VIBR. AND RESPONSE TO RANDOM PRESSURE OF CYL. SHELLS

## ABSTRACT

Author : AOUNI A. LAKIS

Title : Free Vibration and Response to Random Pressure Field of Non-uniform Cylindrical Shells

Department : Mechanical Engineering

Degree : Doctor of Philosophy

Summary :

This thesis presents a new theory for the dynamical and static analysis of axially non-uniform, thin, circular cylindrical shells subjected to random pressure fluctuations. It is a hybrid of finite element and classical shell theories: the shell is subdivided into cylindrical finite elements, and the displacement functions are obtained using Sanders' shell equations (for thin cylindrical shells) in full. Expressions for the mass, stiffness and stress-resultant matrices for one finite element and for the whole structure are obtained.

The free flexural vibration characteristics of thin uniform shells with simply-supported, clamped and free ends are studied, as well as ring-stiffened shells, shells with thickness discontinuities, and shells partially or completely filled with liquid. The frequencies of vibration are compared with those obtained by other theories and with others' experiments. Agreement with other theories

is good and, in the majority of cases, is even better with the experiments.

Finally, an expression of the r.m.s. response of uniform and non-uniform shells subjected to subsonic boundary-layer pressure fluctuations was derived; and a particular simply-supported cylindrical shell subjected to such a pressure field was studied.

## RESUME

Auteur : AOUNI A. LAKIS

Titre : Vibrations dues à un champ de pression aléatoire d'une coque cylindrique non-uniforme

Département : Génie mécanique

Degré : Docteur en philosophie

Sommaire :

Une théorie nouvelle est élaborée dans cette thèse pour analyser dynamiquement et statiquement les coques minces et non uniformes soumises aux fluctuations d'une pression aléatoire. La méthode des éléments-finis est utilisée et les fonctions de déplacement obtenues proviennent de la théorie des coques minces de Sanders. Les matrices de la masse, de la rigidité (stiffness) et des efforts-résultants pour un élément fini ainsi que pour toute la structure sont dérivées.

Les fréquences et les valeurs propres des coques uniforme ou non-uniformes simplement supportée, encastrée, etc., sont déterminées. Aussi, on étudie les effets du liquide sur ces fréquences propres dans le cas d'une coque complètement ou partiellement remplie. Ces résultats sont comparés avec ceux des autres théories et expériences.

Finalement, les déplacements des parois de la coque soumise aux fluctuations d'une pression aléatoire sont dérivés analytiquement et déterminés numériquement.

# FREE VIBRATION
# AND RESPONSE TO RANDOM PRESSURE FIELD
# OF NON-UNIFORM CYLINDRICAL SHELLS

by

AOUNI A. LAKIS

A thesis submitted to the Faculty of Graduate Studies
and Research in partial fulfilment of the
requirements for the degree of
Doctor of Philosophy

Department of Mechanical Engineering
McGill University
Montreal, Que.
Canada

March 1971

To my wife, Michelle

## SUMMARY

This thesis presents a new theory for the dynamical and static analysis of axially non-uniform, thin, circular cylindrical shells subjected to random pressure fluctuations. It is a hybrid of finite element and classical shell theories: the shell is subdivided into cylindrical finite elements, and the displacement functions are obtained using Sanders' shell equations (for thin cylindrical shells) in full. Expressions for the mass, stiffness and stress-resultant matrices for one finite element and for the whole structure are obtained.

The free flexural vibration characteristics of thin uniform shells with simply-supported, clamped and free ends are studied, as well as ring-stiffened shells, shells with thickness discontinuities, and shells partially or completely filled with liquid. The frequencies of vibration are compared with those obtained by other theories and with others' experiments. Agreement with other theories is good and, in the majority of cases, is even better with the experiments.

Finally, an expression of the r.m.s. response of uniform and non-uniform shells subjected to subsonic boundary-layer pressure fluctuations was derived; and a particular simply-supported cylindrical shell subjected to such a pressure field was studied.

## ACKNOWLEDGEMENTS

The author wishes to express his gratitude to Professor M.P. PAIDOUSSIS for his valuable advice and constant encouragement during the conduct of this research, and for providing comments on the draft of this dissertation which were of great value.

This work was supported by a research grant from the National Research Council of Canada and by a contract from Atomic Energy of Canada Ltd. whose assistance the author gratefully acknowledges.

The author also acknowledges the assistance rendered by the Programmers of the McGILL Computing Centre.

His thanks are also due to Mr. HUYNH VAN CHUONG and Mr. QUACH VAN BE who carefully checked the computer programs, the lengthy calculations, and drew the figures.

Finally, his thanks are due to Miss B.E. LOWLES for typing this thesis.

# TABLE OF CONTENTS


| | | | Page |
|---|---|---|---|
| SUMMARY | | | i |
| ACKNOWLEDGEMENTS | | | ii |
| TABLE OF CONTENTS | | | iii |
| LIST OF NOTATIONS | | | vii |
| LIST OF TABLES | | | xvi |
| LIST OF FIGURES | | | xvii |
| CHAPTER I | | INTRODUCTION | 1 |
| | 1.1 | General Introduction | 1 |
| | 1.2 | Literature Review | 4 |
| | 1.3 | The Present Theory | 8 |
| | 1.4 | Organization of this Thesis | 11 |
| CHAPTER II | | BASIC THEORY | 14 |
| | 2.1 | Introduction | 14 |
| | 2.2 | Finite-element Method | 14 |
| | 2.3 | Basic Theory of Thin Elastic Shells | 17 |
| CHAPTER III | | THE DISPLACEMENT FUNCTIONS | 20 |
| | 3.1 | Selection of the Displacement Functions | 20 |
| | 3.2 | Determination of the Displacement Functions | 20 |
| CHAPTER IV | | MATRIX FORMULATION | 25 |
| | 4.1 | Strain Matrix | 25 |

| | | Page |
|---|---|---|
| 4.2 | Elasticity Matrix | 25 |
| 4.3 | Stiffness and Mass Matrices | 26 |
| 4.4 | The Stress-Resultant Matrix | 30 |
| 4.5 | The Stiffness and Mass Matrices for the Whole Shell | 31 |
| 4.6 | Analysis of Shells Subjected to Static Loads | 32 |
| CHAPTER V | FREE VIBRATION AND RESPONSE TO RANDOM PRESSURE FIELD | 34 |
| 5.1 | Introduction | 34 |
| 5.2 | Free, Breathing Vibration | 35 |
| 5.3 | Free Vibration of a Liquid-Filled Cylindrical Shell | 37 |
| 5.4 | Response to Random Pressure Field | 41 |
| 5.5 | Decoupling of the Differential Equations of Motion | 42 |
| 5.6 | Representation of Continuous Random Pressure Field at the Nodal Points | 45 |
| 5.7 | Fourier Transform Representation of Nonperiodic Forces | 47 |
| 5.8 | Cross-correlation Spectral Density of Displacements in Terms of the Cross-correlation Spectral Density of the Pressure Field | 47 |
| 5.9 | Calculation of the Cross-correlation Spectral Density $W_f(\Omega;x\ x';0)$ of the Force Field "f". | 54 |
| 5.10 | Summary | 56 |

| | | | Page |
|---|---|---|---|
| CHAPTER VI | | SHELL RESPONSE TO SUBSONIC BOUNDARY-LAYER PRESSURE FLUCTUATIONS | 59 |
| | 6.1 | Introduction | 59 |
| | 6.2 | Longitudinal and Lateral Correlation Functions | 61 |
| | 6.3 | Mean-Square Response | 64 |
| CHAPTER VII | | METHOD OF CALCULATION | 76 |
| | 7.1 | Computational Method and Computer Program | 76 |
| CHAPTER VIII | | CALCULATIONS AND DISCUSSION | 81 |
| | 8.1 | Introduction | 81 |
| | 8.2 | Rigid-Body Motions | 82 |
| | 8.3 | Characteristic Equations | 83 |
| | 8.4 | Calculations for Uniform Shells | 84 |
| | 8.5 | Calculations for Ring-Stiffened Shells | 89 |
| | 8.6 | Calculations for Shells with Thickness Discontinuity | 91 |
| | 8.7 | Calculations for Shells Completely or Partially Filled with Liquid | 95 |
| | 8.8 | Calculations of the r.m.s. Response for Shells Subjected to Subsonic Boundary Layer Pressure Fluctuations | 96 |
| CHAPTER IX | | CONCLUSION | 99 |
| REFERENCES | | | 105 |
| APPENDIX A | | SANDERS' THEORY OF SHELLS | 113 |
| APPENDIX B | | LIST OF MATRICES | 119 |
| APPENDIX C | | EVALUATION OF SOME INTEGRALS | 121 |

| | | Page |
|---|---|---|
| APPENDIX D | OUTPUT DATA | 132 |
| TABLES | | 152 |
| FIGURES | | 165 |

## LIST OF NOTATIONS

| | |
|---|---|
| $a_{11}, a_{12}, a_{21}, a_{22}, a_{13}, a_{23}$ | parameters defined in equation (3.7) |
| $A_1, A_2$ | the first fundamental magnitude |
| $A_j$ $(j = 1,\ldots,8)$ | constants in equation for U |
| a,b,c,d | constants defined by equations (6.1) and (6.2) |
| A,B | parameters defined in equations (6.10) - (6.12) as $A = a/U_{\mathbb{C}}$, $B = b/U_{\mathbb{C}}$. |
| b/L | liquid depth ratio |
| $B_j, C_j$ $(j = 1,\ldots,8)$ | constants in equation for V and W, respectively |
| $\bar{C}_j$ | elements of vector {C} |
| $c_o$ | velocity of sound in the fluid at the reference pressure |
| $C, C_1, C_2, D, D_1, D_2$ | parameters defined in equation (6.13) |
| D | parameter defined in equation (A.9) |
| E | Young's modulus |
| $f_R(x,t)$, $f_c(x,t)$ | instantaneous radial and circumferential forces per unit length, at time t. |
| $\overline{f_\Omega f'_\Omega}$ | mean per unit band-width |
| $f_o$ | forced frequency in Hz |

| | |
|---|---|
| $f_r$ | $r^{th}$ natural frequency in Hz |
| $F_3^c(\ell_i,\ell_u), F_3^\Delta, F_4^c, F_4^\Delta, F_5^c, F_5^\Delta$. | parameters defined in equations (6.19) - (6.24) |
| $\lvert H_r(\Omega)\rvert$ | magnification factor defined by (5.30) |
| $I_n, J_n$ | modified and ordinary $n^{th}$ order Bessel functions, respectively |
| $I'_n, J'_n$ | first derivative of $I_n$ and $J_n$, respectively |
| $J$ | number of constraint edges imposed |
| $k$ | equal to $(1/12).(t/r)^2$ |
| $k_c$ | parameters given by $k_c = \Omega_i\ r/c_o$ |
| $k_1, k_2$ | constants defined by equation (6.5) |
| $K$ | parameter defined by equation (A.9) |
| $K_1, K_2$ | parameters defined by equation (6.13) |
| $\ell$ | length of finite element |
| $\ell_N^e$ | coordinate of node e in the x-direction |
| $\ell_e, \ell'_e$ | coordinates of the area $S_e$, surrounding the node e, with respect to the origin in the x-direction (figure 7) |
| $\ln$ | Naperian logarithm |
| $L$ | total length of shell |
| $m$ | axial half wave-number |
| $M_{11}, M_{22}, M_{12}, M_{21}$ | stress couples |
| $\bar{M}_{12}$ | modified stress couple |
| $M_x, M_\varphi, \bar{M}_{x\varphi}$ | stress resultants for a circular cylinder |

| | |
|---|---|
| $\bar{\bar{M}}_x$ | value of stress couple at edge (boundary condition) |
| $\mathfrak{M}_r$ | moment acting at each node as shown in figure 7b |
| $n$ | circumferential wave-number |
| $\underline{n}(\xi_1, \xi_2)$ | unit normal vector to the reference surface |
| $N_{11}, N_{22}, N_{12}, N_{21}$ | stress resultants |
| $\bar{N}_{12}$ | modified stress resultants |
| $N_x, N_\varphi, \bar{N}_{x\varphi}$ | stress resultants for a circular cylinder |
| $N$ | number of finite elements in the structure |
| $\bar{\bar{N}}_x$ | stress resultant at an edge (boundary condition) |
| $p(x,\varphi,t)$ | instantaneous pressure on the surface |
| $\overline{p^2(x,\varphi,t)}$ | mean square of pressure fluctuation |
| $\overline{p^2(\Omega,Re)}$ | mean square pressure per unit band-width |
| $q_1, q_2, q_n$ | components of the external force vector along $\xi_1$, $\xi_2$ and along the normal; (functions of time) |
| $Q_1, Q_2$ | transverse stress resultants |
| $Q_x, Q_\varphi$ | transverse stress resultants for a circular cylinder |
| $r$ | mean radius of shell |
| $\underline{r}(\xi_1, \xi_2)$ | position vector of a corresponding point on the reference surface |

| | |
|---|---|
| Re | Reynolds number |
| $R_1, R_2$ | principal radii of curvature of the middle surface |
| $S_\xi, S_\eta$ | axial and circumferential Strouhal numbers, respectively |
| $S_e$ | area surrounding the node e (figure 7) |
| $S_{F_j}(\Omega)$ | Fourier transform of $F_j(t)$ |
| $S^*_{F_j}(\Omega)$ | complex conjugate of $S_{F_j}(\Omega)$ |
| t | wall-thickness of shell |
| $\underline{t_1}$ | unit vector along $\xi_1$. |
| $\underline{t_2}$ | unit vector along $\xi_2$. |
| $\bar{\bar{T}}_x$ | shearing stress resultant at an edge (boundary condition) |
| T | half-period |
| U,V,W | axial, tangential and radial displacements |
| $U_{℄}, U_{CONV}$ | centerline and convection velocities, respectively |
| $\bar{U}_{℄}$ | mean centerline velocity |
| $u_n, v_n, w_n$ | amplitudes of U,V,W associated with $n^{th}$ circumferential wave-number |
| $\bar{\bar{V}}_x$ | stress resultant at an edge (boundary condition) |

| | |
|---|---|
| $W_S$ | work of the body and surface forces |
| $W_{\xi_1}$ | work of the edge stresses on an edge of constant $\xi_1$ |
| $W_{\xi_2}$ | work of the edge stresses on an edge of constant $\xi_2$ |
| $W_f(\Omega;x,x';0)$ | cross-correlation spectral density function of the force field f. |
| x | axial coordinate |
| $\overline{y_t^2(x,\varphi,t)}$ | mean square displacement at node t (subscript t) |
| Z(t) | normal coordinate at time t |
| $\alpha_j, \beta_j$ | defined by (3.6) and given by (3.7) and (3.8) |
| $\bar{\alpha}_j, \bar{\beta}_j$ | defined by (3.8) |
| $\Gamma^F_{im}, \Gamma^M_{ki}, \Gamma^{MM}_{jk}$ | parameters defined in equations (6.15) - (6.18) |
| $\gamma_1(l_i, l_m), \gamma_2, \ldots, \gamma_8$ | parameters defined in equation (6.31) |
| $\epsilon_x, \epsilon_\varphi, \epsilon_{x\varphi}$ | axial, circumferential and shear strains of middle surface |
| $\varphi_R$ | generalized damping factor |
| $\zeta_1, \zeta_2, \eta_1, \eta_2$ | defined in Appendix B |

| | |
|---|---|
| $\eta$ | equal to $\lvert r(\varphi - \varphi')\rvert$; $\lvert\,\rvert$ denotes absolute value |
| $\Theta_r$ | phase lag of the displacement relative to the driving force; defined by equation (5.28) |
| $\kappa_1, \kappa_2$ | real parts of $\lambda_j$ |
| $\kappa_x, \kappa_\varphi, \bar{\kappa}_{x\varphi}$ | axial, circumferential and modified twisting strains |
| $\lambda_j$ | roots of characteristic equation |
| $\lambda_m$ | equal to $m\,\pi r/\ell$ |
| $\mu$ | dynamic viscosity (lb.sec/ft$^2$) |
| $\mu_1, \mu_2$ | imaginary parts of $\lambda_j$ |
| $\nu_F$ | kinematic viscosity (ft$^2$/sec.) |
| $\nu$ | Poisson's ratio |
| $\xi$ | equal to $\lvert x-x'\rvert$; $\lvert\ \rvert$ denotes absolute value |
| $\rho$ | density of material of the shell |
| $\rho_F$ | fluid density |
| $\tau$ | time delay |
| $\varphi$ | circumferential coordinate |
| $\psi_1, \psi_2, \omega_1, \omega_2$ | defined in Appendix B |
| $\Psi_{y_{ij}}(x,\varphi,\tau)$ | spatial correlation function of the displacement defined by equation (5.23) |

| | |
|---|---|
| $\psi_p(\xi,\eta,\tau)$ | normalized space-time correlation function of the fluctuating pressure |
| $\psi_{p,\Omega,Re}(\xi,\eta,0)$ | spatial correlation function of the fluctuating pressure in frequency domain |
| $\psi_{p,\Omega,Re}(\xi,0,0)$ | longitudinal correlation function of the fluctuating pressure in frequency domain |
| $\psi_{p,\Omega,Re}(0,\eta,0)$ | lateral correlation function |
| $\Omega_i$ | $i^{th}$ natural frequency (rad./sec.) |
| $\Omega$ | forced frequency (rad./sec.) |

<u>Matrices</u>

| | |
|---|---|
| $[A]$ | defined by equation (3.11) |
| $[A_1],[B_1],[C_1]$ | defined by equation (4.10) |
| $\{C\}$ | defined by (3.10) |
| $[C_n]$ | diagonal damping matrix defined by (5.13) |
| $[D_1]$ to $[D_4]$ | defined by (4.11) |
| $[E_1]$ to $[E_4]$ | defined by (4.13a) |
| $\{F(x,\phi,t)\}$ | vector of external forces |
| $[G]$ | defined by equation (4.5) |
| $[k]$ | stiffness matrix for one finite element |
| $[K]$ | stiffness matrix for the whole shell |
| $[K_n],[M_n]$ | diagonal matrices defined by equation (5.12) |

| | |
|---|---|
| [N] | defined by (3.13) |
| [m] | mass matrix for one finite element |
| [M] | mass matrix for the whole shell |
| [P] | elasticity matrix |
| [Q] | defined by equation (4.1) |
| $[Q_i]$,$[Q_j]$ | defined by (4.14a) and (4.14b) |
| [R] | defined by equation (3.9) |
| [S] | defined by (4.6) |
| [ST] | stress-resultant matrix for one finite element |
| [T] | matrix for circumferential variation of displacements, etc., defined by (3.9) |
| {y} | displacement vector defined by (5.1) |
| {Z(t)} | normal coordinates vector |
| [ZY],[Y] and [ZJ],[RJ] | matrices defined by equations (4.8) and (4.9), respectively |
| [Z] | matrix (function of x) defined by equation (4.7) |
| $[\Gamma]$ | matrix of constant elements defined by equation (4.7) |
| $\{\delta_i\}$,$\{\delta_j\}$ | nodal displacement vectors, at points i and j, respectively |
| $[\Delta]$ | matrix of constant elements defined by equation (4.7) |
| $\{\varepsilon\}$ | strain vector |

| | |
|---|---|
| $\{\sigma\}$ | stress-resultant vector |
| $[\Phi]$ | modal matrix of the system |
| $\{\Phi_t\}_i$ | modal column of the system corresponding to the $i^{th}$ natural frequency |

# LIST OF TABLES


| | |
|---|---|
| Table 1. | Matrices [R] and [T] |
| Table 2. | Matrix [A] |
| Table 3. | Matrix [Q] |
| Table 4. | Matrix [Γ] |
| Table 5. | Matrices [Δ] and [Z] |
| Table 6. | Matrix [ZY] |
| Table 7. | Matrices [$A_1$], [$B_1$] and [$C_1$] |
| Table 8. | Matrices [$D_1$] to [$D_4$] |
| Table 9. | Matrix [$Q_i$] |
| Table 10. | Roots of characteristic equations for $(1-\nu^2)/k = 4 \times 10^4$ and $\nu = 0.3$. |
| Table 11. | The elements of the displacement function matrix for $x = 0$, $x = \ell$. |
| Table 12. | The eigenvectors of the first and second modes of a free element. |
| Table 13. | Natural frequencies, in Hz, for a particular uniform shell, as calculated by various theories ($m = 1$). |

## LIST OF FIGURES


| | |
|---|---|
| Figure 1. | Cylindrical finite element defined by nodes i and j. |
| Figure 2. | Nodal displacements at points i and j. |
| Figure 3. | Illustration of the construction of stiffness and mass matrices for the whole shell. |
| Figure 4. | Parametric curves of the surface where $A_1^2 = \vec{r}_{,1} \cdot \vec{r}_{,1}$ and $A_2^2 = \vec{r}_{,2} \cdot \vec{r}_{,2}$. |
| Figure 5. | Differential element of a shell. |
| Figure 6a. | Stress resultants and surface loads acting on a differential element. |
| Figure 6b. | Stress couples acting on a differential element. |
| Figure 7. | Illustration of the construction of the continuous random pressure field at the nodal points. |
| Figure 8. | Magnification factors for a lightly damped multi-degree-of-freedom system. |
| Figure 9. | Longitudinal correlation versus Strouhal Number based on convection velocity. |
| Figure 10. | Lateral correlation versus Strouhal Number based on centreline velocity. |

Figure 11. The non-dimensionalized frequency spectrum.

Figure 12. Computational flow diagram.

Figure 13. Normalized eigenvectors for n = 2,3,4,5 and m = 1 for a uniform, simply-supported shell.

Figure 14a. Natural frequencies of a uniform simply-supported shell as a function of the number of finite elements, N, for m = 1.

Figure 14b. Natural frequencies of a uniform simply-supported shell as a function of N, for m = 2 and 3.

Figure 15. Natural frequencies of a free-free uniform shell as a function of the number of circumferential waves, n.

Figure 16. Natural frequencies of a clamped-clamped uniform shell.

Figure 17. Natural frequencies of a clamped-free uniform shell.

Figure 18. Natural frequencies of the unstiffened shell studied by Weingarten (50).

Figure 19. Natural frequencies of the ring-stiffened shell first studied by Weingarten (50); m = 1.

Figure 20. Natural frequencies of the ring-stiffened shell first studied by Weingarten (50); $m = 2$.

Figure 21. Natural frequencies of the ring-stiffened shell first studied by Weingarten (50); $m = 3$.

Figure 22. Some natural frequencies of a simply-supported shell with thickness discontinuity ($t_1 = 0.1875$ in., $t_2 = 0.25$ in.).

Figure 23. Natural frequencies of a simply-supported shell with thickness discontinuity ($t_1 = 0.125$ in., $t_2 = 0.25$ in.); $n = 4$.

Figure 24. Natural frequencies of a simply-supported shell with thickness discontinuity ($t_1 = 0.125$ in., $t_2 = 0.25$ in.); $n = 5$.

Figure 25. Variation of natural frequencies with liquid depth of a liquid-filled shell, based upon this theory; $m = 1$.

Figure 26. Variation of natural frequencies with liquid depth of a liquid-filled shell, based upon this theory; $m = 2$.

Figure 27. Variation of natural frequencies with liquid depth of a liquid-filled shell based upon this theory; $m = 3$.

Figure 28. Comparison of this theory with experiments of (36) for liquid-filled shells; m = 1.

Figure 29. Comparison of this theory with experiments of (36) for liquid-filled shells; m = 2.

Figure 30. Comparison of this theory with experiments of (36) for liquid-filled shells; m = 2 and 3.

Figure 31. Eigenvectors of liquid-filled shells, as functions of liquid depth, b; for n = 5, m = 1.

Figure 32. Eigenvectors of liquid-filled shells, as functions of liquid depth, b; for n = 5, m = 2.

Figure 33. Eigenvectors of liquid-filled shells, as functions of liquid depth, b; for n = 5, m = 3.

Figure 34. Maximum of r.m.s. displacements as functions of n; Re = $10^5$ and $\varphi_x = 10^{-5}$.

Figure 35. Maximum of r.m.s. displacements as functions of the mean centre line velocity, $\bar{U}_{\text{℄}}$; n = 3.

# CHAPTER I

# INTRODUCTION

## 1.1 General Introduction

Thin shells appear as components in practically every type of modern industrial equipment, in aerospace, nuclear, marine and petrochemical industries. Accordingly, the study of the dynamical characteristics of thin elastic shells is of considerable practical, as well as theoretical, interest.

As in all dynamical problems, interest commonly lies in the determination of the free vibration characteristics of such shells, and in their response characteristics when subjected to prescribed force fields.

In this thesis we are concerned with the dynamics of thin *cylindrical* shells. Such shells are commonly used to contain or convey fluids, and this, to a certain extent, determines the classes of problems in which interest is focused. Thus, in addition to the determination of the vibration characteristics of the shells *in vacuo*, it is also of considerable interest to determine the dynamical characteristics of shells containing either stationary or flowing fluid - which is the realm of fluidelasticity.

There are many ways in which the presence of the fluid may influence the dynamics of the shell. If the shell contains a stationary gas at low pressure, then the vibration of the shell differs only slightly from that of the same shell in vacuo. This is not the case, however, if the shell is substantially pressurized by the enclosed fluid, as this entails additional strain energy in the shell. Moreover, if the fluid is compressible, the compressibility of the fluid alters the effective stiffness of the system. Also, if the density of the enclosed fluid is relatively high, as is the case with liquids, then the fluid exerts considerable inertial loading on the shell, and this results in diminishing the resonant frequencies significantly.

Coupling between the fluid and the shell can manifest itself in several other ways. In the case of shells partially filled with liquid free-surface motions may be coupled to the shell motions. This is of particular interest in liquid-propelled rockets; in cases of proximity or coincidence of the natural frequencies of the free-surface motion and that of the shell, large oscillations may develop in the propellant tanks and are normally referred to as sloshing. Nonlinear coupling may also induce sloshing; in this case subharmonic excitation of free-surface modes is involved.

Other effects of coupled fluid-shell motions occur when the fluid is flowing. Depending upon the boundary conditions, if the flow velocities are large, buckling or oscillatory flexural instabilities are possible (§1.2). More recently, the existence of flutter in the shell-modes was discovered (§1.2).

Similarly, in considering the response of cylindrical shells, considerable interest exists in the case where the excitation is transmitted through, or arises from, the contained fluid. This could take the form of pressure waves transmitted through the fluid; or, if the fluid is flowing, the excitation could arise from gross pressure perturbations due to disturbances in the flow, or from boundary-layer perturbations. It is known that vibration caused by these pressure fluctuations may, in certain circumstances, cause fatigue failures of the structures involved.

In this thesis we shall concern ourselves with the development of a novel theory for the dynamical analysis of axially non-uniform shells. We shall study (a) the free vibration characteristics of such shells empty, and completely or partially filled with liquid, and (b) the response of such shells to an arbitrary pressure field, and specifically to a pressure field arising from the subsonic boundary layer of an internally flowing fluid.

## 1.2 Literature Review

The first attempt to formulate a bending theory of thin shells from the general equations of elasticity was made by Aron in 1874, and was followed in 1888 by a successful approximate theory known as Love's first approximation (1)* - (3). Since then, the theory of elastic shells has repeatedly been re-examined in the literature, e.g. (3) - (9).

Several methods have been developed for the dynamical analysis of shells. Of these the most versatile have proved to be Rayleigh-Ritz methods, e.g. (10), (11), Stodola-type iteration methods, e.g. (12), finite-difference methods, e.g. (13), and finite-element methods (14) - (20). All these methods and their variants have their advantages and disadvantages. One of the criteria of success of a method may be considered to be its capability of yielding the high as well as the low characteristic frequencies and modal shapes with comparable, high accuracy. This requirement is not really met by the finite-difference and Stodola-type methods [cf. (12)]. The Rayleigh-Ritz and finite-element methods, on the other hand, are satisfactory from this point of view; furthermore, because they lead to a symmetric

* Underlined numbers in parentheses denote references, listed separately.

eigenvalue problem, they are easily amenable to solution by digital computer, which is a great advantage. The finite-element method has added advantages in terms of ease of formulation, and because numerical convergence is not as sensitive to particular sets of boundary conditions as is the case with the Rayleigh-Ritz method (21).

Here we are specifically interested in free vibration and response to random pressure fluctuations of uniform and non-uniform thin cylindrical shells. Accordingly, we shall review the pertinent literature in these areas, as follows: firstly, on free vibration of empty cylindrical shells; secondly, on free vibration of fluid-filled shells; thirdly, on the response of cylindrical shells subjected to random force fields.

Arnold and Warburton's (47) pioneering work on the vibration of uniform cylindrical shells derives the frequency equation by the energy method using Timoshenko's strain relations. Lagrange's equations are used to derive the dynamical equations, eventually leading to a determinantal equation which yields the frequencies. Baron and Bleich (48) have based their theory on an energy method in which the shell is first treated as a membrane and the bending effects are subsequently introduced as corrections. Galletly (49) extends Arnold and Warburton's theory to ring-stiffened shells. Michalopoulos and Muster (46), also studying ring-stiffened shells, proceed essentially as in (47), but express displacements in the kinetic and strain energy expressions in general, series form; the frequencies are found by the Jacobi iteration method. Sewall and Naumann (11) studied uniform and axially stiffened shells; they obtained their natural frequencies by application of the energy method, using Novozhilov's strain-displacement relations and employing the Rayleigh-Ritz procedure. Weingarten (50) neglecting rotary inertia effects, derived a Donnell-type equation for a general orthotropic conical shell. He then reduced the ring-stiffened shell to an equivalent orthotropic conical shell. The cylindrical shell in this case may be considered as the limiting case of a conical one. Finally, the free vibration characteristics of shells with a thickness discontinuity were studied theoretically by Warburton and Al-Najafi (51) and both theoretically and experimentally by Falkiewicz (52).

The above is not meant to be an exhaustive literature survey of the field of free vibration of thin cylindrical shells; no such survey is presented here, mainly because most of the papers are concerned with uniform cylindrical shells, whereas we are here interested in (axially) non-uniform ones. In this latter category there are few papers indeed, namely Warburton's and Al-Najafi's (51) work, and the work on ring-stiffened shells discussed above.

Considering fluid-filled shells next, a considerable volume of work exists dealing with the effect of the fluid on the dynamics of the shell. Once again, we shall not attempt a complete literature review, for similar reasons to those given above. Niordson (33), in 1953, was the first to present a systematic - and elegant - theory for the effect of internal and external fluids on the vibration of shells (also considering the case of flowing fluids). Fung et al. (37), and Berry and Reissner (32) investigated the effect of pressurization (by compressible fluids) on the vibration of freely supported cylindrical shells, both theoretically and experimentally. Lindholm et al. (36) studied the free vibration of a completely liquid-filled tank, essentially unpressurized. They also performed experiments in the case of partially liquid-filled shells.

Parenthetically considering coupled fluid-shell motions in cases when the fluid is flowing, it was found that, depending on the boundary conditions, if the flow velocities are large enough, buckling or oscillatory instabilities are possible (33), (34). More recently, the existence of flutter instabilities in the shell modes was discovered by Paidoussis (35).

Finally, we consider the literature on the vibration of shells subjected to a random force field. We shall by-pass references on the response of cylindrical shells subjected to either static or dynamic deterministic force fields, which are of no interest to us here. Several theories do exist for the response of bars, beams and plates subjected to general, random pressure fields, and in the particular case of a boundary-layer pressure field, e.g. (53) - (57). To the author's knowledge no such general theory exists for cylindrical shells. However, a study concerned "with the vibratory motion of a simply supported finite, elastic, circular cylindrical shell due to random pressure field" was made by Cottis et al. (45). That study, apart from being limited to simply-supported shells, derives only the space-time correlation function, rather than the mean-square response; moreover, numerical solution of the problem is not attempted.

## 1.3 The Present Theory

In this Thesis we are concerned with the dynamics of thin cylindrical shells. Such shells can vibrate in many ways. Here we shall only concern ourselves with the class of vibrations where the shell motions are predominantly radial. More specifically, we shall only consider flexural vibrations of the shell walls, in the modes sometimes designated as "breathing" vibrations, thus excluding the particularly simple case where the shell vibrates essentially as a beam.

The theory to be developed will be capable of analysing geometrically axially-symmetric shells which are not necessarily uniform, i.e. allowing for axial variations in wall-thickness and elastic properties. The theory will be capable of yielding the free-vibration characteristics of such shells, and their response when subjected to a random pressure field. The theory can also deal with shells partially filled with liquid.

This theory is a hybrid finite-element theory in the sense that, whereas it uses the framework of the finite-element method, the displacement functions are determined by classical shell theory. The finite element chosen is a cylindrical frustum, rather than the more usual triangular or rectangular flat plate elements [cf. (22) - (25)]. This allows us to use the thin shell equations in full for the determination of the displacement functions, and hence the mass, stiffness and stress-resultant matrices - instead of the more usual polynomial displacement functions.

As no geometric modelling of the structure is involved, and as the shell equations are used for the determination of displacements within each finite element, it is reasonable to expect that this approach is capable of high accuracy.

Calculations of the free vibration characteristics (i.e. the eigenvalues and modal shapes) of uniform and non-uniform shells will be presented. In the latter case, shells with a thickness discontinuity and ring-stiffened shells are analysed, as well as shells partially filled with liquid. Specifically, for particular uniform or axially non-uniform cylindrical shells, the flexural natural frequencies and the eigenvectors are calculated for various combinations of the circumferential wave-number, n, and number of axial half-waves, m. The calculations are confined to $n \geq 2$ which is a limitation of the theory as it stands. In this connection, it should be remarked that for $n = 1$ the vibration is essentially that of a beam and its characteristics may be determined by much simpler theory. For $n = 0$ the deformation of the shell is axially symmetric, and this case will likewise not be considered here.

Finally, the r.m.s. response of uniform and axially non-uniform shells subjected to subsonic boundary-layer pressure fluctuations is also calculated, analytically and numerically. In all the above cases, whenever possible, the theoretical results will be compared with available experimental data and with others' theories.

The original contributions of this Thesis may be considered to be the following: (i) the development of a new concept for the analysis of shells, by utilizing the versatility of the finite-element method, on the one hand, and the precision of classical shell theory, on the other; (ii) the use of this concept in developing a new finite element formulation for thin cylindrical, axially non-uniform or uniform, shells; (iii) the development of a theory capable of statically and dynamically analysing <u>any</u> axially non-uniform shell, including the case of partially liquid-filled shells (as will be seen, with consistently good accuracy); (iv) the analysis of uniform and non-uniform thin cylindrical shells subjected to a subsonic boundary-layer pressure field, to the point of predicting r.m.s. amplitudes of vibration.

## 1.4 Organization of this Thesis

The study is divided into nine Chapters. We shall briefly outline the contents of each.

<u>Chapter II</u> is devoted to general, theoretical aspects of the finite-element method, and to the basic theory of thin elastic shells, with particular attention to Sanders' theory.

In <u>Chapter III</u> we establish the pertinent displacement functions for the finite element selected from the theory of thin elastic shells.

The construction of the stiffness, mass and stress-resultant matrices for one finite element and for the whole shell is developed in <u>Chapter IV</u>, as well as an outline of the method of analysis of shells subjected to static loads.

<u>Chapter V</u> considers the free vibration characteristics, the effect of enclosed stationary liquid on the dynamics of

partially filled shells, and the determination of the response to random pressure fields, of uniform and non-uniform shells.

In Chapter VI we determine the longitudinal and lateral spatial correlation functions for the case of subsonic boundary-layer pressure fluctuations. We also obtain expressions for the r.m.s. response of shells subjected to such pressure fluctuations.

Chapter VII describes a procedure for computing the vibration modes and frequencies, both for the case of empty shells and also for the case of shells completely or partially filled with liquid; also the method of computing the r.m.s. response to subsonic boundary-layer pressure fluctuations.

In Chapter VIII are presented the results of some calculations undertaken to test the theory.

The first set of calculations involves uniform shells, the main aim being (i) to check the correctness of the mass and stiffness matrices as derived in Chapter IV, (ii) to test the rate of convergence of the computed natural frequencies to the correct value with increasing number of finite elements, and (iii) to test the sensitivity of the new theory to boundary conditions.

The second set of calculations is with non-uniform shells. A shell made up of two segments of unequal wall-thickness and another which is ring-stiffened are analysed. The third set involves natural frequencies of uniform shell completely or partially - filled with liquid.

Finally, the r.m.s. response to subsonic boundary-layer pressure fluctuations is determined for one specific shell configuration.

Finally, Chapter IV presents some general conclusions.

# CHAPTER II

# BASIC THEORY

## 2.1 Introduction

The general method used in this study is the finite-element method. The shell is subdivided into cylindrical finite elements, and the displacement functions are obtained using Sanders' equations for thin cylindrical shells in full. This approach appears to offer considerable advantages, and its relatively simple logic makes it ideally suited for the computer.

As this is a relatively new technique, a short outline of the finite-element method and of Sanders' theory for thin shells will be given next. For further information, the reader is referred to (25) and (8).

## 2.2 Finite-element Method

### 2.2.1 General outline of the procedure

The finite-element method proceeds as follows (25):

(i) the continuum is separated by imaginary lines or surfaces into a number of 'finite elements';

(ii) the elements are assumed to be interconnected at a discrete number of nodal points situated at their boundaries, the displacements of these nodal points being the basic unknown parameters of the problem;

(iii) functions are chosen to uniquely define displacement within each finite element in terms of its nodal displacements;

(iv) as the displacement functions uniquely define the state of strain within each element, this strain, together with any initial strain, and the elastic properties of the material will define the state of stress throughout the element and on its boundaries.

Suppose that we have a cylindrical finite element defined by two nodes i and j and nodal surface boundaries (figure 1). Then the displacements within the element, i.e. the displacement functions, may be defined by

$$\begin{Bmatrix} U(x,\phi) \\ W(x,\phi) \\ V(x,\phi) \end{Bmatrix} = [N] \begin{Bmatrix} \delta_i \\ \delta_j \end{Bmatrix} , \tag{2.1}$$

where $\begin{Bmatrix} \delta_i \\ \delta_j \end{Bmatrix}$ represents the nodal displacements, and the elements of [N] are in general functions of position.

With displacements now known throughout the element, the strain matrix $\{\varepsilon\}$ may be written as

$$\{\epsilon\} = [B] \begin{Bmatrix} \delta_i \\ \delta_j \end{Bmatrix} . \tag{2.2}$$

Assuming general elastic behaviour, the relationship between the stress matrix, $\{\sigma\}$, and the strain matrix will be linear and of the form

$$\{\sigma\} = [P]\{\epsilon\} = [P][B] \begin{Bmatrix} \delta_i \\ \delta_j \end{Bmatrix} = [ST] \begin{Bmatrix} \delta_i \\ \delta_j \end{Bmatrix} , \tag{2.3}$$

where [P] is the elasticity matrix containing the appropriate material properties.

Finally, the equivalent values of the nodal forces, $\{F\}^e$, may be written as follows (25):

$$\{F\}^e = \left[\int [B]^T [P][B]\, d(\text{volume})\right] \begin{Bmatrix} \delta_i \\ \delta_j \end{Bmatrix} + \left[\rho \int [N]^T [N]\, d(\text{volume})\right] \begin{Bmatrix} \ddot{\delta}_i \\ \ddot{\delta}_j \end{Bmatrix} \quad , \tag{2.4}$$

where $\rho$ is the density. Equation (2.4) simply states that the equivalent force is due to stress, within the element, associated with deformation and inertial loading, and is recognized as the typical dynamical equation for any structural element. Accordingly, it defines the stiffness and mass matrices, [k] and [m], respectively, associated with the finite element, i.e.

$$[k] = \int [B]^T [P][B]\, d(\text{volume}) \;, \tag{2.5}$$

and

$$[m] = \rho \int [N]^T [N]\, d(\text{volume}) \;. \tag{2.6}$$

### 2.2.2 Convergence criteria

It is noted that the finite-element method yields useful results provided that the displacement functions chosen represent well the true displacements. To this end, the displacement functions should satisfy the following 'convergence' criteria (25):

(i) the displacement functions should be such that they do not permit straining of an element when the nodal displacements are generated solely by rigid-body displacements;

(ii) the displacement functions should be such that if the nodal displacements are compatible with a constant strain condition, such constant strain will in fact be obtained.

It is noted that the second criterion incorporates the requirements of the first one, as rigid body displacements are a particular case of constant strain, namely zero strain.

## 2.3 Basic Theory of Thin Elastic Shells

The linear theories of thin elastic shells may be divided into two categories:

(a) Theories based on Love's first approximation

The assumptions in this case are the following: (i) the thickness of the shell is small compared with the least radius of curvature ($R_{min}$) of the middle surface, i.e. ($t/R_{min} << 1$); (ii) the strains and displacements are sufficiently small, so that the quantities of the second- and higher-order magnitudes in the strain-displacement relations may be neglected in comparison with the first-order terms; (iii) the component of stress normal to the middle surface is small compared with other normal components of stress and may be neglected in the stress-strain relations, and (iv) the normals to the undeformed middle surface remain normal to the deformed middle surface and suffer no extension.

(b) Theories based on Love's second approximation

These are distinguished from those of (a) in that here the effects of transverse shear and normal strain are not neglected.

The first assumption in (a) defines what is meant by a "thin shell". The second assumption ensures the linearity of the resultant differential equations. The third and fourth assumptions, respectively, imply the neglect of transverse normal stress ($\sigma_n = 0$) and transverse shear deformation.

Here we shall use a theory based on Love's first approximation which is quite adequate for thin shells. However, most forms of the equations based on this approximation contain an inconsistency; this is that, except for the special case of axisymmetric loading of shells of revolution, the strains do not all vanish for small rigid-body rotations of the shell (e.g. theories of Love (1), Vlasov (4), Reissner (3), Timoshenko (26)). On the other hand, Sanders (8), and Budiansky and Sanders (9) developed a modified theory based on Love's first approximation which removes this inconsistency without complicating the equations; (in Sanders' theory all strains vanish for small rigid body motions). This is the theory we shall use.

The analysis proceeds as follows. First, an appropriate system of coordinates on the shell is introduced (figure 4) and certain geometrical relations established; then the strain-displacement relations are derived from strictly geometrical considerations of the process of deformation. Then, the equations of motion which are obtained from a balance of the forces acting on some fundamental element of the medium are considered (figure 6). Finally, the system of equations is completed by deriving the relations between displacement components and stress-resultant components in the elastic medium by using the law of elasticity (Hooke's Law).

This matter (Sanders' theory of shells) is further elaborated in Appendix A, where the equilibrium equations are also given, in terms of the axial, circumferential and radial displacements of the middle surface, U, V and W, respectively.

# CHAPTER III

## THE DISPLACEMENT FUNCTIONS

### 3.1 Selection of the Displacement Functions

The finite element used in this theory, as shown in figure 1, is a cylindrical frustum defined by two nodal circles and two nodal points i and j. As stated in the Introduction, in the present theory we shall employ Sanders' equations of thin cylindrical shells to obtain the pertinent displacement functions, rather than using the more common arbitrary polynomial forms. This is the point of departure of the present theory from, what might be termed, the classical finite-element theory.

We now consider the effects of loads applied to the nodes i and j. Three components of displacement (U,V,W) describe the movement of a point of the middle surface (see figures 1 and 2). The general expression for the edge displacement must be found from equation (A.10) of the shell theory. See also (59) for further details.

### 3.2 Determination of the Displacement Functions

We assume, in the normal manner [cf. (6)], that

$$U = u_n(x)\cos n\varphi, \quad V = v_n(x)\sin n\varphi, \quad W = w_n(x)\cos n\varphi, \qquad (3.1)$$

where n is the circumferential wave-number. Upon substituting into (A.10) we find that we can further assume

$$u_n(x) = A e^{\lambda x/r}, \; v_n(x) = B e^{\lambda x/r}, \; w_n(x) = C e^{\lambda x/r}, \tag{3.2}$$

which substituted into the equations yield three ordinary linear equations in A,B,C of the form

$$[H] \begin{Bmatrix} A \\ B \\ C \end{Bmatrix} = \{0\}. \tag{3.3}$$

For non-trivial solution the determinant of [H] must vanish yielding the characteristic equation

$$\lambda^8 - 4n^2\lambda^6 + \left[\frac{1-\nu^2}{k} + 6n^2(n^2-1)\right]\lambda^4 - 4n^2(n^2-1)^2\lambda^2 + n^4(n^2-1)^2 = 0 . \tag{3.4}$$

This is a quartic in $\lambda^2$ and its roots may be written in the form

$$\left.\begin{array}{ll} \lambda_1 = -\kappa_1 + i\mu_1 , & \lambda_5 = \kappa_1 + i\mu_1 , \\ \lambda_2 = -\kappa_1 - i\mu_1 , & \lambda_6 = \kappa_1 - i\mu_1 , \\ \lambda_3 = -\kappa_2 + i\mu_2 , & \lambda_7 = \kappa_2 + i\mu_2 , \\ \lambda_4 = -\kappa_2 - i\mu_2 , & \lambda_8 = \kappa_2 - i\mu_2 , \end{array}\right\} \tag{3.5}$$

where $\kappa_i$ and $\mu_i$ are real. Each $\lambda_i$ yields a solution of equations (A.10), the complete solution being obtained by the sum of all eight and involving the constants $A_j$, $B_j$, $C_j$ where $j = 1,2,\cdots,8$.

As the $A_j$, $B_j$ and $C_j$ are not independent, we shall next express the $A_j$ and $B_j$ in terms of $C_j$ so that the $u_n$, $v_n$ and $w_n$ can be expressed in terms of only eight constants. To this end we let

$$A_j = \alpha_j C_j \ , \ B_j = \beta_j C_j \ , \ j = 1, 2, \ldots, 8 \tag{3.6}$$

where $\alpha_j$ and $\beta_j$ are complex. Substituting (3.6) into (3.3) we may now determine $\alpha_j$ and $\beta_j$. The $\alpha_j$ and $\beta_j$ are so interconnected, because of the form of (3.3), that we need only solve two pairs of equations, (say obtaining the real and imaginary parts of $\alpha_1$, $\beta_1$, $\alpha_3$ and $\beta_3$), the remainder being obtainable from them, as done by Flügge (6). Thus for j = 1 and 3 we obtain

$$\begin{bmatrix} a_{11} & a_{12} \\ a_{21} & a_{22} \end{bmatrix} \begin{bmatrix} \alpha_j \\ \beta_j \end{bmatrix} = \begin{bmatrix} -a_{13} \\ -a_{23} \end{bmatrix} \ , \tag{3.7}$$

where

$$a_{11} = \left[ \lambda_j^2 - \frac{(1-\nu)}{2} n^2 \left(1 + \frac{k}{4}\right) \right] \ , \qquad a_{22} = \left[ -\frac{(1-\nu)}{2} \lambda_j^2 + n^2(1+k) - \frac{9(1-\nu)}{8} k \lambda_j^2 \right] \ ,$$

$$a_{12} = \frac{n\lambda_j}{2} \left[ \nu\left(1 + \frac{3k}{4}\right) + \left(1 - \frac{3k}{4}\right) \right] \ , \qquad a_{13} = \left[ \nu\lambda_j - \frac{(1-\nu)}{2} k \lambda_j n^2 \right] \ ,$$

$$a_{21} = a_{12} \ , \qquad a_{23} = \left[ n(1 + n^2 k) - \frac{(3-\nu)}{2} k n \lambda_j^2 \right] \ ,$$

noting that $a_{11}a_{22} - a_{21}a_{12} = -\frac{(1-\nu)}{2}(\lambda^2 - n^2)^2 \neq 0$ . The other $\alpha_j$, $\beta_j$ may be obtained from the following relationships:

$$\left.\begin{aligned}
\alpha_1 &= \bar{\alpha}_1 + i\bar{\alpha}_2 \ , & \alpha_5 &= -\alpha_2 \ , \\
\alpha_2 &= \bar{\alpha}_1 - i\bar{\alpha}_2 \ , & \alpha_6 &= -\alpha_1 \ , \\
\alpha_3 &= \bar{\alpha}_3 + i\bar{\alpha}_4 \ , & \alpha_7 &= -\alpha_4 , \\
\alpha_4 &= \bar{\alpha}_3 - i\bar{\alpha}_4 \ , & \alpha_8 &= -\alpha_3 \ , \\
\beta_1 &= \bar{\beta}_1 + i\bar{\beta}_2 , & \beta_5 &= \beta_2 \ , \\
\beta_2 &= \bar{\beta}_1 - i\bar{\beta}_2 , & \beta_6 &= \beta_1 \ , \\
\beta_3 &= \bar{\beta}_3 + i\bar{\beta}_4 , & \beta_7 &= \beta_4 \ , \\
\beta_4 &= \bar{\beta}_3 - i\bar{\beta}_4 , & \beta_8 &= \beta_3 \ .
\end{aligned}\right\} \tag{3.8}$$

Since the displacements are real functions, the final form of $u_n$, $v_n$ and $w_n$ must also be real. The final expressions may be written as

$$\begin{Bmatrix} U \\ W \\ V \end{Bmatrix} = [T]\ [R]\ \{C\}, \tag{3.9}$$

where the matrices [T] and [R] are shown in Appendix B and

$$\{C\} = \begin{Bmatrix} \bar{C}_1 \\ \vdots \\ \bar{C}_8 \end{Bmatrix} \tag{3.10}$$

is a set of constants [the $\bar{C}_j$ being linear combinations of the $C_j$, (6)]. The $\bar{C}_j$ are the only free constants in our problem and must be determined from eight boundary conditions, four at each edge of constant x.

We are now in a position to specify the displacement functions. At each node (figure 2), the axial, circumferential and radial displacements, as well as a rotation will be prescribed. The 'displacement' of node i can thus be defined by the vector

$$\{\delta_i\} = \begin{Bmatrix} u_{n_i} \\ w_{n_i} \\ (dw_n/dx)_i \\ v_{n_i} \end{Bmatrix},$$

where all these components represent amplitudes of U,V,W and dW/dx associated with the $n^{th}$ circumferential wave-number. The element, having two nodes and eight nodal degrees of freedom, will have nodal displacements

$$\begin{Bmatrix} \delta_i \\ \delta_j \end{Bmatrix} = \begin{Bmatrix} u_{n_i} \\ w_{n_i} \\ (dw_n/dx)_i \\ v_{n_i} \\ u_{n_j} \\ w_{n_j} \\ (dw_n/dx)_j \\ v_{n_j} \end{Bmatrix} = [A]\{C\} , \tag{3.11}$$

where [A] is given in Appendix B, the terms of [A] being obtainable from the terms of [R]. Now pre-multiplying by $[A]^{-1}$, we obtain

$$\{C\} = [A]^{-1}\begin{Bmatrix} \delta_i \\ \delta_j \end{Bmatrix} , \tag{3.12}$$

and substituting into (3.9) we obtain

$$\begin{Bmatrix} U \\ W \\ V \end{Bmatrix} = [T][R][A]^{-1}\begin{Bmatrix} \delta_i \\ \delta_j \end{Bmatrix} = [N]\begin{Bmatrix} \delta_i \\ \delta_j \end{Bmatrix} . \tag{3.13}$$

This equation defines the displacement functions.

In Chapter VIII, rigid-body motions are considered, with the aim of testing whether the displacement functions selected above satisfy the convergence criteria of the finite-element method. It is shown that they do.

# CHAPTER IV

## MATRIX FORMULATION

In this section, expressions for the strain, elasticity, mass, stiffness and stress-resultant matrices are obtained, and the method for constructing the equivalent global matrices is given. Also a method of solving problems of cylindrical shells subjected to static loads is mentioned.

### 4.1 Strain Matrix

The strain vector may be found by using equations (2.2), (A.7) and (3.12), i.e.

$$\{\epsilon\} = \begin{Bmatrix} \epsilon_x \\ \epsilon_\varphi \\ 2\epsilon_{x\varphi} \\ \kappa_x \\ \kappa_\varphi \\ 2\bar{\kappa}_{x\varphi} \end{Bmatrix} = \begin{bmatrix} [T] & [0] \\ [0] & [T] \end{bmatrix} [Q] [A]^{-1} \begin{Bmatrix} \delta_i \\ \delta_j \end{Bmatrix} = [B] \begin{Bmatrix} \delta_i \\ \delta_j \end{Bmatrix} \quad , \qquad (4.1)$$

where the matrices [T], [A] and [Q] are given in Appendix B.

### 4.2 Elasticity Matrix

Similarly, the stress-resultant matrix may be found from equations (2.3), (A.8) and (4.1), i.e.

$$\{\sigma\} = \begin{Bmatrix} N_x \\ N_\varphi \\ \bar{N}_{x\varphi} \\ M_x \\ M_\varphi \\ \bar{M}_{x\varphi} \end{Bmatrix} = [P]\{\epsilon\} = [P][B] \begin{Bmatrix} \delta_i \\ \delta_j \end{Bmatrix} = [ST] \begin{Bmatrix} \delta_i \\ \delta_j \end{Bmatrix} \quad , \qquad (4.2)$$

where [P], the elasticity matrix, is given by

$$[P] = \begin{bmatrix} D & \nu D & 0 & 0 & 0 & 0 \\ \nu D & D & 0 & 0 & 0 & 0 \\ 0 & 0 & \frac{D(1-\nu)}{2} & 0 & 0 & 0 \\ 0 & 0 & 0 & K & \nu K & 0 \\ 0 & 0 & 0 & \nu K & K & 0 \\ 0 & 0 & 0 & 0 & 0 & \frac{K(1-\nu)}{2} \end{bmatrix} , \qquad (4.3)$$

D and K being given by (A.9) for an isotropic elastic material. We note, however, that [P] can be quite general, so that the theory may also apply to anisotropic shells provided their characteristics are known.

## 4.3 Stiffness and Mass Matrices

The stiffness and mass matrices may now be expressed as in (2.5) and (2.6)

$$[k] = \iint [B]^T [P][B]\, dA ,$$

$$[m] = \rho t \iint [N]^T [N]\, dA , \qquad (4.4)$$

where $dA = r\,d\varphi\,dx$.

Here [N], [B] and [P] are defined in (3.13), (4.1) and (4.3). Using these equations in (4.4) and integrating over $\varphi$ we obtain

$$[k] = \left[[A]^{-1}\right]^T \left[\pi r \int_0^{\ell} [Q]^T [P][Q]\, dx\right] [A]^{-1} = \left[[A]^{-1}\right]^T [G]\, [A]^{-1} , \qquad (4.5)$$

$$[m] = \rho t \left[[A]^{-1}\right]^T \left[\pi r \int_0^{\ell} [R]^T [R]\, dx\right] [A]^{-1} = \rho t \left[[A]^{-1}\right]^T [S]\, [A]^{-1} , \qquad (4.6)$$

where [G] and [S] are defined by the above equations.

4.3.1 Determination of the terms of [G] and [S]

Before integrating over x in equations (4.5) and (4.6), it was found advantageous to express [Q] and [R] as follows:

$$[Q]=[\Gamma][Z] \quad , \quad [R]=[\Delta][Z] \, , \tag{4.7}$$

where [Γ] and [Δ] are given in Appendix B and their elements are constants; the elements of [Z], which is also given in Appendix B, are functions of x.

Substituting [Q] and [R] into (4.5) and (4.6) we obtain for [G] and [S]

$$[G] = \pi r \int_0^{\ell} [Z]^T [\Gamma]^T [P][\Gamma][Z] \, dx = \pi r \int_0^{\ell} [Z]^T [Y][Z] \, dx = \pi r \int_0^{\ell} [ZY] \, dx \, , \tag{4.8}$$

$$[S] = \pi r \int_0^{\ell} [Z]^T [\Delta]^T [\Delta][Z] \, dx = \pi r \int_0^{\ell} [Z]^T [RJ][Z] \, dx = \pi r \int_0^{\ell} [ZJ] \, dx \, , \tag{4.9}$$

the advantage in introducing [Γ], [Δ] and [Z] via (4.7) becoming obvious upon realizing that $[Y] = [\Gamma]^T [P] \; [\Gamma]$ and $[RJ] = [\Delta]^T [\Delta]$ are constant matrices. [ZY] and [ZJ] are given in Appendix B.

We now proceed to obtain [G] and [S]. We may write the general term of [G] as follows:

$$
\left.\begin{aligned}
G(i,j) = \pi r \Big\{ &\int_0^{\ell} D_1(i,j)\, e^{A_1(i,j)x} \cos[B_1(i,j)x] \cos[C_1(i,j)x]\, dx \\
&+ \int_0^{\ell} D_2(i,j)\, e^{A_1(i,j)x} \sin[B_1(i,j)x] \cos[C_1(i,j)x]\, dx \\
&+ \int_0^{\ell} D_3(i,j)\, e^{A_1(i,j)x} \cos[B_1(i,j)x] \sin[C_1(i,j)x]\, dx \\
&+ \int_0^{\ell} D_4(i,j)\, e^{A_1(i,j)x} \sin[B_1(i,j)x] \sin[C_1(i,j)x]\, dx \Big\} ,
\end{aligned}\right\} \tag{4.10}
$$

which apply to all i, j = 1, 2, ····, 8, except for the following elements:

G(1,5), G(1,6), G(2,5), G(2,6), G(3,7), G(3,8), G(4,7), G(4,8), G(5,1), G(6,1), G(5,2), G(6,2), G(7,3), G(8,3), G(7,4), G(8,4),

which can be written as follows:

$$
\begin{aligned}
G(i,j) = \pi r \Big\{ &\int_0^{\ell} D_1(i,j) \cos^2[B_1(i,j)x]\, dx \\
&+ \int_0^{\ell} [D_2(i,j) + D_3(i,j)] \sin[B_1(i,j)x] \cos[B_1(i,j)x]\, dx \\
&+ \int_0^{\ell} D_4(i,j) \sin^2[B_1(i,j)x]\, dx .
\end{aligned} \tag{4.11}
$$

The matrices $[A_1]$, $[B_1]$, $[C_1]$, $[D_1]$, $[D_2]$, $[D_3]$, $[D_4]$ are given in Appendix B. Now, integrating over x, we obtain equations (4.12a) and (4.12b), where the indices (i,j) have been omitted from elements $A_1(i,j)$, $B_1(i,j)$, etc., for simplicity.

The $(i,j)^{th}$ term of [G] is given by

$$\frac{2}{\pi r}G(i,j) = \left. e^{A_1\ell}\left\{ \frac{[(D_1-D_4)A_1-(D_2+D_3)(B_1+C_1)]\cos[(B_1+C_1)\ell]}{[A_1^2+(B_1+C_1)^2]} + \frac{[(D_1-D_4)(B_1+C_1)+(D_2+D_3)A_1]\sin[(B_1+C_1)\ell]}{[A_1^2+(B_1+C_1)^2]} + \frac{[(D_1+D_4)A_1-(D_2-D_3)(B_1-C_1)]\cos[(B_1-C_1)\ell]}{[A_1^2+(B_1-C_1)^2]} + \frac{[(D_1+D_4)(B_1-C_1)+(D_2-D_3)A_1]\sin[(B_1-C_1)\ell]}{[A_1^2+(B_1-C_1)^2]} \right\} + \frac{(B_1+C_1)(D_2+D_3)-A_1(D_1-D_4)}{[A_1^2+(B_1+C_1)^2]} + \frac{(B_1-C_1)(D_2-D_3)-A_1(D_1+D_4)}{[A_1^2+(B_1-C_1)^2]}, \right\} \tag{4.12a}$$

for all i, j = 1, 2, $\cdots$, 8, except for the following elements:

G(1,5), G(1,6), G(2,5), G(2,6), G(3,7), G(3,8), G(4,7), G(4,8), G(5,1), G(6,1), G(5,2), G(6,2), G(7,3), G(8,3), G(7,4), G(8,4),

which can be written as follows:

$$G(i,j) = \frac{\pi r}{2}\left[\frac{(D_1-D_4)\sin(2B_1\ell) + 2(D_2+D_3)\sin^2(B_1\ell)}{2B_1} + (D_1+D_4)\ell\right] . \tag{4.12b}$$

Similarly, after integrating the general term of matrix [ZJ], we obtain the general term of matrix [S], as follows:

$$
\left.
\begin{aligned}
\frac{2}{\pi r} S(i,j) = e^{A_1 \ell} \Bigg\{ & \frac{[(E_1-E_4)A_1 - (E_2+E_3)(B_1+C_1)] \cos[(B_1+C_1)\ell]}{[A_1^2 + (B_1+C_1)^2]} \\
& + \frac{[(E_1-E_4)(B_1+C_1) + (E_2+E_3)A_1] \sin[(B_1+C_1)\ell]}{[A_1^2 + (B_1+C_1)^2]} \\
& + \frac{[(E_1+E_4)A_1 - (E_2-E_3)(B_1-C_1)] \cos[(B_1-C_1)\ell]}{[A_1^2 + (B_1-C_1)^2]} \\
& + \frac{[(E_1+E_4)(B_1-C_1) + (E_2-E_3)A_1] \sin[(B_1-C_1)\ell]}{[A_1^2 + (B_1-C_1)^2]} \Bigg\} \\
+ \frac{(B_1+C_1)(E_2+E_3) - A_1(E_1-E_4)}{[A_1^2 + (B_1+C_1)^2]} & + \frac{(B_1-C_1)(E_2-E_3) - A_1(E_1+E_4)}{[A_1^2 + (B_1-C_1)^2]},
\end{aligned}
\right\} \qquad (4.13\text{a})
$$

for all i, j = 1, 2, $\cdots$, 8, except for the following elements:

S(1,5), S(1,6), S(2,5), S(2,6), S(3,7), S(3,8), S(4,7), S(4,8), S(5,1), S(6,1), S(5,2), S(6,2), S(7,3), S(8,3), S(7,4), S(8,4),

which can be written as follows:

$$
S(i,j) = \frac{\pi r}{2} \left[ \frac{(E_1-E_4)\sin(2B_1\ell) + 2(E_2+E_3)\sin^2(B_1\ell)}{2B_1} + (E_1+E_4)\ell \right]. \qquad (4.13\text{b})
$$

Here again, $E_1$, $E_2$, $E_3$, $E_4$, $B_1$ and $C_1$, in (4.13a) and (4.13b), represent the $(i,j)^{th}$ elements of the corresponding matrices given in Appendix B.

## 4.4 The Stress-Resultant Matrix

Finally, the stress-resultant matrix for the stress resultants at node i (x = 0; see figure 2) may be obtained from equation (4.2), such that

$$\{\sigma_i\} = \begin{bmatrix} [T] & [0] \\ [0] & [T] \end{bmatrix} [P][Q_i][A]^{-1} \begin{Bmatrix} \delta_i \\ \delta_j \end{Bmatrix} \tag{4.14a}$$

where $[Q_i]$ is obtained from $[Q]$ by putting $x = 0$. Similarly the stress-resultant matrix of node j $(x = \ell)$ is given by

$$\{\sigma_j\} = \begin{bmatrix} [T] & [0] \\ [0] & [T] \end{bmatrix} [P][Q_j][A]^{-1} \begin{Bmatrix} \delta_i \\ \delta_j \end{Bmatrix}. \tag{4.14b}$$

The corresponding stress-resultant matrix for both nodes of the finite element is given by

$$\begin{Bmatrix} \sigma_i \\ \sigma_j \end{Bmatrix} = \begin{bmatrix} \begin{matrix} [T] & [0] \\ [0] & [T] \end{matrix} & \begin{bmatrix} 0 \end{bmatrix} \\ \begin{bmatrix} 0 \end{bmatrix} & \begin{matrix} [T] & [0] \\ [0] & [T] \end{matrix} \end{bmatrix} \begin{bmatrix} [P][Q_i][A]^{-1} \\ [P][Q_j][A]^{-1} \end{bmatrix} \begin{Bmatrix} \delta_i \\ \delta_j \end{Bmatrix} = [ST] \begin{Bmatrix} \delta_i \\ \delta_j \end{Bmatrix}, \tag{4.15}$$

where $[A]$, $[Q_i]$ and $[Q_j]$ are given in Appendix B.

## 4.5 The Stiffness and Mass Matrices for the Whole Shell

As previously mentioned, the complete shell is divided into finite elements each of which is a cylindrical frustum (figure 3). The position of the nodal points (nodal circles) may be chosen arbitrarily.

The vectors $\{F_i\}$, $\{F_j\}$ represent the internal forces acting at nodes i and j, respectively, and $\{\delta_i\}$, $\{\delta_j\}$ are the corresponding displacements. As the shell is continuous, the sum of forces and moments at a particular node must be equal to the external forces and moments applied at the node. Thus

$$\{F\}^e = \{F_j\} + \{F_{i+1}\} ;$$

moreover, the displacements must be continuous, and

$$\{\delta_j\} = \{\delta_{i+1}\} .$$

These relationships allow us to superimpose the mass and stiffness matrices of individual finite elements, to obtain the global mass and stiffness matrices [M] and [K] for the whole shell. This is shown diagrammatically in figure 3. [K] and [M] will be square matrices of order 4(N+1), where N is the number of finite elements.

## 4.6 Analysis of Shells Subjected to Static Loads

We are now in a position to solve problems of cylindrical shells subjected to static loads. The dynamical problem will be discussed in Chapter V.

From equation (2.4) we see that for static loads we can write

$$[K]\ \{\delta\} = \{F\}^e \tag{4.16}$$

where [K] is the global stiffness matrix, $\{\delta\}$ the vector of all nodal displacements, and $\{F\}^e$ the nodal load vector. We may partition (4.16) as follows:

$$\begin{bmatrix} K_{11} & \vdots & K_{12} \\ \hdashline K_{21} & \vdots & K_{22} \end{bmatrix} \begin{Bmatrix} \delta_1 \\ \hdashline \delta_2 \end{Bmatrix} = \begin{Bmatrix} F_1 \\ \hdashline F_2 \end{Bmatrix} \tag{4.17}$$

where $\{F_1\}$ represents the loads applied to the shell and $\{F_2\}$ are unknown reactions at points where the displacements are specified, and $\{\delta_1\}$ and $\{\delta_2\}$ are the unknown and specified displacements, respectively.

Equation (4.17) may be solved to give

$$\begin{aligned} \{\delta_1\} &= [K_{11}]^{-1}\left(\{F_1\} - [K_{12}]\{\delta_2\}\right), \\ \{F_2\} &= [K_{21}]\{\delta_1\} + [K_{22}]\{\delta_2\}. \end{aligned} \tag{4.18}$$

Finally, the stresses can then be found from the displacements by a relationship of the type

$$\{\sigma\} = [ST]\{\delta_1\}\ , \tag{4.19}$$

where [ST] is given by equation (4.15).

# CHAPTER V

## FREE VIBRATION AND RESPONSE TO RANDOM PRESSURE FIELD

### 5.1 Introduction

Vibrations of shells in which the wall motions are predominantly radial, such that flexure and stretching of the wall occur while the longitudinal axis of the shell remains straight, are often referred to as "breathing vibrations". For the purposes of this thesis, the term "breathing vibration" will include shell modes for various combinations of the circumferential wave-number, n, and number of axial half-waves, m; however, the rotationally symmetric modes, where n = 0, are excluded. This type of vibration is very important in shell structures where the walls are thin compared to other dimensions.

The differential equations of motion for a system in which viscous damping is present are given by

$$[M]\{\ddot{y}\} + [C]\{\dot{y}\} + [K]\{y\} = \{F(x,\varphi,t)\} \quad , \tag{5.1}$$

where $\{y(x,\varphi,t)\}$ is the displacement vector, $\{F(x,\varphi,t)\}$ is a vector of external forces; [M], [C] and [K] are the mass, damping and stiffness matrices, respectively. The study of vibration of non-uniform thin cylindrical shells, subjected to a random pressure field, was divided into two parts, namely free vibration and response, following the normal procedure for the study of dynamical problems. Sections 5.4 et seq. all deal with the response aspect of the problem.

## 5.2 Free, Breathing Vibration

If no external forces are operative, the equations of motion (5.1) may be written in the form

$$[M]\begin{Bmatrix} \ddot{\delta}_1 \\ \vdots \\ \ddot{\delta}_{N+1} \end{Bmatrix} + [K]\begin{Bmatrix} \delta_1 \\ \vdots \\ \delta_{N+1} \end{Bmatrix} = \{0\}\,, \qquad (5.2)$$

where N is the total number of finite elements (see figure 3), [M] and [K] are real, symmetric matrices of order $4(N+1) \times 4(N+1)$; the nodal displacement vectors $\{\delta_i\}$ are of the form

$$\{\delta_i\} = \begin{Bmatrix} u_{ni} \\ w_{ni} \\ (dw_n/dx)_i \\ v_{ni} \end{Bmatrix} \qquad (5.3)$$

where $u_{ni}$, $w_{ni}$, and $v_{ni}$ are respectively, the axial, radial and circumferential displacement amplitudes associated with the $n^{th}$ circumferential wave-number at node i.

Introducing now

$$\begin{Bmatrix} \delta_1 \\ \vdots \\ \delta_{N+1} \end{Bmatrix} = \begin{Bmatrix} \delta_{10} \\ \vdots \\ \delta_{(N+1)_0} \end{Bmatrix} \quad \sin(\Omega_i t + \Theta)$$

and substituting into (5.1) we obtain

$$([K] - \Omega_i^2 [M]) \begin{Bmatrix} \delta_{10} \\ \vdots \\ \delta_{(N+1)_0} \end{Bmatrix}_i = \{0\}, \tag{5.4}$$

which leads to the standard eigenvalue problem. Here $\Omega_i$ is the $i^{th}$ natural frequency. [K] and [M] being of $4(N+1)^{th}$ order, we shall obtain 4(N+1) natural frequencies, each of which will be associated with a particular eigenvector $\begin{Bmatrix} \delta_{10} \\ \vdots \\ \delta_{(N+1)_0} \end{Bmatrix}_i$, also called a modal column of the system. The matrix

$$[\Phi] = \left[ \begin{Bmatrix} \delta_{10} \\ \vdots \\ \delta_{(N+1)_0} \end{Bmatrix}_1 \cdots \begin{Bmatrix} \delta_{10} \\ \vdots \\ \delta_{(N+1)_0} \end{Bmatrix}_i \cdots \begin{Bmatrix} \delta_{10} \\ \vdots \\ \delta_{(N+1)_0} \end{Bmatrix}_{4(N+1)} \right] \tag{5.5}$$

is called the modal matrix of the system.

Of course, before the eigenvalues and eigenvectors of a particular shell can be computed, the boundary conditions must be specified and taken into account. This aspect of the problem, as well as a fairly detailed description of the computational method employed, will be discussed in Chapter VII.

## 5.3 Free Vibration of a Liquid-Filled Cylindrical Shell

The previous section dealt, strictly speaking, with vibration of shells in vacuo. We can usually assume that the effect of the surrounding fluid (normally air at normal pressures) on vibration is negligible. This is not the case, however, if the shell contains, or for that matter is immersed in, a fluid of considerable density.

We shall now consider cylindrical shells either partially or completely filled with stationary liquid. In cases where the shell is partially filled, it is assumed that it is vertical so that there is a horizontal free surface. Free surface effects are neglected. This may be justified as follows: the natural frequencies of the empty shells in the modes under consideration are likely to be high (certainly in the $10^2$ Hz region); on the other hand, the natural frequencies of free surface phenomena are likely to be low, at least in the lowest modes; moreover, the amplitudes associated with the higher free-surface modes may be expected to be small because of dissipation. Accordingly, it may be concluded that coupling between the shell modes under consideration and the free-surface resonances would normally be weak and hence negligible. Actually, as Lindholm et al. (36) have found experimentally, there is a possibility of nonlinear coupling between the free-surface motion and that of the shell, resulting in subharmonic excitation of the free surface at low frequencies, while the shell itself is vibrating at high frequency. This phenomenon, however, is incompletely understood and it will not be attempted to take it into account here.

It is also assumed that the effect of the internal static pressure is small and may be neglected. This means that (a) in the case of completely filled shells we shall not consider pressurized shells, and (b) in the case of partially filled shells, which must be vertical, we shall not consider very long shells. However, static pressure effects can be taken into account, by slightly extending the present theory, essentially by taking into account the initial strain energy induced by the gravity potential. Finally, it is assumed that the contained liquid is incompressible. Here again compressibility could have been taken into account, as was done by Niordson (33) for instance. However, Niordson found that for water-filled shells the effect of compressibility is negligible.

Having made these assumptions, it is clear that the only effect the fluid will have on motions of the shell will be that of inertial hydrodynamic loading. The dynamical effect of the contained fluid can be taken into account by taking into consideration the apparent, or virtual, mass of the fluid, which is added to the mass of the shell itself (33). For beam vibration the apparent mass of the fluid is simply the mass of the enclosed fluid, at least at low frequencies, as no deformation of the cross-section is involved. For shell vibrations, on the other hand, the situation is not so simple, and it is found that the apparent mass is a function of frequency. In order to determine the apparent mass of the fluid in such cases the fluid mechanics of the enclosed fluid must be studied.

Fung et al. (37) and Berry and Reissner (32) studied the effect of pressurization on cylindrical shells containing compressible fluid, using the wave equation to describe the motion of the contained fluid. For small motions, they obtained the following expressions for the fluid apparent mass:

$$m_F = \rho_F r \left[ \frac{I_m\left(\sqrt{\lambda_1^2 - k_c^2}\right)}{\sqrt{\lambda_1^2 - k_c^2} \cdot I_m'\left(\sqrt{\lambda_1^2 - k_c^2}\right)} \right] \quad \text{for } k_c < \lambda_1 ,$$

and (5.6)

$$m_F = \rho_F r \left[ \frac{J_m\left(\sqrt{k_c^2 - \lambda_1^2}\right)}{\sqrt{k_c^2 - \lambda_1^2} \cdot J_m'\left(\sqrt{k_c^2 - \lambda_1^2}\right)} \right] \quad \text{for } k_c > \lambda_1 ,$$

where $\rho_F$ is the fluid density, $\lambda_1 = \pi r/\ell$, $k_c = \Omega_i r/c_o$, $c_o$ being the velocity of sound in the fluid and $J_n$ and $I_n$ are the ordinary and modified $n^{th}$ order Bessel functions, respectively.

On the other hand, Lindholm et al. (36) developed a frequency equation for completely liquid-filled cylindrical shells. Incompressible fluid theory was used and Laplace's equation was utilized to describe the motion of the fluid. The liquid apparent mass per unit area in this case is

$$m_F = r\rho_F \left[ I_n(\lambda_m) / \lambda_m I_n'(\lambda_m) \right] , \tag{5.7}$$

where $\lambda_m = m\pi r/\ell$ .

It is noted that this expression is the same as equation (5.6) when $k_c \to 0$ or when $c_o \to \infty$. Here we shall use $m_F$ as given by (5.7), as we are only concerned with incompressible fluids.

In the present theory, as the only effect of the enclosed liquid to be taken into account is that of inertial hydrodynamic loading, the analysis of liquid-filled shells is particularly simple. Thus, for a partially-filled shell, the shell is first subdivided into two: one part is empty and the other liquid-filled; then in the formulation of the mass matrix, the mass per unit area of the elements in the empty shell is $\rho t$ (see equation (4.6)), while that of the filled-shell finite elements is $(\rho t + m_F)$, where $m_F$ is given by equation (5.7).

5.4 Response to Random Pressure Field

The external forces $\{F\}$ of equation (5.1) may be harmonic, periodic, aperiodic or random. In this thesis we shall only concern ourselves with the last eventuality: the vector $\{F\}$ is considered to represent nonperiodic, random forces. Moreover, we shall assume that these forces are due to pressure fluctuations so that they are normal to the surface of the cylinder. A method of solution for such (vibration) problems is developed in this section.

It is important, at first, to emphasize that while the pressure field varies from point to point at any instant, its variation at any given point fluctuates irregularly with time, and the frequency spectrum results in many modes of vibration being excited with a statistical dependence between them. However, the forced vibration can be represented by synthesis of the natural modes; this assumption is generally permissible only for such structures where nonlinearities can be ignored.

After solving the usual equations of motion for an uncoupled mode, a generalization is made by putting the solution in the form of spectra. The cross-correlation spectral density of displacements at some point in the structure, can then be determined in terms of the cross-correlation spectral density of the pressure perturbations. This allows the r.m.s. value of the displacements to be determined.

We restrict ourselves to weak stationary random processes. Weak stationarity implies that the expected value and the covariance of $F(t+\tau)$ in the sample space are identical with those of $F(t)$ independently of $\tau$. It is also assumed that the random process has a weak ergodic property. This means that a statistical average of $F(t)$, or any function of $F(t)$, over the sample space, can be replaced by a "long" time average over a single sample function $F(t)$. Finally, it is assumed that the variables have a Gaussian (normal) probability distribution.

Before we can proceed with the evaluation of the response, we must first decouple the equations of motion .

## 5.5 Decoupling of the Differential Equations of Motion

Any arbitrary motion $\{y\}$ can be expressed by superposition of all of the normal modes taken in appropriate proportions. Therefore

$$\left\{y(x,\varphi,t)\right\} = \left[\left\{\Phi_t\right\}_1, \left\{\Phi_t\right\}_2, \cdots, \left\{\Phi_t\right\}_A\right] \left\{Z(t)\right\} \equiv \left[\Phi\right]\left\{Z(t)\right\} , \quad (5.8)$$

where $\{Z(t)\}$ represents the normal coordinates, and $[\Phi]$ is the modal matrix in which each column is a modal column of the system. Substituting equations (5.8) into (5.1) and premultiplying by the transpose of [$\Phi$], equation (5.1) becomes

$$[\Phi]^T[M][\Phi]\{\ddot{z}\} + [\Phi]^T[C][\Phi]\{\dot{z}\} + [\Phi]^T[K][\Phi]\{z\} = [\Phi]^T\{F\} \quad . \tag{5.9}$$

Due to the orthogonality of the normal modes, products such as

$$\{\Phi\}_r^T[M]\{\Phi\}_s = 0 \qquad \text{for } r \neq s . \tag{5.10}$$

Furthermore, it is always possible to normalize the modes such that

$$\{\Phi\}_r^T[M]\{\Phi\}_s = M_i \quad \text{when } r = s = i . \tag{5.11}$$

A similar result is valid for the matrix [K]. It follows, therefore, that

$$\begin{aligned} [\Phi]^T[M][\Phi] &= [\,^\diagdown M_r{}_\diagdown] , \\ [\Phi]^T[K][\Phi] &= [\,^\diagdown \Omega_r^2{}_\diagdown][\,^\diagdown M_r{}_\diagdown] = [\,^\diagdown K_r{}_\diagdown] , \end{aligned} \tag{5.12}$$

where [$^\diagdown M_r{}_\diagdown$] and [$^\diagdown K_r{}_\diagdown$] are diagonal matrices. Comparing now the triple matrix product $[\phi]^T[C]\,[\phi]$ with equation (5.12), it becomes apparent that this triple product will result in a diagonal matrix only when the damping matrix [C] is proportional to either [M] or [K], or to a linear combination of the two. If [C] is taken to be proportional to [M] and [K], then,

$$[\Phi]^T [C] [\Phi] = \lceil C_r \rfloor = 2. \lceil \Omega_r \zeta_r \rfloor \lceil M_r \rfloor , \tag{5.13}$$

where $\Omega_r$ is the $r^{th}$ natural frequency, $\zeta_r$ is the generalized damping factor and $\lceil C_r \rfloor$ is the diagonal viscous damping matrix in which a typical element can be written as

$$C_r = 2 . \zeta_r \sqrt{K_r M_r} \quad . \tag{5.14}$$

Substitution of relations (5.12) and (5.13) in equation (5.9) results in a set of 4(N+1)-J decoupled differential equations of motion

$$\lceil M_r \rfloor \{\ddot{Z}\} + 2. \lceil \Omega_r \zeta_r \rfloor \lceil M_r \rfloor \{\dot{Z}\} + \lceil \Omega_r^2 \rfloor \lceil M_r \rfloor \{Z\} = [\Phi]^T \{F\} \tag{5.15}$$

where N is the number of finite elements and J is the number of constraint equations imposed (see Chapter VII). The $r^{th}$ equation of (5.15) has the form

$$\ddot{Z}_r + 2 \zeta_r \Omega_r \dot{Z}_r + \Omega_r^2 Z_r = \frac{1}{M_r} \{\Phi\}_r^T \{F\} \quad . \tag{5.16}$$

From equation (5.8), the response $y_t(x,\varphi,t)$ of point t, defined by the coordinates $(x,\varphi)$ at time t, can be expressed in terms of the normal modes $\Phi_r(x,\varphi)$ and normal coordinates $Z_r(t)$ such that

$$y_t(x,\varphi,t) = \sum_{r=1}^{4(N+1)-J} \Phi_{tr}(x,\varphi)\, Z_r(t) \,. \qquad (5.17)$$

## 5.6 Representation of Continuous Random Pressure Field at the Nodal Points

It is well known that a set of forces on a rigid body may be represented by another set of forces acting at a different point, along with appropriate couples. The continuous random pressure field of the deformable body will be approximated here by a finite set of discrete forces and moments acting at the nodal points (60).

As previously mentioned in Chapter IV, the complete shell is divided into N finite elements each of which is a cylindrical frustum. The position of the (N+1) nodal points may be chosen arbitrarily (figure 3).

Any pressure field is considered to be acting on an area $S_e$ surrounding the node e of coordinate $\ell_N^e$ as shown in figure 7a. This area $S_e$ is limited by the positions $\ell_e$ and $\ell_e'$ with respect to the origin in the x direction. It is therefore possible to approximate the pressure distribution acting over the area $S_e$ by two mutually perpendicular forces per unit length. These forces $f_R(x,t)$

and $f_C(x,t)$ , at time t, are at distance $x_o$ from the origin of the shell as shown in figure 7a; and these values are simply

$$f_R(x,t) = r\int_0^{2\pi} p(x,\varphi,t)\cos(\varphi)\,d\varphi, \tag{5.18}$$

$$f_C(x,t) = r\int_0^{2\pi} p(x,\varphi,t)\sin(\varphi)\,d\varphi, \tag{5.19}$$

where $p(x,\varphi,t)$ is the instantaneous pressure on the surface.

These two forces, $f_R$ and $f_C$ , acting at point 'A' are transformed to two forces and one moment ($M_r$) acting at the node e as shown in figure 7b.

The external force vector at a typical node e can be written in the following form:

$$\left\{F(x,t)\right\}_e = \left\{\begin{array}{l} 0 \\ \int_{l'_i}^{l_i} f_R(x_i,t)\,dx_i \\ \int_{l'_j}^{l_j} (x_j - l_N^j)\, f_R(x_j,t)\,dx_j \\ \int_{l'_p}^{l_p} f_C(x_p,t)\,dx_p \end{array}\right\}_e, \tag{5.20}$$

where $l_i = l_j = l_p = l_e$ , $l'_i = l'_j = l'_p = l'_e$ and $l_N^e = l_N^j$ .

## 5.7 Fourier Transform Representation of Nonperiodic Forces

As previously mentioned, the vector $\{F(t)\}$ represents the nonperiodic forces due to the pressure fluctuations. This nonperiodic force can be treated as a periodic one having a period 2T of infinite duration $(T\to\infty)$. It follows then, that the nonperiodic force function can be synthesized from harmonic components whose frequencies form a continuous spectrum. This synthesis is accomplished by the use of the Fourier integral. It is known that in general we may write

$$F_j(t) = \frac{1}{2\pi}\int_{-\infty}^{\infty} S_{F_j}(\Omega)\, e^{i\Omega t}\, d\Omega \;, \qquad (5.21)$$

where $\Omega$ is the forced frequency in radians per second, and $S_{F_j}(\Omega)$, called the Fourier transform of $F_j(t)$, is given by

$$S_{F_j}(\Omega) = \int_{-\infty}^{\infty} F_j(t)\, e^{-i\Omega t}\, dt \;. \qquad (5.22)$$

## 5.8 Cross-correlation Spectral Density of Displacements in Terms of the Cross-Correlation Spectral Density of the Pressure Field

The excitation spatial correlation function is defined as

$$\Psi_{y_{ij}}(x,\varphi,\tau) = \overline{y_i(x,\varphi,t)\, y_j(x,\varphi,t+\tau)} \quad , \tag{5.23}$$

where $\tau$ is the time delay, and the barred quantity denotes a time average. The stationary random process being ergodic, we can write

$$\begin{aligned} \Psi_{y_{ij}}(x,\varphi,\tau) &= \overline{y_i(x,\varphi,t)\, y_j(x,\varphi,t+\tau)} \\ &= \lim_{T\to\infty} \frac{1}{2T}\int_{-T}^{T} y_i(x,\varphi,t)\, y_j(x,\varphi,t+\tau)\, dt \, , \end{aligned} \tag{5.24}$$

where 2T is the period.

By using the correlation theorem, we can also write

$$\Psi_{y_{ij}}(x,\varphi,\tau) = \lim_{T\to\infty} \frac{1}{4\pi T}\int_{-\infty}^{\infty} S^{*}_{y_i}(x,\varphi,\Omega,T)\, S_{y_j}(x,\varphi,\Omega,T)\, e^{i\Omega\tau}\, d\Omega \, , \tag{5.25}$$

where $S_{y_i}(x,\varphi,\Omega,T)$ , $S_{y_j}(x,\varphi,\Omega,T)$ are the finite Fourier transforms of $y_i(x,\varphi,t)$ and $y_j(x,\varphi,t)$ , respectively, such that $S_{y_i}(x,\varphi,\Omega,T) = \int_{-T}^{T} y_i(x,\varphi,t)\, e^{-i\Omega t}\, dt$ , and similarly for $S_{y_j}$; the asterisk denotes the complex conjugate. Now for $\tau = 0$ and i = j = t, equation (5.25) becomes

$$\Psi_{y_t}(x,\varphi,0) = \overline{y_t^2(x,\varphi,t)} = \lim_{T\to\infty} \frac{1}{4\pi T}\int_{-\infty}^{\infty} S_{y_t}^{*}(x,\varphi,\Omega,T)\, S_{y_t}(x,\varphi,\Omega,T)\, d\Omega . \tag{5.26}$$

Since $\frac{1}{2T} S_{y_t}^{*}(x,\varphi,\Omega,T)\, S_{y_t}(x,\varphi,\Omega,T)$ is an even function of $\Omega$, equation (5.26) can be written in the form

$$\Psi_{y_t}(x,\varphi,0) = \overline{y_t^2(x,\varphi,t)} = \lim_{T\to\infty} \frac{1}{2\pi T}\int_{0}^{\infty} S_{y_t}^{*}(x,\varphi,\Omega,T)\, S_{y_t}(x,\varphi,\Omega,T)\, d\Omega . \tag{5.27}$$

By taking the Fourier transform of equations (5.16) and (5.17), the following relation is obtained

$$S_{z_r}(\Omega,T) = \frac{e^{-i\theta_r}\, \{\Phi\}_r^{T} \{S_F(\Omega,T)\}}{\Omega_r^2 M_r \left[\left[1-\left(\frac{\Omega}{\Omega_r}\right)^2\right]^2 + \left(2\zeta_r \frac{\Omega}{\Omega_r}\right)^2\right]^{1/2}} , \tag{5.28}$$

where $\Omega_r$ is the $r^{th}$ natural frequency, $\Omega$ is the forced frequency, and $\Theta_r$ is the phase lag of the displacement relative to the driving force and is given by

$$\theta_r = \tan^{-1}\left(\frac{2\zeta_r \frac{\Omega}{\Omega_r}}{1-\left(\frac{\Omega}{\Omega_r}\right)^2}\right) .$$

Also

$$S_{y_t}(x,\varphi,\Omega,T) = \sum_{r=1}^{4(N+1)-J} \Phi_{tr}(x,\varphi)\, S_{z_r}(\Omega,T) \tag{5.29}$$

By introducing equations (5.28) and (5.29) in (5.27), we obtain

$$\begin{aligned} \Psi_{y_t}(x,\varphi,0) &= \overline{y_t^2(x,\varphi,t)} \\ &= \sum_{r=1}^{4(N+1)-J} \sum_{s=1}^{4(N+1)-J} \frac{\Phi_{tr}(x,\varphi)\,\Phi_{ts}(x,\varphi)}{\Omega_r^2\,\Omega_s^2\, M_r\, M_s} \,\cdot \\ &\quad \cdot \lim_{T\to\infty} \frac{1}{2\pi T} \int_0^\infty e^{i(\theta_s-\theta_r)} \cdot |H_r(\Omega)| \cdot |H_s(\Omega)| \cdot \{\Phi\}_r^T \cdot \{S_F(\Omega,T)\} \cdot \{\Phi\}_s^T \cdot \{S_F^*(\Omega,T)\} \cdot d\Omega, \end{aligned} \tag{5.30}$$

where

$$|H_r(\Omega)| = \left\{ \left[1 - \left(\frac{\Omega}{\Omega_r}\right)^2\right]^2 + \left(2\zeta_r \frac{\Omega}{\Omega_r}\right)^2 \right\}^{-1/2},$$

is the magnification factor. Figure 8 shows $|H_r(\Omega)|$ for a lightly damped multi-degree-of-freedom system. This magnification factor has regions of pronounced peaks in the neighbourhood of the corresponding natural frequencies $\Omega_r$. The products $|H_r(\Omega)||H_s(\Omega)|$ for $r \neq s$ are seen to be small in comparison with the same products for $r = s$. In addition, the terms in equation (5.30) with $r \neq s$ may be negative or positive depending upon the sign of the product

$\Phi_{tr}(x,\varphi)\ \Phi_{ts}(x,\varphi)$, while terms with r = s are always positive. Therefore, the contribution of cross-product terms ($r \neq s$) to the mean square response will always be small and can be ignored (38): equation (5.30) can then be written as

$$\Psi_y(x,\varphi,0) = \overline{y_t^2(x,\varphi,t)} = \sum_{r=1}^{4(N+1)-J} \frac{\Phi_{tr}^2(x,\varphi)}{\Omega_r^4\ M_r^2} \cdot \lim_{T\to\infty} \frac{1}{2\pi T}\int_0^\infty |H_r(\Omega)|^2 \cdot \{\Phi\}_r^T \cdot \{S_F(\Omega,T)\} \{\Phi\}_r^T \cdot \{S_F^*(\Omega,T)\}\, d\Omega . \tag{5.31}$$

The external force vector at each node is given by equation (5.20); the corresponding Fourier integral and its conjugate can be written as

$$\{S_F(\Omega,T)\} = \left\{ \begin{array}{c} 0 \\ \int_{l_i'}^{l_i} S_{f_R}(x_i,\Omega,T)\, dx_i \\ \int_{l_j'}^{l_j} (x_j - l_N^j)\, S_{f_R}(x_j,\Omega,T)\, dx_j \\ \int_{l_p'}^{l_p} S_{f_C}(x_p,\Omega,T)\, dx_p \end{array} \right\} , \tag{5.32}$$

$$\left\{ S_F^*(\Omega,T) \right\} = \left\{ \begin{matrix} 0 \\ \int_{\ell'_u}^{\ell_u} S_{f_R}^*(x_u,\Omega,T)\, dx_u \\ \int_{\ell'_k}^{\ell_k} (x_k - \ell_N^k)\, S_{f_R}^*(x_k,\Omega,T)\, dx_p \\ \int_{\ell'_v}^{\ell_v} S_{f_C}^*(x_v,\Omega,T)\, dx_v \end{matrix} \right\} \tag{5.32 cont'}$$

where the indices i and u represent the radial forces, and p and v the circumferential forces. The indices j and k correspond to the moments.

Substituting equation (5.32) into (5.31) and expanding, we obtain

$$\Psi_{y_t}(x,\varphi,0) = \overline{y_t^2(x,\varphi,t)} = \sum_{r=1}^{4(N+1)-J} \frac{\Phi_{tr}^2(x,\varphi)}{\Omega_r^4 M_r^2 2.\pi} \cdot \int_0^\infty \left| H_r(\Omega) \right|^2 \cdot$$

$$\cdot \left\{ \sum_{i=1}^{N+1} \sum_{u=1}^{N+1} \Phi_{ir} \Phi_{ur} \left| \int_{\ell'_i}^{\ell_i} \int_{\ell'_u}^{\ell_u} W_{f_R}(\Omega; x_i, x_u; 0)\, dx_i\, dx_u \right| \right.$$

$$+ \sum_{i=1}^{N+1} \sum_{k=1}^{N+1} \Phi_{ir} \Phi_{kr} \left| \int_{\ell'_i}^{\ell_i} \int_{\ell'_k}^{\ell_k} (x_k - \ell_N^k) W_{f_R}(\Omega; x_i, x_k; 0)\, dx_i\, dx_k \right|$$

$$+ \sum_{i=1}^{N+1} \sum_{v=1}^{N+1} \Phi_{ir} \Phi_{vr} \left| \int_{\ell'_i}^{\ell_i} \int_{\ell'_v}^{\ell_v} W_{f_{RC}}(\Omega; x_i, x_v; 0)\, dx_i\, dx_v \right| + \tag{5.33}$$

$$+\sum_{j=1}^{N+1}\sum_{u=1}^{N+1}\Phi_{jr}\Phi_{ur}\left|\int_{\ell'_j}^{\ell_j}\int_{\ell'_u}^{\ell_u}\left(x_j-\ell_N^j\right)W_{f_R}(\Omega;x_j,x_u;0)\,dx_j\,dx_u\right|$$

$$+\sum_{j=1}^{N+1}\sum_{k=1}^{N+1}\Phi_{jr}\Phi_{kr}\left|\int_{\ell'_j}^{\ell_j}\int_{\ell'_k}^{\ell_k}\left(x_j-\ell_N^j\right)\left(x_k-\ell_N^k\right)W_{f_R}(\Omega;x_j,x_k;0)\,dx_j\,dx_k\right|$$

$$+\sum_{j=1}^{N+1}\sum_{v=1}^{N+1}\Phi_{jr}\Phi_{vr}\left|\int_{\ell'_j}^{\ell_j}\int_{\ell'_v}^{\ell_v}\left(x_j-\ell_N^j\right)W_{f_{RC}}(\Omega;x_j,x_v;0)\,dx_j\,dx_v\right|$$

$$+\sum_{p=1}^{N+1}\sum_{u=1}^{N+1}\Phi_{pr}\Phi_{ur}\left|\int_{\ell'_p}^{\ell_p}\int_{\ell'_u}^{\ell_u}W_{f_{CR}}(\Omega;x_p,x_u;0)\,dx_p\,dx_u\right| \qquad \text{(5.33) cont'}$$

$$+\sum_{p=1}^{N+1}\sum_{k=1}^{N+1}\Phi_{pr}\Phi_{kr}\left|\int_{\ell'_p}^{\ell_p}\int_{\ell'_k}^{\ell_k}\left(x_k-\ell_N^k\right)W_{f_{CR}}(\Omega;x_k,x_p;0)\,dx_p\,dx_k\right|$$

$$+\sum_{p=1}^{N+1}\sum_{v=1}^{N+1}\Phi_{pr}\Phi_{vr}\left|\int_{\ell'_p}^{\ell_p}\int_{\ell'_v}^{\ell_v}W_{f_C}(\Omega;x_p,x_v;0)\,dx_p\,dx_v\right|\Bigg\}\,d\Omega,$$

where $W_f(\Omega; x, x'; 0) = \lim_{T\to\infty}\left[\frac{1}{T}S_f(x,\Omega,T)\,S_f^*(x',\Omega,T)\right]$ is the cross-correlation spectral density function of the force field '$f$'.

5.9 <u>Calculation of the Cross-Correlation Spectral Density $W_f(\Omega;x,x';0)$ of the Force Field 'f'.</u>

This quantity $W_f(\Omega;x,x';0)$ can be obtained electronically by multiplying $f(x,t)$ and $f(x',t)$ and passing it through a narrow-band filter whose central frequency is varied slowly through the desired frequency range. (Here $f(x,t)$ represents the force per unit length.) Then

$$\overline{f_{\Omega}(x,t)\, f_{\Omega}(x',t)} = W_f(\Omega;x,x';0), \tag{5.34}$$

where the quantity $\overline{f_{\Omega}f'_{\Omega}}$ denotes the mean per unit band-width.

The pressure field is assumed to be homogeneous, and hence the resultant force field will also be homogeneous. This assumption permits writing the cross-correlation spectral density of the force field as a function of the separation $(x-x')$ and the frequency $\Omega$; thus

$$W_f(\Omega;x,x';0) = W_f(\Omega;\xi;0), \tag{5.35}$$

where $\xi = |x-x'|$. Substituting equations (5.18) and (5.19) in (5.34), the mean-square values of the fluctuating radial and circumferential forces per unit band-width are

$$W_{f_R}(\Omega,\xi,0) = \overline{f_{R,\Omega}(x,t) \cdot f_{R,\Omega}(x',t)} \tag{5.36}$$
$$= r^2 \int_0^{2\pi}\int_0^{2\pi} \overline{p_\Omega(x,\varphi,t)\, p_\Omega(x',\varphi',t)} \cos(\ \varphi) \cdot \cos(\ \varphi')\, d\varphi\, d\varphi',$$

$$W_{f_C}(\Omega,\xi,0) = \overline{f_{C,\Omega}(x,t) \cdot f_{C,\Omega}(x',t)} \tag{5.37}$$
$$= r^2 \int_0^{2\pi}\int_0^{2\pi} \overline{p_\Omega(x,\varphi,t)\, p_\Omega(x',\varphi',t)} \sin(\ \varphi) \cdot \sin(\ \varphi')\, d\varphi\, d\varphi',$$

$$W_{f_{RC}}(\Omega,\xi,0) = \overline{f_{R,\Omega}(x,t)\, f_{C,\Omega}(x',t)} \tag{5.38}$$
$$= r^2 \int_0^{2\pi}\int_0^{2\pi} \overline{p_\Omega(x,\varphi,t)\, p_\Omega(x',\varphi',t)} \cos(\ \varphi) \cdot \sin(\ \varphi')\, d\varphi\, d\varphi',$$

$$W_{f_{CR}}(\Omega,\xi,0) = W_{f_{RC}}(\Omega,\xi,0) \, . \tag{5.39}$$

### 5.9.1 Calculation of $\overline{p_\Omega(x,\varphi,t) \cdot p_\Omega(x',\varphi',t)}$

The normalized space-time correlation function of the fluctuating pressure is defined as

$$\Psi_p(\xi,\eta,\tau) = \frac{\overline{p(x,\varphi,t)\, p(x+\xi,\varphi+\eta,t+\tau)}}{\overline{p^2(x,\varphi,t)}}, \tag{5.40}$$

where $\xi = |x-x'|$, $\eta = |(\varphi-\varphi')r|$, $\tau$ is the time delay and $\overline{p^2(x,\varphi,t)}$ is the mean square of pressure fluctuations. The spatial correlation function in the frequency domain, for $\tau = 0$, becomes

$$\Psi_{p,\Omega,Re}(\xi,\eta,0) = \frac{\overline{p_{\Omega,Re}(x,\varphi,t)\cdot p_{\Omega,Re}(x+\xi,\varphi+\eta,t)}}{\overline{p^2(\Omega,Re)}} \, , \tag{5.41}$$

where the subscript $\Omega$ represents the geometric mean centre-frequency of the octave band (forced frequency, rad/sec), $\overline{p^2(\Omega,Re)}$ is the mean-square pressure per unit band-width, and the subscript Re indicates the Reynolds number for a given measurement. The longitudinal and lateral spatial correlation functions are particular cases of the space-time correlation function $\Psi_{p,\Omega,Re}(\xi,\eta,0)$ and are given respectively by $\Psi_{p,\Omega,Re}(\xi,0,0)$ and $\Psi_{p,\Omega,Re}(0,\eta,0)$. Assuming that

$$\Psi_{p,\Omega,Re}(\xi,\eta,0) = \Psi_{p,\Omega,Re}(\xi,0,0)\cdot\Psi_{p,\Omega,Re}(0,\eta,0) \, , \tag{5.42}$$

and substituting equation (5.42) into (5.41) we obtain

$$\overline{p_{\Omega,Re}(x,\varphi,t)\cdot p_{\Omega,Re}(x+\xi,\varphi+\eta,t)} = \Psi_{p,\Omega,Re}(\xi,0,0)\cdot\Psi_{p,\Omega,Re}(0,\eta,0)\,\overline{p^2(\Omega,Re)} \, . \tag{5.43}$$

## 5.10 Summary

In §5.2 was presented the general formulation for obtaining the free vibration characteristics of non-uniform cylindrical shells. Solution of equation (5.4), with the pertinent boundary conditions taken into account, will yield the eigenvalues (and hence the natural frequencies) and eigenvectors of the system.

The necessary modifications for the analysis of shells partially or completely filled with liquid were presented in § 5.3. To obtain the free vibration characteristics of liquid-filled shells, we must again solve equation (5.4), where [M] must now be modified to take into account the virtual mass of the fluid.

The subsequent sections dealt with the response of a shell subjected to an arbitrary random pressure field. Equation (5.33) in § 5.8 gives the mean-square response of the shell in terms of the cross-correlation spectral density of the pressure field. In § 5.9 this cross-correlation spectral density is expressed in terms of the pertinent pressure correlations [equations (5.36) - (5.39)]. Finally, these pressure correlations are expressed in terms of spatial cross-correlation functions of the pressure field and the mean-square spectral density, by equations (5.43), in the particular case of a homogeneous pressure field.

Thus, if the mean-square spectral density, $\overline{p^2(\Omega, Re)}$, and the spatial cross-correlation functions, $\psi(\xi, 0, 0)$ and $\psi(0, \eta, 0)$, of the pressure field are known, the cross-correlation spectral density of the field is known, in terms of equations (5.36) - (5.39): the response may then be computed by using equations (5.33).

## CHAPTER VI

## SHELL RESPONSE TO SUBSONIC BOUNDARY-LAYER PRESSURE FLUCTUATIONS

### 6.1 Introduction

In the previous Chapter we obtained expressions for the response of a shell subjected to an arbitrary random pressure field. The origin of the pressure field was left undefined, although the indicial notation 'Re' for Reynolds number anticipated a flow situation. In this Chapter we shall consider the particular case where the pressure field arises from pressure fluctuations in the subsonic, turbulent boundary layer of a fluid flowing inside the shell.

In the previous Chapter we have indicated how the inertial effects of a fluid contained by the shell may be taken into account. However, when the fluid is flowing, there are additional factors that must be considered; thus the shell will be subjected to centrifugal forces proportional to $\bar{U}_{\mathbb{C}}^2\left(\partial^2 w/\partial x^2\right)$ and Coriolis forces proportional to $2\bar{U}_{\mathbb{C}}(\partial^2 w/\partial x\, \partial t)$, where $\bar{U}_{\mathbb{C}}$ is the mean flow velocity (33). The former have the effect of decreasing the natural frequencies of the system (34), (35), while the latter effectively have a damping effect on vibrations in cases where one end of the shell is free (34). The magnitude of these effects depends on a dimensionless flow velocity given by $\bar{U} = \bar{U}_{\not{c}}\left(\rho \frac{1-\nu^2}{E}\right)^{1/2}$. Unless we are dealing with very flexible shells (e.g. rubber shells), where E is very small, or with very high flow velocities, these effects are small and may be neglected. Thus for a cylindrical shell with $L/r = 26$, $t/a \simeq 2.3 \times 10^{-2}$ and both ends clamped, the frequencies for $n = 2$ are diminished by 3% when $\bar{U} = 0.20$ (58); for a steel shell containing air flow, the dimensional velocity associated with this $\bar{U}$ is 3330 ft/sec, which is beyond the range we shall be considering. (Actually, the Coriolis forces may be taken into account by incorporating their effect in the overall damping of the system.) In any case, for metal shells conveying fluid with flow velocity in the normal engineering range, these effects are negligible and will not be taken into account in the present theory.

It is also assumed that the internal pressures are not unduly high, so that pressurization of the shell is negligible. We further assume that pressure drop in the length of the shell is sufficiently small for the mean pressure to be considered constant over the length of the shell (thus excluding very long, slender shells); this, however, is not a limitation of the theory, but a simplification introduced for convenience.

For the case of subsonic boundary-layer pressure fluctuations, the longitudinal and lateral space correlation functions have been determined experimentally and theoretically by several investigators, (39) - (44). Bakewell, (39)and(44), has measured, and derived a formula for, the longitudinal and lateral spatial correlation functions over a range of Reynolds numbers from 100,000 to 300,000. In the experiments, the fluid was air. Compressibility effects were ignored because the highest local Mach number was 0.185, which is well below the nominal 0.3 Mach number generally used as the lower limit of compressibility phenomena.

## 6.2 Longitudinal and Lateral Correlation Functions

The longitudinal correlation function $\psi_{p,f_o,Re}(\xi,0,0)$ and the lateral correlation function $\psi_{p,f_o,Re}(0,\eta,0)$ are plotted against the axial and circumferential Strouhal numbers, $S_\xi = f_o^* \xi / U_{CONV.}$ and $S_\eta = f_o \eta / U_{\mathbb{C}}$ , in figures 3 and 4 as given by references (39) and (44). $U_{\mathbb{C}}$ and $U_{CONV}$ are the centreline and convection velocities, respectively.

The data of the longitudinal and lateral correlation functions, for all Reynolds numbers, frequencies, and separations plotted in figures 9 and 10 respectively, appear

---

* $f_o$ and $\Omega$ both represent the forced frequency; $f_o$ is given in Hz and $\Omega$ in radians per second.

to define the following curves [given by (39) and (44)]

$$\psi_{p,f_o,Re}(\xi,0,0) \approx e^{-b|S_\xi|}\cos aS_\xi \quad , \tag{6.1}$$

$$\psi_{p,f_o,Re}(0,\eta,0) \approx \left(1+c\,S_\eta^2\right)^{-1}\cdot\left(2-e^{-d\,S_\eta^2}\right)^{-1} \quad , \tag{6.2}$$

where a,b,c and d are constants determined from experimental data.

The values of the constants used in these two expressions for longitudinal and lateral correlations depend on the fluid. For turbulent flow in air, the values of a,b,c and d for Strouhal number based on centre-line velocity $U_{\mathbb{C}}$, as given in (39) and (44) are

$$\begin{aligned} a &= 8.7266 \;,\; b = 1.0 \;, \text{ for } S_\xi = \xi f_o/U_{\mathbb{C}} \;, \\ c &= 20 \;,\; d = 100 \;, \text{ for } S_\eta = \eta f_o/U_{\mathbb{C}} \;. \end{aligned} \tag{6.3}$$

Bakewell (44) reported that work to determine these constants, for turbulent flow in water, is in progress at the Underwater Sound Laboratory (U.S. Navy). It may be expected, nevertheless, that these constants would be the same for different fluids at the same Strouhal number, at least for sufficiently high Reynolds number.

It should also be noted that the empirical expressions for the lateral and longitudinal correlation functions satisfy the following general requirements (39):

$$\Psi_{p,f_0,Re}(0,0,0) = 1 ,$$

$$\lim_{\xi \to \infty} \Psi_{p,f_0,Re}(\xi,0,0) = 0 ,$$

$$\lim_{\eta \to \infty} \Psi_{p,f_0,Re}(0,\eta,0) = 0 ,$$

$$\left.\frac{\partial \Psi_{p,f_0,Re}(\xi,0,0)}{\partial \xi}\right|_{\xi=0} = \left.\frac{\partial \Psi_{p,f_0,Re}(0,\eta,0)}{\partial \eta}\right|_{\eta=0} = 0 , \quad (6.4)$$

$$\Psi_{p,f_0,Re}(\xi,0,0) = \Psi_{p,f_0,Re}(-\xi,0,0) ,$$

$$\Psi_{p,f_0,Re}(0,\eta,0) = \Psi_{p,f_0,Re}(0,-\eta,0) .$$

On the other hand, the mean square pressure per unit band-width, $\overline{p^2(f_0,Re)}$ in equation (5.43), is plotted in non-dimensional form against the Strouhal number $\left(S = 2 f_0 r / U_{\mathfrak{C}}\right)$. This plot, also obtained by Bakewell (39), is reproduced here in figure 11. For the purposes of this analysis, a functional expression for this curve was obtained, as follows

$$\overline{p^2(f_0,Re)} = 2 k_2 \rho_F^2 r U_{\mathfrak{C}}^3 e^{-2 k_1 \frac{f_0 r}{U_{\mathfrak{C}}}} , \quad (6.5)$$

where $k_2 = 2 \times 10^{-6}$ and $k_1 = 0.25$.

Substitution of relations (5.43) in equations (5.36) - (5.39) gives

$$W_{f_R}(f_0;\xi;0) = \pi^2 . \overline{p^2(f_0, Re)} . \Psi_{p,f_0,Re}(\xi,0,0) . \int_0^{2\pi}\int_0^{2\pi} \Psi_{p,f_0,Re}(0,\eta,0) . \cos(\varphi) . \cos(\varphi') . d\varphi . d\varphi', \qquad (6.6)$$

$$W_{f_C}(f_0;\xi;0) = \pi^2 . \overline{p^2(f_0, Re)} . \Psi_{p,f_0,Re}(\xi,0,0) . \int_0^{2\pi}\int_0^{2\pi} \Psi_{p,f_0,Re}(0,\eta,0) . \sin(\varphi) . \sin(\varphi') . d\varphi . d\varphi', \qquad (6.7)$$

$$W_{f_{RC}}(f_0;\xi;0) = \pi^2 . \overline{p^2(f_0, Re)} . \Psi_{p,f_0,Re}(\xi,0,0) . \int_0^{2\pi}\int_0^{2\pi} \Psi_{p,f_0,Re}(0,\eta,0) . \cos(\varphi) . \sin(\varphi') . d\varphi . d\varphi', \qquad (6.8)$$

where $\Psi_{p,f_0,Re}(\xi,0,0)$, $\Psi_{p,f_0,Re}(0,\eta,0)$ and $\overline{p^2(f_0, Re)}$ are given by equations (6.1), (6.2) and (6.5), respectively; and the integrals of equations (6.6) - (6.8) are evaluated in Appendix C.

## 6.3 Mean Square Response

Substitution of equations (12C) - (14C) into (5.33) leads to the following expression:

$$\Psi_{y_t}(x,\varphi,o) = \overline{y_t^2(x,\varphi,t)} = \sum_{r=1}^{4(N+1)-J} \frac{\Phi_{tr}^2(x,\varphi).r^2}{16.\pi^2.f_r^4 M_r^2} \cdot$$

$$\cdot \int_0^\infty \overline{p^2(f_o,Re)} \cdot T(f_o) \cdot |H_r(f_o)|^2 \cdot$$

$$\cdot \Bigg\{ \sum_{i=1}^{N+1} \sum_{u=1}^{N+1} \Phi_{ir} \Phi_{ur} \left| \int_{l'_i}^{l_i} \int_{l'_u}^{l_u} \Psi_{p,f_o,Re}(\xi,o,o).dx_i.dx_u \right|$$

$$+ 2. \sum_{i=1}^{N+1} \sum_{k=1}^{N+1} \Phi_{ir} \Phi_{kr} \left| \int_{l'_i}^{l_i} \int_{l'_k}^{l_k} (x_k - l_N^k).\Psi_{p,f_o,Re}(\xi,o,o).dx_i.dx_k \right| \tag{6.9}$$

$$+ \sum_{j=1}^{N+1} \sum_{k=1}^{N+1} \Phi_{jr} \Phi_{kr} \left| \int_{l'_j}^{l_j} \int_{l'_k}^{l_k} (x_j - l_N^j).(x_k - l_N^k) \cdot \right.$$

$$\left. \cdot \Psi_{p,f_o,Re}(\xi,o,o).dx_j.dx_k \right|$$

$$+ \sum_{p=1}^{N+1} \sum_{v=1}^{N+1} \Phi_{pr} \Phi_{vr} \left| \int_{l'_p}^{l_p} \int_{l'_v}^{l_v} \Psi_{p,f_o,Re}(\xi,o,o).dx_p.dx_v \right| \Bigg\} df_o \ ,$$

where $\overline{p^2(f_o,Re)}$ is given by the equation (6.5), $T(f_o)$ is evaluated in Appendix C, equation (11C), and can be written as follows

$$T(f_o) = \frac{e^{-1/f_o\sqrt{C}}}{f_o\sqrt{C}\left[2 - e^{D/C}\right]} + \frac{e^{-\sqrt{\ln 2}/f_o\sqrt{D}}}{2f_o\sqrt{D\ln 2}\left[1 - \frac{C}{D}\ln 2\right]} \ ,$$

$$C = c\,r^2/U_\mathfrak{t}^2 \ , \ D = d\,r^2/U_\mathfrak{t}^2 \ ,$$

$$|H_r(f_o)| = \left\{ \left[1 - \left(\frac{f_o}{f_r}\right)^2\right]^2 + \left(2\xi_r \frac{f_o}{f_r}\right)^2 \right\}^{-1/2} \ ,$$

$f_r$ is the $r^{th}$ natural frequency in Hz and $f_o$ is the forced frequency in Hz.

By substituting relations (6.1) in equation (6.9) and integrating over x and x', the following is obtained

$$
\begin{aligned}
&\int_{\ell'_j}^{\ell_j}\int_{\ell'_k}^{\ell_k}(x_j-\ell_N^j)(x_k-\ell_N^k)\,\psi_{f_o,Re}(\xi,0,0)\,dx_j\,dx_k = \\
&\frac{1}{f_o^2(A^2+B^2)^2}\cdot\Big\{\ (B^2-A^2)(\ell_N^k-\ell_k)(\ell_N^j-\ell_j)\,e^{-f_oB|\ell_j-\ell_k|}\cos[f_oA|\ell_j-\ell_k|] \\
&\qquad -2AB(\ell_N^k-\ell_k)(\ell_N^j-\ell_j)\,e^{-f_oB|\ell_j-\ell_k|}\sin[f_oA|\ell_j-\ell_k|] \\
&\qquad -(B^2-A^2)(\ell_N^k-\ell_k)(\ell_N^j-\ell'_j)\,e^{-f_oB|\ell'_j-\ell_k|}\cos[f_oA|\ell'_j-\ell_k|] \\
&\qquad +2AB(\ell_N^k-\ell_k)(\ell_N^j-\ell'_j)\,e^{-f_oB|\ell'_j-\ell_k|}\sin[f_oA|\ell'_j-\ell_k|] \\
&\qquad -(B^2-A^2)(\ell_N^k-\ell'_k)(\ell_N^j-\ell_j)\,e^{-f_oB|\ell_j-\ell'_k|}\cos[f_oA|\ell_j-\ell'_k|] \qquad (6.10) \\
&\qquad +2AB(\ell_N^k-\ell'_k)(\ell_N^j-\ell_j)\,e^{-f_oB|\ell_j-\ell'_k|}\sin[f_oA|\ell_j-\ell'_k|] \\
&\qquad +(B^2-A^2)(\ell_N^k-\ell'_k)(\ell_N^j-\ell'_j)\,e^{-f_oB|\ell'_j-\ell'_k|}\cos[f_oA|\ell'_j-\ell'_k|] \\
&\qquad -2AB(\ell_N^k-\ell'_k)(\ell_N^j-\ell'_j)\,e^{-f_oB|\ell'_j-\ell'_k|}\sin[f_oA|\ell'_j-\ell'_k|]\ \Big\} \\
&+\frac{1}{f_o^3(A^2+B^2)^3}\cdot\Big\{\ B(3A^2-B^2)(\ell_N^k+\ell_N^j-\ell_j-\ell_k)\,e^{-f_oB|\ell_j-\ell_k|}\cos[f_oA|\ell_j-\ell_k|] \\
&\qquad +A(3B^2-A^2)(\ell_N^k+\ell_N^j-\ell_j-\ell_k)\,e^{-f_oB|\ell_j-\ell_k|}\sin[f_oA|\ell_j-\ell_k|] \\
&\qquad -B(3A^2-B^2)(\ell_N^k+\ell_N^j-\ell'_j-\ell_k)\,e^{-f_oB|\ell'_j-\ell_k|}\cos[f_oA|\ell'_j-\ell_k|] \\
&\qquad -A(3B^2-A^2)(\ell_N^k+\ell_N^j-\ell'_j-\ell_k)\,e^{-f_oB|\ell'_j-\ell_k|}\sin[f_oA|\ell'_j-\ell_k|]
\end{aligned}
$$

$$-B(3A^2-B^2)\left(l_N^k+l_N^j-l_j-l_k'\right)e^{-f_oB|l_j-l_k'|}\cos\left[f_oA|l_j-l_k'|\right]$$

$$-A(3B^2-A^2)\left(l_N^k+l_N^j-l_j-l_k'\right)e^{-f_oB|l_j-l_k'|}\sin\left[f_oA|l_j-l_k'|\right]$$

$$+B(3A^2-B^2)\left(l_N^k+l_N^j-l_j'-l_k'\right)e^{-f_oB|l_j'-l_k'|}\cos\left[f_oA|l_j'-l_k'|\right]$$

$$+A(3B^2-A^2)\left(l_N^k+l_N^j-l_j'-l_k'\right)e^{-f_oB|l_j'-l_k'|}\sin\left[f_oA|l_j'-l_k'|\right]\Big\}$$

$$+\frac{1}{f_o^4(A^2+B^2)^4}\cdot\Big\{\left[(A^2-B^2)^2-4A^2B^2\right]e^{-f_oB|l_j-l_k|}\cos\left[f_oA|l_j-l_k|\right]$$

$$+4AB(A^2-B^2)\,e^{-f_oB|l_j-l_k|}\sin\left[f_oA|l_j-l_k|\right]$$

$$-\left[(A^2-B^2)^2-4A^2B^2\right]e^{-f_oB|l_j'-l_k|}\cos\left[f_oA|l_j'-l_k|\right]$$

$$-4AB(A^2-B^2)\,e^{-f_oB|l_j'-l_k|}\sin\left[f_oA|l_j'-l_k|\right] \qquad (6.10)\ \text{cont'}$$

$$-\left[(A^2-B^2)^2-4A^2B^2\right]e^{-f_oB|l_j-l_k'|}\cos\left[f_oA|l_j-l_k'|\right]$$

$$-4AB(A^2-B^2)\,e^{-f_oB|l_j-l_k'|}\sin\left[f_oA|l_j-l_k'|\right]$$

$$+\left[(A^2-B^2)^2-4A^2B^2\right]e^{-f_oB|l_j'-l_k'|}\cos\left[f_oA|l_j'-l_k'|\right]$$

$$+4AB(A^2-B^2)\,e^{-f_oB|l_j'-l_k'|}\sin\left[f_oA|l_j'-l_k'|\right]\Big\}\ ,$$

$$\int_{l_i'}^{l_i}\int_{l_k'}^{l_k}\left(x_k-l_N^k\right)\psi_{f_o,Re}(\xi,0,0)\,dx_i\,dx_k =$$

$$\frac{1}{f_o^3(A^2+B^2)^3}\cdot\Big\{\left[B^3-3A^2B\right]e^{-f_oB|l_k-l_i|}\cos\left[f_oA|l_k-l_i|\right]$$

$$+\left[A^3-3AB^2\right]e^{-f_oB|l_k-l_i|}\sin\left[f_oA|l_k-l_i|\right]$$

$$-\left[B^3-3A^2B\right]e^{-f_oB|l_k'-l_i|}\cos\left[f_oA|l_k'-l_i|\right] \qquad (6.11)$$

$$-\left[A^3-3AB^2\right]e^{-f_oB|l_k'-l_i|}\sin\left[f_oA|l_k'-l_i|\right]$$

$$
\begin{aligned}
&-\left[B^3-3A^2B\right] e^{-f_0 B|\ell_k-\ell_i'|} \cos\left[f_0 A|\ell_k-\ell_i'|\right] \\
&-\left[A^3-3AB^2\right] e^{-f_0 B|\ell_k-\ell_i'|} \sin\left[f_0 A|\ell_k-\ell_i'|\right] \\
&+\left[B^3-3A^2B\right] e^{-f_0 B|\ell_k'-\ell_i'|} \cos\left[f_0 A|\ell_k'-\ell_i'|\right] \\
&+\left[A^3-3AB^2\right] e^{-f_0 B|\ell_k'-\ell_i'|} \sin\left[f_0 A|\ell_k'-\ell_i'|\right]\Big\}
\end{aligned}
$$

$$
\begin{aligned}
+\frac{1}{f_0^2(A^2+B^2)^2}\Big\{ &(B^2-A^2)(\ell_k-\ell_N^k)\, e^{-f_0 B|\ell_k-\ell_i|} \cos\left[f_0 A|\ell_k-\ell_i|\right] \\
&-2AB(\ell_k-\ell_N^k)\, e^{-f_0 B|\ell_k-\ell_i|} \sin\left[f_0 A|\ell_k-\ell_i|\right] \\
&-(B^2-A^2)(\ell_k'-\ell_N^k)\, e^{-f_0 B|\ell_k'-\ell_i|} \cos\left[f_0 A|\ell_k'-\ell_i|\right] \\
&+2AB(\ell_k'-\ell_N^k)\, e^{-f_0 B|\ell_k'-\ell_i|} \sin\left[f_0 A|\ell_k'-\ell_i|\right] \\
&-(B^2-A^2)(\ell_k-\ell_N^k)\, e^{-f_0 B|\ell_k-\ell_i'|} \cos\left[f_0 A|\ell_k-\ell_i'|\right] \\
&+2AB(\ell_k-\ell_N^k)\, e^{-f_0 B|\ell_k-\ell_i'|} \sin\left[f_0 A|\ell_k-\ell_i'|\right] \\
&+(B^2-A^2)(\ell_k'-\ell_N^k)\, e^{-f_0 B|\ell_k'-\ell_i'|} \cos\left[f_0 A|\ell_k'-\ell_i'|\right] \\
&-2AB(\ell_k'-\ell_N^k)\, e^{-f_0 B|\ell_k'-\ell_i'|} \sin\left[f_0 A|\ell_k'-\ell_i'|\right]\Big\},
\end{aligned}
\qquad \text{(6.11) cont'}
$$

$$
\int_{\ell_i'}^{\ell_i}\int_{\ell_\mu'}^{\ell_\mu} \psi_{f_0,Re}(\xi,0,0)\, dx_i\, dx_\mu =
$$

$$
\begin{aligned}
\frac{1}{f_0^2(B^2+A^2)^2}\cdot\Big\{ &(B^2-A^2)\, e^{-f_0 B|\ell_i-\ell_\mu|} \cos\left[f_0 A|\ell_i-\ell_\mu|\right] - 2AB\, e^{-f_0 B|\ell_i-\ell_\mu|} \sin\left[f_0 A|\ell_i-\ell_\mu|\right] \\
&-(B^2-A^2)\, e^{-f_0 B|\ell_i'-\ell_\mu|} \cos\left[f_0 A|\ell_i'-\ell_\mu|\right] + 2AB\, e^{-f_0 B|\ell_i'-\ell_\mu|} \sin\left[f_0 A|\ell_i'-\ell_\mu|\right] \\
&-(B^2-A^2)\, e^{-f_0 B|\ell_i-\ell_\mu'|} \cos\left[f_0 A|\ell_i-\ell_\mu'|\right] \\
&+2AB\, e^{-f_0 B|\ell_i-\ell_\mu'|} \sin\left[f_0 A|\ell_i-\ell_\mu'|\right] \\
&+(B^2-A^2)\, e^{-f_0 B|\ell_i'-\ell_\mu'|} \cos\left[f_0 A|\ell_i'-\ell_\mu'|\right] \\
&-2AB\, e^{-f_0 B|\ell_i'-\ell_\mu'|} \sin\left[f_0 A|\ell_i'-\ell_\mu'|\right]\Big\},
\end{aligned}
\qquad \text{(6.12)}
$$

where A = a/$U_{\mathbb{C}}$ , B = b/$U_{\mathbb{C}}$, 'a' and 'b' are given by equation (6.5), and $\ell_e$, $\ell'_e$, $\ell_N^e$ represent the coordinates of the area surrounding the node e (figure 7). In this case e may have the values i,j,k,p,u or v. The expression $\int_{\ell'_p}^{\ell_p}\int_{\ell'_v}^{\ell_v} \Psi_{p,f_0,Re}(\xi,0,0).dx_p.dx_v$ can also be obtained from equation (6.12) by substituting in this equation the indices p and v in place of i and u, respectively.

Next, the product $\overline{p^2(f_0,Re).T(f_0).|H_r(f_0)|^2}$ , in equation (6.9), gives the relation

$$\overline{p^2(f_0,Re)}.T(f_0).\left|H_r(f_0)\right|^2 =$$

$$\frac{K_2\, e^{-(K_1 f_0 + C_1/f_0)}}{f_0 C_2\left[\left(\frac{1}{f_r^4}\right)f_0^4 + \frac{(4\varphi_r^2-2)}{f_r^2}f_0^2+1\right]} + \tag{6.13}$$

$$+ \frac{K_2\, e^{-(K_1 f_0 + D_1/f_0)}}{f_0 D_2\left[\left(\frac{1}{f_r^4}\right)f_0^4 + \frac{(4\varphi_r^2-2)}{f_r^2}f_0^2+1\right]} ,$$

where $K_2 = 2k_2\rho^2 r U_{\mathbb{C}}^3$, $K_1 = 2k_1 r/U_{\mathbb{C}}$, $C_1 = 1/\sqrt{C}$, $C_2 = \sqrt{C}\left[2 - e^{D/C}\right]$, $D_1 = \sqrt{\ln 2/D}$, $D_2 = 2\sqrt{D \ln 2}\left[1 - \frac{C}{D}\ln 2\right]$, $C = cr^2/U_{\mathbb{C}}^2$, $D = dr^2/U_{\mathbb{C}}^2$; $k_1$, $k_2$ and a,b,c,d are constants given by equations (6.5) and (6.3), respectively.

Substitution of relations (6.10) - (6.13) in equation (6.9) results in an expression of the following form:

$$\Psi_{y_t}(x,\varphi,0) = \overline{y_t^2(x,\varphi,t)} = \sum_{r=1}^{4(N+1)-J} \Phi_{tr}^2(x,\varphi) \cdot \frac{r^2}{16 \cdot \pi^2 \cdot f_r^4 \cdot M_r^2} \cdot$$

$$\cdot \left[ \sum_{i=1}^{N+1} \sum_{u=1}^{N+1} \Phi_{ir} \Phi_{ur} \left| \Gamma_{iu}^{F} \right| + 2 \cdot \sum_{i=1}^{N+1} \sum_{k=1}^{N+1} \Phi_{ir} \Phi_{kr} \left| \Gamma_{ki}^{M} \right| \right. \tag{6.14}$$

$$\left. + \sum_{j=1}^{N+1} \sum_{k=1}^{N+1} \Phi_{jr} \Phi_{kr} \left| \Gamma_{jk}^{MM} \right| + \sum_{p=1}^{N+1} \sum_{v=1}^{N+1} \Phi_{pr} \Phi_{vr} \left| \Gamma_{pv}^{F} \right| \right] ,$$

$$\Gamma_{iu}^{F} = \frac{1}{(B^2+A^2)^2} \cdot \Big\{ (B^2-A^2) \left[ F_3^{c}(\ell_i,\ell_u) - F_3^{c}(\ell_i',\ell_u) - F_3^{c}(\ell_i,\ell_u') + F_3^{c}(\ell_i',\ell_u') \right]$$

$$+ 2 \cdot AB \left[ -F_3^{s}(\ell_i,\ell_u) + F_3^{s}(\ell_i',\ell_u) + F_3^{s}(\ell_i,\ell_u') - F_3^{s}(\ell_i',\ell_u') \right] \Big\} ,$$

(6.15)

$$\Gamma_{ki}^{M} = \frac{1}{(A^2+B^2)^3} \cdot \Big\{ (B^3-3A^2B) \left[ F_4^{c}(\ell_k,\ell_i) - F_4^{c}(\ell_k',\ell_i) - F_4^{c}(\ell_k,\ell_i') + F_4^{c}(\ell_k',\ell_i') \right]$$

$$+ (A^3-3AB^2) \left[ F_4^{s}(\ell_k,\ell_i) - F_4^{s}(\ell_k',\ell_i) - F_4^{s}(\ell_k,\ell_i') + F_4^{s}(\ell_k',\ell_i') \right] \Big\}$$

$$+ \frac{1}{(A^2+B^2)^2} \cdot \Big\{ (B^2-A^2)(\ell_k - \ell_N^{k}) \left[ F_3^{c}(\ell_k,\ell_i) - F_3^{c}(\ell_k,\ell_i') \right] \tag{6.16}$$

$$- (B^2-A^2)(\ell_k' - \ell_N^{k}) \left[ F_3^{c}(\ell_k',\ell_i) - F_3^{c}(\ell_k',\ell_i') \right]$$

$$- 2AB(\ell_k - \ell_N^{k}) \left[ F_3^{s}(\ell_k,\ell_i) - F_3^{s}(\ell_k,\ell_i') \right]$$

$$+ 2AB(\ell_k' - \ell_N^{k}) \left[ F_3^{s}(\ell_k',\ell_i) - F_3^{s}(\ell_k',\ell_i') \right] \Big\} ,$$

$$
\begin{aligned}
\Gamma_{jk}^{MM} = {} & \frac{1}{(A^2+B^2)^2}\cdot\Big\{ (B^2-A^2)(\ell_N^k-\ell_k)\Big[(\ell_N^j-\ell_j)F_3^c(\ell_k,\ell_j)-(\ell_N^j-\ell_j')F_3^c(\ell_k,\ell_j')\Big] \\
& -(B^2-A^2)(\ell_N^k-\ell_k')\Big[(\ell_N^j-\ell_j)F_3^c(\ell_k',\ell_j)-(\ell_N^j-\ell_j')F_3^c(\ell_k',\ell_j')\Big] \\
& -2.AB(\ell_N^k-\ell_k)\Big[(\ell_N^j-\ell_j)F_3^s(\ell_k,\ell_j)-(\ell_N^j-\ell_j')F_3^s(\ell_k,\ell_j')\Big] \\
& +2.AB(\ell_N^k-\ell_k')\Big[(\ell_N^j-\ell_j)F_3^s(\ell_k',\ell_j)-(\ell_N^j-\ell_j')F_3^s(\ell_k',\ell_j')\Big]\Big\} \\
& +\frac{1}{(A^2+B^2)^3}\cdot\Big\{(\ell_N^k+\ell_N^j-\ell_j-\ell_k)\Big[B(3A^2-B^2)F_4^c(\ell_k,\ell_j)+A(3B^2-A^2)F_4^s(\ell_k,\ell_j)\Big] \\
& -(\ell_N^k+\ell_N^j-\ell_j'-\ell_k)\Big[B(3A^2-B^2)F_4^c(\ell_k,\ell_j')+A(3B^2-A^2)F_4^s(\ell_k,\ell_j')\Big] \\
& -(\ell_N^k+\ell_N^j-\ell_j-\ell_k')\Big[B(3A^2-B^2)F_4^c(\ell_k',\ell_j)+A(3B^2-A^2)F_4^s(\ell_k',\ell_j)\Big] \\
& +(\ell_N^k+\ell_N^j-\ell_j'-\ell_k')\Big[B(3A^2-B^2)F_4^c(\ell_k',\ell_j')+A(3B^2-A^2)F_4^s(\ell_k',\ell_j')\Big]\Big\} \\
& +\frac{1}{(A^2+B^2)^4}\cdot\Big\{\Big[(A^2-B^2)^2-4A^2B^2\Big]\Big[F_5^c(\ell_k,\ell_j)-F_5^c(\ell_k,\ell_j')-F_5^c(\ell_k',\ell_j)+F_5^c(\ell_k',\ell_j')\Big] \\
& +4.AB(A^2-B^2)\Big[F_5^s(\ell_k,\ell_j)-F_5^s(\ell_k,\ell_j')-F_5^s(\ell_k',\ell_j)+F_5^s(\ell_k',\ell_j')\Big]\Big\}\,,
\end{aligned}
\tag{6.17}
$$

$$
\begin{aligned}
\Gamma_{j\mu}^{M} = {} & \frac{1}{(A^2+B^2)^3}\Big\{(B^3-3A^2B)\Big[F_4^c(\ell_j,\ell_\mu)-F_4^c(\ell_j',\ell_\mu)-F_4^c(\ell_j,\ell_\mu')+F_4^c(\ell_j',\ell_\mu')\Big] \\
& +(A^3-3AB^2)\Big[F_4^s(\ell_j,\ell_\mu)-F_4^s(\ell_j',\ell_\mu)-F_4^s(\ell_j,\ell_\mu')+F_4^s(\ell_j',\ell_\mu')\Big]\Big\} \\
& +\frac{1}{(A^2+B^2)^2}\cdot\Big\{(B^2-A^2)(\ell_j-\ell_N^j)\Big[F_3^c(\ell_j,\ell_\mu)-F_3^c(\ell_j,\ell_\mu')\Big] \\
& -(B^2-A^2)(\ell_j'-\ell_N^j)\Big[F_3^c(\ell_j',\ell_\mu)-F_3^c(\ell_j',\ell_\mu')\Big] \\
& -2.AB(\ell_j-\ell_N^j)\Big[F_3^s(\ell_j,\ell_\mu)-F_3^s(\ell_j,\ell_\mu')\Big] \\
& +2.AB(\ell_j'-\ell_N^j)\Big[F_3^s(\ell_j',\ell_\mu)-F_3^s(\ell_j',\ell_\mu')\Big]\Big\}\,,
\end{aligned}
\tag{6.18}
$$

$$F_3^c(\ell_i,\ell_\mu)=\frac{K_2}{C_2}\int_0^\infty \frac{e^{-\left[(K_1+B|\ell_i-\ell_\mu|)f_0+\frac{C_1}{f_0}\right]}\cos[A|\ell_i-\ell_\mu|f_0]}{f_0^3\left[\left(\frac{1}{f_\pi^4}\right)f_0^4+\frac{(4\varphi_\pi^2-2)}{f_\pi^2}f_0^2+1\right]}df_0 \tag{6.19}$$

$$+\frac{K_2}{D_2}\int_0^\infty \frac{e^{-\left[(K_1+B|\ell_i-\ell_\mu|)f_0+(D_1/f_0)\right]}\cos[A|\ell_i-\ell_\mu|f_0]}{f_0^3\left[\left(\frac{1}{f_\pi^4}\right)f_0^4+\frac{(4\varphi_\pi^2-2)}{f_\pi^2}f_0^2+1\right]}df_0\,,$$

$$F_3^s(\ell_i,\ell_\mu)=\frac{K_2}{C_2}\int_0^\infty \frac{e^{-\left[(K_1+B|\ell_i-\ell_\mu|)f_0+(C_1/f_0)\right]}\sin[A|\ell_i-\ell_\mu|f_0]}{f_0^3\left[\left(\frac{1}{f_\pi^4}\right)f_0^4+\frac{(4\varphi_\pi^2-2)}{f_\pi^2}f_0^2+1\right]}df_0 \tag{6.20}$$

$$+\frac{K_2}{D_2}\int_0^\infty \frac{e^{-\left[(K_1+B|\ell_i-\ell_\mu|)f_0+(D_1/f_0)\right]}\sin[A|\ell_i-\ell_\mu|f_0]}{f_0^3\left[\left(\frac{1}{f_\pi^4}\right)f_0^4+\frac{(4\varphi_\pi^2-2)}{f_\pi^2}f_0^2+1\right]}df_0\,,$$

$$F_4^c(\ell_i,\ell_\mu)=F_3^c(\ell_i,\ell_\mu)\Big/f_0\,, \tag{6.21}$$

$$F_4^s(\ell_i,\ell_\mu)=F_3^s(\ell_i,\ell_\mu)\Big/f_0\,, \tag{6.22}$$

$$F_5^c(\ell_i,\ell_\mu)=F_3^c(\ell_i,\ell_\mu)\Big/f_0^2\,, \tag{6.23}$$

$$F_5^s(\ell_i,\ell_\mu)=F_3^s(\ell_i,\ell_\mu)\Big/f_0^2\,, \tag{6.24}$$

The above integrals, (6.19) - (6.24), are evaluated and listed in Appendix C, [(25C) - (30C)]; they are given by

$$F_3^{c}(\ell_i,\ell_\mu)=\frac{\pi K_2}{8C_2 f_r^2}\left[4e^{-\gamma_1}\sin\gamma_2-4e^{-\gamma_3}\sin\gamma_4+\frac{1}{\varphi_r}\left(e^{-\gamma_1}\cos\gamma_2+e^{-\gamma_3}\cos\gamma_4\right)\right]$$
$$+\frac{\pi K_2}{8D_2 f_r^2}\left[4e^{-\gamma_5}\sin\gamma_6-4e^{-\gamma_7}\sin\gamma_8+\frac{1}{\varphi_r}\left(e^{-\gamma_5}\cos\gamma_6+e^{-\gamma_7}\cos\gamma_8\right)\right], \tag{6.25}$$

$$F_3^{s}(\ell_i,\ell_\mu)=\frac{\pi K_2}{8C_2 f_r^2}\left[4e^{-\gamma_3}\cos\gamma_4-4e^{-\gamma_1}\cos\gamma_2+\frac{1}{\varphi_r}\left(e^{-\gamma_1}\sin\gamma_2+e^{-\gamma_3}\sin\gamma_4\right)\right]$$
$$+\frac{\pi K_2}{8D_2 f_r^2}\left[4e^{-\gamma_7}\cos\gamma_8-4e^{-\gamma_5}\cos\gamma_6+\frac{1}{\varphi_r}\left(e^{-\gamma_5}\sin\gamma_6+e^{-\gamma_7}\sin\gamma_8\right)\right], \tag{6.26}$$

$$F_4^{c}(\ell_i,\ell_\mu)=\frac{\pi K_2}{8C_2 f_r^3}\left[e^{-\gamma_1}\sin\gamma_2-e^{-\gamma_3}\sin\gamma_4\right]+\frac{\pi K_2}{8D_2 f_r^3}\left[e^{-\gamma_5}\sin\gamma_6-e^{-\gamma_7}\sin\gamma_8\right]$$
$$+\frac{1}{f_r}F_3^{c}(\ell_i,\ell_\mu), \tag{6.27}$$

$$F_4^{s}(\ell_i,\ell_\mu)=\frac{\pi K_2}{8C_2 f_r^3}\left[e^{-\gamma_3}\cos\gamma_4-e^{-\gamma_1}\cos\gamma_2\right]+\frac{\pi K_2}{8D_2 f_r^3}\left[e^{-\gamma_7}\cos\gamma_8-e^{-\gamma_5}\cos\gamma_6\right]$$
$$+\frac{1}{f_r}F_3^{s}(\ell_i,\ell_\mu), \tag{6.28}$$

$$F_5^{c}(\ell_i,\ell_\mu)=\frac{2}{f_r}F_4^{c}-\frac{1}{f_r^2}F_3^{c}, \tag{6.29}$$

$$F_5^{s}(\ell_i,\ell_\mu)=\frac{2}{f_r}F_4^{s}-\frac{1}{f_r^2}F_3^{s}, \tag{6.30}$$

where

$$\gamma_1^* = \left[K_1 + |\ell_i - \ell_u| \left(A\varphi_r + B\right)\right] f_r + \frac{C_1}{f_r\left(1+\varphi_r^2\right)},$$

$$\gamma_2 = \left[-K_1\varphi_r + |\ell_i - \ell_u| \left(A - B\varphi_r\right)\right] f_r + \frac{C_1\varphi_r}{f_r\left(1+\varphi_r^2\right)},$$

$$\gamma_3 = \left[-K_1 + |\ell_i - \ell_u| \left(A\varphi_r - B\right)\right] f_r - \frac{C_1}{f_r\left(1+\varphi_r^2\right)},$$

$$\gamma_4 = \left[-K_1\varphi_r - |\ell_i - \ell_u| \left(A + B\varphi_r\right)\right] f_r + \frac{C_1\varphi_r}{f_r\left(1+\varphi_r^2\right)},$$

$$\gamma_5 = \left[K_1 + |\ell_i - \ell_u| \left(A\varphi_r + B\right)\right] f_r + \frac{D_1}{f_r\left(1+\varphi_r^2\right)}, \qquad (6.31)$$

$$\gamma_6 = \left[-K_1\varphi_r + |\ell_i - \ell_u| \left(A - B\varphi_r\right)\right] f_r + \frac{D_1\varphi_r}{f_r\left(1+\varphi_r^2\right)},$$

$$\gamma_7 = \left[-K_1 + |\ell_i - \ell_u| \left(A\varphi_r - B\right)\right] f_r - \frac{D_1}{f_r\left(1+\varphi_r^2\right)},$$

$$\gamma_8 = \left[-K_1\varphi_r - |\ell_i - \ell_u| \left(A + B\varphi_r\right)\right] f_r + \frac{D_1\varphi_r}{f_r\left(1+\varphi_r^2\right)},$$

$$K_1 = 2k_1 r/U_\ell, \quad K_2 = 2k_2\rho_F^2 r U_\ell^3,$$

$$C_1 = 1/\sqrt{C}, \quad C_2 = \sqrt{C}\left(2 - e^{D/C}\right),$$

$$D_1 = \sqrt{\ln 2/D}, \quad D_2 = 2\sqrt{D\ln 2}\left[1 - \frac{C}{D}\ln 2\right],$$

---

* here the arguments $(\ell_i, \ell_u)$ have been omitted from $\gamma_1(\ell_i, \ell_u)$, $\gamma_2(\ell_i, \ell_u)$, etc., for simplicity.

$$A = a / U_{¢} \quad , \quad B = b / U_{¢} \, ,$$
$$C = c r^2 / U_{¢}^2 \quad , \quad D = d r^2 / U_{¢}^2 \, ,$$

$k_2$, $k_1$ and a,b,c,d are constants given by equations (6.5) and (6.3) respectively, $f_r$ is the $r^{th}$ natural frequency in Hz, r is the mean radius in inches, $M_r$ is the element of the matrix given by equation (5.12), $U_{¢}$ is the centre-line velocity in in./sec., $\rho_F$ is the fluid density in (lb.sec.$^2$/in.$^4$), $\zeta_r$ is the generalized damping factor given by equation (5.14), ( $\ell_i$ , $\ell_i'$ , $\ell_N^i$ , $\ell_j$ , $\ell_j'$ , $\ell_N^j$, etc...) are the coordinates of the field force (figure 7) surrounding the nodes (i,j, etc...) given in inches; and $\Phi_{ir}$ , $\Phi_{mr}$ , $\Phi_{jr}$ , $\Phi_{kr}$, $\Phi_{pr}$, $\Phi_{nr}$ represent the elements of the modal column of the $r^{th}$ natural frequency in the modal matrix corresponding to the radial displacement, rotation and circumferential displacement, in respective pairs. Finally $\overline{y_t^2(x,\varphi,t)}$ is the mean square response (displacements) at the node t.

# CHAPTER VII

## METHOD OF CALCULATION

This Chapter describes a procedure for computing the vibration modes and frequencies, both for the case of the empty non-uniform cylindrical shell and also for the case of the shell completely or partially filled with fluid. Also, the root-mean-square (r.m.s.) response to subsonic boundary-layer pressure fluctuations is obtained. The procedure is based on the theory developed in the previous Chapters.

### 7.1 Computational Method and Computer Program

To determine the eigenvalues, eigenvectors and the response of a given uniform or non-uniform cylindrical shell, we first subdivide it into a sufficient number of finite elements (sufficiency in this context will be discussed later). The calculation is then done with the aid of a digital computer program which, for given input data, calculates the mass, stiffness and stress-resultant matrices for each element, assembles the global mass and stiffness matrices for the whole shell, and calculates the natural frequencies, the eigenvectors, and finally the r.m.s.

response at each node.

In this section, the necessary steps of the computational method will be outlined. The steps are specific enough to allow a digital computer program to be written by using them as a guide.

The basic organization of the computer program used in the present analysis is shown in figure 12.

A - The necessary input data are the mean radius, wall thickness, and length of each individual element, and the respective modulus of elasticity, Poisson's ratio, material density and fluid density; also the values of $n(\geq 2)$ which should be calculated. To find the r.m.s. response, additional input data are required at each node such as the centreline velocity, viscous damping or damping factor, and the constants $a, b, c, d, k_1$ and $k_2$ given by the expressions (6.3) and (6.5).

B - The computer program then proceeds as follows for each element:

(i) the eight complex roots of the characteristic equation, $\lambda_j$, are calculated by the Newton-Raphson iterative technique, and hence, we obtain $\kappa_1$, $\kappa_2$, $\mu_1$, $\mu_2$, $\alpha_j$, $\beta_j$, $(j = 1,2,\cdots,8)$, and $\bar{\alpha}_j$, $\bar{\beta}_j$;

(ii) the intermediate matrices $[R]$, $[A]$, $[\Gamma]$, $[\Delta]$, $[RJ] = [\Delta]^T[\Delta]$ and $[Y] = [\Gamma]^T[P][\Gamma]$ given in Appendix B are determined;

(iii) the displacement functions, mass, stiffness and stress-resultant matrices, [N], [m], [k] and [ST], respectively, are computed by the relationships given by equations (3.13), (4.5), (4.6) and (4.15).

C - When the stiffness and mass matrices have thus been computed for each element, the matrices are superimposed to form the global shell stiffness and mass matrices, in the manner described in § 4.5.

D - If the shell has rigid edge constraints, then appropriate rows and columns of $[K] - \Omega_i^2\ [M]$ given by equation (5.4), are deleted to satisfy these constraints. Accordingly, [K] and [M] are reduced to square matrices of order 4(N+1)-J, where J is the number of constraint equations imposed. The form and character of equation (5.4) is not affected, except in that the reduced [K] and [M] are positive definite instead of being, generally, positive semi-definite. It is noted that only kinematic boundary conditions are specified. Thus for a free shell, no specification of boundary conditions need be made, and J = 0; for a shell with two edges simply supported ($v_n = w_n = 0$) J = 4, and for one with two clamped edges J = 8.

E - With the reduced [M] and [K] determined, the computer program proceeds to find the natural frequencies, $\Omega_i$, where $i = 1,2,\cdots, 4(N+1)-J$ for each n, and the corresponding eigenvectors of a real square non-symmetric matrix of the special form $[M]^{-1}$ $[K]$, where both $[M]$ and $[K]$ are real, symmetric matrices and $[M]$ is positive definite (31).

F - Finally, if the r.m.s. response to a subsonic boundary layer is required, the diagonal matrices $\left[M_{\kappa}\right]$ and $\left[K_{\kappa}\right]$ must be computed by the relationships given by equation (5.6). It follows that the calculation of the amplitude of the r.m.s. axial, radial, circumferential displacements and the rotation at each node can be done with the aid of equation (6.14).

A computer program, based on this procedure, has been coded in FORTRAN IV for the IBM 360/75 computer. Double precision arithmetic was used throughout the eight overlays shown in figure 12. The maximum capability of the solution for the eigenvalue problem is limited to 30 elements, which corresponds to 400K bytes of core memory.

The program, involving approximately five thousand cards, is compiled in 3 minutes, and the necessary time for the calculation of the eigenvalues and eigenvectors of a given shell subdivided into 15 elements is about 2.5 minutes for each value of n. But, for the calculation of r.m.s. response due to random pressure, the execution time for a typical case involving five finite elements is approximately 30 minutes. However, for the case of 10 elements, the time involved is around 130 minutes of CPU.

The computer time for the calculation of r.m.s. response seems to be high. The time quoted above refers to the case where all the computed natural frequencies are used in the calculation of response. However, if only a few of the lowest natural frequencies are used in the calculation, the response may be computed to an acceptable degree of accuracy, but with a considerable saving in computational cost; thus, if only 15% of the natural frequencies are utilized, then the time given above may be reduced by a factor of 1/8 approximatively.

To illustrate the utility of the computer program described above, the results (INPUT, OUTPUT) for one example problem are listed in Appendix D.

## CHAPTER VIII

## CALCULATIONS AND DISCUSSION

### 8.1 Introduction

The aim of the calculations presented in this Chapter was to test the theory as to correctness, precision and versatility and, accordingly, a wide variety of cylindrical shells and boundary conditions was chosen. Most of the calculations were aimed at determining the free vibration characteristics of shells.

The first set of calculations (§8.3, § 8.4) were all for uniform shells with various boundary conditions. In each case the eigenvalues and eigenvectors were calculated for various combinations of n and m. The first calculation in this set (§8.3) was with a single, completely free, finite element in order to investigate rigid-body motions, with the aim of testing whether the displacement functions selected satisfy the convergence criteria of the finite-element method.

The second set of calculations (§ 8.5, § 8.6) deals with the free vibration characteristics of non-uniform shells. A shell made up of two segments of unequal wall-thickness and another which is ring-stiffened are analysed.

The third set (§8.7) deals with the free-vibration characteristics of a uniform shell completely or partially-filled with liquid.

Finally, the r.m.s. response to subsonic boundary-layer pressure fluctuations is determined for one particular case in §8.8.

In all cases but the last, the results obtained by this theory are compared with other theories or experiments, or both.

## 8.2 Characteristic Equation

The computational task is quite complex and the author was constantly aware that it would be easy for an error to slip into the computer program and remain undetected. For this reason the results were checked at each stage. Starting with the characteristic equation, the values of $\lambda_j$ obtained by the computer program were compared with existing values using other theories. One such set of calculations is shown in Table 10, where it may be seen that the computed values based on Sanders' characteristic equation are comparable with those from other theories.

Next, the elements of the displacement function matrix, [N], were calculated for a wide variety of input parameters. The results for a typical case are shown in Table 11, where the elements of [N] were calculated at $x = 0$ and $x = \ell$ respectively. In such a case we should obtain a matrix with zero elements throughout, except for some elements equal to unity corresponding to displacements being equal to nodal displacements. As may be seen this is indeed the case, and with very good accuracy.

## 8.3 Rigid-Body Motions

For a finite-element free at both ends the solution of equation (5.4) should give the rigid-body modes of vibration, which should be two in number (for $n \geq 2$) and have zero frequencies in addition to the flexural modes.

The results of one such calculation will be given here for a particular element with $E = 10^6$ lb/in.$^2$, $\nu = 0.3$, $\rho = 1$ lb. sec$^2$/in.$^4$, $r = 60.523$ in., $t = 1$ in., $\ell = 40$ in., for $n = 2$. The computer program, described in Chapter VII, yields the following eight eigenvalues:

$$\Omega_1^2 = 0.0478 \qquad \Omega_5^2 = 1390.8$$

$$\Omega_2^2 = 0.2187 \qquad \Omega_6^2 = 3072.4$$

$$\Omega_3^2 = 348.22 \qquad \Omega_7^2 = 5585.6$$

$$\Omega_4^2 = 424.28 \qquad \Omega_8^2 = 6273.9$$

all in (rad/sec)$^2$.

We see that the first two eigenvalues are essentially zero when compared with the others, within the accuracy of the computer manipulation (although double precision was used). The corresponding eigenvectors associated with the first and second modes are listed in Table 12.

We note that for the first mode $u_{n_i} = u_{n_j} \approx 0$, $(dw_n/dx)_i = (dw_n/dx)_j \approx 0$, $w_{n_i} = w_{n_j}$ and $v_{n_i} = v_{n_j}$, i.e. this mode involves pure translation in w and v. The second mode, on the other hand involves rotation about the centre of the element and axial translation.

Taking $\partial \underset{\sim}{v}/\partial x = (v_{n_j} - v_{n_i})/\ell$, etc. and using equations (3.1), (A.7) and the values of Table 10, the strains are found to be all of order $10^{-4}$ or less. This is not true for eigenvectors corresponding to $\Omega_3$ and higher.

It may be concluded, therefore, that the displacement functions chosen satisfy the convergence criteria of the finite-element method with good accuracy.

## 8.4 Calculations for Uniform Shells

The eigenvalues and eigenvectors of uniform shells may, of course, be calculated by much simpler methods than by this theory. The main aim here is to test the correctness of the mass and stiffness matrices in their general form as derived in previous Chapters.

The first calculation involves the determination of the natural frequencies and eigenvectors of a particular simply-supported shell which has been analysed by Michalopoulos and Muster (46), not only by their own theory but also by the theory of three other investigators. The data for the shell are as follows: $r = 4.08$ in., $t = 0.047$ in., $L = 18.54$ in., $E = 3 \times 10^7$ lb/in.$^2$, $\nu = 0.3$ and $\rho = 7.324 \times 10^{-4}$ lb. sec.$^2$/in.$^4$. The natural frequencies of this shell for $n = 2$ to $5$ and $m = 1$ are shown in Table 13, as calculated by Michalopoulos and Muster according to various theories, and by the author.

Arnold and Warburton's (47) pioneering work derives the frequency equation by the energy method using Timoshenko's strain relations; the strain and kinetic energies are evaluated and, with the nodal configuration assumed, Lagrange's equations are used to derive the dynamical equations, eventually leading to a determinantal equation which yields the frequencies. Three natural frequencies are obtained for each nodal configuration, of which only the lowest is of interest here and corresponds to vibration mainly radial in character. Baron and Bleich's (48) theory is based on an energy method in which the shell is first treated as a membrane and the bending effects are subsequently introduced as corrections. Galletly's theory (49) is quite similar to Arnold and Warburton's but is extended to ring-stiffened shells. Finally, Michalopoulos and Muster's (46) theory which also deals with ring-stiffened shells, proceeds essentially as in (47), but expresses displacements in the kinetic and strain energy expressions in general, series form; the equations of motion are written in matrix form and the frequencies are found by the Jacobi iteration method, yielding also the eigenvectors.

The results obtained by our theory were calculated using ten equal finite elements. As may be seen in Table 13, the results obtained by this theory are in quite good agreement with those from other theories, and particularly those of (46) which may be considered to be the most precise.

We also note in Table 13 that the frequencies are not in ascending order of magnitude with increasing n, and that the lowest frequency is not associated with n = 2, in this particular case at least. This matter was first observed and explained by Arnold and Warburton (47) and will not be elaborated upon here.

The eigenvectors were also computed for this shell and are shown in figure 13 in normalized form. Once normalized, the eigenvectors are identical for n = 2,3,4 and 5 to eight significant figures; moreover, they are indistinct from the corresponding sine and cosine half-waves, as they should be for a simply-supported shell. As may be seen in the table at the bottom of the figure the motion is mainly radial; thus $v_{max}/w_{max} \approx 1/n$ and $u_{max}/w_{max} \leq 0(10^{-1})$.

Accordingly, the computed frequencies correspond to the lowest of the three frequencies determined by Arnold and Warburton's and Michalopoulos and Muster's theories, as expected.

Another set of calculations was undertaken to determine the requisite number of finite elements for a precise determination of the natural frequencies. Calculations were made for the same shell as above for $n = 2$ to 5, and with the number of finite elements $N = 2,4,6,8$ and 10. The results for $m = 1$ are shown in figure 14a and those for $m = 2$ and 3 in figure 14b. From figure 14a it is clear that for $m = 1$, the higher n is, the larger the number of finite elements required; thus for $n = 2$ and 3 the frequencies may be adequately determined with $N = 6$, while for the higher n at least $N = 8$ or 10 is required. However, the rate of convergence is not the same for different m as may be seen by comparing figures 14a and 14b. For $m = 2$ and 3 it is the frequencies associated with $n = 2$ which converge slowest, while for $m = 1$ the frequency for $n = 2$ converges fastest. Finally, attention is drawn to the purposely expanded ordinate of the figures which accentuates differences in frequency; thus, in all cases shown, the values for $N = 8$ differ from those of $N = 10$ by less than 2%.

Next, the natural frequencies of another uniform shell were calculated for various boundary conditions and combinations of n and m. The shell analysed is one already studied, both theoretically and experimentally, by Sewall and Naumann (11), with whose results those of this theory will be compared. The data for the shell are as follows: $r = 9.538$ in., $t = 0.0255$ in., $E = 10^7$ lb/in.$^2$, $\nu = 0.315$, $\rho = 2.54 \times 10^{-4}$ lb.sec$^2$/in.$^4$; the length is $L = 25.125$ in., 24.625 in. and 24.0 in., respectively, for the free-free, clamped-free, and clamped-clamped configurations.

The analytical natural frequencies in (11) were obtained by application of the energy method using Novozhilov's strain-displacement relations and employing the Rayleigh-Ritz procedure. The modal functions used in connection with the Rayleigh-Ritz procedure assume axial variation in displacements proportional to the corresponding beam eigenfunctions; this has certain inherent limitations, namely (i) in connection with free-free boundary conditions, not all possible rigid-body motions are allowed, and (ii) in cases of a clamped end, there is the contradiction of having both $v = 0$ and $N_{x\varphi} = 0$ at that end (11).

The results obtained by our theory were computed with $N = 10$, and are compared with those of (11) in figures 15 - 17. As may be seen, the results obtained by this theory are in fairly good agreement with those of (11) and, what is more gratifying, they are in better agreement with the experiments of (11)*. This is particularly noticeable in the case of both ends clamped (figure 16), where the effect of the aforementioned difficulty arising from the modal functions chosen in (11) would be greatest.

Detailed discussion of the results obtained and their significance will not be undertaken here as this has already been done by others, notably in (47) and (46).

The evident success of this theory in analysing uniform cylindrical shells is considered to have provided adequate proof of the soundness of the theory as a whole and of the correctness of the expressions of the stiffness and mass matrices derived here.

## 8.5 Calculations for Ring-Stiffened Shells

A particular ring-stiffened cylindrical shell with clamped ends is analysed. This shell was first studied, theoretically and experimentally, by Weingarten (50) and, subsequently, also by Sewall and Naumann (11). The shell data are as follows: $r = 3.03$ in., $t = 0.06$ in., $L = 5.375$ in., $E = 10^7$ lb./in.$^2$, $\nu = 0.315$ and $\rho = 2.54 \times 10^{-4}$ lb. sec$^2$/in.$^4$. The 'rings', eleven in number, are actually integral with the shell in the form of external ribs of height 0.095 in. (measured from the shell mean radius), of width 0.125 in. each, and equispaced at a pitch of 0.50 in.

* It is possible, of course, that the better agreement is fortuitous, arising from the difficulty of obtaining truly a clamped boundary condition in the experiments.

Weingarten (50) neglecting rotary inertia effects, derived a Donnell-type vibration equation for a general orthotropic conical shell, so that the cylindrical configuration is a particular case. He then reduced the ring-stiffened shell to an equivalent orthotropic shell using Bodner's method. The free vibration characteristics of this equivalent shell were then determined by application of the Galerkin method, using matrix iteration techniques.

Sewall and Naumann's (11) method of analysis has already been outlined. In dealing with stiffened shells (mainly with axial stiffeners) they assumed the stiffeners to be sufficiently closely spaced for their effect to be averaged, or 'smeared' as they put it, over the whole shell surface; eccentricity effects are explicitly taken into account.

In the calculations done by our theory the shell was divided into 23 finite elements, each corresponding alternately to stiffened and unstiffened portions of the shell. The difference in mean radii of stiffened and unstiffened sections was taken into account.

The natural frequencies of both the stiffened and the 'unstiffened' shell were calculated, the latter being a uniform shell with the rings obliterated, for $n = 2$ to $14$ and $m = 1,2,3 \ldots 4(N+1)-J$.

The results for the unstiffened shell are shown in figure 18 for m = 1,2 and 3 where they are compared with Weingarten's theoretical and experimental results. Agreement with both Weingarten's theory and experiments is fairly good.

The results for the stiffened shell are shown in figures 19 - 21, where they are compared with Weingarten's theory and experiments and with Sewall and Naumann's theory. We note that the theories of (11) and (50) are in close agreement, but they both somewhat overestimate the frequencies, particularly at high n - assuming, of course, that the experimental values are correct. This theory, on the other hand, is in considerably closer agreement with the experiments.*

8.6 Calculations for Shells with Thickness Discontinuity

The particular shells considered here are made up of a length $L_1$ of uniform thickness $t_1$ and a length $L_2$ of uniform thickness $t_2 > t_1$ and a constant mean radius over the total length L; they are simply-supported. The free vibration characteristics of such shells were recently studied theoretically by Warburton and Al-Najafi (51) and both theoretically and experimentally by Falkiewicz (52).

Falkiewicz's theoretical results were not available to the authors at the time of writing and will not be discussed. Warburton and Al-Najafi presented two theories.

* See footnote on p. 89.

One is based on a classical theory which has been used by Warburton previously for uniform shells, and is extended in (51) to deal with shells with a thickness discontinuity by using appropriate continuity conditions at the intersection of the two segments. Their second method is a finite-element method employing ring-type elements with displacement functions which are polynomials in x and trigonometric functions in $n\varphi$.

Calculations for three different steel shells were undertaken in (51) involving different $t_1$ and $t_2$, for various values of $L_1/L$ and some values of n and m. Here only two of the cases are analysed, one with $t_1 = 0.1875$ in. and the other with $t_1 = 0.125$ in., and both with $r = 2.073$ in., $L = 17.56$ in. and $t_2 = 0.25$ in.; attention was focused on only those of the cases presented in (51) where there were appreciable discrepancies between theory and experiment.

The calculations by our theory were done using 20 finite elements throughout. The results are shown in figures 22 - 24 where they are compared with Warburton and Al-Najafi's theoretical results and Falkiewicz's experimental results. In figure 22, where $t_1 = 0.1875$ in., the finite-element calculations of (51) were done using nine or ten finite elements. In figure 23, where $t_1 = 0.125$ in. and $n = 4$, the corresponding calculations of (51) were done with 25 finite elements; in this case the dashed line for m = 1 is not shown as it essentially coincides with the full one, i.e. the results of the two finite-element theories coincide. Finally, in figure 24, where $t_1 = 0.125$ in. and n = 5, the finite-element calculations of (51) were done using ten elements. This figure also shows the frequencies for m = 3 and 4 which are not available in (51).

We note that in most cases the classical shell theory of (51) agrees well with the experiments; that theory, however, was only used to obtain frequencies for a limited range of $L_1/L$. The agreement with the finite-element method of (51), on the other hand, is generally not as good. The results obtained by our theory are seen to be generally in quite good agreement with the classical theory of (51) and also with the experiments of (52), with some notable exceptions. Thus for m = 1 and n = 2 (figure 10), n = 4 (figure 23), and n = 5 (figure 24), the experimental points for $L_1/L < 0.25$ are at variance with all theories, which throws some doubt on these specific measurements. There are also some discrepancies between our theory and the classical theory of (51), for $L_1/L < 0.125$ and m = 1 in figure 24, which remain unexplained.

It may be said that, on the whole, the frequencies obtained by this theory are superior to those calculated by the finite-element theory of (51). The reason for this lies in the better choice of displacement functions, and also because in figures 22 and 24 more finite elements were employed. However, our theory has been shown to yield equally good results for any set of boundary conditions; this is not generally true with ordinary type of finite-element theories.

It is also noted that the computational task for the full analysis is comparable in the two finite-element methods. Thus for ten elements both Warburton and Al Najafi's matrices and ours are of order 40 x 40. However, in (51) the problem is reduced prior to calculation, by Guyan's method, by expressing u, v and dw/dx in terms of w; this reduces the 40 x 40 matrices to order 9 x 9, but raises the frequencies, as additional constraints are thus imposed on the system.

Now comparing the classical theory of (51) with our theory it is noted that they yield comparable results. Accordingly, there is no advantage either way, for this particular shell. However, in dealing with a shell with several discontinuities, or a ring-stiffened shell such as the one of the previous section, Warburton and Al Najafi's analysis, or any other truly classical theory, would have to be reformulated for the particular shell at hand. Our theory, on the other hand, because it employs the finite-element framework, requires no special reformulation.

## 8.7 Calculations for Shells Completely or Partially Filled with Liquid

A particular simply-supported cylindrical shell partially filled with water is analysed. The free vibration characteristics of such a shell were studied experimentally by Lindholm et al. (36). Based on the theory discussed in section 5.3, Lindholm et al. (36) developed a frequency equation for the completely liquid filled tank, using incompressible theory for the fluid, in an unpressurized circular cylindrical shell. Also experimental data was obtained in (36) in order to determine the effect of the liquid on frequency at partial liquid depths. The shell data are as follows: $r = 1.48425$ in., $t = 0.0090157$ in., $L = 9.2126$ in., $E = 0.29 \times 10^8$ lb./in.$^2$, $\nu = 0.29$, $\rho = 0.75017 \times 10^{-3}$ lb.sec.$^2$/in.$^4$ and $\rho_F = 0.096066 \times 10^{-3}$ lb.sec.$^2$/in.$^4$.

The investigations made in (36) involve different values of b/L (= 0, 0.25, 0.5, 0.75, 1.0), where b is the depth of liquid, and some values of n and m. The calculations by our theory were done using 10 finite elements and with b/L = 0.0, 0.125, 0.25, 0.375, 0.5, 0.625, 0.75, 1.0. The results are shown in figures 25 - 33.

Our theoretical results are plotted on figures 25 - 27 for m = 1,2 and 3. We note that for m = 1 all the curves have same form, with the change of curvature of the curves occurring at a fractional depth of about 1/4. As shown in figures 28-30, agreement between the present theory and experiment of (36) is seen to be relatively good. Also, it can be seen that the natural frequencies decrease significantly with the liquid depth.

On the other hand, figures 31 - 33 show the modal shapes of the system for $n = 5$, and $m = 1,2$, and 3 for the empty, 1/4-, 1/2-, 3/4-, and completely-filled shells. It is clear that the peaks of the displacements tend to shift towards the base of the tank as the depth is decreased (but non-zero).

However, for the cases of an empty ($b/L = 0.0$) or a full shell ($b/L = 1$), the modal shapes are theoretically the same. But for the experimental modes ($m = 3$ and 4) reported in (36), difference was noted between the shapes corresponding to the empty and full cases. This difference according to Lindholm et al. (36) is "not felt to be significant because of the difficulty in obtaining a clean mode shape at the higher frequencies".

## 8.8 Calculations of the r.m.s. Response for Shells Subjected to Subsonic Boundary Layer Pressure Fluctuations

As developed in Chapter VI, the present theory is capable of determining the r.m.s. response for the most general case: axially non-uniform, thin cylindrical shells, subjected to subsonic boundary layer pressure fluctuations with arbitrary boundary conditions, are within the capabilities of the computer program described in Chapter VII.

However, due to the high computational cost of this analysis (cf. Chapter VII), only one case of a simply-supported uniform shell was treated. The free vibration characteristics of this particular shell was studied in section 8.4. From figures 14a and 14b, it is clear that an idealization of 5 elements is sufficient to yield reasonably accurate results for low as well as high natural frequencies.

The shell dimensions and material properties are as follows: $r = 4.08$ in., $t = 0.047$ in., $L = 18.54$ in., $E = 3 \times 10^7$ lb./in.$^2$, $\nu = 0.3$ and $\rho = 7.324 \times 10^{-4}$ lb.-sec.$^2$/in.$^4$.

The fluid is air at 70°F and atmospheric pressure, flowing through the shell. The fluid properties are: $\rho_F = 0.23292 \times 10^{-2}$ lb.sec.$^2$/ft.$^4$, $\mu = 0.038 \times 10^{-5}$ lb.sec./ft.$^2$, and $\nu_F = 1.63147 \times 10^{-4}$ ft.$^2$/sec..

The first case studied was for mean centreline velocity of 24 ft./sec. corresponding to $Re = 10^5$ and a damping factor of $\zeta_n = 10^{-5}$. The results of maximum r.m.s. response for n = 2,3,4 and 5 are shown in figure 34. The peak values for $\left(\sqrt{\overline{v_n^2}}\right)_{max.}$, $\left(\sqrt{\overline{u_n^2}}\right)_{max.}$ and $\left(\sqrt{\overline{w_n^2}}\right)_{max.}$ are at n = 3. This confirms the theoretical derivations as obtained in equation (6.14) where the r.m.s. response is inversely proportional to the square of the natural frequency, $f_r$.

It is evident, therefore, that the r.m.s. response of interest, for this particular case, is at n = 3. Consequently all subsequent calculations will be confined to this particular value of the circumferential wave-number.

Figure 35 shows the r.m.s. response for different mean velocities, namely 24, 75, 120 and 240 ft./sec., using $\varphi_n = 10^{-5}$ and $10^{-2}$ as damping factors. It is seen, from the results plotted in figure 35, that the r.m.s. displacement is inversely proportional to the damping factor and proportional to the mean axial flow velocity raised approximately to a power 2, both effects being as could have been anticipated.

Unfortunately, in this case no experimental results are available to check the theory.

# CHAPTER IX

## CONCLUSION

The accuracy of the finite-element method depends primarily on the number and size of the finite elements into which the structure is divided. Good accuracy can generally be obtained with a sufficiently large number of small elements.

The optimum degree of approximation in the element stiffness and mass matrices will depend on many factors, the most important perhaps being the choice of the displacement functions and the degree to which they satisfy the convergence criteria of the finite-element method. (Here we do not mean numerical convergence but absolute convergence to the continuum.) The usual type of displacement functions are polynomials of the type

$$U = C_1 + C_2 x,$$
$$W = C_3 + C_4 x + C_5 x^2 + C_6 x^3,$$

(15) - (17), (20) and (22) - (25). Such displacement functions can never exactly satisfy the convergence criteria, but may satisfy them approximately if a sufficiently large number of small finite elements is used.

In this work the displacement functions are derived from the equations of thin cylindrical shells based on Sanders' theory. As Sanders showed (8), for small rigid-body motions the strains all vanish for his theory, while they do not if the strain-displacement relations are taken as given by Love (2), or Novozhilov (27), for instance. This is because the sixth equation of motion (A.5) is violated in all but Sanders' theory. Flügge puts the matter as follows: "There is one point of fundamental interest which may be discussed at once. In the simplified formulas the difference between the shearing forces $N_{\varphi x}$ and $N_{x\varphi}$ has disappeared. The sixth condition of equilibrium, ($rN_{x\varphi} - rN_{\varphi x} + M_{\varphi x} = 0$), is therefore no longer satisfied if $M_{\varphi x} \neq 0$, which is generally the case. This violation of one of the fundamental principles of mechanics is a serious drawback for all theory founded thereon. In most cases, small and otherwise insignificant changes of $N_{\varphi x}$ and $N_{x\varphi}$ will be sufficient to adjust the equilibrium, but during the mathematical handling of the equations it may happen that the large terms cancel and just the small ones become decisive."

The difficulties anticipated by Flügge were by-passed in this work by the use of Sanders' theory. As was shown in Chapter VIII no strains are induced by rigid-body motions, as evidenced by the fact that the frequencies associated with rigid-body motions of a free-free element are zero. Accordingly, one of the main practical difficulties associated with the use of the finite-element method, is absent from this theory.

The hybrid finite-element, classical theory developed in this thesis has been used, with considerable success, to obtain the free vibration characteristics of a variety of uniform and non-uniform circular cylindrical shells, empty and partially or completely filled with liquid. The data obtained was compared with that of other theories and experiments. If one accepts the validity and precision of the available experimental data for the shells used, then it may be stated that this theory is, in general, more successful than at least some of the others already referred to in this Thesis. This is hardly surprising if one considers that it is basically a classical theory put on a finite-element framework for the sake of versatility. Moreover, the shell equations employed, which are solved for the determination of the displacement functions, are such that the convergence criteria of the finite-element method are satisfied.

It is clear that this theory enjoys at once the advantages of the finite-element method and the precise formulation of classical shell theory. Yet the difficulties often encountered by classical analysis with certain boundary conditions (e.g. clamped-free), even for uniform shells, are absent here. Also the computational difficulties in classical analysis arising from the vanishing determinant of the boundary conditions, which contains both large and small terms of the type $e^{\pm \lambda_j L/r}$, are not encountered here; difficulties due to such terms in this theory are easily overcome either by increasing N or by matrix manipulations.

Only a few cases have been presented here, a sufficient number, the author believes, to illustrate the capabilities of the theory. Several other cases could also have been tackled, but were not because of the computational cost. Thus shells with several discontinuities in thickness and material properties, conical shells, and non-isotropic shells can be easily analysed by this theory.

The second part of this thesis dealt with the response of thin circular cylindrical shells (uniform or axially non-uniform) when subjected to a random pressure field. The theory was developed in general for an arbitrary random pressure field, and in particular in the case where the pressure field arises from pressure fluctuations in the turbulent, subsonic boundary layer of an internally flowing fluid (air). This latter case was incorporated in the computer program, which also determines the free-vibration characteristics of the shell, and yields the r.m.s. response of the shell. One calculation was undertaken, the results of which appear to be reasonable; however, the absence of data precludes comparison with experiment.

This theory may also be applied to shells subjected to subsonic boundary-layer pressure fluctuations when the fluid is other than air, by using the values of the constants a,b,c and d given by expression (6.3). Further work on boundary-layer pressure fluctuations by Willmarth and Wooldridge (61), Willmarth and Roos (62) support the original measurements and assumptions made by Bakewell (39), (44) and used in this thesis.

The analysis of the random vibration of the shell is restricted to light damping ($\zeta_r << 1$); this restriction can be relaxed by considering the contribution of cross-product terms in equation (5.30). However, the results obtained here, for $\zeta_r << 1$, will still constitute an important part of the total solution. Finally, it is stressed that pressure correlation functions used in the analysis are applicable only for flow velocities corresponding to Mach number 0.3 or less; there is no assurance that such correlation functions can be applied at higher Mach numbers when compressibility effects become important.

## Future Work

This theory can of course only deal with geometrically axially-symmetric, non-uniform cylindrical and conical shells.

Nevertheless, considering the extensive literature on the topic, it is clear that the analysis of such shells is of considerable practical importance. Accordingly, the effort involved in producing a theory such as this, of superior precision and accuracy than existing theories, is deemed to be justified. Moreover, the success of this theory indicates that the basic approach adopted, namely using classical theory for the determination of the displacement functions, is both sound and practicable. Therefore, its extension to the more general case of curved-shell finite elements is envisaged, with which shells of any shape could be analysed with enhanced precision.

Another extension to this work will be to consider the effects of all the components arising from the presence of flowing or stationary fluids, on the natural frequencies for the cases of completely or partially-filled shells. Finally, it would be of interest to compare the theoretical r.m.s. response of this theory to experimental data which will hopefully become available in future.

## REFERENCES

(1) LOVE, A.E.H.
'A Treatise on the Mathematical Theory of Elasticity'
1944, 4th Edition, Chap. 24, (Dover, New York).

(2) GREEN, A.E. and ZERNA, W.
'Theoretical Elasticity'
1954, (Oxford University Press).

(3) REISSNER, E.
'A New Derivation of the Equations for the Deformation of Elastic Shells'
Amer. J. Math., 1941, 63, 177.

(4) VLASOV, V.S.
'Basic Differential Equations in General Theory of Elastic Shells'
NACA TM 1241, 1951.

(5) NAGHDI, P.M.
'On the Theory of Thin Elastic Shells'
Quart. Appl. Math., 1957, 14, 369.

(6) FLÜGGE, W.
'Stresses in Shells'
1960, (Springer-Verlag, Berlin).

(7) HEARMON, R.F.S.
'Introduction to Applied Anisotropic Elasticity'
1961, (Oxford University Press, London).

(8) SANDERS, J.L.
'An Improved First Approximation Theory for Thin Shells'
NASA-TR-R24, 1959.

(9) BUDIANSKY, B. and SANDERS, J.L.
'On the 'Best' First Order Linear Shell Theory'
Progress in Applied Mechanics, The Prager Anniversary Volume, 1963, (Macmillan, New York), pp. 129-140.

(10) NAUMANN, E.C.
'On the Prediction of Vibration Behaviour of Free-Free Truncated Conical Shells'
NASA TN D-4772, 1968.

(11) SEWALL, J.L. and NAUMANN, E.C.
'An Experimental and Analytical Vibration Study of Thin Cylindrical Shells with and without Longitudinal Stiffeners'
NASA TN D-4705, 1968.

(12) COHEN, G.A.
'Computer Analysis of Asymmetric Free Vibrations of Ring-Stiffened Orthotropic Shells of Revolution'
AIAA. J., 1965, 3, 2305.

(13) COOPER, P.A.
'Vibration and Buckling of Prestressed Shells of Revolution'
NASA TN D-3831, 1967.

(14) POPOV, E.P., PENZIEN, J. and LU, Z.A.
'Finite Element Solution for Axisymmetric Shells'
Proc. A.S.C.E. EM 5, 1964, 90, 119.

(15) JONES, R.E. and STROME, D.R.
'Direct Stiffness Method of Analysis of Shells of Revolution Utilizing Curved Elements'
AIAA. J., 1966, 4, 1519.

(16) PERCY, J.H., PIAN, T.H., KLEIN, S. and NAVARATNA, D.R.
'Application of Matrix Displacement Method to Linear Elastic Analysis of Shells of Revolution'
AIAA. J., 1965, 3, 2138.

(17) JONES, R.E. and STROME, D.R.
'A Survey of Analysis of Shells by the Displacement Method'
Proc. Conf. on Matrix Methods in Structural Mech., Air Force Inst. of Technology, Wright Patterson A.F. Base, Ohio, October 1965.

(18) WEBSTER, J.J.
'Free Vibrations of Shells of Revolution Using Ring Finite Elements'
Int. J. Mech. Sci., 1967, 9, 559.

(19) BACON, M.D. and BERT, C.W.
'Unsymmetrical Free Vibrations of Orthotropic Sandwich Shells of Revolution'
AIAA. J., 1967, 5, 413.

(20) ADELMAN, H.M., CATHERINES, D.S. and WALTON, W.D., Jr.
'A Method for Computation of Vibration Modes and Frequencies of Orthotropic Thin Shells of Revolution having General Meridional Curvature'
NASA TN D-4972, 1969.

(21) FORSBERG, K.
'Influence of Boundary Conditions on the Modal Characteristics of Thin Cylindrical Shells'
AIAA. J., 1964, 2, 2150.

(22) CLOUGH, R.L. and TOCHER, J.L.
'Analysis of Thin Arch Dams by the Finite Element Method'
Proc. Symposium on Theory of Arch Dams, Southampton University, 1964, (Pergamon Press, 1965).

(23) BAZELEY, G.P., CHEUNG, Y.K., IRONS, B.M. and ZIENKIEWICZ, O.C.
'Triangular Elements in Bending - Conforming and Non-conforming Solutions'
Proc. Conf. Matrix Methods in Struct. Mech., Air Force Inst. of Tech., Wright Patterson A.F. Base, Ohio, October 1965.

(24) ZIENKIEWICZ, O.C. and CHEUNG, Y.K.
'Finite Element Method of Analysis for Arch Dam Shells and Comparison with Finite Difference Procedures'
Proc. of Symposium on Theory of Arch Dams, Southampton University, 1964 (Pergamon Press, 1965).

(25) ZIENKIEWICZ, O.C. and CHEUNG, Y.K.
'The Finite Element Method in Structural and Continuum Mechanics'
1968, (McGraw-Hill, New York).

(26) TIMOSHENKO, S.
'Theory of Plates and Shells'
1959, (McGraw-Hill, New York).

(27) NOVOZHILOV, V.V.
'The Theory of Thin Shells'
1959, (Noordhoff, Groningen).

(28) HOUGHTON, D.S. and JOHNS, D.J.
'A Comparison of the Characteristic Equations in the Theory of Circular Cylindrical Shells'
Aero. Quart., 1961, <u>12</u>, 228.

(29) WASHIZU, K.
'Variational Methods in Elasticity and Plasticity'
1968, (Pergamon Press, London).

(30) KRAUSS, H.
'Thin Elastic Shells'
1967, (John Wiley and Sons, New York).

(31) COOLEY, W.W. and LOHNES, P.R.
'Multivariate Procedures for the Behavioral Sciences'
Chapter III, 1962, (John Wiley and Sons).

(32) BERRY, J.G. and REISSNER, E.
'The Effect of an Internal Compressible Fluid Column on the Breathing Vibrations of a Thin Pressurized Cylindrical Shell'
Journal of the Aerospace Sciences, 1958, <u>25</u>, 288.

(33) NIORDSON, F.I.N.
'Vibrations of a Cylindrical Tube Containing Flowing Fluid'
1953, Transactions of the Royal Institute of Technology, Stockholm, Sweden, No. 73.

(34) GREGORY, R.W. and PAIDOUSSIS, M.P.
'Unstable Oscillation of Tubular Cantilevers Conveying Fluid - I. Theory'
Proc. Roy. Soc., 1966, 293(A), 512.

(35) PAIDOUSSIS, M.P. and DENISE, J.P.
'Instabilities of Cylindrical Shells Containing Flow'
1970, M.E.R.L. T.N. 70-5, McGill University.

(36) LINDHOLM, U.S., KANA, D.D., and ABRAMSON, H.N.
'Breathing Vibrations of a Circular Cylindrical Shell with an Internal Liquid'
Journal of the Aerospace Sciences, 1962, 29, 1052.

(37) FUNG, Y.C., SECHLER, E.E. and KAPLAN, A.
'On the Vibration of Thin Cylindrical Shells under Internal Pressure'
Journal of the Aeronautical Sciences, 1957, 24, 650.

(38) BOZICH, D.J.
'Spatial-Correlation in Acoustic-Structural Coupling'
J. Acoust. Soc. Amer., 1964, 36, 52.

(39) BAKEWELL, H.P. Jr., CAREY, G.F., LIBUHA, J.J., SCHLOEMER, H.H. and VONWINKLE, W.A.
'Wall Pressure Fluctuations in Turbulent Pipe Flow'
U.S. Navy Underwater Sound Lab. Dept., No. 559, 1962.

(40) SMITH, M.W. and LAMBERT, R.F.
'Propagation of Band Limited Noise'
Acoust. Soc. Amer., 1960, 32, 512.

(41) WILLMARTH, W.W.
'Wall Pressure Fluctuations in a Turbulent Boundary Layer'
NACA TN-4139, 1958.

(42) WEYERS, P.F.R.
'Vibration and Near-Field Sound of Thin-Walled Cylinders Caused by Internal Turbulent Flow'
NASA TN-D-430, 1960.

(43) CORCOS, G.M. and LIEPMANN, H.W.
'On the Contribution of Turbulent Boundary Layers to the Noise Inside a Fuselage'
NACA TM-1420, 1956.

(44) BAKEWELL, H.P. Jr.
'Narrow-Band Investigations of the Longitudinal Space-Time Correlation Function in Turbulent Airflow'
J. Acoust. Soc. Amer., 1964, 36, 146.

(45) COTTIS, M.G. and JASONIDES, J.G.
'The Response of a Finite Thin Cylindrical Shell to Random Pressure Fields'
Acoustical Fatigue in Aerospace Structures: Proceedings of the Second International Conference, Conference sponsored by USAF, Materials Lab., Dayton, Ohio, April 29th - May 1st, 1964.

(46) MICHALOPOULOS, C.D. and MUSTER, D.
'The in-vacuo Vibrations of a Simply Supported, Ring-stiffened, Mass-loaded Cylindrical Shell'
1967, Proc. Symposium on the Theory of Shells, Edited by D. Muster, University of Houston, p. 345.

(47) ARNOLD, R.N. and WARBURTON, G.B.
'Flexural Vibrations of the Walls of Thin Cylindrical Shells having Freely Supported Ends'
Proc. Roy. Soc. (A), 1949, 197, 238.

(48) BARON, M.L. and BLEICH, H.H.
'Tables of Frequencies and Modes of Free Vibration of Infinitely Long Thin Cylindrical Shells'
J. Appl. Mech., 1954, 21, 178.

(49) GALLETLY, G.D.
'On the in-vacuo Vibrations of Simply Supported, Ring-stiffened Cylindrical Shells'
Proc. 2nd (U.S.) Nat. Congr. Appl. Mech., 1954, 225.

(50) WEINGARTEN, V.I.
'Free Vibrations of Ring-stiffened Conical Shells'
A.I.A.A. J., 1965, 3, 1475.

(51) WARBURTON, G.B. and AL-NAJAFI, A.M.J.
'Free Vibration of Thin Cylindrical Shells with a Discontinuity in the Thickness'
J. Sound Vib., 1969, 9, 373.

(52) FALKIEWICZ, A.T.
'Vibration of Thin Cylindrical Shells of Variable Thickness'
1952, Ph.D. Thesis, University of Edinburgh.

(53) POWELL, A.
'On the Fatigue Failure of Structures due to Vibrations Excited by Random Pressure Fields'
J. Acoust. Soc. Amer., 1958, 30, 1130.

(54) POWELL, A.
'On the Approximation to the "Infinite" Solution by the Method of Normal Modes for Random Vibrations'
J. Acoust. Soc. Amer., 1958, 30, 1136.

(55) TACK, D.H. and LAMBERT, R.F.
'Response of Bars and Plates to Boundary-Layer Turbulence'
J. of Aerospace Sciences, 1962, 29, 311.

(56) BURGREEN, D. et al.
'Vibration of Rods Induced by Water in Parallel Flow'
Trans. ASME, 1958, 80, 991.

(57) REAVIS, J.R.
'WVI-Westinghouse Vibration Correlation for Maximum Fuel Element Displacement in Parallel Turbulent Flow'
Trans. Am. Nucl. Soc., 1967, 10, 369.

(58) PAIDOUSSIS, M.P. and DENISE, J.P.
'Flutter of Cylindrical Shells Conveying Fluid'
A paper submitted for publication to J. Sound Vib. (Feb. 1971).

(59) LAKIS, A.A.
'Cylindrical Finite Elements for Analysis of Cylindrical Structures'
M.Eng. Thesis, 1969, McGill University.

(60) MERCER, C.A. and HAMMOND, J.K.
'On the Representation of Continuous Random Pressure Fields at a Finite Set of Points'
J. Sound Vib., 1968, 7, 49.

(61) WILLMARTH, W.W. and WOOLDRIDGE, C.E.
'Measurements of the Fluctuating Pressure at the Wall Beneath a Thick Turbulent Boundary Layer'
J. Fluid Mech., 1962, 14, 187.

(62) WILLMARTH, W.W. and ROOS, F.W.
'Resolution and Structure of the Wall Pressure Field Beneath a Turbulent Boundary Layer'
J. Fluid Mech., 1965, 22, 81.

## APPENDIX A

## SANDERS' THEORY OF SHELLS

### A.1 The Coordinate System

The location of a point of the shell is given by three parameters, two of which are along the middle surface of the shell and the third along the normal to the middle surface. The condition we impose on the parametric curves is that they form a three-dimensional orthogonal system (see figure 4).

To describe the location of an arbitrary point in the space occupied by a thin shell, we define the following position vector (see figures 4 and 5):

$$\underline{R}(\xi_1, \xi_2, \zeta) = \underline{r}(\xi_1, \xi_2) + \zeta \underline{n}(\xi_1, \xi_2) \qquad \text{(A.1)}$$

where $\underline{r}$ is the position vector of a corresponding point on the reference surface, $\underline{n}$ is the unit vector from the reference surface to the point in question, $\xi_1$ = constant and $\xi_2$ = constant are the parametric curves which follow the lines of principal curvature of the shell on the middle surface, and $\zeta$ is the distance of the point from the middle surface measured along the unit normal vector $\underline{n}$. All of the necessary concepts and results from differential geometry are developed in (29) and (30).

A.2 Equations of Motion

Consider an element of the shell bounded by surfaces $\xi$ = constant, $\xi + d\xi$ = constant, and $\zeta = \pm t/2$. Forces and moments acting on all six faces must be in equilibrium (see figure 6). We denote by $\underline{N}$ the force resultants and by $\underline{M}$ the moment resultants, per unit of length measured along the parametric curves on the middle surface. By $\underline{q}$ we denote the external force per unit of area of the middle surface.

We may use Hamilton's principle for the derivation of the equations of motion of a thin elastic shell because it gives us, at the same time, the natural boundary conditions that are to be used with the theory.

Hamilton's principle states that the actual path followed by a dynamical process is such as to make

$$\delta \int_{t_0}^{t_1} (\pi - K)\, dt = 0 , \tag{A.2}$$

where $\pi$ is the potential energy, and $K$ is the kinetic energy. If the process is steady, the above principle reduces to the principle of minimum potential energy, or

$$\delta \pi = 0 \quad , \quad \pi = \text{minimum}, \tag{A.3}$$

For a thin elastic shell this may be written in the form

$$\delta\int_{t_0}^{t_1}(U - W_S - W_{\xi_1} - W_{\xi_2} - K)\,dt = 0, \tag{A.4}$$

where U is the strain energy, $W_S$ is the work of the body and surface forces, $W_{\xi_1}$ and $W_{\xi_2}$ represent the work of the edge stresses on edges of constant $\xi_1$ and $\xi_2$, respectively, and K is the kinetic energy. The development of the equations of static equilibrium from (A.4) can be found in many papers, e.g. (29), (30), (3). Here we only list the final six scalar equations of motion, as follows:

$$\begin{aligned}
&\frac{\partial A_2 N_{11}}{\partial \xi_1} + \frac{\partial A_1 N_{21}}{\partial \xi_2} + N_{12}\frac{\partial A_1}{\partial \xi_2} - N_{22}\frac{\partial A_2}{\partial \xi_1} + \frac{A_1 A_2}{R_1} Q_1 = 0\,, \\
&\frac{\partial A_2 N_{12}}{\partial \xi_1} + \frac{\partial A_1 N_{22}}{\partial \xi_2} + N_{21}\frac{\partial A_2}{\partial \xi_1} - N_{11}\frac{\partial A_1}{\partial \xi_2} + \frac{A_1 A_2}{R_2} Q_2 = 0\,, \\
&\frac{\partial A_2 Q_1}{\partial \xi_1} + \frac{\partial A_1 Q_2}{\partial \xi_2} - A_1 A_2\left(\frac{N_{11}}{R_1} + \frac{N_{22}}{R_2}\right) = 0\,, \\
&\frac{\partial A_2 M_{11}}{\partial \xi_1} + \frac{\partial A_1 M_{21}}{\partial \xi_2} + \frac{\partial A_1}{\partial \xi_2} M_{12} - \frac{\partial A_2}{\partial \xi_1} M_{22} - A_1 A_2 Q_1 = 0\,, \\
&\frac{\partial A_2 M_{12}}{\partial \xi_1} + \frac{\partial A_1 M_{22}}{\partial \xi_2} + \frac{\partial A_2}{\partial \xi_1} M_{21} - \frac{\partial A_1}{\partial \xi_2} M_{11} - A_1 A_2 Q_2 = 0\,, \\
&N_{12} - N_{21} + \frac{M_{12}}{R_1} - \frac{M_{21}}{R_2} = 0\,.
\end{aligned} \tag{A.5}$$

(figure 6), where distributed load terms have been omitted for simplicity.

In the usual derivation of the equations based on Love's first approximation, the distinction between $M_{12}$ and $M_{21}$ is dropped and the last of equations (A.5) is suppressed. Accordingly, most theories violate this equation, unless the shell is spherical, or a flat plate, or if it is a symmetrically loaded shell of revolution. This is not the case with Sanders' theory; consequently, as is shown in (8), all strains vanish for small rigid-body motions. Accordingly, if we select displacement functions based on this theory, we should expect to be able to satisfy the convergence criteria of the finite-element method.

We now consider a circular cylindrical shell and express the movement of the middle surface in terms of the axial, tangential and radial displacements, U,V and W, respectively. In equations (A.5) we now have

$$\left.\begin{aligned} &\xi_1 = x \;, \; U_1 = U \;, \; R_1 = \infty \;, \; A_1 = 1 \;, \\ &\xi_2 = \varphi \;, \; U_2 = V \;, \; R_2 = r \;, \; A_2 = r \,. \end{aligned}\right\} \qquad \text{(A.6)}$$

The modified strain-displacement relations are given by

$$\left.\begin{aligned} &\epsilon_x = \frac{\partial U}{\partial x} \;, \qquad \kappa_x = -\frac{\partial^2 W}{\partial x^2} \;, \\ &\epsilon_\varphi = \frac{1}{r}\frac{\partial V}{\partial \varphi} + \frac{W}{r} \;, \quad \kappa_\varphi = -\frac{1}{r^2}\frac{\partial^2 W}{\partial \varphi^2} + \frac{1}{r^2}\frac{\partial V}{\partial \varphi} \;, \\ &\epsilon_{x\varphi} = \frac{1}{2}\left(\frac{\partial V}{\partial x} + \frac{1}{r}\frac{\partial U}{\partial \varphi}\right) , \; \kappa_{x\varphi} = -\frac{1}{r}\frac{\partial^2 W}{\partial x \partial \varphi} + \frac{3}{4r}\frac{\partial V}{\partial x} - \frac{1}{4r^2}\frac{\partial U}{\partial \varphi} . \end{aligned}\right\} \qquad \text{(A.7)}$$

The appropriate set of stress-strain relations (see figure 1b) are given by

$$\left.\begin{array}{ll} N_x = D(\epsilon_x + \nu\epsilon_\varphi) \;, & M_x = K(\kappa_x + \nu\kappa_\varphi) , \\ N_\varphi = D(\epsilon_\varphi + \nu\epsilon_x) \;, & M_\varphi = K(\kappa_\varphi + \nu\kappa_x) , \\ \bar{N}_{x\varphi} = D(1-\nu)\epsilon_{x\varphi} \;, & \bar{M}_{x\varphi} = K(1-\nu)\bar{\kappa}_{x\varphi} , \end{array}\right\} , \qquad \text{(A.8)}$$

where $\bar{N}_{x\varphi} = \frac{1}{2}(N_{x\varphi} + N_{\varphi x})$ and $\bar{M}_{x\varphi} = \frac{1}{2}(M_{x\varphi} + M_{\varphi x})$; for an isotropic elastic material, the stiffness parameters K and D are given by

$$K = Et^3/12(1-\nu^2), \qquad D = Et/(1-\nu^2). \qquad \text{(A.9)}$$

Upon substituting (A.6), (A.7) and (A.8) into (A.5), after considerable manipulation, one obtains the equations of equilibrium in terms of U,V and W, namely (8)

$$\left.\begin{array}{l} r^2\frac{\partial^2 U}{\partial x^2} + \frac{(1-\nu)}{2}\frac{\partial^2 U}{\partial\varphi^2} + \frac{r(1+\nu)}{2}\frac{\partial^2 V}{\partial x\partial\varphi} + r\nu\frac{\partial W}{\partial x} + k\Big[\frac{(1-\nu)}{8}\frac{\partial^2 U}{\partial\varphi^2} \\ \quad - \frac{3(1-\nu)}{8}r\frac{\partial^2 V}{\partial x\partial\varphi} + \frac{(1-\nu)}{2}r\frac{\partial^3 W}{\partial x\partial\varphi^2}\Big] \qquad = 0, \\ \frac{(1+\nu)r}{2}\frac{\partial^2 U}{\partial x\partial\varphi} + \frac{\partial^2 V}{\partial\varphi^2} + \frac{(1-\nu)r^2}{2}\frac{\partial^2 V}{\partial x^2} + \frac{\partial W}{\partial\varphi} + k\Big[-\frac{3(1-\nu)r}{8}\frac{\partial^2 U}{\partial x\partial\varphi} \\ \quad + \frac{9}{8}(1-\nu)r^2\frac{\partial^2 V}{\partial x^2} + \frac{\partial^2 V}{\partial\varphi^2} - \frac{(3-\nu)r^2}{2}\frac{\partial^3 W}{\partial x^2\partial\varphi} - \frac{\partial^3 W}{\partial\varphi^3}\Big] \qquad = 0, \\ -\nu r\frac{\partial U}{\partial x} - \frac{\partial V}{\partial\varphi} - W + k\Big[\frac{(\nu-1)r}{2}\frac{\partial^3 U}{\partial x\partial\varphi^2} + \frac{(3-\nu)r}{2}\frac{\partial^3 V}{\partial x^2\partial\varphi} \\ \quad + \frac{\partial^3 V}{\partial\varphi^3} - r^4\frac{\partial^4 W}{\partial x^4} - 2r^2\frac{\partial^4 W}{\partial x^2\partial\varphi^2} - \frac{\partial^4 W}{\partial\varphi^4}\Big] \qquad = 0, \end{array}\right\} \qquad \text{(A.10)}$$

where $k = (1/12)(t/r)^2$.

For an edge of constant x, the boundary conditions are given by specified values of the following quantities

$$\left.\begin{aligned}
\bar{\bar{N}}_x &= N_x \quad \text{or} \quad \bar{\bar{U}} = U\,, \\
\bar{\bar{T}}_{x\varphi} &= \bar{N}_{x\varphi} + \frac{3}{2r}\bar{M}_{x\varphi} \quad \text{or} \quad \bar{\bar{V}} = V\,, \\
\bar{\bar{V}}_x &= Q_x + \frac{1}{r}\frac{\partial \bar{M}_{x\varphi}}{\partial \varphi} \quad \text{or} \quad \bar{\bar{W}} = W\,, \\
\bar{\bar{M}}_x &= M_x \quad \text{or} \quad \overline{\overline{\left(\frac{\partial W}{\partial X}\right)}} = \frac{\partial W}{\partial X}\,.
\end{aligned}\right\} \tag{A.11}$$

where the double-barred quantities refer to the boundary values.

# APPENDIX B

## List of Matrices

This appendix contains the matrices referred to in the text which were too large to be included therein.

The matrices are listed as follows:

| | |
|---|---|
| [R], [T] | in Table 1 |
| [A] | " " 2 |
| [Q] | " " 3 |
| [Γ] | " " 4 |
| [Δ], [Z] | " " 5 |
| [ZY]* | " " 6 |
| $[A_1]$, $[B_1]$, $[C_1]$ | " " 7 |
| $[D_1]$, $[D_2]$, $[D_3]$, $[D_4]$* | " " 8 |
| $[Q_i]$ | " " 9 |

The matrices [ZJ] and $[E_1]$, $[E_2]$, $[E_3]$, $[E_4]$ are obtained respectively, from matrices [ZY] and $[D_1]$, $[D_2]$, $[D_3]$, $[D_4]$ by substituting in these matrices the elements of matrix $[Y] = [\Gamma]^T[P][\Gamma]$ by the elements of matrix $[RJ] = [\Delta]^T[\Delta]$.

The matrix $[Q_j]$ is obtained from matrix [Q] by substituting in this matrix $\psi_1$, $\psi_2$, $\zeta_1$, $\zeta_2$ by $\omega_1$, $\omega_2$, $\eta_1$, $\eta_2$,

---

* $y_{ij}$ in these matrices are elements of the [Y] matrix given above.

respectively, where these terms are defined in Table 4.

# APPENDIX C

## EVALUATION OF SOME INTEGRALS OF CHAPTER VI

### C-1 Evaluation of the Integrals given by Equations (6.6) - (6.8)

$$P_1 = \int_0^{2\pi}\int_0^{2\pi} \Psi_{p,f_o,Re}(0,\eta,0).\cos(\varphi).\cos(\varphi').\,d\varphi.d\varphi', \qquad (C.1)$$

$$P_2 = \int_0^{2\pi}\int_0^{2\pi} \Psi_{p,f_o,Re}(0,\eta,0).\sin(\varphi).\sin(\varphi').d\varphi.d\varphi', \qquad (C.2)$$

$$P_3 = \int_0^{2\pi}\int_0^{2\pi} \Psi_{p,f_o,Re}(0,\eta,0).\cos(\varphi).\sin(\varphi').d\varphi.d\varphi', \qquad (C.3)$$

where $\Psi_{p,f_o,Re}(0,\eta,0) = \left(1+c\,S_\eta^2\right)^{-1}.\left(2-e^{-d\,S_\eta^2}\right)^{-1}$ and

$$S_\eta = f_o\eta/U_{\not{c}} = f_o r(\varphi-\varphi')/U_{\not{c}} .$$

Equation (C.1) can be written as

$$P_1 = \int_0^{2\pi}\cos(\varphi)\,d\varphi\int_0^{2\pi}\frac{\cos(\varphi')\,d\varphi'}{\left[1+C_3(\varphi-\varphi')^2\right]\left[2-e^{-D_3(\varphi-\varphi')^2}\right]}, \qquad (C.4)$$

where $C_3 = c\,f_o^2 r^2/U_{\not{c}}^2$ and $D_3 = d\,f_o^2 r^2/U_{\not{c}}^2$.

Consider $$\omega_R = \int_0^{2\pi}\frac{e^{i\varphi'}\,d\varphi'}{\left[1+C_3(\varphi-\varphi')^2\right].\left[2-e^{-D_3(\varphi-\varphi')^2}\right]}$$ and let

$z = e^{i\varphi'}$, where $i = \sqrt{-1}$. Then

$dz = iz\,d\varphi'$, $\varphi' = -i\ln z$ such that

$$w_R = \frac{1}{i}\oint_{C'} \frac{dz}{\left[1 + C_3(\varphi + i\ln z)^2\right]\left[2 - e^{-D_3(\varphi + i\ln z)^2}\right]}, \qquad \text{(C.5)}$$

where C' is the circle of unit radius with center at the origin 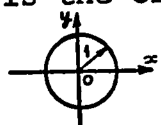 . The integrand (C.5) has simple poles at

$$1 + C_3(\varphi + i\ln z)^2 = 0, \quad \text{or} \quad z = e^{i\varphi}e^{\pm 1/\sqrt{C_3}}, \qquad \text{(C.6)}$$

and other simple poles at

$$2 - e^{-D_3(\varphi + i\ln z)^2} = 0, \qquad z = e^{i\varphi}e^{\pm\sqrt{\ln 2/D_3}}. \qquad \text{(C.7)}$$

Finally, the integrand has a simple pole at

$z = e^{i\varphi}e^{\pm 1/\sqrt{C_3}}$ and at $z = e^{i\varphi}e^{\pm\sqrt{\ln 2/D_3}}$ ; however

only $z = e^{i\varphi}e^{-1/\sqrt{C_3}}$ and $z = e^{i\varphi}e^{-\sqrt{\ln 2/D_3}}$

lie inside C'.

$$\left\{\begin{matrix}\text{Residue of } i w_R \\ \text{at } e^{i\varphi}e^{-1/\sqrt{C_3}}\end{matrix}\right\} = \lim_{z \to e^{i\varphi - 1/\sqrt{C_3}}} \left\{ \frac{\left(z - e^{i\varphi}e^{-1/\sqrt{C_3}}\right)}{\left[1 + C_3(\varphi + i\ln z)^2\right]\left[2 - e^{-D_3(\varphi + i\ln z)^2}\right]} \right\} \qquad \text{(C.8)}$$

$$= \frac{e^{i\varphi}\, e^{-1/\sqrt{C_3}}}{2\sqrt{C_3}\left[2 - e^{D_3/C_3}\right]},$$

and

$$\left\{\begin{matrix}\text{Residue of } i\omega_R \\ \text{at } e^{i\varphi}\, e^{-\sqrt{\ln 2/D_3}}\end{matrix}\right\} = \frac{e^{i\varphi}\; e^{-\sqrt{\ln 2/D_3}}}{4\sqrt{D_3 \ln 2}\left[1-\frac{C_3}{D_3}\ln 2\right]} \,. \tag{C.9}$$

Then, equation (C.5) becomes

$$\omega_R = 2\pi e^{i\varphi}\left\{\frac{e^{-1/\sqrt{C_3}}}{2\sqrt{C_3}\left[2-e^{D_3/C_3}\right]} + \frac{e^{-\sqrt{\ln 2/D_3}}}{4\sqrt{D_3\ln 2}\left[1-\frac{C_3}{D_3}\ln 2\right]}\right\}. \tag{C.10}$$

The expression $\displaystyle\int_0^{2\pi} \frac{\cos(\varphi')\,d\varphi'}{\left[1+C_3(\varphi-\varphi')^2\right]\cdot\left[2-e^{-D_3(\varphi-\varphi')^2}\right]}$ of equation (C.4) is equal to the real part of $\omega_R$; therefore

$$P_1 = 2\pi\left\{\frac{e^{-1/\sqrt{C_3}}}{2\sqrt{C_3}\left[2-e^{D_3/C_3}\right]} + \frac{e^{-\sqrt{\ln 2/D_3}}}{4\sqrt{D_3\ln 2}\left[1-\frac{C_3}{D_3}\ln 2\right]}\right\}\int_0^{2\pi}\cos^2(\varphi)\,d\varphi \,.$$

or

$$P_1 = \pi^2\, T(f_0)\,, \tag{C.11}$$

where $$T(f_0) = \frac{e^{-1/f_0\sqrt{C}}}{f_0\sqrt{C}\left[2-e^{D/C}\right]} + \frac{e^{-\sqrt{\ln 2}/f_0\sqrt{D}}}{2f_0\sqrt{D\ln 2}\left[1-\frac{C}{D}\ln 2\right]}\,,$$

$$C = c r^2/U_\mathrm{\text{¢}}^2 \quad\text{and}\quad D = d r^2/U_\mathrm{\text{¢}}^2 \,.$$

Similarly, $P_2$ becomes equal to $P_1$, $P_3$ is zero and equations (6.6) - (6.8) give

$$W_{f_R}(f_o, \xi, 0) = \pi^2 \cdot r^2 \cdot \overline{p^2(f_o, Re)} \cdot T(f_o) \cdot \Psi_{p, f_o, Re}(\xi, 0, 0) , \qquad (C.12)$$

$$W_{f_C}(f_o, \xi, 0) = \pi^2 \cdot r^2 \cdot \overline{p^2(f_o, Re)} \cdot T(f_o) \cdot \Psi_{p, f_o, Re}(\xi, 0, 0) , \qquad (C.13)$$

$$W_{f_{RC}}(f_o, \xi, 0) = 0.0 , \qquad (C.14)$$

where $T(f_o)$ is given by the equation (C.11).

C-2 <u>Evaluation of the Integrals given by the Equations (6.19) - (6.24) in the Main Text</u>

We consider
$$\oint_C \frac{e^{-[MZ - iNZ + P/Z]} \, dZ}{Z^3\left[\left(\frac{1}{f_r^4}\right)Z^4 + \frac{(4\xi_r^2 - 2)}{f_r^2} Z^2 + 1\right]} , \qquad (C.15)$$

where C is the semi-circular arc of radius R shown here

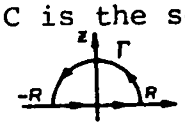


, (M,N,P) are positive constants,

$i = \sqrt{-1}$ and Z is a complex variable.

The integrand has pole of order 3 at Z = 0, and 4 simple poles at

$$Z = -f_r \sqrt{1 - 2\xi_r^2 + i\,2\xi_r\left(\sqrt{1 - \xi_r^2}\right)} ,$$

$$Z = f_n\sqrt{1-2\zeta_n^2+i\,2\,\zeta_n\left(\sqrt{1-\zeta_n^2}\right)}\ ,$$

$$Z = -f_n\sqrt{1-2\zeta_n^2-i\,2\,\zeta_n\left(\sqrt{1-\zeta_n^2}\right)}\ ,$$

and

$$Z = f_n\sqrt{1-2\zeta_n^2-i\,2\,\zeta_n\left(\sqrt{1-\zeta_n^2}\right)}\ ,$$

but only

$$a)\ Z=0\ ,$$

$$b)\ Z = f_n\left(1-2\zeta_n^2+i\,2\,\zeta_n\left(1-\zeta_n^2\right)^{1/2}\right)^{1/2},$$

$$c)\ Z = -f_n\left(1-2\zeta_n^2-i\,2\,\zeta_n\left(1-\zeta_n^2\right)^{1/2}\right)^{1/2},$$

lie within C.

a) Residue at Z = 0 is

$$\lim_{Z\to 0}\frac{d^2}{dZ^2}\left\{\frac{Z^3\,e^{-[MZ-iNZ+P/Z]}}{Z^3\left[\left(\frac{1}{f_n^4}\right)Z^4+\frac{(4\zeta_n^2-2)}{f_n^2}Z^2+1\right]}\right\}=0. \qquad \text{(C.16)}$$

b) Residue at

$$Z = f_n\left(1-2\zeta_n^2+i\,2\,\zeta_n\left(1-\zeta_n^2\right)^{1/2}\right)^{1/2} = f_n(\quad)^{1/2}$$

is

$$\lim_{Z\to f_n(\quad)^{1/2}}\left\{\frac{\left[Z-f_n(\quad)^{1/2}\right]e^{-[MZ-iNZ+P/Z]}}{Z^3\left[\left(\frac{1}{f_n^4}\right)Z^4+\left(\frac{4\zeta_n^2-2}{f_n^2}\right)Z^2+1\right]}\right\}.$$

By neglecting the terms of third and higher-order of magnitude for the generalized damping factor $\varphi_n$, we obtain

The residue at

$$\left\{ Z = f_n\left( \quad \right)^{1/2} \right\} =$$

$$\frac{e^{-[A_i^+]}}{8\ f_n^2}\left[-4 - i\ \frac{\varphi_n\left(1-8\varphi_n^2\right)}{\varphi_n^2}\right], \qquad \text{(C.17)}$$

where $\quad A_i^+ = f_n\left(1-2\varphi_n^2+i2\varphi_n\left(1-\varphi_n^2\right)^{1/2}\right)^{1/2}\left(M-iN\right) + \dfrac{P}{\left(1-2\varphi_n^2+i2\varphi_n\left(1-\varphi_n^2\right)^{1/2}\right)^{1/2}}.$

c) Similarly, the residue of (C.15) at

$$\left\{ Z = -f_n\left(1-2\varphi_n^2-i2\varphi_n\left(1-\varphi_n^2\right)^{1/2}\right)^{1/2} \right\} \quad \text{becomes}$$

$$\frac{e^{-[A_i^-]}}{8\ f_n^2}\left[4 - i\ \frac{\varphi_n\left(1-8\varphi_n^2\right)}{\varphi_n^2}\right], \qquad \text{(C.18)}$$

where $\quad A_i^- = -f_n\left(1-2\varphi_n^2-i2\varphi_n\left(1-\varphi_n^2\right)^{1/2}\right)^{1/2}\left(M-iN\right) - \dfrac{P}{\left(1-2\varphi_n^2-i2\varphi_n\left(1-\varphi_n^2\right)^{1/2}\right)^{1/2}}.$

By considering equations (C.16), (C.17) and (C.18); we obtain

$$\oint_C \frac{e^{-[MZ-iNZ+P/Z]}\,dZ}{Z^3\left[\left(\frac{1}{f_n^4}\right)Z^4+\left(\frac{4\varphi_n^2-2}{f_n^2}\right)Z^2+1\right]} = \frac{\pi i}{f_n^2}\left\{e^{-[A_i^-]} - e^{-[A_i^+]} - \frac{i}{4\varphi_n}\left[e^{-[A_i^-]} + e^{-[A_i^+]}\right]\right\}.$$

(C.19)

This equation (C.19) can be reduced to the following expression

$$\oint_C = \frac{\pi}{4f_r^2}\left\{4e^{-\gamma_1'}\sin(\gamma_2') - 4e^{-\gamma_3'}\sin(\gamma_4') + \frac{1}{\xi_r}\left[e^{-\gamma_3'}\cos(\gamma_4') + e^{-\gamma_1'}\cos(\gamma_2')\right]\right.$$
$$\left. + i\left[4e^{-\gamma_3'}\cos(\gamma_4') - 4e^{-\gamma_1'}\cos(\gamma_2') + \frac{1}{\xi_r}\left(e^{-\gamma_3'}\sin(\gamma_4') + e^{-\gamma_1'}\sin(\gamma_2')\right)\right]\right\},$$

(C.20)

where
$$\gamma_1' = M f_r + N f_r \xi_r + \left(P/f_r(1+\xi_r^2)\right),$$
$$\gamma_2' = -M f_r \xi_r + N f_r + \left(P\xi_r/f_r(1+\xi_r^2)\right),$$
$$\gamma_3' = -M f_r + N f_r \xi_r - \left(P/f_r(1+\xi_r^2)\right),$$
$$\gamma_4' = -M f_r \xi_r - N f_r + \left(P\xi_r/f_r(1+\xi_r^2)\right).$$

On the other hand, since

$$\oint_C \frac{e^{-[Mz+P/z]}\,e^{iNz}\,dz}{z^3\left[\left(\frac{1}{f_r^4}\right)z^4 + \left(\frac{4\xi_r^2-2}{f_r^2}\right)z^2 + 1\right]} = \tag{C.21}$$
$$\int_{-R}^{R}\frac{e^{-[Mf_0+P/f_0]}\,e^{iNf_0}\,df_0}{f_0^3\left[\left(\frac{1}{f_r^4}\right)f_0^4 + \left(\frac{4\xi_r^2-2}{f_r^2}\right)f_0^2 + 1\right]} + \int_\Gamma \frac{e^{-[Mz+P/z]}\,e^{iNz}\,dz}{z^3\left[\left(\frac{1}{f_r^4}\right)z^4 + \left(\frac{4\xi_r^2-2}{f_r^2}\right)z^2 + 1\right]},$$

where C is the semi-circular arc of radius R and Γ is the curve 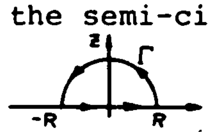

.

Taking the limit of equation (C.21) as $R \to \infty$ and using the theorem* which proves that the integral around $\Gamma$ approaches zero, the following is obtained

$$\oint_C \frac{e^{-[MZ+P/Z]} e^{iNZ}}{Z^3[\qquad]} dZ =$$

$$2\int_0^{\infty} \frac{e^{-[Mf_o+P/f_o]}\cos(Nf_o)\,df_o}{f_o^3\left[\left(\frac{1}{f_n^4}\right)f_o^4+\left(\frac{4\varphi_n^2-2}{f_n^2}\right)f_o^2+1\right]} + i2\int_0^{\infty} \frac{e^{-[Mf_o+P/f_o]}\sin(Nf_o)\,df_o}{f_o^3\left[\left(\frac{1}{f_n^4}\right)f_o^4+\left(\frac{4\varphi_n^2-2}{f_n^2}\right)f_o^2+1\right]} . \tag{C.22}$$

Comparing equation (C.22) with (C.21), then

$$\int_0^{\infty} \frac{e^{-[Mf_o+P/f_o]}\cos(Nf_o)}{f_o^3[\qquad]} df_o = \frac{\pi}{2f_n^2}\left\{e^{-\gamma_1'}\sin(\gamma_2') - e^{-\gamma_3'}\sin(\gamma_4') + \frac{1}{4\varphi_n}\left[e^{-\gamma_3'}\cos(\gamma_4') + e^{-\gamma_1'}\cos(\gamma_2')\right]\right\}, \tag{C.23}$$

$$\int_0^{\infty} \frac{e^{-[Mf_o+P/f_o]}\sin(Nf_o)}{f_o^3[\qquad]} df_o = \frac{\pi}{2f_n^2}\left\{e^{-\gamma_3'}\cos(\gamma_4') - e^{-\gamma_1'}\cos(\gamma_2') + \frac{1}{4\varphi_n}\left[e^{-\gamma_3'}\sin(\gamma_4') + e^{-\gamma_1'}\sin(\gamma_2')\right]\right\}, \tag{C.24}$$

where $\gamma_1'$, $\gamma_2'$, $\gamma_3'$ and $\gamma_4'$ are given by equation (C.20).

---

* If $|f(z)| \leq M/R^k$, for $Z = Re^{i\theta}$, where $(k>0)$ and M are constants, then $\lim_{R\to\infty}\int_{\Gamma} e^{imz} f(z)\,dz = 0$.

By using the above two equations (C.23) and (C.24), the expressions $F_3^c(\ell_i, \ell_\mu)$ and $F_3^s(\ell_i, \ell_\mu)$, given by (6.19) and (6.20) in the main text, can be written as follows:

$$F_3^c(\ell_i, \ell_\mu) = \frac{\pi K_2}{8 C_2 f_n^2}\left[4 e^{-\gamma_1} \sin\gamma_2 - 4 e^{-\gamma_3} \sin\gamma_4 + \frac{1}{\varphi_{gn}}\left(e^{-\gamma_1}\cos\gamma_2 + e^{-\gamma_3}\cos\gamma_4\right)\right]$$
$$+ \frac{\pi K_2}{8 D_2 f_n^2}\left[4 e^{-\gamma_5} \sin\gamma_6 - 4 e^{-\gamma_7} \sin\gamma_8 + \frac{1}{\varphi_{gn}}\left(e^{-\gamma_5}\cos\gamma_6 + e^{-\gamma_7}\cos\gamma_8\right)\right],$$

(C.25)

$$F_3^s(\ell_i, \ell_\mu) = \frac{\pi K_2}{8 C_2 f_n^2}\left[4 e^{-\gamma_3} \cos\gamma_4 - 4 e^{-\gamma_1} \cos\gamma_2 + \frac{1}{\varphi_{gn}}\left(e^{-\gamma_1}\sin\gamma_2 + e^{-\gamma_3}\sin\gamma_4\right)\right]$$
$$+ \frac{\pi K_2}{8 D_2 f_n^2}\left[4 e^{-\gamma_7} \cos\gamma_8 - 4 e^{-\gamma_5} \cos\gamma_6 + \frac{1}{\varphi_{gn}}\left(e^{-\gamma_5}\sin\gamma_6 + e^{-\gamma_7}\sin\gamma_8\right)\right],$$

(C.26)

Using the same method, developed in this Appendix to evaluate $F_3^c(\ell_i, \ell_\mu)$ and $F_3^s(\ell_i, \ell_\mu)$ given above, integration of the expressions given by the equations (6.21) - (6.24) can be performed. Thus

$$F_4^{c}(l_i,l_u)=\frac{\pi K_2}{8C_2 f_r^3}\left[e^{-\gamma_1}\sin\gamma_2-e^{-\gamma_3}\sin\gamma_4\right]+\frac{\pi K_2}{8D_2 f_r^3}\left[e^{-\gamma_5}\sin\gamma_6-e^{-\gamma_7}\sin\gamma_8\right] \tag{C.27}$$

$$+\frac{1}{f_r}F_3^{s}(l_i,l_u)\ ,$$

$$F_4^{s}(l_i,l_u)=\frac{\pi K_2}{8C_2 f_r^3}\left[e^{-\gamma_3}\cos\gamma_4-e^{-\gamma_1}\cos\gamma_2\right]+\frac{\pi K_2}{8D_2 f_r^3}\left[e^{-\gamma_7}\cos\gamma_8-e^{-\gamma_5}\cos\gamma_6\right] \tag{C.28}$$

$$+\frac{1}{f_r}F_3^{s}(l_i,l_u)\ ,$$

$$F_5^{c}(l_i,l_u)=\frac{2}{f_r}F_4^{c}-\frac{1}{f_r^2}F_3^{c}\ , \tag{C.29}$$

$$F_5^{s}(l_i,l_u)=\frac{2}{f_r}F_4^{s}-\frac{1}{f_r^2}F_3^{s}\ , \tag{C.30}$$

where

$$\gamma_1^* = \left[K_1 + |\ell_i - \ell_u|\left(A\varphi_r + B\right)\right] f_r + \frac{C_1}{f_r\left(1+\varphi_r^2\right)} ,$$

$$\gamma_2 = \left[-K_1\varphi_r + |\ell_i - \ell_u|\left(A - B\varphi_r\right)\right] f_r + \frac{C_1\varphi_r}{f_r\left(1+\varphi_r^2\right)} ,$$

$$\gamma_3 = \left[-K_1 + |\ell_i - \ell_u|\left(A\varphi_r - B\right)\right] f_r - \frac{C_1}{f_r\left(1+\varphi_r^2\right)} ,$$

$$\gamma_4 = \left[-K_1\varphi_r - |\ell_i - \ell_u|\left(A + B\varphi_r\right)\right] f_r + \frac{C_1\varphi_r}{f_r\left(1+\varphi_r^2\right)} ,$$

$$\gamma_5 = \left[K_1 + |\ell_i - \ell_u|\left(A\varphi_r + B\right)\right] f_r + \frac{D_1}{f_r\left(1+\varphi_r^2\right)} ,$$

$$\gamma_6 = \left[-K_1\varphi_r + |\ell_i - \ell_u|\left(A - B\varphi_r\right)\right] f_r + \frac{D_1\varphi_r}{f_r\left(1+\varphi_r^2\right)} ,$$

$$\gamma_7 = \left[-K_1 + |\ell_i - \ell_u|\left(A\varphi_r - B\right)\right] f_r - \frac{D_1}{f_r\left(1+\varphi_r^2\right)} ,$$

$$\gamma_8 = \left[-K_1\varphi_r - |\ell_i - \ell_u|\left(A + B\varphi_r\right)\right] f_r + \frac{D_1\varphi_r}{f_r\left(1+\varphi_r^2\right)} ,$$

$$K_1 = 2k_1 r/U_{\mathfrak{C}} , \quad K_2 = 2k_2\rho_F^2 r\, U_{\mathfrak{C}}^3 ,$$

$$C_1 = 1/\sqrt{C} , \quad C_2 = \sqrt{C}\left(2 - e^{D/C}\right) ,$$

$$D_1 = \sqrt{\ln 2/D} , \quad D_2 = 2\sqrt{D\ln 2}\left[1 - \frac{C}{D}\ln 2\right] ,$$

$$A = a/U_{\mathfrak{C}} , \quad B = b/U_{\mathfrak{C}} , \quad C = c r^2/U_{\mathfrak{C}}^2 , \quad D = d r^2/U_{\mathfrak{C}}^2 .$$

---

* here the arguments ($\ell_i$, $\ell_u$) have been omitted from $\gamma_1(\ell_i, \ell_u)$, $\gamma_2(\ell_i, \ell_u)$, etc., for simplicity.

## APPENDIX D

## OUTPUT DATA

```
NATURAL VIBRATION OF NONUNIFORM THIN  CYLIND  SHELLS BY FINITE-ELEMENTS METHOD
------------------------------------------------------------------------------


INPUT  DATA
---------------


                                       SECTION  NUMBER          1
YOUNG.S MODULUS OF ELASTICITY E=LB/(IN-SQUARE) 0.30000D 08
POISSON.S  RATIO   NU .                        0.30000D 00
MEAN RADIUS OF SHELL ELEMENT RA=IN ----------- 0.40800D 01
THICKNESS OF SHELL ELEMENT TH=IN ------------- 0.47000D-01
LENGTH OF AN INDIVIDUAL SHELL ELEMEN  LE=IN.   0 46350D 01
MASS PER UNIT VOLUME OF THE SHELL ELEMENT RHO  0.73240D-03
COEFFICIENTS IN SHELL EQUATION D=E*T/(1-NU**2) 0.15495D 07
                          K  =E*T**3/12*(1-NU**2) 0 28523D 03
                          SMALL K  =T**2/12*RA**2 0.11058D-04

N.B.   RHO=(LB/IN/SEC**2)/(IN**3)
----
FLUID DENSITY= 0.11233D-06


SECTION  NUMBER    1
ELASTICITY MATRIX      P%I,6,6< -FOR ISOTROPIC MATERIAL-
 0.15495D 07  0.46484D 06  0 0           0.0          0.0          0.0
 0.46484D 06  0 15495D 07  0.0           0.0          0.0          0.0
 0.0          0.0          0 54231D 06   0.0          0.0          0.0
 0.0          0 0          0 0           0.28523D 03  0.85568D 02  0.0
 0.0          0.0          0.0           0.85568D 02  0.28523D 03  0.0
 0.0          0.0          0.0           0.0          0.0          0.99830D 02
```

- 132 -

```
NATURAL VIBRATICN CF NCNUNIFORM THIN  CYLIND. SHELLS BY FINITE-ELEMENTS METHOD
------------------------------------------------------------------------------

        THE NUMBER OF CIRCUMFERENTIAL  WAVES IS N =  3.
        --------------------------------------------


                  SECTION  NUMBER   1
                  ------------------

----A--------------------CHARACTERISTIC   EQUATION-------------------------

 THE EIGHT RCCTS CF THE CHARACTERISTIC EQUATICN ARE =

LAMDA1 = -0.363490 C0 0.34382C C0 *I    LAMDA5 =  0.363490 00 0.343820 00 *I
LAMDA2 = -0.363490 00-0.343820 00 *I    LAMDA6 =  0.363490 00-0.343820 00 *I
LAMDA3 = -0.12361C 02 0.11611C 02 *I    LAMDA7 =  0.123610 02 0.116110 02 *I
LAMDA4 = -0.12361C 02-0.116110 C2 *I    LAMDA8 =  0.123610 02-0.116110 02 *I


         EACH OF THE 8 VALUES -LAMDA- YIELDS CNE  SOLUTION
         OF EQUATICNS OF MOTICN, AND THE COMPLETE SOLUTION
         IS THE SUM OF ALL THEM WITH 8 INDEPEADENT SETS OF
         CCNSTANTS   A(J) , B(J) , C(J) =

              A(J) = CONSTANTS OF U = AXIAL DISPLACEMENT EQUATION
              B(J) = CCNSTANTS CF V = TANGENTIAL DISPLACEMENT EQUATION
              C(J) = CCNSTANTS OF W = RADIAL DISPLACEMENT EQUATION

         SUCH THAT = A(J) = ALPHA(J) * C(J)
                     B(J) = BETA(J) * C(J)
         AND=
         ------


ALPHA1 =  0.37981D-01-0.40830C-01 *I    BETA1 = -0.33362D 00-0.28048D-02 *I
ALPHA2 =  0.37981C-01 C.40830D-01 *I    BETA2 = -0.33362D 00 0 28048D-02 *I
ALPHA3 =  0.1C868C-01 0.14268C-01 *I    BETA3 =  C.19894D-03 0.24038D-01 *I
ALPHA4 =  0.1C868D-01-0.14268C-01 *I    BETA4 =  C.19894D-03-0.24038D-01 *I
ALPHA5 = -0.37981C-01-0.40830C-01 *I    BETA5 = -0.33362D 00 0.28048D-02 *I
ALPHA6 = -0.37981D-01 0.40830C-01 *I    BETA6 = -C.33362D 00-0.28048D-02 *I
ALPHA7 = -C.1C868C-01 0.14268C-01 *I    BETA7 =  C.19894D-03-0.24038D-01 *I
ALPHA8 = -0.1C868C-01-0.14268C-01 *I    BETA8 =  0.19894D-03 0.24038D-01 *I

CMEGA1 =  0.41293C 00    ETA1 =  C.39059D 0C
CMEGA2 =  C.14043C 02    ETA2 =  C.13190D 02

CISPLACEMENT FUNCTION MATRIX AT X=LE= 0.0
                                          -0.40477D-16  0.29779D-15 -0.90917D-17  0.10981D-17  0 91304D-16
 C.1C000D 01   0.17919D-16   0.41637D-18  -C.28184D-14 -0.45658D-14 -0 16569D-15  0.50624D-16 -0.22568D-15
-0.36549C-14   0.1C000D 01   C.69812D-16   C.1000CD 01  0.13072D-14  C.62551D-16  0 14346D-16  C.14763D-15
 0.12307D-14  -0.74606D-16  -0.69117D-17

CISPLACEMENT FUNCTION MATRIX AT X=LE= 0.46350C 01
                                           0.37242D-15  0.1C000D 01  C.52530D-16 -0 76436D-17 -0.30444D-15
 0.25815D-15  -C.20085D-16  -0.5046CD-17   0.82434D-14  0.13475D-13  0.10000D 01 -0.97145D-16 -C 44409D-14
 0.10575D-13  -0.67741D-15  -C.12983D-15   0.18171D-14  0.48373D-14  0.14572D-15 -0 36429D-16  0 1000D 01
 0.40206D-14  -0.24136D-15  -C.52987D-16
```

NATURAL VIBRATION OF NONUNIFORM THIN  CYLIND. SHELLS BY FINITE-ELEMENTS METHOD
---

THE NUMBER OF CIRCUMFERENTIAL  WAVES IS N =  3.

SECTION  NUMBER  1

----B------------------------OUTPUT  MATRICES------------------------------

```
THE MATRIX A ( 3,8,8 )  IS
                                                         -0.37981D-01  -0.40830D-01  -0.10868D-01   0.14268D-01
 0.37981D-01  -0.40830D-01   0.10868D-01   0.14268D-01                                 0.10000D 01   0.0
 0.10000D 01   0.0           0.10000D 01   0.0           0.10000D 01   0.0
                                                          0.89091D-01   0.84270D-01   0.30297D 01   0.28458D 01
-0.89091D-01   0.84270D-01  -0.30297D 01   0.28458D 01   0.89091D-01   0.28048D-02   0.19894D-03  -0.24038D-01
-0.33362D 00  -0.28048D-02   0.19894D-03   0.24038D-01  -0.33362D 00  -0.78910D-01  -0.21532D 05   0.65640D 04
 0.33526D-01  -0.15414D-01   0.38541D-09   0.14286D-07  -0.29583D-01   0.57538D 00   0.10186D 07   0.73327D 06
 0.61187D 00   0.25193D 00   0.64664D-06   0.46552D-06   0.13974D 01   0.16902D 00   0.99919D 06   0.51202D 07
-0.75742D-01   0.29117D-01  -0.32839D-05   0.42982D-06   0.76010D-01  -0.18804D 00   0.17829D 05  -0.24338D 05
-0.20343D 00  -0.85766D-01  -0.11062D-07   0.15636D-07  -0.46782D 00
```

```
THE TRANSFORMATION MATRIX  -INVERSE OF A-  IS
                                            -0.18178D 02  -0.33301D 02  -0.12814D 01   0.30244D 00   0.16039D 02
-0.26966D 02   0.11715D 01   0.28875D 00  -0.19542D 02  -0.28084D 02  -0.13102D 01   0.33025D 00   0.22428D 02
-0.66445D 02   0.22458D 01   0.50159D 00   0.27140D 01   0.61732D-01  -0.11689D-02   0.60002D-03   0.10766D 00
-0.48457D 00   0.94264D 00  -0.20493D-01   0.27134D 01  -0.18308D 00  -0.10766D-01   0.28809D-02   0.23238D 00
 0.80633D-02   0.99443D 00   0.32843D 00   0.15464D 02   0.33239D 02   0.12826D 01  -0.30304D 00  -0.16147D 02
 0.27451D 02  -0.11142D 01  -0.26626D 00  -0.96820D 01  -0.33862D 02  -0.10790D 01   0.23416D 00   0.76223D 01
-0.87938D 01   0.47885D 00   0.12587D 00   0.17780D-06   0.30985D-06   0.10725D-05  -0.13964D-06   0.30182D-05
 0.45308D-07  -0.57676D-08  -0.17291D-08  -0.10015D-06   0.23098D-06  -0.20422D-06   0.22192D-06  -0.49117D-06
-0.14712D-06   0.64175D-08   0.15836D-08
```

```
THE GENERALIZED COORDINATE STIFFNESS OF THE ELEMENT  G ( 1,8,8 )  IS
                                                                        0.13728D 04   0.21912D 09  -0.20604D 10
 0.27804D 04   0.79896D 02  -0.13183D 04   0.11549D 04   0.33341D 04  -0.33342D 04  -0.14804D 10  -0.60013D 09
 0.79896D 02   0.28475D 04  -0.17564D 04  -0.19696D 04   0.13728D 04   0.12578D 04   0.17064D 06   0.12285D 06
-0.13183D 04  -0.17564D 04   0.18795D 06   0.33509D 04  -0.18540D 04   0.12461D 04   0.12284D 06  -0.17064D 06
 0.11549D 04  -0.19696D 04   0.33509D 04   0.19519D 06   0.18312D 04  -0.18386D 03  -0.25534D 10  -0.25814D 10
 0.33341D 04   0.13728D 04  -0.18540D 04   0.18312D 04   0.65009D 04   0.63534D 04   0.42329D 10  -0.22367D 10
 0.13728D 04  -0.33342D 04   0.12578D 04   0.12461D 04  -0.18386D 03   0.42329D 10   0.30495D 18  -0.70786D 16
 0.21912D 09  -0.14804D 10   0.17064D 06   0.12284D 06  -0.25534D 10  -0.22367D 10  -0.70786D 16   0.29855D 18
-0.20604D 10  -0.60013D 09   0.12285D 06  -0.17064D 06  -0.25814D 10
```

```
TRANSFORM MATRIX  G  TO THE DESIRED NODAL POINT STIFFNESS ,SUCH THAT
K  = (TRANSPOSE OF INVERSE OF A) * G * ( INVERSE OF A )
                                                         -0.73926D 06   0.27069D 05  -0.11468D 05  -0.17966D 07
 0.71227D 07  -0.80806D 05  -0.74142D 03   0.16419D 07  -0.27069D 05  -0.23883D 04   0.68678D 03   0.65226D 05
-0.80806D 05   0.35911D 06   0.59658D 05   0.10034D 07  -0.11468D 05  -0.68678D 03   0.18451D 03   0.15038D 05
-0.74142D 03   0.59658D 05   0.20807D 05   0.15999D 06   0.17966D 07   0.65226D 05  -0.15038D 05  -0.71397D 06
 0.16419D 07   0.10034D 07   0.15999D 06   0.39330D 07   0.71227D 07   0.80806D 05  -0.74142D 03  -0.16419D 07
-0.73926D 06  -0.27069D 05  -0.11468D 05   0.17966D 07   0.80806D 05   0.35911D 06  -0.59658D 05   0.10034D 07
 0.27069D 05  -0.23883D 04  -0.68678D 03   0.65226D 05  -0.74142D 03  -0.59658D 05   0.20807D 05  -0.15999D 06
-0.11468D 05   0.68678D 03   0.18451D 03  -0.15038D 05  -0.16419D 07   0.10034D 07  -0.15999D 06   0.39330D 07
-0.17966D 07   0.65226D 05   0.15038D 05  -0.71397D 06
```

THIS MATRIX K IS THE STIFFNESS MATRIX OF ANY FORM OF STRUCTURAL ELEMENT

THE NODAL DISPLACEMENTS ARE IN THE FOLLOWING ORDER =
(U,W,BETA,V) AT POINTS  I(X=0)  AND  J(X=LE) RESPECTIVELY

```
NATURAL VIBRATICN OF NONUNIFORM THIN  CYLIND. SHELLS BY FINITE-ELEMENTS METHOD
-------------------------------------------------------------------------------

        THE NUMBER OF CIRCUMFERENTIAL  WAVES IS N =  3.   FLUID DENSITY= 0.11233D-06
        ------------------------------------------------
NC.    LAMCA         I (LAMDA)    I   (LAMDA)  TOTAL MASS PER UNIT SURFACE
                      N            N+1           STRUCTURE+FLUID
   1   0.27654D 01    0.69603D 0C   0.22072D 0C    0.34541D-04
```

NATURAL VIBRATION OF NONUNIFORM THIN CYLIND. SHELLS BY FINITE-ELEMENTS METHOD

THE NUMBER OF CIRCUMFERENTIAL WAVES IS N = 3.

SECTION NUMBER 1

----B------------------------OUTPUT MATRICES------------------------------

THE MATRIX A ( I,8,8 ) IS

| | | | | | | | |
|---|---|---|---|---|---|---|---|
| 0.37981D-01 | -0.40830D-01 | 0.10868D-01 | 0.14268D-01 | -0.37981D-01 | -0.40830D-01 | -0.10868D-01 | 0.14268D-01 |
| 0.10000D 01 | 0.0 | 0.10000D 01 | 0.0 | 0.10000D 01 | 0.0 | 0.10000D 01 | 0.0 |
| -0.89091D-01 | 0.84270D-01 | -0.30297D 01 | 0.28458D 01 | 0.89091D-01 | 0.84270D-01 | 0.30297D 01 | 0.28458D 01 |
| -0.33362D 00 | -0.28048D-02 | 0.19894D-03 | 0.24038D-01 | -0.33362D 00 | 0.28048D-02 | 0.19894D-03 | -0.24038D-01 |
| 0.33526D-01 | -0.15414D-01 | 0.38541D-09 | 0.14286D-07 | -0.29583D-01 | -0.78910D-01 | -0.21532D 05 | 0.65640D 04 |
| 0.61187D 00 | 0.25153D 00 | 0.64664D-06 | 0.46552D-06 | 0.13974D 01 | 0.57538D 00 | 0.10186D 07 | 0.73327D 06 |
| -0.75742D-01 | 0.29117D-01 | -0.32839D-05 | 0.42982D-06 | 0.76010D-01 | 0.16902D 00 | 0.99919D 06 | 0.51202D 07 |
| -0.20343D 00 | -0.85766D-01 | -0.11062D-07 | 0.15636D-07 | -0.46782D 00 | -0.18804D 00 | 0.17829D 05 | -0.24338D 05 |

THE TRANSFORMATION MATRIX -INVERSE OF A- IS

| | | | | | | | |
|---|---|---|---|---|---|---|---|
| -0.26966D 02 | 0.11715D 01 | 0.28875D 00 | -0.18178D 02 | -0.33301D 02 | -0.12814D 01 | 0.30244D 00 | 0.16039D 02 |
| -0.66445D 02 | 0.22458D 01 | 0.50159D 00 | -0.19942D 02 | -0.28084D 02 | -0.13102D 01 | 0.33025D 00 | 0.22428D 02 |
| -0.48497D 00 | 0.94264D 00 | -0.20493D-01 | 0.27140D 01 | 0.61732D-01 | -0.11689D-02 | 0.60002D-03 | 0.10766D 00 |
| 0.80633D-02 | 0.99443D 00 | 0.32843D 00 | 0.27134D 01 | -0.18308D 00 | -0.10766D-01 | 0.28809D-02 | 0.23238D 00 |
| 0.27451D 02 | -0.11142D 01 | -0.26826D 00 | 0.15464D 02 | 0.33239D 02 | 0.12826D 01 | -0.30304D 00 | -0.16147D 02 |
| -0.87938D 01 | 0.47885D 00 | 0.12587D 00 | -0.96820D 01 | -0.33862D 02 | -0.10790D 01 | 0.23416D 00 | 0.76223D 01 |
| 0.45308D-07 | -0.57676D-08 | -0.17291D-08 | 0.17780D-06 | 0.30985D-06 | 0.10725D-05 | -0.13964D-06 | 0.30182D-05 |
| -0.14712D-06 | 0.64175D-08 | 0.15836D-08 | -0.10015D-06 | 0.23098D-06 | -0.20422D-06 | 0.22192D-06 | -0.49117D-06 |

THE GENERALIZED COORDINATE MASS OF THE ELEMENT RHO*T*S%I,8,8< IS

| | | | | | | | |
|---|---|---|---|---|---|---|---|
| 0.46771D 02 | -0.25850D 01 | -0.72784D 00 | 0.51683D 02 | -0.30180D 02 | -0.24579D 01 | 0.72641D 00 | 0.54654D 02 |
| -0.25850D 01 | 0.36456D 01 | 0.47201D 00 | -0.75037D 01 | 0.24579D 01 | 0.17050D 00 | -0.48416D-01 | -0.35662D 01 |
| -0.72784D 00 | 0.47201D 00 | 0.91222D-01 | -0.21826D 01 | 0.72641D 00 | 0.48416D-01 | -0.13606D-01 | -0.99558D 00 |
| 0.51683D 02 | -0.75037D 01 | -0.21826D 01 | 0.12325D 03 | -0.54654D 02 | -0.35662D 01 | 0.99558D 00 | 0.71574D 02 |
| -0.30180D 02 | 0.24579D 01 | 0.72641D 00 | -0.54654D 02 | 0.46771D 02 | 0.25850D 01 | -0.72784D 00 | -0.51683D 02 |
| -0.24579D 01 | 0.17050D 00 | 0.48416D-01 | -0.35662D 01 | 0.25850D 01 | 0.36456D 01 | -0.47201D 00 | -0.75037D 01 |
| 0.72641D 00 | -0.48416D-01 | -0.13606D-01 | 0.99558D 00 | -0.72784D 00 | -0.47201D 00 | 0.91222D-01 | 0.21826D 01 |
| 0.54654D 02 | -0.35662D 01 | -0.99558D 00 | 0.71574D 02 | -0.51683D 02 | -0.75037D 01 | 0.21826D 01 | 0.12325D 03 |

TRANSFORM -MATRIX RHO*T*S(I,8,8)- TO THE DESIRED NODAL POINT MASS SUCH THAT
M = (TRANSPOSE OF INVERSE OF A) * RHO*T*S(I,8,8) * (INVERSE OF A )

| | | | | | | | |
|---|---|---|---|---|---|---|---|
| 0.16155D-02 | -0.89288D-04 | -0.25140D-04 | 0.17852D-02 | -0.10424D-02 | -0.84899D-04 | 0.25091D-04 | 0.18878D-02 |
| -0.89288D-04 | 0.12592D-03 | 0.16304D-04 | -0.25918D-03 | 0.84899D-04 | 0.58893D-05 | -0.16723D-05 | -0.12318D-03 |
| -0.25140D-04 | 0.16304D-04 | 0.31509D-05 | -0.75388D-04 | 0.25091D-04 | 0.16723D-05 | -0.46996D-06 | -0.34388D-04 |
| 0.17852D-02 | -0.25918D-03 | -0.75388D-04 | 0.42573D-02 | -0.18878D-02 | -0.12318D-03 | 0.34388D-04 | 0.24722D-02 |
| -0.10424D-02 | 0.84899D-04 | 0.25091D-04 | -0.18878D-02 | 0.16155D-02 | 0.89288D-04 | -0.25140D-04 | -0.17852D-02 |
| -0.84899D-04 | 0.58893D-05 | 0.16723D-05 | -0.12318D-03 | 0.89288D-04 | 0.12592D-03 | -0.16304D-04 | -0.25918D-03 |
| 0.25091D-04 | -0.16723D-05 | -0.46996D-06 | 0.34388D-04 | -0.25140D-04 | -0.16304D-04 | 0.31509D-05 | 0.75388D-04 |
| 0.18878D-02 | -0.12318D-03 | -0.34388D-04 | 0.24722D-02 | -0.17852D-02 | -0.25918D-03 | 0.75388D-04 | 0.42573D-02 |

THIS MATRIX M IS THE MASS MATRIX OF ANY FORM OF STRUCTURAL ELEMENT

THE NODAL DISPLACEMENTS ARE IN THE FOLLOWING ORDER =
(U,W,BETA,V) AT POINTS I(X=0) AND J(X=LE) RESPECTIVELY

NATURAL VIBRATICN OF NCNUNIFORM THIN CYLIND. SHELLS BY FINITE-ELEMENTS METHCD

THE NUMBER OF CIRCUMFERENTIAL WAVES IS N = 3. FLUID DENSITY= 0.11233D-06

GECMETRICAL ANC ELASTIC PRCPERTIES OF STRUCTURE

| ELEMENT NC. | NODE NOS. | CCORDINATES X(IN) | R(IN) | THICKNESS(IN) | ELASTIC CONSTANTS E(LB/IN**2) | NU | MASS/UNIT VOLUME (LB/IN/SEC**2)/(IN**3) |
|---|---|---|---|---|---|---|---|
| 1 | 1 | 0.0 | C.408C0D 01 | 0.47000D-01 | C.30000D 08 | 0.30000D 00 | 0 73240D-03 |
| | 2 | C.4635CD C1 | 0.40800D 01 | | | | |
| 2 | 2 | 0.4635CD C1 | C.408C0D 01 | 0.47000D-01 | 0.30000D 08 | 0 30000D OC | 0.73240D-03 |
| | 3 | C.927)CD C1 | 0.40800D 01 | | | | |
| 3 | 3 | 0.927'CD C1 | 0.408C0D 01 | 0.47000D-01 | 0.30C00D 08 | 0 30000D 00 | 0.73240D-03 |
| | 4 | 0.13905D C2 | 0.40800D 01 | | | | |
| 4 | 4 | 0.13905D 02 | 0.408C0D 01 | 0.47000D-01 | C.3000GD 08 | 0 30000D 00 | 0.73240D-03 |
| | 5 | 0.1854CD 02 | 0.40800D 01 | | | | |

| | | | | | | | |
|---|---|---|---|---|---|---|---|
| THE EIGENVALUES | | | | | | | |
| 0.27470D 04 | 0.87226D 04 | 0.17573D 05 | 0.49083D 05 | 0.56113D 05 | 0.62677D 05 | 0.67181D 05 | 0.85701D 05 |
| 0.87788D 05 | 0.88260D 05 | 0.88332D 05 | 0.97318D 05 | 0.10436D 06 | 0.10567D 06 | 0.11544D 06 | 0.12046D 06 |
| ROW NUMBER 1 | | | | | | | |
| -0.44748D-01 | 0.61183D-01 | 0.50341D-01 | 0.40230D-01 | -0.46561D-01 | 0.49822D-01 | 0.55369D-01 | 0.15432D-02 |
| 0.14276D-02 | -0.26387D-02 | 0.27654D-02 | 0.12562D-01 | -0.31608D-01 | -0.27221D 00 | -0.50308D 00 | -0.12816D 00 |
| ROW NUMBER 2 | | | | | | | |
| 0.11105D 00 | -0.20821D 00 | -0.25529D 00 | -0.44540D 00 | 0.55407D 00 | -0.50289D 00 | -0.37272D 00 | -0.57363D 00 |
| 0.57695D 00 | -0.57729D 00 | 0.44721D 00 | 0.44704D 00 | -0.57498D 00 | 0.35482D 00 | -0.41077D-01 | -0.55024D 00 |
| ROW NUMBER 3 | | | | | | | |
| -0.31641D-01 | 0.57532D-14 | -0.35597D-01 | -0.40230D-01 | 0.32924D-01 | -0.86998D-13 | 0.39152D-01 | -0.10912D-02 |
| -0.76747D-12 | -0.18658D-02 | 0.27654D-02 | -0.12562D-01 | 0.22350D-01 | -0.27221D 00 | -0.35573D 00 | -0.41487D-13 |
| ROW NUMBER 4 | | | | | | | |
| 0.46346D 00 | -0.62073D 00 | -0.42555D 00 | -0.24072D-12 | -0.13458D 00 | 0.34173D 00 | 0.37777D 00 | -0.54643D-01 |
| 0.25066D-01 | -0.64025D-02 | -0.23307D-12 | -0.10028D-12 | 0.32923D-01 | -0.71483D-11 | 0.21904D 00 | 0.12756D 00 |
| ROW NUMBER 5 | | | | | | | |
| 0.78525D-01 | 0.11872D-12 | 0.18052D 00 | 0.44540D 00 | -0.39179D 00 | -0.13403D-11 | -0.26355D 00 | 0.40562D 00 |
| 0.43172D-11 | -0.40821D 00 | 0.44721D 00 | -0.44704D 00 | 0.40657D 00 | 0.35482D 00 | -0.29046D-01 | 0.79071D-11 |
| ROW NUMBER 6 | | | | | | | |
| -0.15638D 00 | 0.20588D 00 | 0.13464D 00 | -0.47244D-13 | 0.36444D-02 | 0.12224D-01 | 0.28280D-01 | -0.15025D-01 |
| 0.73923D-02 | -0.19348D-02 | -0.12750D-12 | -0.25866D-13 | 0.14616D-01 | -0.23783D-11 | 0.10458D 00 | 0.70291D-01 |
| ROW NUMBER 7 | | | | | | | |
| 0.59534D-15 | -0.61183D-01 | -0.57100D-13 | 0.40230D-01 | 0.21823D-13 | -0.49822D-01 | -0.12551D-12 | 0.19653D-14 |
| -0.14276D-02 | 0.62788D-14 | 0.27654D-02 | 0.12562D-01 | 0.98004D-14 | -0.27221D 00 | 0.15448D-12 | 0.12816D 00 |
| ROW NUMBER 8 | | | | | | | |
| 0.65543D 00 | -0.81944D-13 | 0.60182D 00 | -0.26443D-12 | 0.19032D 00 | -0.15667D-11 | 0.53425D 00 | 0.77277D-01 |
| -0.16635D-12 | -0.90545D-02 | -0.19969D-13 | -0.10195D-12 | -0.46560D-01 | 0.21988D-11 | 0.30977D 00 | 0.49853D-12 |
| ROW NUMBER 9 | | | | | | | |
| -0.47075D-14 | 0.20821D 00 | -0.20770D-13 | -0.44540D 00 | 0.16445D-12 | 0.50289D 00 | -0.77423D-12 | 0.67542D-14 |
| -0.57695D 00 | 0.17843D-13 | 0.44721D 00 | 0.44704D 00 | 0.32921D-13 | 0.35482D 00 | 0.97399D-12 | 0.55024D 00 |
| ROW NUMBER10 | | | | | | | |
| -0.22119D 00 | 0.25578D-13 | -0.19040D 00 | 0.74924D-14 | -0.51540D-02 | 0.64623D-13 | 0.39994D-01 | 0.21248D-01 |
| 0.14903D-13 | -0.27363D-02 | 0.41866D-14 | 0.10821D-13 | -0.20670D-01 | -0.10821D-12 | 0.14790D 00 | -0.31983D-13 |
| ROW NUMBER11 | | | | | | | |
| 0.31641D-01 | -0.53062D-14 | 0.35597D-01 | -0.40230D-01 | -0.32924D-01 | 0.67368D-13 | -0.39152D-01 | 0.10912D-02 |
| -0.75347D-12 | 0.18658D-02 | 0.27654D-02 | -0.12562D-01 | -0.22350D-01 | -0.27221D 00 | 0.35573D 00 | -0.80595D-13 |
| ROW NUMBER12 | | | | | | | |
| 0.46346D 00 | 0.62073D 00 | -0.42555D 00 | -0.22210D-12 | -0.13458D 00 | -0.34173D 00 | 0.37777D 00 | -0.54643D-01 |
| -0.25066D-01 | -0.64025D-02 | 0.26440D-12 | 0.68423D-14 | 0.32923D-01 | 0.10522D-10 | 0.21904D 00 | -0.12756D 00 |
| ROW NUMBER13 | | | | | | | |
| -0.78525D-01 | -0.44426D-12 | -0.18052D 00 | 0.44540D 00 | 0.39179D 00 | -0.37019D-11 | 0.26355D 00 | -0.40562D 00 |
| 0.75445D-11 | 0.40821D 00 | 0.44721D 00 | -0.44704D 00 | -0.40657D 00 | 0.35482D 00 | 0.29046D-01 | 0.47943D-11 |
| ROW NUMBER14 | | | | | | | |
| -0.15638D 00 | -0.20588D 00 | 0.13464D 00 | 0.90865D-15 | 0.36444D-02 | -0.12224D-01 | 0.28280D-01 | -0.15025D-01 |
| -0.73923D-02 | -0.19348D-02 | 0.11605D-12 | -0.57499D-14 | 0.14616D-01 | 0.28599D-11 | 0.10458D 00 | -0.70291D-01 |
| ROW NUMBER15 | | | | | | | |
| 0.44748D-01 | 0.61183D-01 | -0.50341D-01 | 0.40230D-01 | 0.46561D-01 | 0.49822D-01 | -0.55369D-01 | -0.15432D-02 |
| 0.14276D-02 | 0.26387D-02 | 0.27654D-02 | 0.12562D-01 | 0.31608D-01 | -0.27221D 00 | 0.50308D 00 | -0.12816D 00 |
| ROW NUMBER16 | | | | | | | |
| -0.11105D 00 | -0.20821D 00 | 0.25529D 00 | -0.44540D 00 | -0.55407D 00 | -0.50289D 00 | 0.37272D 00 | 0.57363D 00 |
| 0.57695D 00 | 0.57729D 00 | 0.44721D 00 | 0.44704D 00 | 0.57498D 00 | 0.35482D 00 | 0.41077D-01 | -0.55024D 00 |

NATURAL VIBRATION OF NONUNIFORM THIN CYLIND. SHELLS BY FINITE-ELEMENTS METHOD
---------------------------------------------------------------------------------

THE NUMBER OF CIRCUMFERENTIAL WAVES IS N = 3. FLUID DENSITY= 0.11233D-06
----------------------------------------------------

THE FREQUENCY IS = 0.27470D 04 RAD./SEC. = 0.43720D 03 CYCLES/SEC. FREQ. NO. 1

THE CORRESPONDING SHAPE IS

| NODE NO. | X/L | UMAX= 0.44748D-01<br>AXIAL/UMAX | WMAX= 0.65543D 00<br>RADIAL/WMAX | BMAX= 0.11105D 00<br>ANGULAR/BMAX | VMAX= 0.22115D 00<br>CIRCUMFERENTIAL/VMAX |
|---|---|---|---|---|---|
| 1 | 0.0 | -0.10000000D 01 | 0.0 | 0.10000000D 01 | 0.0 |
| 2 | 0.25000D 00 | -0.70710678D 00 | 0.70710678D 00 | 0.70710678D 00 | -0.70710678D 00 |
| 3 | 0.50000D 00 | 0.13393678D-13 | 0.10000000D 01 | -0.42393767D-13 | -0.10000000D 01 |
| 4 | 0.75000D 00 | 0.70710678D 00 | 0.70710678D 00 | -0.70710678D 00 | -0.70710678D 00 |
| 5 | 0.10000D 01 | 0.10000000D 01 | 0.0 | -0.10000000D 01 | 0.0 |

REMARK= LISTED ABOVE,ONE HARMONIC AT A TIME, ARE THE AMPLITUDES OF THE VARIATION IN CIRCUMFERENTIAL DIRECTION
THESE SHOULD BE MULTIPLIED RESPECTIVELY BY COS(N*PHI),COS(N*PHI),COS(N*PHI) AND SIN(N*PHI)
FOR CIRCUMFERENTIAL WAVE NUMBER N AND CIRCUMFERENTIAL ANGLE PHI.

NATURAL VIBRATION OF NONUNIFORM THIN CYLIND. SHELLS BY FINITE-ELEMENTS METHOD

THE NUMBER OF CIRCUMFERENTIAL WAVES IS N = 3. FLUID DENSITY= 0.11233D-06

THE FREQUENCY IS = 0.87226D 04 RAD./SEC. = 0.13883D 04 CYCLES/SEC. FREQ. NO. 2

THE CORRESPONDING SHAPE IS

| | | UMAX= 0.61183D-01 | WMAX= 0.62073D 00 | BMAX= 0.20821D 00 | VMAX= 0.20988D 00 |
|---|---|---|---|---|---|
| NODE NO. | X/L | AXIAL/UMAX | RADIAL/WMAX | ANGULAR/BMAX | CIRCUMFERENTIAL/VMAX |
| 1 | 0.0 | 0.10000000D 01 | 0.0 | -0.10000000D 01 | 0.0 |
| 2 | 0.25000D 00 | 0.94032658D-13 | -0.10000000D 01 | 0.57019738D-12 | 0.10000000D 01 |
| 3 | 0.50000D 00 | -0.10000000D 01 | -0.13201128D-12 | 0.10000000D 01 | 0.12377378D-12 |
| 4 | 0.75000D 00 | -0.86725820D-13 | 0.10000000D 01 | -0.21337016D-11 | -0.10000000D 01 |
| 5 | 0.10000D 01 | 0.10000000D 01 | 0.0 | -0.10000000D 01 | 0.0 |

REMARK= LISTED ABOVE,ONE HARMONIC AT A TIME, ARE THE AMPLITUDES OF THE VARIATION IN CIRCUMFERENTIAL DIRECTION
THESE SHOULD BE MULTIPLIED RESPECTIVELY BY COS(N*PHI),COS(N*PHI),COS(N*PHI) AND SIN(N*PHI)
FOR CIRCUMFERENTIAL WAVE NUMBER N AND CIRCUMFERENTIAL ANGLE PHI.

NATURAL VIBRATICN OF NCNUNIFORM THIN CYLIND. SHELLS BY FINITE-ELEMENTS METHOD

THE NUMBER OF CIRCUMFERENTIAL WAVES IS N = 3. FLUID DENSITY= 0.11233D-06

THE FREQUENCY IS = 0.17573D C5 RAD./SEC. = 0.27968D 04 CYCLES/SEC. FREQ. NO. 3

THE CORRESPONDING SHAPE IS

| NODE NO. | X/L | UMAX= 0.50341D-01 AXIAL/UMAX | WMAX= 0.60182D 00 RADIAL/WMAX | BMAX= 0.25529D 00 ANGULAR/BMAX | VMAX= 0 19040D 00 CIRCUMFERENTIAL/VMAX |
|---|---|---|---|---|---|
| 1 | 0.0 | 0.10000000D 01 | 0.0 | -0 10000000D 01 | 0.0 |
| 2 | 0.25000D 00 | -0.70710678D 00 | -0.70710678D 00 | 0.70710678D 00 | 0.70710678D 00 |
| 3 | 0.50000D 00 | -0.11342531D-11 | 0.10000000D 01 | -0.81356860D-13 | -0.10000000D 01 |
| 4 | 0.75000D 00 | 0.70710678D 00 | -0.70710678D 00 | -0.70710678D 00 | 0.70710678D 00 |
| 5 | 0.10000D 01 | -0.10000000D 01 | 0.0 | 0 10000000D 01 | 0.0 |

REMARK= LISTED ABOVE,ONE HARMONIC AT A TIME, ARE THE AMPLITUDES OF THE VARIATION IN CIRCUMFERENTIAL DIRECTION
THESE SHOULD BE MULTIPLIED RESPECTIVELY BY COS(N*PHI),COS(N*PHI),COS(N*PHI) AND SIN(N*PHI)
FOR CIRCUMFERENTIAL WAVE NUMBER N AND CIRCUMFERENTIAL ANGLE PHI.

NATURAL VIBRATION OF NONUNIFORM THIN CYLIND. SHELLS BY FINITE-ELEMENTS METHOD

THE NUMBER OF CIRCUMFERENTIAL WAVES IS N = 3. FLUID DENSITY= 0.11233D-06



THE FREQUENCY IS = 0.49083D 05 RAD./SEC. = 0.78118D 04 CYCLES/SEC. FREQ. NO. 4

THE CORRESPONDING SHAPE IS

| NODE NO. | X/L | UMAX= 0.40230D-01 AXIAL/UMAX | WMAX= 0.26443D-12 RADIAL/WMAX | BMAX= 0.44540D 00 ANGULAR/BMAX | VMAX= 0.47244D-13 CIRCUMFERENTIAL/VMAX |
|---|---|---|---|---|---|
| 1 | 0.0 | 0.10000000D 01 | 0.0 | -0.10000000D 01 | 0.0 |
| 2 | 0.25000D 00 | -0.10000000D 01 | -0.91034271D 00 | 0.10000000D 01 | -0.10000000D 01 |
| 3 | 0.50000D 00 | 0.10000000D 01 | -0.10000000D 01 | -0.10000000D 01 | 0.15859002D 00 |
| 4 | 0.75000D 00 | -0.10000000D 01 | -0.83991669D 00 | 0.10000000D 01 | 0.19233108D-01 |
| 5 | 0.10000D 01 | 0.10000000D 01 | 0.0 | -0.10000000D 01 | 0.0 |

REMARK= LISTED ABOVE,ONE HARMONIC AT A TIME, ARE THE AMPLITUDES OF THE VARIATION IN CIRCUMFERENTIAL DIRECTION
THESE SHOULD BE MULTIPLIED RESPECTIVELY BY COS(N*PHI),COS(N*PHI),COS(N*PHI) AND SIN(N*PHI)
FOR CIRCUMFERENTIAL WAVE NUMBER N AND CIRCUMFERENTIAL ANGLE PHI.

NATURAL VIBRATION OF NONUNIFORM THIN CYLIND. SHELLS BY FINITE-ELEMENTS METHOD



THE NUMBER OF CIRCUMFERENTIAL WAVES IS N = 3. FLUID DENSITY= 0.11233D-06

THE FREQUENCY IS = 0.56113D 05 RAD./SEC. = 0.89307D 04 CYCLES/SEC FREQ. NO. 5

THE CORRESPONDING SHAPE IS

| NODE NO. | X/L | UMAX= 0.46561D-01 AXIAL/UMAX | WMAX= 0.19032D 00 RADIAL/WMAX | BMAX= 0.55407D 00 ANGULAR/BMAX | VMAX= 0.51540D-02 CIRCUMFERENTIAL/VMAX |
|---|---|---|---|---|---|
| 1 | 0.0 | -0.10000000D 01 | 0.0 | 0.10000000D 01 | 0.0 |
| 2 | 0.25000D 00 | 0.70710678D 00 | -0.70710678D 00 | -0.70710678D 00 | 0.70710678D 00 |
| 3 | 0.50000D 00 | 0.46869375D-12 | 0.10000000D 01 | 0.29680394D-12 | -0.10000000D 01 |
| 4 | 0.75000D 00 | -0.70710678D 00 | -0.70710678D 00 | 0.70710678D 00 | 0.70710678D 00 |
| 5 | 0.10000D 01 | 0.10000000D 01 | 0.0 | -0.10000000D 01 | 0.0 |

REMARK= LISTED ABOVE,ONE HARMONIC AT A TIME, ARE THE AMPLITUDES OF THE VARIATION IN CIRCUMFERENTIAL DIRECTION
THESE SHOULD BE MULTIPLIED RESPECTIVELY BY COS(N*PHI),COS(N*PHI),COS(N*PHI) AND SIN(N*PHI)
FOR CIRCUMFERENTIAL WAVE NUMBER N AND CIRCUMFERENTIAL ANGLE PHI.

NATURAL VIERATICN OF NCNUNIFORM THIN CYLIND. SHELLS BY FINITE-ELEMENTS METHCD

THE NUMBER OF CIRCLMFERENTIAL WAVES IS N = 3. FLUID DENSITY= 0.11233D-06

THE FREQUENCY IS = 0.62677C C5 RAD./SEC. = 0.99753D 04 CYCLES/SEC. FREQ. NO. 6

THE CCRRESPCNCING SHAPE IS

| | | UMAX= 0.49822D-01 | WMAX= 0.34173D 00 | BMAX= 0.50289D 00 | VMAX= 0.12224D-01 |
|---|---|---|---|---|---|
| NODE NO. | X/L | AXIAL/UMAX | RADIAL/WMAX | ANGULAR/BMAX | CIRCUMFERENTIAL/VMAX |
| 1 | 0.0 | C.10000000D 01 | 0.0 | -0.10000000D 01 | 0.0 |
| 2 | 0.25000D 00 | -C.17461742D-11 | 0.10000000D 01 | -0.26651565D-11 | 0.10000000D 01 |
| 3 | 0.50000D 00 | -C.10000000D 01 | -C.45845132D-11 | 0.10000000D 01 | 0.52868034D-11 |
| 4 | 0.75000D 00 | C.13521561D-11 | -0.10000000D 01 | -0.73612046D-11 | -0.10000000D 01 |
| 5 | 0.10000D 01 | 0.10000000D 01 | 0.0 | -0.10000000D 01 | 0.0 |

REMARK= LISTEC ABOVE,CNE HARMCNIC AT A TIME, ARE THE AMPLITUDES OF THE VARIATION IN CIRCUMFERENTIAL DIRECTION
THESE SHOULD BE MULTIPLIED RESPECTIVELY BY COS(N*PHI),COS(N*PHI),COS(N*PHI) AND SIN(N*PHI)
FOR CIRCUMFERENTIAL WAVE NUMBER N ANC CIRCUMFERENTIAL ANGLE PHI.

NATURAL VIBRATION OF NONUNIFORM THIN CYLIND. SHELLS BY FINITE-ELEMENTS METHOD

THE NUMBER OF CIRCUMFERENTIAL WAVES IS N = 3. FLUID DENSITY= 0.11233D-06

THE FREQUENCY IS = 0.67181D 05 RAD./SEC. = 0.10692D 05 CYCLES/SEC. FREQ. NO. 7

THE CORRESPONDING SHAPE IS

| | | UMAX= 0.55369D-01 | WMAX= 0.53425D 00 | BMAX= 0.37272D 00 | VMAX= 0.39994D-01 |
|---|---|---|---|---|---|
| NODE NO. | X/L | AXIAL/UMAX | RADIAL/WMAX | ANGULAR/BMAX | CIRCUMFERENTIAL/VMAX |
| 1 | 0.0 | 0.10000000D 01 | 0.0 | -0.10000000D 01 | 0.0 |
| 2 | 0.250000D 00 | 0.70710678D 00 | 0.70710678D 00 | -0.70710678D 00 | 0.70710678D 00 |
| 3 | 0.500000D 00 | -0.22667516D-11 | 0.10000000D 01 | -0.20772472D-11 | 0.10000000D 01 |
| 4 | 0.750000D 00 | -0.70710678D 00 | 0.70710678D 00 | 0.70710678D 00 | 0.70710678D 00 |
| 5 | 0.100000D 01 | -0.10000000D 01 | 0.0 | 0.10000000D 01 | 0.0 |

REMARK= LISTED ABOVE,ONE HARMONIC AT A TIME, ARE THE AMPLITUDES OF THE VARIATION IN CIRCUMFERENTIAL DIRECTION
THESE SHOULD BE MULTIPLIED RESPECTIVELY BY COS(N*PHI),COS(N*PHI),COS(N*PHI) AND SIN(N*PHI)
FOR CIRCUMFERENTIAL WAVE NUMBER N AND CIRCUMFERENTIAL ANGLE PHI.

```
NATURAL VIBRATION OF NONUNIFORM THIN CYLIND. SHELLS BY FINITE-ELEMENTS METHOD
-----------------------------------------------------------------------------

        THE NUMBER OF CIRCUMFERENTIAL  WAVES IS N =  3.   FLUID DENSITY= 0.11233D-06
        -------------------------------------------

 THE FREQUENCY IS = 0.85701D 05 RAD./SEC. = 0.13640D 05 CYCLES/SEC.          FREQ. NO.    8

THE CORRESPONDING SHAPE IS

                             UMAX= 0.15432D-02   WMAX= 0.77277D-01  BMAX= 0.57363D 00  VMAX= 0.21248D-01
  NODE NO.        X/L          AXIAL/UMAX        RADIAL/WMAX       ANGULAR/BMAX       CIRCUMFERENTIAL/VMAX
       1        0.0             0.10000000D 01    0.0              -0.10000000D 01      0.0
       2        0.25000D 00    -0.70710678D 00   -0.70710678D 00    0.70710678D 00    -0.70710678D 00
       3        0.50000D 00     0.12735384D-11    0.10000000D 01    0.11774475D-13     0.10000000D 01
       4        0.75000D 00     0.70710678D 00   -0.70710678D 00   -0.70710678D 00    -0.70710678D 00
       5        0.10000D 01    -0.10000000D 01    0.0               0.10000000D 01     0.0

REMARK= LISTED ABOVE,ONE HARMONIC AT A TIME, ARE THE AMPLITUDES OF THE VARIATION IN CIRCUMFERENTIAL DIRECTION
        THESE SHOULD BE MULTIPLIED RESPECTIVELY BY COS(N*PHI),COS(N*PHI),COS(N*PHI) AND SIN(N*PHI)
        FOR CIRCUMFERENTIAL WAVE NUMBER  N AND CIRCUMFERENTIAL ANGLE PHI.
```

NATURAL VIBRATION OF NONUNIFORM THIN CYLIND. SHELLS BY FINITE-ELEMENTS METHOD

THE NUMBER OF CIRCUMFERENTIAL WAVES IS N = 3. FLUID DENSITY= 0.11233D-06

THE FREQUENCY IS = 0.87788D 05 RAD./SEC. = 0.13972D 05 CYCLES/SEC. FREQ. NO. 9

THE CORRESPONDING SHAPE IS

| NODE NO. | X/L | UMAX= 0.14276D-02<br>AXIAL/UMAX | WMAX= 0.25066D-01<br>RADIAL/WMAX | BMAX= 0.57695D 00<br>ANGULAR/BMAX | VMAX= 0.73923D-02<br>CIRCUMFERENTIAL/VMAX |
|---|---|---|---|---|---|
| 1 | 0.0 | 0.10000000D 01 | 0.0 | 0.10000000D 01 | 0.0 |
| 2 | 0.25000D 00 | -0.53758070D-09 | 0.10000000D 01 | 0.74826714D-11 | 0.10000000D 01 |
| 3 | 0.50000D 00 | -0.10000000D 01 | -0.66364218D-11 | -0.10000000D 01 | 0.20159661D-11 |
| 4 | 0.75000D 00 | -0.52778602D-09 | -0.10000000D 01 | 0.13076497D-10 | -0.10000000D 01 |
| 5 | 0.10000D 01 | 0.10000000D 01 | 0.0 | 0.10000000D 01 | 0.0 |

REMARK= LISTED ABOVE,ONE HARMONIC AT A TIME, ARE THE AMPLITUDES OF THE VARIATION IN CIRCUMFERENTIAL DIRECTION
THESE SHOULD BE MULTIPLIED RESPECTIVELY BY COS(N*PHI),COS(N*PHI),COS(N*PHI) AND SIN(N*PHI)
FOR CIRCUMFERENTIAL WAVE NUMBER N AND CIRCUMFERENTIAL ANGLE PHI.

NATURAL VIBRATION OF NONUNIFORM THIN CYLIND. SHELLS BY FINITE-ELEMENTS METHOD



THE NUMBER OF CIRCUMFERENTIAL WAVES IS N = 3. FLUID DENSITY= 0.11233D-06

THE FREQUENCY IS = 0.88260D 05 RAD./SEC. = 0.14047D 05 CYCLES/SEC. FREQ. NO. 10

THE CORRESPONDING SHAPE IS

| | | UMAX= 0.26387D-02 | WMAX= 0.90545D-02 | BMAX= 0.57729D 00 | VMAX= 0.27363D-02 |
|---|---|---|---|---|---|
| NODE NO. | X/L | AXIAL/UMAX | RADIAL/WMAX | ANGULAR/BMAX | CIRCUMFERENTIAL/VMAX |
| 1 | 0.0 | -0.10000000D 01 | 0.0 | -0.10000000D 01 | 0.0 |
| 2 | 0.250000D 00 | -0.70710678D 00 | -0.70710678D 00 | -0.70710678D 00 | -0.70710678D 00 |
| 3 | 0.500000D 00 | 0.23795308D-11 | -0.10000000D 01 | 0.30907372D-13 | -0.10000000D 01 |
| 4 | 0.750000D 00 | 0.70710678D 00 | -0.70710678D 00 | 0.70710678D 00 | -0.70710678D 00 |
| 5 | 0.100000D 01 | 0.10000000D 01 | 0.0 | 0.10000000D 01 | 0.0 |

REMARK= LISTED ABOVE,ONE HARMONIC AT A TIME, ARE THE AMPLITUDES OF THE VARIATION IN CIRCUMFERENTIAL DIRECTION
THESE SHOULD BE MULTIPLIED RESPECTIVELY BY COS(N*PHI),COS(N*PHI),COS(N*PHI) AND SIN(N*PHI)
FOR CIRCUMFERENTIAL WAVE NUMBER N AND CIRCUMFERENTIAL ANGLE PHI.

```
MEAN SQUARE RESPONSE OF NONUNIFORM THIN CYLIND.  SHELLS
-------------------------------------------------------
SUBJECTED TO INTERNAL RANDOM PRESSURE
--------------------------------------
 CIRCUMFERENTIAL WAVES NUMBER N =3. FLUID DENSITY= 0.11233D-06 LB-SEC**2/(IN**4)


CENTRE LINE VELOCITY VECTOR,  (UCL(I),I=1,NNODES)= (IN./SEC.)
 0.28800D 03  0.28800D 03  0.28800D 03  0.28800D 03  0.28800D 03

 DIAGONAL MASS VECTOR,  (M(I),I=1,NREDUC)= (LB-SEC*SEC/IN)
 0.19327D-02  0.14752D-02  0.85499D-03  0.54562D-04  0.44417D-04  0.73997D-04
 0.15177D-03  0.78454D-05  0.40610D-05  0.36534D-05  0.43234D-05  0.46310D-05
 0.75809D-05  0.34250D-03  0.61786D-03  0.54269D-04

 DIAGONAL STIFFNESS VECTOR,  (K(I),I=1,NREDUC)= (LB/IN)
 0.14584D 05  0.11224D 06  0.26403D 06  0.13145D 06  0.13985D 06  0.29069D 06
 0.68496D 06  0.57622D 05  0.31297D 05  0.28459D 05  0.33734D 05  0.43859D 05
 0.82559D 05  0.38241D 07  0.82340D 07  0.78748D 06

 VISCOUS DAMPING VECTOR,  (C(I),I=1,NREDUC)= (LB-SEC/IN)
 0.10618D-03  0.25734D-03  0.30050D-03  0.53562D-04  0.49847D-04  0.92758D-04
 0.20392D-03  0.13447D-04  0.71302D-05  0.64489D-05  0.76380D-05  0.90137D-05
 0.15822D-04  0.72382D-03  0.14265D-02  0.13075D-03

 DAMPING FACTOR,  (ZETA(I),I=1,NREDUC),
 0.10000D-04  0.10000D-04  0.10000D-04  0.10000D-04  0.10000D-04  0.10000D-04
 0.10000D-04  0.10000D-04  0.10000D-04  0.10000D-04  0.10000D-04  0.10000D-04
 0.10000D-04  0.10000D-04  0.10000D-04  0.10000D-04
```

MEAN SQUARE RESPONSE OF NONUNIFORM THIN CYLIND. SHELLS

SUBJECTED TO INTERNAL RANDOM PRESSURE

CIRCUMFERENTIAL WAVES NUMBER N =3. FLUID DENSITY= 0.11233D-06 LB-SEC**2/(IN**4)

| NODE NO. | X(I) | R.M.S. AXIAL DISPL. | R.M.S. RADIAL DISPL. | R.M.S. ANGULAR DISPL. | R.M.S. CIRCUMFERENTIAL DISPL. |
|---|---|---|---|---|---|
| 1 | 0.0 | 0.16194D-08 | 0.0 | 0.40188D-08 | 0.0 |
| 2 | 0.46350D 01 | 0.11451D-08 | 0.16772D-07 | 0.28417D-08 | 0.56592D-08 |
| 3 | 0.92700D 01 | 0.26460D-11 | 0.23719D-07 | 0.90044D-11 | 0.80033D-08 |
| 4 | 0.13905D 02 | 0.11451D-08 | 0.16772D-07 | 0.28417D-08 | 0.56592D-08 |
| 5 | 0.18540D 02 | 0.16194D-08 | 0.0 | 0.40188D-08 | 0.0 |

BECAUSE THE EXCITATION IS APPROX. NORMALLY DISTRIBUTED
WITH ZERO MEANS. IT FOLLOWS THAT THE RESPONSE IS ALSO
APPROX. NORMALLY DISTRIBUTED WITH ZERO MEANS AND
THE VARIANCES ARE GIVEN BY THE RMS VALUES LISTED ABOVE
THEREFORE
THE PROBABILITY THAT THE DISPL. AT NODE (I) WILL EXCEED
THE 1.*(RMS RESPONSE) IS = 0.31731D 00
THE 2.*(RMS RESPONSE) IS = 0.45500D-01
THE 3.*(RMS RESPONSE) IS = 0.26999D-02

MEAN SQUARE RESPONSE OF NONUNIFORM THIN CYLIND. SHELLS

SUBJECTED TO INTERNAL RANDOM PRESSURE

CIRCUMFERENTIAL WAVES NUMBER N =3. FLUID DENSITY= 0.11233D-06 LB-SEC**2/(IN**4)

UMAX= 0.16194D-08 WMAX= 0.23719D-07 BMAX= 0.40188D-08 VMAX= 0.80033D-08

| NODE NO. | X/L | RMS AXIAL DISP./UMAX. | RMS RADIAL DISP./WMAX. | RMS ANGULAR DISP./BMAX. | RMS CIRCUMFERENTIAL DISPL./VMAX. |
|---|---|---|---|---|---|
| 1 | 0.0 | 0.10000D 01 | 0.0 | 0.10000D 01 | 0.0 |
| 2 | 0.25000D 00 | 0.70711D 00 | 0.70711D 00 | 0.70711D 00 | 0.70711D 00 |
| 3 | 0.50000D 00 | 0.16340D-02 | 0.10000D 01 | 0.22406D-02 | 0.10000D 01 |
| 4 | 0.75000D 00 | 0.70711D 00 | 0.70711D 00 | 0.70711D 00 | 0.70711D 00 |
| 5 | 0.10000D 01 | 0.10000D 01 | 0.0 | 0.10000D 01 | 0.0 |

$$
[R] = \begin{bmatrix}
e^{-\psi_1}[\bar\alpha_1\cos\zeta_1-\bar\alpha_2\sin\zeta_1] & e^{-\psi_1}[\bar\alpha_2\cos\zeta_1+\bar\alpha_1\sin\zeta_1] & e^{-\psi_2}[\bar\alpha_3\cos\zeta_2-\bar\alpha_4\sin\zeta_2] & e^{-\psi_2}[\bar\alpha_4\cos\zeta_2+\bar\alpha_3\sin\zeta_2] & e^{\psi_1}[\bar\alpha_5\cos\zeta_1-\bar\alpha_6\sin\zeta_1] & e^{\psi_1}[\bar\alpha_6\cos\zeta_1+\bar\alpha_5\sin\zeta_1] & e^{\psi_2}[\bar\alpha_7\cos\zeta_2-\bar\alpha_8\sin\zeta_2] & e^{\psi_2}[\bar\alpha_8\cos\zeta_2+\bar\alpha_7\sin\zeta_2] \\
e^{-\psi_1}\cos\zeta_1 & e^{-\psi_1}\sin\zeta_1 & e^{-\psi_2}\cos\zeta_2 & e^{-\psi_2}\sin\zeta_2 & e^{\psi_1}\cos\zeta_1 & e^{\psi_1}\sin\zeta_1 & e^{\psi_2}\cos\zeta_2 & e^{\psi_2}\sin\zeta_2 \\
e^{-\psi_1}[\bar\beta_1\cos\zeta_1-\bar\beta_2\sin\zeta_1] & e^{-\psi_1}[\bar\beta_2\cos\zeta_1+\bar\beta_1\sin\zeta_1] & e^{-\psi_2}[\bar\beta_3\cos\zeta_2-\bar\beta_4\sin\zeta_2] & e^{-\psi_2}[\bar\beta_4\cos\zeta_2+\bar\beta_3\sin\zeta_2] & e^{\psi_1}[\bar\beta_5\cos\zeta_1-\bar\beta_6\sin\zeta_1] & e^{\psi_1}[\bar\beta_6\cos\zeta_1+\bar\beta_5\sin\zeta_1] & e^{\psi_2}[\bar\beta_7\cos\zeta_2-\bar\beta_8\sin\zeta_2] & e^{\psi_2}[\bar\beta_8\cos\zeta_2+\bar\beta_7\sin\zeta_2]
\end{bmatrix}
$$

$$
\omega_1 = \frac{\kappa_1 \ell}{r}, \quad \eta_1 = \frac{\mu_1 \ell}{r}, \quad \psi_1 = \frac{\kappa_1 x}{r}, \quad \zeta_1 = \frac{\mu_1 x}{r}
$$

$$
\omega_2 = \frac{\kappa_2 \ell}{r}, \quad \eta_3 = \frac{\mu_2 \ell}{r}, \quad \psi_2 = \frac{\kappa_2 x}{r}, \quad \zeta_2 = \frac{\mu_2 x}{r}
$$

;

$$
[T] = \begin{bmatrix} \cos n\varphi & 0 & 0 \\ 0 & \cos n\varphi & 0 \\ 0 & 0 & \sin n\varphi \end{bmatrix}
$$

$$
\{f\} = \begin{Bmatrix} U \\ W \\ V \end{Bmatrix} = [T][R]\{C\} = [T][R][A^{-1}]\{\delta_n\} = [N]\{\delta_n\}
$$

TABLE 1. Matrices [R] and [T] and definition of $\omega_1$, $\omega_2$, $\eta_1$, $\eta_2$, $\psi_1$, $\psi_2$ and $\zeta_1$, $\zeta_2$.

$$
[A] = \begin{bmatrix}
\bar{\alpha}_1 & \bar{\alpha}_2 & \bar{\alpha}_3 & \bar{\alpha}_4 & \bar{\alpha}_5 & \bar{\alpha}_6 & \bar{\alpha}_7 & \bar{\alpha}_8 \\
1 & 0 & 1 & 0 & 1 & 0 & 1 & 0 \\
-\kappa_1/r & \mu_1/r & -\kappa_2/r & \mu_2/r & \kappa_1/r & \mu_1/r & \kappa_2/r & \mu_2/r \\
\bar{\beta}_1 & \bar{\beta}_2 & \bar{\beta}_3 & \bar{\beta}_4 & \bar{\beta}_5 & \bar{\beta}_6 & \bar{\beta}_7 & \bar{\beta}_8 \\
e^{-\omega_1}[\bar{\alpha}_1 \cos\eta_1 - \bar{\alpha}_2 \sin\eta_1] & e^{-\omega_1}[\bar{\alpha}_2 \cos\eta_1 + \bar{\alpha}_1 \sin\eta_1] & e^{-\omega_2}[\bar{\alpha}_3 \cos\eta_2 - \bar{\alpha}_4 \sin\eta_2] & e^{-\omega_2}[\bar{\alpha}_4 \cos\eta_2 + \bar{\alpha}_3 \sin\eta_2] & e^{\omega_1}[\bar{\alpha}_5 \cos\eta_1 - \bar{\alpha}_6 \sin\eta_1] & e^{\omega_1}[\bar{\alpha}_6 \cos\eta_1 + \bar{\alpha}_5 \sin\eta_1] & e^{\omega_2}[\bar{\alpha}_7 \cos\eta_2 - \bar{\alpha}_8 \sin\eta_2] & e^{\omega_2}[\bar{\alpha}_8 \cos\eta_2 + \bar{\alpha}_7 \sin\eta_2] \\
e^{-\omega_1}\cos\eta_1 & e^{-\omega_1}\sin\eta_1 & e^{-\omega_2}\cos\eta_2 & e^{-\omega_2}\sin\eta_2 & e^{\omega_1}\cos\eta_1 & e^{\omega_1}\sin\eta_1 & e^{\omega_2}\cos\eta_2 & e^{\omega_2}\sin\eta_2 \\
\frac{e^{-\omega_1}}{r}[-\kappa_1 \cos\eta_1 - \mu_1 \sin\eta_1] & \frac{e^{-\omega_1}}{r}[\mu_1 \cos\eta_1 - \kappa_1 \sin\eta_1] & \frac{e^{-\omega_2}}{r}[-\kappa_2 \cos\eta_2 - \mu_2 \sin\eta_2] & \frac{e^{-\omega_2}}{r}[\mu_2 \cos\eta_2 - \kappa_2 \sin\eta_2] & \frac{e^{\omega_1}}{r}[\kappa_1 \cos\eta_1 - \mu_1 \sin\eta_1] & \frac{e^{\omega_1}}{r}[\mu_1 \cos\eta_1 + \kappa_1 \sin\eta_1] & \frac{e^{\omega_2}}{r}[\kappa_2 \cos\eta_2 - \mu_2 \sin\eta_2] & \frac{e^{\omega_2}}{r}[\mu_2 \cos\eta_2 + \kappa_2 \sin\eta_2] \\
e^{-\omega_1}[\bar{\beta}_1 \cos\eta_1 - \bar{\beta}_2 \sin\eta_1] & e^{-\omega_1}[\bar{\beta}_2 \cos\eta_1 + \bar{\beta}_1 \sin\eta_1] & e^{-\omega_2}[\bar{\beta}_3 \cos\eta_2 - \bar{\beta}_4 \sin\eta_2] & e^{-\omega_2}[\bar{\beta}_4 \cos\eta_2 + \bar{\beta}_3 \sin\eta_2] & e^{\omega_1}[\bar{\beta}_5 \cos\eta_1 - \bar{\beta}_6 \sin\eta_1] & e^{\omega_1}[\bar{\beta}_6 \cos\eta_1 + \bar{\beta}_5 \sin\eta_1] & e^{\omega_2}[\bar{\beta}_7 \cos\eta_2 - \bar{\beta}_8 \sin\eta_2] & e^{\omega_2}[\bar{\beta}_8 \cos\eta_2 + \bar{\beta}_7 \sin\eta_2]
\end{bmatrix}
$$

TABLE 2. Matrix [A]

$$
[Q] = \left[\begin{array}{c|c|c|c|c|c|c|c}
\begin{gathered}\frac{e^{-\psi_1}}{r}\left[(-\kappa_1\bar{\alpha}_1-\mu_1\bar{\alpha}_2)\cos\zeta_1\right.\\ \left.+(\kappa_1\bar{\alpha}_2-\mu_1\bar{\alpha}_1)\sin\zeta_1\right]\end{gathered} &
\begin{gathered}\frac{e^{-\psi_1}}{r}\left[(-\kappa_1\bar{\alpha}_2+\mu_1\bar{\alpha}_1)\cos\zeta_1\right.\\ \left.-(\kappa_1\bar{\alpha}_1+\mu_1\bar{\alpha}_2)\sin\zeta_1\right]\end{gathered} &
\begin{gathered}\frac{e^{-\psi_2}}{r}\left[(-\kappa_2\bar{\alpha}_3-\mu_2\bar{\alpha}_4)\cos\zeta_2\right.\\ \left.+(\kappa_2\bar{\alpha}_4-\mu_2\bar{\alpha}_3)\sin\zeta_2\right]\end{gathered} &
\begin{gathered}\frac{e^{-\psi_2}}{r}\left[(-\kappa_2\bar{\alpha}_4+\mu_2\bar{\alpha}_3)\cos\zeta_2\right.\\ \left.-(\kappa_2\bar{\alpha}_3+\mu_2\bar{\alpha}_4)\sin\zeta_2\right]\end{gathered} &
\begin{gathered}\frac{e^{\psi_1}}{r}\left[(\kappa_1\bar{\alpha}_5-\mu_1\bar{\alpha}_6)\cos\zeta_1\right.\\ \left.-(\kappa_1\bar{\alpha}_6+\mu_1\bar{\alpha}_5)\sin\zeta_1\right]\end{gathered} &
\begin{gathered}\frac{e^{\psi_1}}{r}\left[(\kappa_1\bar{\alpha}_6+\mu_1\bar{\alpha}_5)\cos\zeta_1\right.\\ \left.+(\kappa_1\bar{\alpha}_5-\mu_1\bar{\alpha}_6)\sin\zeta_1\right]\end{gathered} &
\begin{gathered}\frac{e^{\psi_2}}{r}\left[(\kappa_2\bar{\alpha}_7-\mu_2\bar{\alpha}_8)\cos\zeta_2\right.\\ \left.-(\kappa_2\bar{\alpha}_8+\mu_2\bar{\alpha}_7)\sin\zeta_2\right]\end{gathered} &
\begin{gathered}\frac{e^{\psi_2}}{r}\left[(\kappa_2\bar{\alpha}_8+\mu_2\bar{\alpha}_7)\cos\zeta_2\right.\\ \left.+(\kappa_2\bar{\alpha}_7-\mu_2\bar{\alpha}_8)\sin\zeta_2\right]\end{gathered} \\ \hline
\begin{gathered}\frac{e^{-\psi_1}}{r}\left[(n\bar{\beta}_1+1)\cos\zeta_1\right.\\ \left.-n\bar{\beta}_2\sin\zeta_1\right]\end{gathered} &
\begin{gathered}\frac{e^{-\psi_1}}{r}\left[n\bar{\beta}_2\cos\zeta_1\right.\\ \left.+(n\bar{\beta}_1+1)\sin\zeta_1\right]\end{gathered} &
\begin{gathered}\frac{e^{-\psi_2}}{r}\left[(n\bar{\beta}_3+1)\cos\zeta_2\right.\\ \left.-n\bar{\beta}_4\sin\zeta_2\right]\end{gathered} &
\begin{gathered}\frac{e^{-\psi_2}}{r}\left[n\bar{\beta}_4\cos\zeta_2\right.\\ \left.+(n\bar{\beta}_3+1)\sin\zeta_2\right]\end{gathered} &
\begin{gathered}\frac{e^{\psi_1}}{r}\left[(n\bar{\beta}_5+1)\cos\zeta_1\right.\\ \left.-n\bar{\beta}_6\sin\zeta_1\right]\end{gathered} &
\begin{gathered}\frac{e^{\psi_1}}{r}\left[n\bar{\beta}_6\cos\zeta_1\right.\\ \left.+(n\bar{\beta}_5+1)\sin\zeta_1\right]\end{gathered} &
\begin{gathered}\frac{e^{\psi_2}}{r}\left[(n\bar{\beta}_7+1)\cos\zeta_2\right.\\ \left.-n\bar{\beta}_8\sin\zeta_2\right]\end{gathered} &
\begin{gathered}\frac{e^{\psi_2}}{r}\left[n\bar{\beta}_8\cos\zeta_2\right.\\ \left.+(n\bar{\beta}_7+1)\sin\zeta_2\right]\end{gathered} \\ \hline
\begin{gathered}\frac{e^{-\psi_1}}{r}\left[(-\kappa_1\bar{\beta}_1-\mu_1\bar{\beta}_2-n\bar{\alpha}_1)\right.\\ \cos\zeta_1+(\kappa_1\bar{\beta}_2-\mu_1\bar{\beta}_1\\ \left.+n\bar{\alpha}_2)\sin\zeta_1\right]\end{gathered} &
\begin{gathered}\frac{e^{-\psi_1}}{r}\left[(-\kappa_1\bar{\beta}_2+\mu_1\bar{\beta}_1-n\bar{\alpha}_2)\cdot\right.\\ \cos\zeta_1-(\kappa_1\bar{\beta}_1+\mu_1\bar{\beta}_2\\ \left.+n\bar{\alpha}_1)\sin\zeta_1\right]\end{gathered} &
\begin{gathered}\frac{e^{-\psi_2}}{r}\left[(-\kappa_2\bar{\beta}_3-\mu_2\bar{\beta}_4-n\bar{\alpha}_3)\cdot\right.\\ \cos\zeta_2+(\kappa_2\bar{\beta}_4-\mu_2\bar{\beta}_3\\ \left.+n\bar{\alpha}_4)\sin\zeta_2\right]\end{gathered} &
\begin{gathered}\frac{e^{-\psi_2}}{r}\left[(-\kappa_2\bar{\beta}_4+\mu_2\bar{\beta}_3-n\bar{\alpha}_4)\cdot\right.\\ \cos\zeta_2-(\kappa_2\bar{\beta}_3+\mu_2\bar{\beta}_4\\ \left.+n\bar{\alpha}_3)\sin\zeta_2\right]\end{gathered} &
\begin{gathered}\frac{e^{\psi_1}}{r}\left[(\kappa_1\bar{\beta}_5-\mu_1\bar{\beta}_6-n\bar{\alpha}_5)\cdot\right.\\ \cos\zeta_1-(\kappa_1\bar{\beta}_6+\mu_1\bar{\beta}_5\\ \left.-n\bar{\alpha}_6)\sin\zeta_1\right]\end{gathered} &
\begin{gathered}\frac{e^{\psi_1}}{r}\left[(\kappa_1\bar{\beta}_6+\mu_1\bar{\beta}_5-n\bar{\alpha}_6)\cdot\right.\\ \cos\zeta_1+(\kappa_1\bar{\beta}_5-\mu_1\bar{\beta}_6\\ \left.-n\bar{\alpha}_5)\sin\zeta_1\right]\end{gathered} &
\begin{gathered}\frac{e^{\psi_2}}{r}\left[(\kappa_2\bar{\beta}_7-\mu_2\bar{\beta}_8-n\bar{\alpha}_7)\cdot\right.\\ \cos\zeta_2-(\kappa_2\bar{\beta}_8+\mu_2\bar{\beta}_7\\ \left.-n\bar{\alpha}_8)\sin\zeta_2\right]\end{gathered} &
\begin{gathered}\frac{e^{\psi_2}}{r}\left[(\kappa_2\bar{\beta}_8+\mu_2\bar{\beta}_7-n\bar{\alpha}_8)\cdot\right.\\ \cos\zeta_2+(\kappa_2\bar{\beta}_7-\mu_2\bar{\beta}_8\\ \left.-n\bar{\alpha}_7)\sin\zeta_2\right]\end{gathered} \\ \hline
\begin{gathered}\frac{-e^{-\psi_1}}{r^2}\left[(\kappa_1^2-\mu_1^2)\cos\zeta_1\right.\\ +2\kappa_1\mu_1\sin\zeta_1\end{gathered} &
\begin{gathered}\frac{-e^{-\psi_1}}{r^2}\left[-2\kappa_1\mu_1\cos\zeta_1\right.\\ +(\kappa_1^2-\mu_1^2)\sin\zeta_1\end{gathered} &
\begin{gathered}\frac{-e^{-\psi_2}}{r^2}\left[(\kappa_2^2-\mu_2^2)\cos\zeta_2\right.\\ \left.+2\kappa_2\mu_2\sin\zeta_2\right]\end{gathered} &
\begin{gathered}\frac{-e^{-\psi_2}}{r^2}\left[-2\kappa_2\mu_2\cos\zeta_2\right.\\ \left.+(\kappa_2^2-\mu_2^2)\sin\zeta_2\right]\end{gathered} &
\begin{gathered}\frac{-e^{\psi_1}}{r^2}\left[(\kappa_1^2-\mu_1^2)\cos\zeta_1\right.\\ \left.-2\kappa_1\mu_1\sin\zeta_1\right]\end{gathered} &
\begin{gathered}\frac{-e^{\psi_1}}{r^2}\left[2\kappa_1\mu_1\cos\zeta_1\right.\\ \left.+(\kappa_1^2-\mu_1^2)\sin\zeta_1\right]\end{gathered} &
\begin{gathered}\frac{-e^{\psi_2}}{r^2}\left[(\kappa_2^2-\mu_2^2)\cos\zeta_2\right.\\ \left.-2\kappa_2\mu_2\sin\zeta_2\right]\end{gathered} &
\begin{gathered}\frac{-e^{\psi_2}}{r^2}\left[2\kappa_2\mu_2\cos\zeta_2\right.\\ \left.+(\kappa_2^2-\mu_2^2)\sin\zeta_2\right]\end{gathered} \\ \hline
\begin{gathered}\frac{e^{-\psi_1}}{r^2}\left[(n^2+n\bar{\beta}_1)\cos\zeta_1\right.\\ \left.-n\bar{\beta}_2\sin\zeta_1\right]\end{gathered} &
\begin{gathered}\frac{e^{-\psi_1}}{r^2}\left[n\bar{\beta}_2\cos\zeta_1\right.\\ \left.+(n^2+n\bar{\beta}_1)\sin\zeta_1\right]\end{gathered} &
\begin{gathered}\frac{e^{-\psi_2}}{r^2}\left[(n^2+n\bar{\beta}_3)\cos\zeta_2\right.\\ \left.-n\bar{\beta}_4\sin\zeta_2\right]\end{gathered} &
\begin{gathered}\frac{e^{-\psi_2}}{r^2}\left[n\bar{\beta}_4\cos\zeta_2\right.\\ \left.+(n^2+n\bar{\beta}_3)\sin\zeta_2\right]\end{gathered} &
\begin{gathered}\frac{e^{\psi_1}}{r^2}\left[(n^2+n\bar{\beta}_5)\cos\zeta_1\right.\\ \left.-n\bar{\beta}_6\sin\zeta_1\right]\end{gathered} &
\begin{gathered}\frac{e^{\psi_1}}{r^2}\left[n\bar{\beta}_6\cos\zeta_1\right.\\ \left.+(n^2+n\bar{\beta}_5)\sin\zeta_1\right]\end{gathered} &
\begin{gathered}\frac{e^{\psi_2}}{r^2}\left[(n^2+n\bar{\beta}_7)\cos\zeta_2\right.\\ \left.-n\bar{\beta}_8\sin\zeta_2\right]\end{gathered} &
\begin{gathered}\frac{e^{\psi_2}}{r^2}\left[n\bar{\beta}_8\cos\zeta_2\right.\\ \left.+(n^2+n\bar{\beta}_7)\sin\zeta_2\right]\end{gathered} \\ \hline
\begin{gathered}\frac{e^{-\psi_1}}{r^2}\left[(-2n\kappa_1-\tfrac{3}{2}\kappa_1\bar{\beta}_1\right.\\ -\tfrac{3}{2}\mu_1\bar{\beta}_2+\tfrac{n\bar{\alpha}_1}{2})\cos\zeta_1\\ +(-2n\mu_1+\tfrac{3}{2}\kappa_1\bar{\beta}_2\\ \left.-\tfrac{3}{2}\mu_1\bar{\beta}_1-\tfrac{n\bar{\alpha}_2}{2})\sin\zeta_1\right]\end{gathered} &
\begin{gathered}\frac{e^{-\psi_1}}{r^2}\left[(2n\mu_1-\tfrac{3}{2}\kappa_1\bar{\beta}_2\right.\\ +\tfrac{3}{2}\mu_1\bar{\beta}_1+\tfrac{n\bar{\alpha}_2}{2})\cos\zeta_1\\ +(-2n\kappa_1-\tfrac{3}{2}\kappa_1\bar{\beta}_1\\ \left.-\tfrac{3}{2}\mu_1\bar{\beta}_2+\tfrac{n\bar{\alpha}_1}{2})\sin\zeta_1\right]\end{gathered} &
\begin{gathered}\frac{e^{-\psi_2}}{r^2}\left[(-2n\kappa_2-\tfrac{3}{2}\kappa_2\bar{\beta}_3\right.\\ -\tfrac{3}{2}\mu_2\bar{\beta}_4+\tfrac{n\bar{\alpha}_3}{2})\cos\zeta_2\\ +(-2n\mu_2+\tfrac{3}{2}\kappa_2\bar{\beta}_4\\ \left.-\tfrac{3}{2}\mu_2\bar{\beta}_3-\tfrac{n\bar{\alpha}_4}{2})\sin\zeta_2\right]\end{gathered} &
\begin{gathered}\frac{e^{-\psi_2}}{r^2}\left[(2n\mu_2-\tfrac{3}{2}\kappa_2\bar{\beta}_4\right.\\ +\tfrac{3}{2}\mu_2\bar{\beta}_3+\tfrac{n\bar{\alpha}_4}{2})\cos\zeta_2\\ +(-2n\kappa_2-\tfrac{3}{2}\kappa_2\bar{\beta}_3\\ \left.-\tfrac{3}{2}\mu_2\bar{\beta}_4+\tfrac{n\bar{\alpha}_3}{2})\sin\zeta_2\right]\end{gathered} &
\begin{gathered}\frac{e^{\psi_1}}{r^2}\left[(2n\kappa_1+\tfrac{3}{2}\kappa_1\bar{\beta}_5\right.\\ -\tfrac{3}{2}\mu_1\bar{\beta}_6+\tfrac{n\bar{\alpha}_5}{2})\cos\zeta_1\\ +(2n\mu_1-\tfrac{3}{2}\kappa_1\bar{\beta}_6\\ \left.-\tfrac{3}{2}\mu_1\bar{\beta}_5-\tfrac{n\bar{\alpha}_6}{2})\sin\zeta_1\right]\end{gathered} &
\begin{gathered}\frac{e^{\psi_1}}{r^2}\left[(2n\mu_1+\tfrac{3}{2}\kappa_1\bar{\beta}_6\right.\\ +\tfrac{3}{2}\mu_1\bar{\beta}_5+\tfrac{n\bar{\alpha}_6}{2})\cos\zeta_1\\ +(2n\kappa_1+\tfrac{3}{2}\kappa_1\bar{\beta}_5\\ \left.-\tfrac{3}{2}\mu_1\bar{\beta}_6+\tfrac{n\bar{\alpha}_5}{2})\sin\zeta_1\right]\end{gathered} &
\begin{gathered}\frac{e^{\psi_2}}{r^2}\left[(2n\kappa_2+\tfrac{3}{2}\kappa_2\bar{\beta}_7\right.\\ -\tfrac{3}{2}\mu_2\bar{\beta}_8+\tfrac{n\bar{\alpha}_7}{2})\cos\zeta_2\\ +(-2n\mu_2-\tfrac{3}{2}\kappa_2\bar{\beta}_8\\ \left.-\tfrac{3}{2}\mu_2\bar{\beta}_7-\tfrac{n\bar{\alpha}_8}{2})\sin\zeta_2\right]\end{gathered} &
\begin{gathered}\frac{e^{\psi_2}}{r^2}\left[(2n\mu_2+\tfrac{3}{2}\kappa_2\bar{\beta}_8\right.\\ +\tfrac{3}{2}\mu_2\bar{\beta}_7+\tfrac{n\bar{\alpha}_8}{2})\cos\zeta_2\\ +(2n\kappa_2+\tfrac{3}{2}\kappa_2\bar{\beta}_7\\ \left.-\tfrac{3}{2}\mu_2\bar{\beta}_8+\tfrac{n\bar{\alpha}_7}{2})\sin\zeta_2\right]\end{gathered}
\end{array}\right]
$$



$$
\{\epsilon\} = \begin{bmatrix}[T] & [0] \\ [0] & [T]\end{bmatrix}[Q]\{C\} = \begin{bmatrix}[T][0] \\ [0][T]\end{bmatrix}[Q][A^{-1}]\{\delta_n\}
$$

**TABLE 3.** Matrix [Q]

$$[\Gamma] = \begin{bmatrix}
\frac{1}{r^2}\left[-2n\kappa_1 - \frac{3}{2}\kappa_1\bar\beta_1 - \frac{3}{2}\mu_1\bar\beta_2 + \frac{n\bar\alpha_1}{2}\right] & \frac{1}{r^2}\left[n^2 + n\bar\beta_1\right] & -\frac{1}{r^2}\left[\kappa_1^2 - \mu_1^2\right] & \frac{1}{r}\left[-\kappa_1\bar\beta_1 - \mu_1\bar\beta_2 - n\bar\alpha_1\right] & \frac{1}{r}\left[n\bar\beta_1 + 1\right] & \frac{1}{r}\left[-\kappa_1\bar\alpha_1 - \mu_1\bar\alpha_2\right] \\
\frac{1}{r^2}\left[-2n\mu_1 + \frac{3}{2}\kappa_1\bar\beta_2 - \frac{3}{2}\mu_1\bar\beta_1 - \frac{n\bar\alpha_2}{2}\right] & \frac{1}{r^2}\left[-n\bar\beta_2\right] & -\frac{1}{r^2}\left[2\kappa_1\mu_1\right] & \frac{1}{r}\left[\kappa_1\bar\beta_2 - \mu_1\bar\beta_1 + n\bar\alpha_2\right] & \frac{1}{r}\left[-n\bar\beta_2\right] & \frac{1}{r}\left[\kappa_1\bar\alpha_2 - \mu_1\bar\alpha_1\right] \\
\frac{1}{r^2}\left[2n\mu_1 - \frac{3}{2}\kappa_1\bar\beta_2 + \frac{3}{2}\mu_1\bar\beta_1 + \frac{n\bar\alpha_2}{2}\right] & \frac{1}{r^2}\left[n\bar\beta_2\right] & \frac{1}{r^2}\left[2\mu_1\kappa_1\right] & \frac{1}{r}\left[-\kappa_1\bar\beta_2 + \mu_1\bar\beta_1 - n\bar\alpha_2\right] & \frac{1}{r}\left[n\bar\beta_2\right] & \frac{1}{r}\left[-\kappa_1\bar\alpha_2 + \mu_1\bar\alpha_1\right] \\
\frac{1}{r^2}\left[-2n\kappa_1 - \frac{3}{2}\kappa_1\bar\beta_1 - \frac{3}{2}\mu_1\bar\beta_2 + \frac{n\bar\alpha_1}{2}\right] & \frac{1}{r^2}\left[n^2 + n\bar\beta_1\right] & -\frac{1}{r^2}\left[\kappa_1^2 - \mu_1^2\right] & \frac{1}{r}\left[-\kappa_1\bar\beta_1 - \mu_1\bar\beta_2 - n\bar\alpha_1\right] & \frac{1}{r}\left[n\bar\beta_1 + 1\right] & \frac{1}{r}\left[-\kappa_1\bar\alpha_1 - \mu_1\bar\alpha_2\right] \\
\frac{1}{r^2}\left[-2n\kappa_2 - \frac{3}{2}\kappa_2\bar\beta_3 - \frac{3}{2}\mu_2\bar\beta_4 + \frac{n\bar\alpha_3}{2}\right] & \frac{1}{r^2}\left[n^2 + n\bar\beta_3\right] & -\frac{1}{r^2}\left[\kappa_2^2 - \mu_2^2\right] & \frac{1}{r}\left[-\kappa_2\bar\beta_3 - \mu_2\bar\beta_4 - n\bar\alpha_3\right] & \frac{1}{r}\left[n\bar\beta_3 + 1\right] & \frac{1}{r}\left[-\kappa_2\bar\alpha_3 - \mu_2\bar\alpha_4\right] \\
\frac{1}{r^2}\left[-2n\mu_2 + \frac{3}{2}\kappa_2\bar\beta_4 - \frac{3}{2}\mu_2\bar\beta_3 - \frac{n\bar\alpha_4}{2}\right] & -\frac{1}{r^2}\left[n\bar\beta_4\right] & -\frac{1}{r^2}\left[2\kappa_2\mu_2\right] & \frac{1}{r}\left[\kappa_2\bar\beta_4 - \mu_2\bar\beta_3 + n\bar\alpha_4\right] & \frac{1}{r}\left[-n\bar\beta_4\right] & \frac{1}{r}\left[\kappa_2\bar\alpha_4 - \mu_2\bar\alpha_3\right] \\
\frac{1}{r^2}\left[2n\mu_2 - \frac{3}{2}\kappa_2\bar\beta_4 + \frac{3}{2}\mu_2\bar\beta_3 + \frac{n\bar\alpha_4}{2}\right] & \frac{1}{r^2}\left[n\bar\beta_4\right] & \frac{1}{r^2}\left[2\kappa_2\mu_2\right] & \frac{1}{r}\left[-\kappa_2\bar\beta_4 + \mu_2\bar\beta_3 - n\bar\alpha_4\right] & \frac{1}{r}\left[n\bar\beta_4\right] & \frac{1}{r}\left[-\kappa_2\bar\alpha_4 + \mu_2\bar\alpha_3\right] \\
\frac{1}{r^2}\left[-2n\kappa_2 - \frac{3}{2}\kappa_2\bar\beta_3 - \frac{3}{2}\mu_2\bar\beta_4 + \frac{n\bar\alpha_3}{2}\right] & \frac{1}{r^2}\left[n^2 + n\bar\beta_3\right] & -\frac{1}{r^2}\left[\kappa_2^2 - \mu_2^2\right] & \frac{1}{r}\left[-\kappa_2\bar\beta_3 - \mu_2\bar\beta_4 - n\bar\alpha_3\right] & \frac{1}{r}\left[n\bar\beta_3 + 1\right] & \frac{1}{r}\left[-\kappa_2\bar\alpha_3 - \mu_2\bar\alpha_4\right] \\
\frac{1}{r^2}\left[2n\kappa_1 + \frac{3}{2}\kappa_1\bar\beta_5 - \frac{3}{2}\mu_1\bar\beta_6 + \frac{n\bar\alpha_5}{2}\right] & \frac{1}{r^2}\left[n^2 + n\bar\beta_5\right] & -\frac{1}{r^2}\left[\kappa_1^2 - \mu_1^2\right] & \frac{1}{r}\left[\kappa_1\bar\beta_5 - \mu_1\bar\beta_6 - n\bar\alpha_5\right] & \frac{1}{r}\left[n\bar\beta_5 + 1\right] & \frac{1}{r}\left[\kappa_1\bar\alpha_5 - \mu_1\bar\alpha_6\right] \\
\frac{1}{r^2}\left[-2n\mu_1 - \frac{3}{2}\kappa_1\bar\beta_6 - \frac{3}{2}\mu_1\bar\beta_5 - \frac{n\bar\alpha_6}{2}\right] & -\frac{1}{r^2}\left[n\bar\beta_6\right] & \frac{1}{r^2}\left[2\kappa_1\mu_1\right] & \frac{1}{r}\left[-\kappa_1\bar\beta_6 - \mu_1\bar\beta_5 + n\bar\alpha_6\right] & \frac{1}{r}\left[-n\bar\beta_6\right] & \frac{1}{r}\left[-\kappa_1\bar\alpha_6 - \mu_1\bar\alpha_5\right] \\
\frac{1}{r^2}\left[2n\mu_1 + \frac{3}{2}\kappa_1\bar\beta_6 + \frac{3}{2}\mu_1\bar\beta_5 + \frac{n\bar\alpha_6}{2}\right] & \frac{1}{r^2}\left[n\bar\beta_6\right] & -\frac{1}{r^2}\left[2\kappa_1\mu_1\right] & \frac{1}{r}\left[\kappa_1\bar\beta_6 + \mu_1\bar\beta_5 - n\bar\alpha_6\right] & \frac{1}{r}\left[n\bar\beta_6\right] & \frac{1}{r}\left[\kappa_1\bar\alpha_6 + \mu_1\bar\alpha_5\right] \\
\frac{1}{r^2}\left[2n\kappa_1 + \frac{3}{2}\kappa_1\bar\beta_5 - \frac{3}{2}\mu_1\bar\beta_6 + \frac{n\bar\alpha_5}{2}\right] & \frac{1}{r^2}\left[n^2 + n\bar\beta_5\right] & -\frac{1}{r^2}\left[\kappa_1^2 - \mu_1^2\right] & \frac{1}{r}\left[\kappa_1\bar\beta_5 - \mu_1\bar\beta_6 - n\bar\alpha_5\right] & \frac{1}{r}\left[n\bar\beta_5 + 1\right] & \frac{1}{r}\left[\kappa_1\bar\alpha_5 - \mu_1\bar\alpha_6\right] \\
\frac{1}{r^2}\left[2n\kappa_2 + \frac{3}{2}\kappa_2\bar\beta_7 - \frac{3}{2}\mu_2\bar\beta_8 + \frac{n\bar\alpha_7}{2}\right. & \frac{1}{r^2}\left[n^2 + n\bar\beta_7\right] & -\frac{1}{r^2}\left[\kappa_2^2 - \mu_2^2\right] & \frac{1}{r}\left[\kappa_2\bar\beta_7 - \mu_2\bar\beta_8 - n\bar\alpha_7\right] & \frac{1}{r}\left[n\bar\beta_7 + 1\right] & \frac{1}{r}\left[\kappa_2\bar\alpha_7 - \mu_2\bar\alpha_8\right] \\
\frac{1}{r^2}\left[-2n\mu_2 - \frac{3}{2}\kappa_2\bar\beta_8 - \frac{3}{2}\mu_2\bar\beta_7 - \frac{n\bar\alpha_8}{2}\right] & -\frac{1}{r^2}\left[n\bar\beta_8\right] & \frac{1}{r^2}\left[2\kappa_2\mu_2\right] & \frac{1}{r}\left[-\kappa_2\bar\beta_8 - \mu_2\bar\beta_7 + n\bar\alpha_8\right] & \frac{1}{r}\left[-n\bar\beta_8\right] & \frac{1}{r}\left[-\kappa_2\bar\alpha_8 - \mu_2\bar\alpha_7\right] \\
\frac{1}{r^2}\left[2n\mu_2 + \frac{3}{2}\kappa_2\bar\beta_8 + \frac{3}{2}\mu_2\bar\beta_7 + \frac{n\bar\alpha_8}{2}\right] & \frac{1}{r^2}\left[n\bar\beta_8\right] & -\frac{1}{r^2}\left[2\kappa_2\mu_2\right] & \frac{1}{r}\left[\kappa_2\bar\beta_8 + \mu_2\bar\beta_7 - n\bar\alpha_8\right] & \frac{1}{r}\left[n\bar\beta_8\right] & \frac{1}{r}\left[\kappa_2\bar\alpha_8 + \mu_2\bar\alpha_7\right] \\
\frac{1}{r^2}\left[2n\kappa_2 + \frac{3}{2}\kappa_2\bar\beta_7 - \frac{3}{2}\mu_2\bar\beta_8 + \frac{n\bar\alpha_7}{2}\right] & \frac{1}{r^2}\left[n^2 + n\bar\beta_7\right] & -\frac{1}{r^2}\left[\kappa_2^2 - \mu_2^2\right] & \frac{1}{r}\left[\kappa_2\bar\beta_7 - \mu_2\bar\beta_8 - n\bar\alpha_7\right] & \frac{1}{r}\left[n\bar\beta_7 + 1\right] & \frac{1}{r}\left[\kappa_2\bar\alpha_7 - \mu_2\bar\alpha_8\right]
\end{bmatrix}$$

$$[G] = \pi r\int_0^\ell [Q]^T[P][Q]\,dx = \pi r\int_0^\ell [Z]^T[\Gamma]^T[P][\Gamma][Z]\,dx = \pi r\int_0^\ell [Z]^T[Y][Z]\,dx = \pi r\int_0^\ell [ZY]\,dx$$

TABLE 4. Matrix $[\Gamma]$

$$
[\Delta]=\left[\begin{array}{c|c|c|c|c|c|c|c|c|c|c|c|c|c|c|c}
\bar{\alpha}_1 & -\bar{\alpha}_2 & \bar{\alpha}_2 & \bar{\alpha}_1 & \bar{\alpha}_3 & -\bar{\alpha}_4 & \bar{\alpha}_4 & \bar{\alpha}_3 & \bar{\alpha}_5 & -\bar{\alpha}_6 & \bar{\alpha}_6 & \bar{\alpha}_5 & \bar{\alpha}_7 & -\bar{\alpha}_8 & \bar{\alpha}_8 & \bar{\alpha}_7 \\ \hline
1 & 0 & 0 & 1 & 1 & 0 & 0 & 1 & 1 & 0 & 0 & 1 & 1 & 0 & 0 & 1 \\ \hline
\bar{\beta}_1 & -\bar{\beta}_2 & \bar{\beta}_2 & \bar{\beta}_1 & \bar{\beta}_3 & -\bar{\beta}_4 & \bar{\beta}_4 & \bar{\beta}_3 & \bar{\beta}_5 & -\bar{\beta}_6 & \bar{\beta}_6 & \bar{\beta}_5 & \bar{\beta}_7 & -\bar{\beta}_8 & \bar{\beta}_8 & \bar{\beta}_7
\end{array}\right]
$$

$$
[Z]=\left[\begin{array}{c|c|c|c|c|c|c|c}
e^{-\psi_1}\cos\zeta_1 & & & & & & & \\ \hline
e^{-\psi_1}\sin\zeta_1 & & & & & & & \\ \hline
 & e^{-\psi_1}\cos\zeta_1 & & & & & & \\ \hline
 & e^{-\psi_1}\sin\zeta_1 & & & & & & \\ \hline
 & & e^{-\psi_2}\cos\zeta_2 & & & & & \\ \hline
 & & e^{-\psi_2}\sin\zeta_2 & & & & & \\ \hline
 & & & e^{-\psi_2}\cos\zeta_2 & & & & \\ \hline
 & & & e^{-\psi_2}\sin\zeta_2 & & & & \\ \hline
 & & & & e^{\psi_1}\cos\zeta_1 & & & \\ \hline
 & & & & e^{\psi_1}\sin\zeta_1 & & & \\ \hline
 & & & & & e^{\psi_1}\cos\zeta_1 & & \\ \hline
 & & & & & e^{\psi_1}\sin\zeta_1 & & \\ \hline
 & & & & & & e^{\psi_2}\cos\zeta_2 & \\ \hline
 & & & & & & e^{\psi_2}\sin\zeta_2 & \\ \hline
 & & & & & & & e^{\psi_2}\cos\zeta_2 \\ \hline
 & & & & & & & e^{\psi_2}\sin\zeta_2
\end{array}\right]
$$

$$
[G]=\pi r\int_0^{\ell}[Q]^T[P][Q]\,dx=\pi r\int_0^{\ell}[Z]^T[\Gamma]^T[P][\Gamma][Z]\,dx=\pi r\int_0^{\ell}[Z]^T[Y][Z]\,dx=\pi r\int_0^{\ell}[ZY]\,dx
$$

TABLE 5. Matrices $[\Delta]$ and $[Z]$

$$
[ZY]=\left[\begin{array}{llllllll}
\begin{array}{l} y_{11}\,e^{-2\psi_1}\cos^2\xi_1 + \\ y_{21}\,e^{-2\psi_1}\sin\xi_1\cos\xi_1 + \\ y_{12}\,e^{-2\psi_1}\cos\xi_1\sin\xi_1 + \\ y_{22}\,e^{-2\psi_1}\sin^2\xi_1 \end{array} &
\begin{array}{l} y_{13}\,e^{-2\psi_1}\cos^2\xi_1 + \\ y_{23}\,e^{-2\psi_1}\sin\xi_1\cos\xi_1 + \\ y_{14}\,e^{-2\psi_1}\cos\xi_1\sin\xi_1 + \\ y_{24}\,e^{-2\psi_1}\sin^2\xi_1 \end{array} &
\begin{array}{l} y_{15}\,e^{-\psi_1-\psi_2}\cos\xi_1\cos\xi_2 + \\ y_{25}\,e^{-\psi_1-\psi_2}\sin\xi_1\cos\xi_2 + \\ y_{16}\,e^{-\psi_1-\psi_2}\cos\xi_1\sin\xi_2 + \\ y_{26}\,e^{-\psi_1-\psi_2}\sin\xi_1\sin\xi_2 \end{array} &
\begin{array}{l} y_{17}\,e^{-\psi_1-\psi_2}\cos\xi_1\cos\xi_2 + \\ y_{27}\,e^{-\psi_1-\psi_2}\sin\xi_1\cos\xi_2 + \\ y_{18}\,e^{-\psi_1-\psi_2}\cos\xi_1\sin\xi_2 + \\ y_{28}\,e^{-\psi_1-\psi_2}\sin\xi_1\sin\xi_2 \end{array} &
\begin{array}{l} y_{19}\cos^2\xi_1 + \\ y_{29}\sin\xi_1\cos\xi_1 + \\ y_{1,10}\cos\xi_1\sin\xi_1 + \\ y_{2,10}\sin^2\xi_1 \end{array} &
\begin{array}{l} y_{1,11}\cos^2\xi_1 + \\ y_{2,11}\sin\xi_1\cos\xi_1 + \\ y_{1,12}\cos\xi_1\sin\xi_1 + \\ y_{2,12}\sin^2\xi_1 \end{array} &
\begin{array}{l} y_{1,13}\,e^{-\psi_1+\psi_2}\cos\xi_1\cos\xi_2 + \\ y_{2,13}\,e^{-\psi_1+\psi_2}\sin\xi_1\cos\xi_2 + \\ y_{1,14}\,e^{-\psi_1+\psi_2}\cos\xi_1\sin\xi_2 + \\ y_{2,14}\,e^{-\psi_1+\psi_2}\sin\xi_1\sin\xi_2 \end{array} &
\begin{array}{l} y_{1,15}\,e^{-\psi_1+\psi_2}\cos\xi_1\cos\xi_2 + \\ y_{2,15}\,e^{-\psi_1+\psi_2}\sin\xi_1\cos\xi_2 + \\ y_{1,16}\,e^{-\psi_1+\psi_2}\cos\xi_1\sin\xi_2 + \\ y_{2,16}\,e^{-\psi_1+\psi_2}\sin\xi_1\sin\xi_2 \end{array} \\
\begin{array}{l} y_{31}\,e^{-2\psi_1}\cos^2\xi_1 + \\ y_{32}\,e^{-2\psi_1}\sin\xi_1\cos\xi_1 + \\ y_{41}\,e^{-2\psi_1}\cos\xi_1\sin\xi_1 + \\ y_{42}\,e^{-2\psi_1}\sin^2\xi_1 \end{array} &
\begin{array}{l} y_{33}\,e^{-2\psi_1}\cos^2\xi_1 + \\ y_{43}\,e^{-2\psi_1}\sin\xi_1\cos\xi_1 + \\ y_{34}\,e^{-2\psi_1}\cos\xi_1\sin\xi_1 + \\ y_{44}\,e^{-2\psi_1}\sin^2\xi_1 \end{array} &
\begin{array}{l} y_{35}\,e^{-\psi_1-\psi_2}\cos\xi_1\cos\xi_2 + \\ y_{45}\,e^{-\psi_1-\psi_2}\sin\xi_1\cos\xi_2 + \\ y_{36}\,e^{-\psi_1-\psi_2}\cos\xi_1\sin\xi_2 + \\ y_{46}\,e^{-\psi_1-\psi_2}\sin\xi_1\sin\xi_2 \end{array} &
\begin{array}{l} y_{37}\,e^{-\psi_1-\psi_2}\cos\xi_1\cos\xi_2 + \\ y_{47}\,e^{-\psi_1-\psi_2}\sin\xi_1\cos\xi_2 + \\ y_{38}\,e^{-\psi_1-\psi_2}\cos\xi_1\sin\xi_2 + \\ y_{48}\,e^{-\psi_1-\psi_2}\sin\xi_1\sin\xi_2 \end{array} &
\begin{array}{l} y_{39}\cos^2\xi_1 + \\ y_{49}\sin\xi_1\cos\xi_1 + \\ y_{3,10}\cos\xi_1\sin\xi_1 + \\ y_{4,10}\sin^2\xi_1 \end{array} &
\begin{array}{l} y_{3,11}\cos^2\xi_1 + \\ y_{4,11}\sin\xi_1\cos\xi_1 + \\ y_{3,12}\cos\xi_1\sin\xi_1 + \\ y_{4,12}\sin^2\xi_1 \end{array} &
\begin{array}{l} y_{3,13}\,e^{-\psi_1+\psi_2}\cos\xi_1\cos\xi_2 + \\ y_{4,13}\,e^{-\psi_1+\psi_2}\sin\xi_1\cos\xi_2 + \\ y_{3,14}\,e^{-\psi_1+\psi_2}\cos\xi_1\sin\xi_2 + \\ y_{4,14}\,e^{-\psi_1+\psi_2}\sin\xi_1\sin\xi_2 \end{array} &
\begin{array}{l} y_{3,15}\,e^{-\psi_1+\psi_2}\cos\xi_1\cos\xi_2 + \\ y_{4,15}\,e^{-\psi_1+\psi_2}\sin\xi_1\cos\xi_2 + \\ y_{3,16}\,e^{-\psi_1+\psi_2}\cos\xi_1\sin\xi_2 + \\ y_{4,16}\,e^{-\psi_1+\psi_2}\sin\xi_1\sin\xi_2 \end{array} \\
\begin{array}{l} y_{51}\,e^{-\psi_1-\psi_2}\cos\xi_1\cos\xi_2 + \\ y_{52}\,e^{-\psi_1-\psi_2}\sin\xi_1\cos\xi_2 + \\ y_{61}\,e^{-\psi_1-\psi_2}\cos\xi_1\sin\xi_2 + \\ y_{62}\,e^{-\psi_1-\psi_2}\sin\xi_1\sin\xi_2 \end{array} &
\begin{array}{l} y_{53}\,e^{-\psi_1-\psi_2}\cos\xi_1\cos\xi_2 + \\ y_{54}\,e^{-\psi_1-\psi_2}\sin\xi_1\cos\xi_2 + \\ y_{63}\,e^{-\psi_1-\psi_2}\cos\xi_1\sin\xi_2 + \\ y_{64}\,e^{-\psi_1-\psi_2}\sin\xi_1\sin\xi_2 \end{array} &
\begin{array}{l} y_{55}\,e^{-2\psi_2}\cos^2\xi_2 + \\ y_{65}\,e^{-2\psi_2}\sin\xi_2\cos\xi_2 + \\ y_{56}\,e^{-2\psi_2}\cos\xi_2\sin\xi_2 + \\ y_{66}\,e^{-2\psi_2}\sin^2\xi_2 \end{array} &
\begin{array}{l} y_{57}\,e^{-2\psi_2}\cos^2\xi_2 + \\ y_{67}\,e^{-2\psi_2}\sin\xi_2\cos\xi_2 + \\ y_{58}\,e^{-2\psi_2}\cos\xi_2\sin\xi_2 + \\ y_{68}\,e^{-2\psi_2}\sin^2\xi_2 \end{array} &
\begin{array}{l} y_{59}\,e^{\psi_1-\psi_2}\cos\xi_2\cos\xi_1 + \\ y_{69}\,e^{\psi_1-\psi_2}\sin\xi_2\cos\xi_1 + \\ y_{5,10}\,e^{\psi_1-\psi_2}\cos\xi_2\sin\xi_1 + \\ y_{6,10}\,e^{\psi_1-\psi_2}\sin\xi_2\sin\xi_1 \end{array} &
\begin{array}{l} y_{5,11}\,e^{\psi_1-\psi_2}\cos\xi_2\cos\xi_1 + \\ y_{6,11}\,e^{\psi_1-\psi_2}\sin\xi_2\cos\xi_1 + \\ y_{5,12}\,e^{\psi_1-\psi_2}\cos\xi_2\sin\xi_1 + \\ y_{6,12}\,e^{\psi_1-\psi_2}\sin\xi_2\sin\xi_1 \end{array} &
\begin{array}{l} y_{5,13}\cos^2\xi_2 + \\ y_{6,13}\sin\xi_2\cos\xi_2 + \\ y_{5,14}\cos\xi_2\sin\xi_2 + \\ y_{6,14}\sin^2\xi_2 \end{array} &
\begin{array}{l} y_{5,15}\cos^2\xi_2 + \\ y_{6,15}\sin\xi_2\cos\xi_2 + \\ y_{5,16}\cos\xi_2\sin\xi_2 + \\ y_{6,16}\sin^2\xi_2 \end{array} \\
\begin{array}{l} y_{71} \\ y_{72} \\ y_{81} \\ y_{82} \end{array} &
\begin{array}{l} y_{73} \\ y_{74} \\ y_{83} \\ y_{84} \end{array} &
\begin{array}{l} y_{75} \\ y_{76} \\ y_{85} \\ y_{86} \end{array} &
\begin{array}{l} y_{77}\,e^{-2\psi_2}\cos^2\xi_2 + \\ y_{87}\,e^{-2\psi_2}\sin\xi_2\cos\xi_2 + \\ y_{78}\,e^{-2\psi_2}\cos\xi_2\sin\xi_2 + \\ y_{88}\,e^{-2\psi_2}\sin^2\xi_2 \end{array} &
\begin{array}{l} y_{79}\,e^{\psi_1-\psi_2}\cos\xi_2\cos\xi_1 + \\ y_{89}\,e^{\psi_1-\psi_2}\sin\xi_2\cos\xi_1 + \\ y_{7,10}\,e^{\psi_1-\psi_2}\cos\xi_2\sin\xi_1 + \\ y_{8,10}\,e^{\psi_1-\psi_2}\sin\xi_2\sin\xi_1 \end{array} &
\begin{array}{l} y_{7,11}\,e^{\psi_1-\psi_2}\cos\xi_2\cos\xi_1 + \\ y_{8,11}\,e^{\psi_1-\psi_2}\sin\xi_2\cos\xi_1 + \\ y_{7,12}\,e^{\psi_1-\psi_2}\cos\xi_2\sin\xi_1 + \\ y_{8,12}\,e^{\psi_1-\psi_2}\sin\xi_2\sin\xi_1 \end{array} &
\begin{array}{l} y_{7,13}\cos^2\xi_2 + \\ y_{8,13}\sin\xi_2\cos\xi_2 + \\ y_{7,14}\cos\xi_2\sin\xi_2 + \\ y_{8,14}\sin^2\xi_2 \end{array} &
\begin{array}{l} y_{7,15}\cos^2\xi_2 + \\ y_{8,15}\sin\xi_2\cos\xi_2 + \\ y_{7,16}\cos\xi_2\sin\xi_2 + \\ y_{8,16}\sin^2\xi_2 \end{array} \\
\begin{array}{l} y_{91} \\ y_{92} \\ y_{10,1} \\ y_{10,2} \end{array} &
\begin{array}{l} y_{93} \\ y_{94} \\ y_{10,3} \\ y_{10,4} \end{array} &
\begin{array}{l} y_{95} \\ y_{96} \\ y_{10,5} \\ y_{10,6} \end{array} &
\begin{array}{l} y_{97} \\ y_{98} \\ y_{10,7} \\ y_{10,8} \end{array} &
\begin{array}{l} y_{9,9}\,e^{2\psi_1}\cos^2\xi_1 + \\ y_{10,9}\,e^{2\psi_1}\sin\xi_1\cos\xi_1 + \\ y_{9,10}\,e^{2\psi_1}\cos\xi_1\sin\xi_1 + \\ y_{10,10}\,e^{2\psi_1}\sin^2\xi_1 \end{array} &
\begin{array}{l} y_{9,11}\,e^{2\psi_1}\cos^2\xi_1 + \\ y_{10,11}\,e^{2\psi_1}\sin\xi_1\cos\xi_1 + \\ y_{9,12}\,e^{2\psi_1}\cos\xi_1\sin\xi_1 + \\ y_{10,12}\sin^2\xi_1 \end{array} &
\begin{array}{l} y_{9,13}\,e^{\psi_1+\psi_2}\cos\xi_1\cos\xi_2 + \\ y_{10,13}\,e^{\psi_1+\psi_2}\sin\xi_1\cos\xi_2 + \\ y_{9,14}\,e^{\psi_1+\psi_2}\cos\xi_1\sin\xi_2 + \\ y_{10,14}\,e^{\psi_1+\psi_2}\sin\xi_1\sin\xi_2 \end{array} &
\begin{array}{l} y_{9,15}\,e^{\psi_1+\psi_2}\cos\xi_1\cos\xi_2 + \\ y_{10,15}\,e^{\psi_1+\psi_2}\sin\xi_1\cos\xi_2 + \\ y_{9,16}\,e^{\psi_1+\psi_2}\cos\xi_1\sin\xi_2 + \\ y_{10,16}\,e^{\psi_1+\psi_2}\sin\xi_1\sin\xi_2 \end{array} \\
\begin{array}{l} y_{11,1} \\ y_{11,2} \\ y_{12,1} \\ y_{12,2} \end{array} &
\begin{array}{l} y_{11,3} \\ y_{11,4} \\ y_{12,3} \\ y_{12,4} \end{array} &
\begin{array}{l} y_{11,5} \\ y_{11,6} \\ y_{12,5} \\ y_{12,6} \end{array} &
\begin{array}{l} y_{11,7} \\ y_{11,8} \\ y_{12,7} \\ y_{12,8} \end{array} &
\begin{array}{l} y_{11,9} \\ y_{11,10} \\ y_{12,9} \\ y_{12,10} \end{array} &
\begin{array}{l} y_{11,11}\,e^{2\psi_1}\cos^2\xi_1 + \\ y_{12,11}\,e^{2\psi_1}\sin\xi_1\cos\xi_1 + \\ y_{11,12}\,e^{2\psi_1}\cos\xi_1\sin\xi_1 + \\ y_{12,12}\,e^{2\psi_1}\sin^2\xi_1 \end{array} &
\begin{array}{l} y_{11,13}\,e^{\psi_1+\psi_2}\cos\xi_1\cos\xi_2 + \\ y_{12,13}\,e^{\psi_1+\psi_2}\sin\xi_1\cos\xi_2 + \\ y_{11,14}\,e^{\psi_1+\psi_2}\cos\xi_1\sin\xi_2 + \\ y_{12,14}\,e^{\psi_1+\psi_2}\sin\xi_1\sin\xi_2 \end{array} &
\begin{array}{l} y_{11,15}\,e^{\psi_1+\psi_2}\cos\xi_1\cos\xi_2 + \\ y_{12,15}\,e^{\psi_1+\psi_2}\sin\xi_1\cos\xi_2 + \\ y_{11,16}\,e^{\psi_1+\psi_2}\cos\xi_1\sin\xi_2 + \\ y_{12,16}\,e^{\psi_1+\psi_2}\sin\xi_1\sin\xi_2 \end{array} \\
\begin{array}{l} y_{13,1} \\ y_{13,2} \\ y_{14,1} \\ y_{14,2} \end{array} &
\begin{array}{l} y_{13,3} \\ y_{13,4} \\ y_{14,3} \\ y_{14,4} \end{array} &
\begin{array}{l} y_{13,5} \\ y_{13,6} \\ y_{14,5} \\ y_{14,6} \end{array} &
\begin{array}{l} y_{13,7} \\ y_{13,8} \\ y_{14,7} \\ y_{14,8} \end{array} &
\begin{array}{l} y_{13,9} \\ y_{13,10} \\ y_{14,9} \\ y_{14,10} \end{array} &
\begin{array}{l} y_{13,11} \\ y_{13,12} \\ y_{14,11} \\ y_{14,12} \end{array} &
\begin{array}{l} y_{13,13}\,e^{2\psi_2}\cos^2\xi_2 + \\ y_{14,13}\,e^{2\psi_2}\sin\xi_2\cos\xi_2 + \\ y_{13,14}\,e^{2\psi_2}\cos\xi_2\sin\xi_2 + \\ y_{14,14}\,e^{2\psi_2}\sin^2\xi_2 \end{array} &
\begin{array}{l} y_{13,15}\,e^{2\psi_2}\cos^2\xi_2 + \\ y_{14,15}\,e^{2\psi_2}\sin\xi_2\cos\xi_2 + \\ y_{13,16}\,e^{2\psi_2}\cos\xi_2\sin\xi_2 + \\ y_{14,16}\,e^{2\psi_2}\sin^2\xi_2 \end{array} \\
\begin{array}{l} y_{15,1} \\ y_{15,2} \\ y_{16,1} \\ y_{16,2} \end{array} &
\begin{array}{l} y_{15,3} \\ y_{15,4} \\ y_{16,3} \\ y_{16,4} \end{array} &
\begin{array}{l} y_{15,5} \\ y_{15,6} \\ y_{16,5} \\ y_{16,6} \end{array} &
\begin{array}{l} y_{15,7} \\ y_{15,8} \\ y_{16,7} \\ y_{16,8} \end{array} &
\begin{array}{l} y_{15,9} \\ y_{15,10} \\ y_{16,9} \\ y_{16,10} \end{array} &
\begin{array}{l} y_{15,11} \\ y_{15,12} \\ y_{16,11} \\ y_{16,12} \end{array} &
\begin{array}{l} y_{15,13} \\ y_{15,14} \\ y_{16,13} \\ y_{16,14} \end{array} &
\begin{array}{l} y_{15,15}\,e^{2\psi_2}\cos^2\xi_2 + \\ y_{16,15}\,e^{2\psi_2}\sin\xi_2\cos\xi_2 + \\ y_{15,16}\,e^{2\psi_2}\cos\xi_2\sin\xi_2 + \\ y_{16,16}\,e^{2\psi_2}\sin^2\xi_2 \end{array}
\end{array}\right]
$$

$$
[G] = \pi r\int_0^{\ell}[Q]^T[P][Q]\,dx = \pi r\int_0^{\ell}[Z]^T[\Gamma]^T[P][\Gamma][Z]\,dx = \pi r\int_0^{\ell}[Z]^T[Y][Z]\,dx = \pi r\int_0^{\ell}[ZY]\,dx
$$

TABLE 6. Matrix [ZY]

$$[A_1] = \begin{bmatrix}
-2\frac{\kappa_1}{r} & -2\frac{\kappa_1}{r} & -\frac{\kappa_1}{r}-\frac{\kappa_2}{r} & -\frac{\kappa_1}{r}-\frac{\kappa_2}{r} & 0 & 0 & -\frac{\kappa_1}{r}+\frac{\kappa_2}{r} & -\frac{\kappa_1}{r}+\frac{\kappa_2}{r} \\
-2\frac{\kappa_1}{r} & -2\frac{\kappa_1}{r} & -\frac{\kappa_1}{r}-\frac{\kappa_2}{r} & -\frac{\kappa_1}{r}-\frac{\kappa_2}{r} & 0 & 0 & -\frac{\kappa_1}{r}+\frac{\kappa_2}{r} & -\frac{\kappa_1}{r}+\frac{\kappa_2}{r} \\
-\frac{\kappa_1}{r}-\frac{\kappa_2}{r} & -\frac{\kappa_1}{r}-\frac{\kappa_2}{r} & -2\frac{\kappa_2}{r} & -2\frac{\kappa_2}{r} & \frac{\kappa_1}{r}-\frac{\kappa_2}{r} & \frac{\kappa_1}{r}-\frac{\kappa_2}{r} & 0 & 0 \\
-\frac{\kappa_1}{r}-\frac{\kappa_2}{r} & -\frac{\kappa_1}{r}-\frac{\kappa_2}{r} & -2\frac{\kappa_2}{r} & -2\frac{\kappa_2}{r} & \frac{\kappa_1}{r}-\frac{\kappa_2}{r} & \frac{\kappa_1}{r}-\frac{\kappa_2}{r} & 0 & 0 \\
0 & 0 & \frac{\kappa_1}{r}-\frac{\kappa_2}{r} & \frac{\kappa_1}{r}-\frac{\kappa_2}{r} & 2\frac{\kappa_1}{r} & 2\frac{\kappa_1}{r} & \frac{\kappa_1}{r}+\frac{\kappa_2}{r} & \frac{\kappa_1}{r}+\frac{\kappa_2}{r} \\
0 & 0 & \frac{\kappa_1}{r}-\frac{\kappa_2}{r} & \frac{\kappa_1}{r}-\frac{\kappa_2}{r} & 2\frac{\kappa_1}{r} & 2\frac{\kappa_1}{r} & \frac{\kappa_1}{r}+\frac{\kappa_2}{r} & \frac{\kappa_1}{r}+\frac{\kappa_2}{r} \\
\frac{\kappa_2}{r}-\frac{\kappa_1}{r} & \frac{\kappa_2}{r}-\frac{\kappa_1}{r} & 0 & 0 & \frac{\kappa_2}{r}+\frac{\kappa_1}{r} & \frac{\kappa_2}{r}+\frac{\kappa_1}{r} & 2\frac{\kappa_2}{r} & 2\frac{\kappa_2}{r} \\
\frac{\kappa_2}{r}-\frac{\kappa_1}{r} & \frac{\kappa_2}{r}-\frac{\kappa_1}{r} & 0 & 0 & \frac{\kappa_2}{r}+\frac{\kappa_1}{r} & \frac{\kappa_2}{r}+\frac{\kappa_1}{r} & 2\frac{\kappa_2}{r} & 2\frac{\kappa_2}{r}
\end{bmatrix}$$

$$[B_1] = \begin{bmatrix}
\frac{\mu_1}{r} & \frac{\mu_1}{r} & \frac{\mu_1}{r} & \frac{\mu_1}{r} & \frac{\mu_1}{r} & \frac{\mu_1}{r} & \frac{\mu_1}{r} & \frac{\mu_1}{r} \\
\frac{\mu_1}{r} & \frac{\mu_1}{r} & \frac{\mu_1}{r} & \frac{\mu_1}{r} & \frac{\mu_1}{r} & \frac{\mu_1}{r} & \frac{\mu_1}{r} & \frac{\mu_1}{r} \\
\frac{\mu_1}{r} & \frac{\mu_1}{r} & \frac{\mu_2}{r} & \frac{\mu_2}{r} & \frac{\mu_2}{r} & \frac{\mu_2}{r} & \frac{\mu_2}{r} & \frac{\mu_2}{r} \\
\frac{\mu_1}{r} & \frac{\mu_1}{r} & \frac{\mu_2}{r} & \frac{\mu_2}{r} & \frac{\mu_2}{r} & \frac{\mu_2}{r} & \frac{\mu_2}{r} & \frac{\mu_2}{r} \\
\frac{\mu_1}{r} & \frac{\mu_1}{r} & \frac{\mu_2}{r} & \frac{\mu_2}{r} & \frac{\mu_1}{r} & \frac{\mu_1}{r} & \frac{\mu_1}{r} & \frac{\mu_1}{r} \\
\frac{\mu_1}{r} & \frac{\mu_1}{r} & \frac{\mu_2}{r} & \frac{\mu_2}{r} & \frac{\mu_1}{r} & \frac{\mu_1}{r} & \frac{\mu_1}{r} & \frac{\mu_1}{r} \\
\frac{\mu_1}{r} & \frac{\mu_1}{r} & \frac{\mu_2}{r} & \frac{\mu_2}{r} & \frac{\mu_1}{r} & \frac{\mu_1}{r} & \frac{\mu_2}{r} & \frac{\mu_2}{r} \\
\frac{\mu_1}{r} & \frac{\mu_1}{r} & \frac{\mu_2}{r} & \frac{\mu_2}{r} & \frac{\mu_1}{r} & \frac{\mu_1}{r} & \frac{\mu_2}{r} & \frac{\mu_2}{r}
\end{bmatrix}$$

$$[C_1] = \begin{bmatrix}
\frac{\mu_1}{r} & \frac{\mu_1}{r} & \frac{\mu_2}{r} & \frac{\mu_2}{r} & \frac{\mu_1}{r} & \frac{\mu_1}{r} & \frac{\mu_2}{r} & \frac{\mu_2}{r} \\
\frac{\mu_1}{r} & \frac{\mu_1}{r} & \frac{\mu_2}{r} & \frac{\mu_2}{r} & \frac{\mu_1}{r} & \frac{\mu_1}{r} & \frac{\mu_2}{r} & \frac{\mu_2}{r} \\
\frac{\mu_2}{r} & \frac{\mu_2}{r} & \frac{\mu_2}{r} & \frac{\mu_2}{r} & \frac{\mu_1}{r} & \frac{\mu_1}{r} & \frac{\mu_2}{r} & \frac{\mu_2}{r} \\
\frac{\mu_2}{r} & \frac{\mu_2}{r} & \frac{\mu_2}{r} & \frac{\mu_2}{r} & \frac{\mu_1}{r} & \frac{\mu_1}{r} & \frac{\mu_2}{r} & \frac{\mu_2}{r} \\
\frac{\mu_2}{r} & \frac{\mu_2}{r} & \frac{\mu_1}{r} & \frac{\mu_1}{r} & \frac{\mu_1}{r} & \frac{\mu_1}{r} & \frac{\mu_2}{r} & \frac{\mu_2}{r} \\
\frac{\mu_1}{r} & \frac{\mu_1}{r} & \frac{\mu_1}{r} & \frac{\mu_1}{r} & \frac{\mu_1}{r} & \frac{\mu_1}{r} & \frac{\mu_2}{r} & \frac{\mu_2}{r} \\
\frac{\mu_2}{r} & \frac{\mu_2}{r} & \frac{\mu_2}{r} & \frac{\mu_2}{r} & \frac{\mu_2}{r} & \frac{\mu_2}{r} & \frac{\mu_2}{r} & \frac{\mu_2}{r} \\
\frac{\mu_2}{r} & \frac{\mu_2}{r} & \frac{\mu_2}{r} & \frac{\mu_2}{r} & \frac{\mu_2}{r} & \frac{\mu_2}{r} & \frac{\mu_2}{r} & \frac{\mu_2}{r}
\end{bmatrix}$$

TABLE 7. Matrices $[A_1]$, $[B_1]$, and $[C_1]$

$$[D1]=\begin{bmatrix} y_{11} & y_{13} & y_{15} & y_{17} & y_{19} & y_{1,11} & y_{1,13} & y_{1,15} \\ y_{31} & y_{33} & y_{35} & y_{37} & y_{39} & y_{3,11} & y_{3,13} & y_{3,15} \\ y_{51} & y_{53} & y_{55} & y_{57} & y_{59} & y_{5,11} & y_{5,13} & y_{5,15} \\ y_{71} & y_{73} & y_{75} & y_{77} & y_{79} & y_{7,11} & y_{7,13} & y_{7,15} \\ y_{91} & y_{93} & y_{95} & y_{97} & y_{99} & y_{9,11} & y_{9,13} & y_{9,15} \\ y_{11,1} & y_{11,3} & y_{11,5} & y_{11,7} & y_{11,9} & y_{11,11} & y_{11,13} & y_{11,15} \\ y_{13,1} & y_{13,3} & y_{13,5} & y_{13,7} & y_{13,9} & y_{13,11} & y_{13,13} & y_{13,15} \\ y_{15,1} & y_{15,3} & y_{15,5} & y_{15,7} & y_{15,9} & y_{15,11} & y_{15,13} & y_{15,15} \end{bmatrix}$$

$$[D2]=\begin{bmatrix} y_{21} & y_{23} & y_{25} & y_{27} & y_{29} & y_{2,11} & y_{2,13} & y_{2,15} \\ y_{32} & y_{43} & y_{45} & y_{47} & y_{49} & y_{4,11} & y_{4,13} & y_{4,15} \\ y_{52} & y_{54} & y_{65} & y_{67} & y_{69} & y_{6,11} & y_{6,13} & y_{6,15} \\ y_{72} & y_{74} & y_{76} & y_{87} & y_{89} & y_{8,11} & y_{8,13} & y_{8,15} \\ y_{92} & y_{94} & y_{96} & y_{98} & y_{10,9} & y_{10,11} & y_{10,13} & y_{10,15} \\ y_{11,2} & y_{11,4} & y_{11,6} & y_{11,8} & y_{11,10} & y_{12,11} & y_{12,13} & y_{12,15} \\ y_{13,2} & y_{13,4} & y_{13,6} & y_{13,8} & y_{13,10} & y_{13,12} & y_{14,13} & y_{14,15} \\ y_{15,2} & y_{15,4} & y_{15,6} & y_{15,8} & y_{15,10} & y_{15,12} & y_{15,14} & y_{16,15} \end{bmatrix}$$

$$[D3]=\begin{bmatrix} y_{12} & y_{14} & y_{16} & y_{18} & y_{1,10} & y_{1,12} & y_{1,14} & y_{1,16} \\ y_{41} & y_{34} & y_{36} & y_{38} & y_{3,10} & y_{3,12} & y_{3,14} & y_{3,16} \\ y_{61} & y_{63} & y_{56} & y_{58} & y_{5,10} & y_{5,12} & y_{5,14} & y_{5,16} \\ y_{81} & y_{83} & y_{85} & y_{78} & y_{7,10} & y_{7,12} & y_{7,14} & y_{7,16} \\ y_{10,1} & y_{10,3} & y_{10,5} & y_{10,7} & y_{9,10} & y_{9,12} & y_{9,14} & y_{9,16} \\ y_{12,1} & y_{12,3} & y_{12,5} & y_{12,7} & y_{12,9} & y_{11,12} & y_{11,14} & y_{11,16} \\ y_{14,1} & y_{14,3} & y_{14,5} & y_{14,7} & y_{14,9} & y_{14,11} & y_{13,14} & y_{13,16} \\ y_{16,1} & y_{16,3} & y_{16,5} & y_{16,7} & y_{16,9} & y_{16,11} & y_{16,13} & y_{15,16} \end{bmatrix}$$

$$[D4]=\begin{bmatrix} y_{22} & y_{24} & y_{26} & y_{28} & y_{2,10} & y_{2,12} & y_{2,14} & y_{2,16} \\ y_{42} & y_{44} & y_{46} & y_{48} & y_{4,10} & y_{4,12} & y_{4,14} & y_{4,16} \\ y_{62} & y_{64} & y_{66} & y_{68} & y_{6,10} & y_{6,12} & y_{6,14} & y_{6,16} \\ y_{82} & y_{84} & y_{86} & y_{88} & y_{8,10} & y_{8,12} & y_{8,14} & y_{8,16} \\ y_{10,2} & y_{10,4} & y_{10,6} & y_{10,8} & y_{10,10} & y_{10,12} & y_{10,14} & y_{10,16} \\ y_{12,2} & y_{12,4} & y_{12,6} & y_{12,8} & y_{12,10} & y_{12,12} & y_{12,14} & y_{12,16} \\ y_{14,2} & y_{14,4} & y_{14,6} & y_{14,8} & y_{14,10} & y_{14,12} & y_{14,14} & y_{14,16} \\ y_{16,2} & y_{16,4} & y_{16,6} & y_{16,8} & y_{16,10} & y_{16,12} & y_{16,14} & y_{16,16} \end{bmatrix}$$

<u>TABLE 8</u>. Matrices $[D_1]$ to $[D_4]$

$$
[Q_i] = \begin{bmatrix}
\frac{1}{r}\left[-\kappa_1\bar{\alpha}_1-\mu_1\bar{\alpha}_2\right] & \frac{1}{r}\left[-\kappa_1\bar{\alpha}_2+\mu_1\bar{\alpha}_1\right] & \frac{1}{r}\left[-\kappa_2\bar{\alpha}_3-\mu_2\bar{\alpha}_4\right] & \frac{1}{r}\left[-\kappa_2\bar{\alpha}_4+\mu_2\bar{\alpha}_3\right] & \frac{1}{r}\left[\kappa_1\bar{\alpha}_5-\mu_1\bar{\alpha}_6\right] & \frac{1}{r}\left[\kappa_1\bar{\alpha}_6+\mu_1\bar{\alpha}_5\right] & \frac{1}{r}\left[\kappa_2\bar{\alpha}_7-\mu_2\bar{\alpha}_8\right] & \frac{1}{r}\left[\kappa_2\bar{\alpha}_8+\mu_2\bar{\alpha}_7\right] \\
\frac{1}{r}\left[n\bar{\beta}_1+1\right] & \frac{n\bar{\beta}_2}{r} & \frac{1}{r}\left[n\bar{\beta}_3+1\right] & \frac{n\bar{\beta}_4}{r} & \frac{1}{r}\left[n\bar{\beta}_5+1\right] & \frac{n\bar{\beta}_6}{r} & \frac{1}{r}\left[n\bar{\beta}_7+1\right] & \frac{n\bar{\beta}_8}{r} \\
\frac{1}{r}\left[-\kappa_1\bar{\beta}_1-\mu_1\bar{\beta}_2-n\bar{\alpha}_1\right] & \frac{1}{r}\left[-\kappa_1\bar{\beta}_2+\mu_1\bar{\beta}_1-n\bar{\alpha}_2\right] & \frac{1}{r}\left[-\kappa_2\bar{\beta}_3-\mu_2\bar{\beta}_4-n\bar{\alpha}_3\right] & \frac{1}{r}\left[-\kappa_2\bar{\beta}_4+\mu_2\bar{\beta}_3-n\bar{\alpha}_4\right] & \frac{1}{r}\left[\kappa_1\bar{\beta}_5-\mu_1\bar{\beta}_6-n\bar{\alpha}_5\right] & \frac{1}{r}\left[\kappa_1\bar{\beta}_6+\mu_1\bar{\beta}_5-n\bar{\alpha}_6\right] & \frac{1}{r}\left[\kappa_2\bar{\beta}_7-\mu_2\bar{\beta}_8-n\bar{\alpha}_7\right] & \frac{1}{r}\left[\kappa_2\bar{\beta}_8+\mu_2\bar{\beta}_7-n\bar{\alpha}_8\right] \\
\frac{-1}{r^2}\left[\kappa_1^2-\mu_1^2\right] & \frac{1}{r^2}\left[2\kappa_1\mu_1\right] & \frac{-1}{r^2}\left[\kappa_2^2-\mu_2^2\right] & \frac{1}{r}\left[2\kappa_2\mu_2\right] & \frac{-1}{r^2}\left[\kappa_1^2-\mu_1^2\right] & \frac{-1}{r^2}\left[2\kappa_1\mu_1\right] & \frac{-1}{r^2}\left[\kappa_2^2-\mu_2^2\right] & \frac{-1}{r^2}\left[2\kappa_2\mu_2\right] \\
\frac{1}{r^2}\left[n^2+n\bar{\beta}_1\right] & \frac{n\bar{\beta}_2}{r^2} & \frac{1}{r^2}\left[n^2+n\bar{\beta}_3\right] & \frac{n\bar{\beta}_4}{r^2} & \frac{1}{r^2}\left[n^2+n\bar{\beta}_5\right] & \frac{n\bar{\beta}_6}{r^2} & \frac{1}{r^2}\left[n^2+n\bar{\beta}_7\right] & \frac{n\bar{\beta}_8}{r^2} \\
\frac{1}{r^2}\left[-2n\kappa_1-\frac{3}{2}\kappa_1\bar{\beta}_1 -\frac{3}{2}\mu_1\bar{\beta}_2+\frac{n\bar{\alpha}_1}{2}\right] & \frac{1}{r^2}\left[2n\mu_1-\frac{3}{2}\kappa_1\bar{\beta}_2 +\frac{3}{2}\mu_1\bar{\beta}_1+\frac{n\bar{\alpha}_2}{2}\right] & \frac{1}{r^2}\left[-2n\kappa_2-\frac{3}{2}\kappa_2\bar{\beta}_3 -\frac{3}{2}\mu_2\bar{\beta}_4+\frac{n\bar{\alpha}_3}{2}\right] & \frac{1}{r^2}\left[2n\mu_2-\frac{3}{2}\kappa_2\bar{\beta}_4 +\frac{3}{2}\mu_2\bar{\beta}_3+\frac{n\bar{\alpha}_4}{2}\right] & \frac{1}{r^2}\left[2n\kappa_1+\frac{3}{2}\kappa_1\bar{\beta}_5 -\frac{3}{2}\mu_1\bar{\beta}_6+\frac{n\bar{\alpha}_5}{2}\right] & \frac{1}{r^2}\left[2n\mu_1+\frac{3}{2}\kappa_1\bar{\beta}_6 +\frac{3}{2}\mu_1\bar{\beta}_5+\frac{n\bar{\alpha}_6}{2}\right] & \frac{1}{r^2}\left[2n\kappa_2+\frac{3}{2}\kappa_2\bar{\beta}_7 -\frac{3}{2}\mu_2\bar{\beta}_8+\frac{n\bar{\alpha}_7}{2}\right] & \frac{1}{r^2}\left[2n\mu_2+\frac{3}{2}\kappa_2\bar{\beta}_8 +\frac{3}{2}\mu_2\bar{\beta}_7+\frac{n\bar{\alpha}_8}{2}\right]
\end{bmatrix}
$$

<u>TABLE 9</u>. Matrix $[Q_i]$

| | n = 2 | | n = 3 | | n = 10 | |
|---|---|---|---|---|---|---|
| | $\lambda_1$ | $\lambda_2$ | $\lambda_1$ | $\lambda_2$ | $\lambda_1$ | $\lambda_2$ |
| SANDERS * | 10.202 ±9.8026i | .17570 ±.17051i | 10.465 ±9.5682i | .43961 ±.40598i | 15.286 ±7.3965i | 5.2613 ±2.5783 |
| BIEZENO and ** GRAMMEL | 10.1953 ±9.8105i | 0.1758 ±.1704i | 10.4583 ±9.5763i | .4399 ±.4056i | 15.2534 ±7.4853i | 5.2609 ±2.5719i |
| FLUGGE ** | 10.1952 ±9.8104i | .1758 ±.1704i | 10.4581 ±9.576i | .4399 ±.4057i | 15.2533 ±7.4851i | 5.2610 ±2.5719i |
| VLASOV ** | 10.1955 ±9.8107i | .1756 ±.1706i | 10.4591 ±9.5771i | .4396 ±.4059i | 15.2881 ±7.4183i | 5.2579 ±2.5766i |
| MORLEY ** | 10.1781 ±9.8283i | .1761 ±.1701i | 10.4414 ±9.5944i | .4406 ±.4049i | 15.2678 ±7.4348i | 5.2678 ±2.5652i |
| TIMOSHENKO ** | 10.2025 ±9.8027i | .1758 ±.1704i | 10.4652 ±9.5632i | .44 ±.4056i | 15.2840 ±7.3951i | 5.2645 ±2.5741i |
| BIJLAARD ** | 10.2024 ±9.8025i | .1707 ±.1655i | 10.4651 ±9.5681i | .4382 ±.4041i | 15.284 ±7.3950i | 5.2643 ±2.5741i |
| NOVOZHILOV ** | 10.2022 ±9.8024i | .1757± ±.1705i | 10.4645 ±9.5674i | .4396 ±.4060i | 15.2796 ±7.3859i | 5.2657 ±2.5779i |
| NAGHDI and ** BERRY | 10.2027 ±9.803i | .1760 ±.1702i | 10.4660 ±9.569i | .4403 ±.4052i | 15.2737 ±7.4030i | 5.2860 ±2.5342i |
| KENNARD ** | 10.2033 ±9.8036i | .1767 ±.1694i | 10.467 ±9.5703i | .4418 ±.4015i | 15.289 ±7.4137i | 5.2691 ±2.5340i |

TABLE 10 Roots of Characteristic Equations for $(1 - \nu^2)/k = 4 \times 10^4$ and $\nu = 0.3$

* This data comes from the authors' computer program.
** This data is given in Reference (28).

$$
\begin{Bmatrix} u_n(0) \\ w_n(0) \\ v_n(0) \end{Bmatrix} = \begin{bmatrix}
0.10000\mathrm{D}\ 01 & 0.27645\mathrm{D}{-12} & 0.75051\mathrm{D}{-13} & -0.67502\mathrm{D}{-13} & 0.21282\mathrm{D}{-13} & -0.27756\mathrm{D}{-12} & 0.17586\mathrm{D}{-12} & 0.68223\mathrm{D}{-13} \\
0.54179\mathrm{D}{-13} & 0.10000\mathrm{D}\ 01 & -0.27249\mathrm{D}{-11} & 0.12724\mathrm{D}{-11} & -0.27311\mathrm{D}{-13} & 0.33538\mathrm{D}{-11} & -0.25331\mathrm{D}{-11} & -0.81020\mathrm{D}{-12} \\
-0.88037\mathrm{D}{-14} & 0.27436\mathrm{D}{-11} & 0.26562\mathrm{D}{-11} & 0.10000\mathrm{D}\ 01 & -0.15384\mathrm{D}{-13} & -0.33376\mathrm{D}{-11} & 0.21925\mathrm{D}{-11} & 0.47017\mathrm{D}{-12}
\end{bmatrix} \begin{Bmatrix} \delta_i \\ \delta_j \end{Bmatrix}
$$

(a)

$$
\begin{Bmatrix} u_n(\ell) \\ w_n(\ell) \\ v_n(\ell) \end{Bmatrix} = \begin{bmatrix}
-0.68323\mathrm{D}{-14} & 0.16029\mathrm{D}{-12} & 0.79046\mathrm{D}{-13} & -0.55844\mathrm{D}{-13} & 0.10000\mathrm{D}\ 01 & -0.19785\mathrm{D}{-12} & 0.71275\mathrm{D}{-13} & 0.54873\mathrm{D}{-13} \\
0.42175\mathrm{D}{-13} & -0.41034\mathrm{D}{-11} & -0.34582\mathrm{D}{-11} & 0.18238\mathrm{D}{-11} & -0.39094\mathrm{D}{-13} & 0.10000\mathrm{D}\ 01 & -0.21778\mathrm{D}{-11} & -0.17639\mathrm{D}{-11} \\
-0.10281\mathrm{D}{-13} & 0.34892\mathrm{D}{-11} & 0.40867\mathrm{D}{-11} & -0.57385\mathrm{D}{-12} & -0.10198\mathrm{D}{-13} & -0.41265\mathrm{D}{-11} & 0.32150\mathrm{D}{-11} & 0.10000\mathrm{D}\ 01
\end{bmatrix} \begin{Bmatrix} \delta_i \\ \delta_j \end{Bmatrix}
$$

(b)



TABLE 11. The elements of the displacement function matrix for (a) $x = 0$, and (b) $x = \ell$.

Note: Terms such as 0.54179D-13 mean $0.54179 \times 10^{-13}$

| | $u_{n_i}$ | $w_{n_i}$ | $(dw_n/dx)_i$ | $v_{n_i}$ | $u_{n_j}$ | $w_{n_j}$ | $(dw_n/dx)_j$ | $v_{n_j}$ |
|---|---|---|---|---|---|---|---|---|
| First Mode | $-.55\times10^{-5}$ | $-.633$ | $.927\times10^{-3}$ | $.31515$ | $.55\times10^{-5}$ | $-.633$ | $-.927\times10^{-3}$ | $.31515$ |
| Second Mode | $.3967$ | $.5227$ | $-.02633$ | $-.262$ | $.3967$ | $-.5227$ | $-.02633$ | $.262$ |

TABLE 12. The eigenvectors of the first and second modes of a free element.

| n | Arnold and Warburton | Baron and Bleich | Galletly | Michalopoulos and Muster | This theory |
|---|---|---|---|---|---|
| 2 | 748 | 760 | 744 | 750 | 752.3 |
| 3 | 435 | 435 | 435 | 436 | 436.3 |
| 4 | 469 | 463 | 467 | 467 | 468.7 |
| 5 | 675 | 670 | 675 | 675 | 678.3 |

TABLE 13. Natural frequencies, in Hz, for a particular uniform shell, as calculated by various theories ($m = 1$)

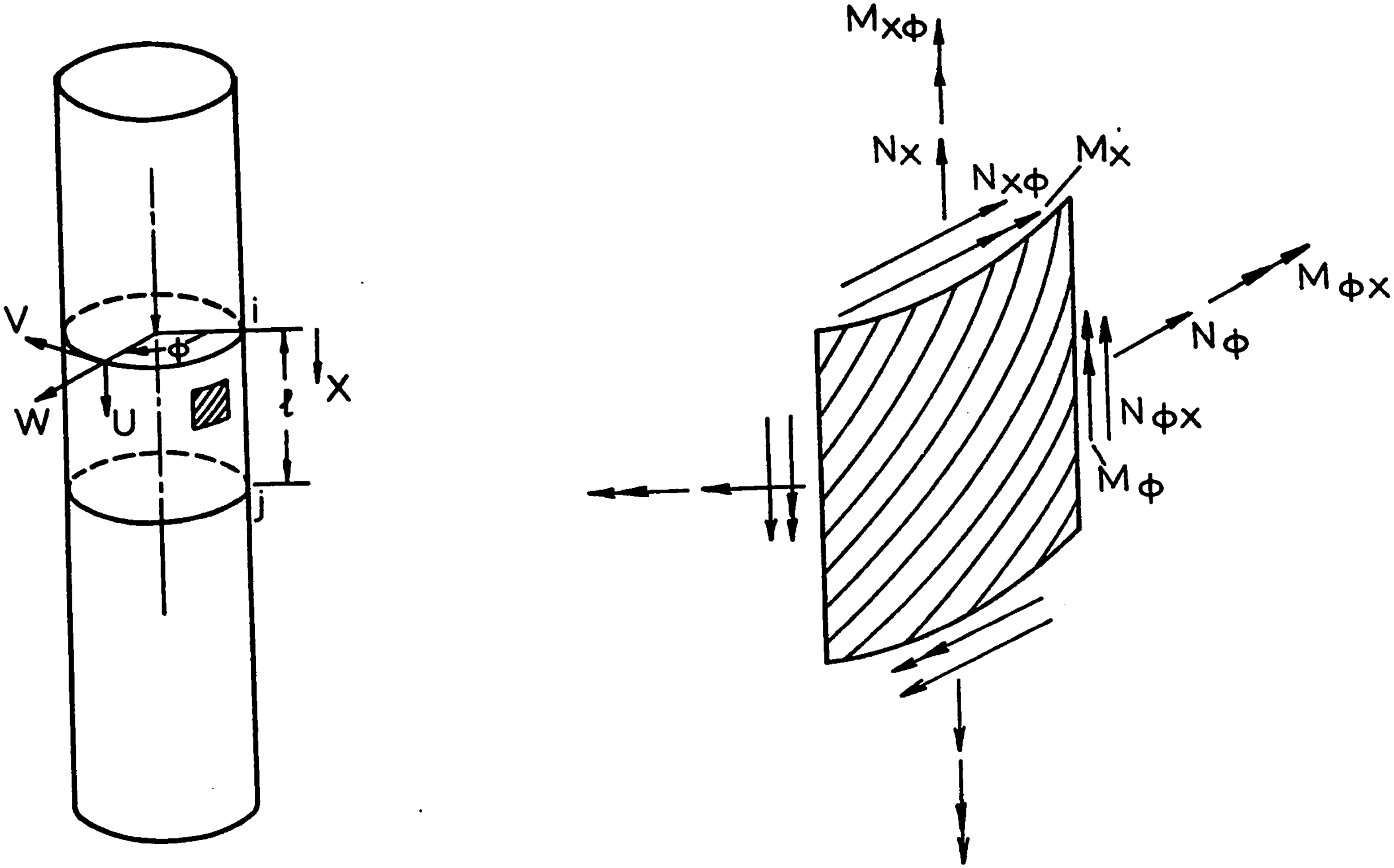


(a) (b)

FIGURE 1. (a) Axi-symmetric shell showing a cylindrical finite element defined by nodes i and j;
(b) Stress resultants on an element of the shell within the finite element (with transverse shear forces omitted for clarity).

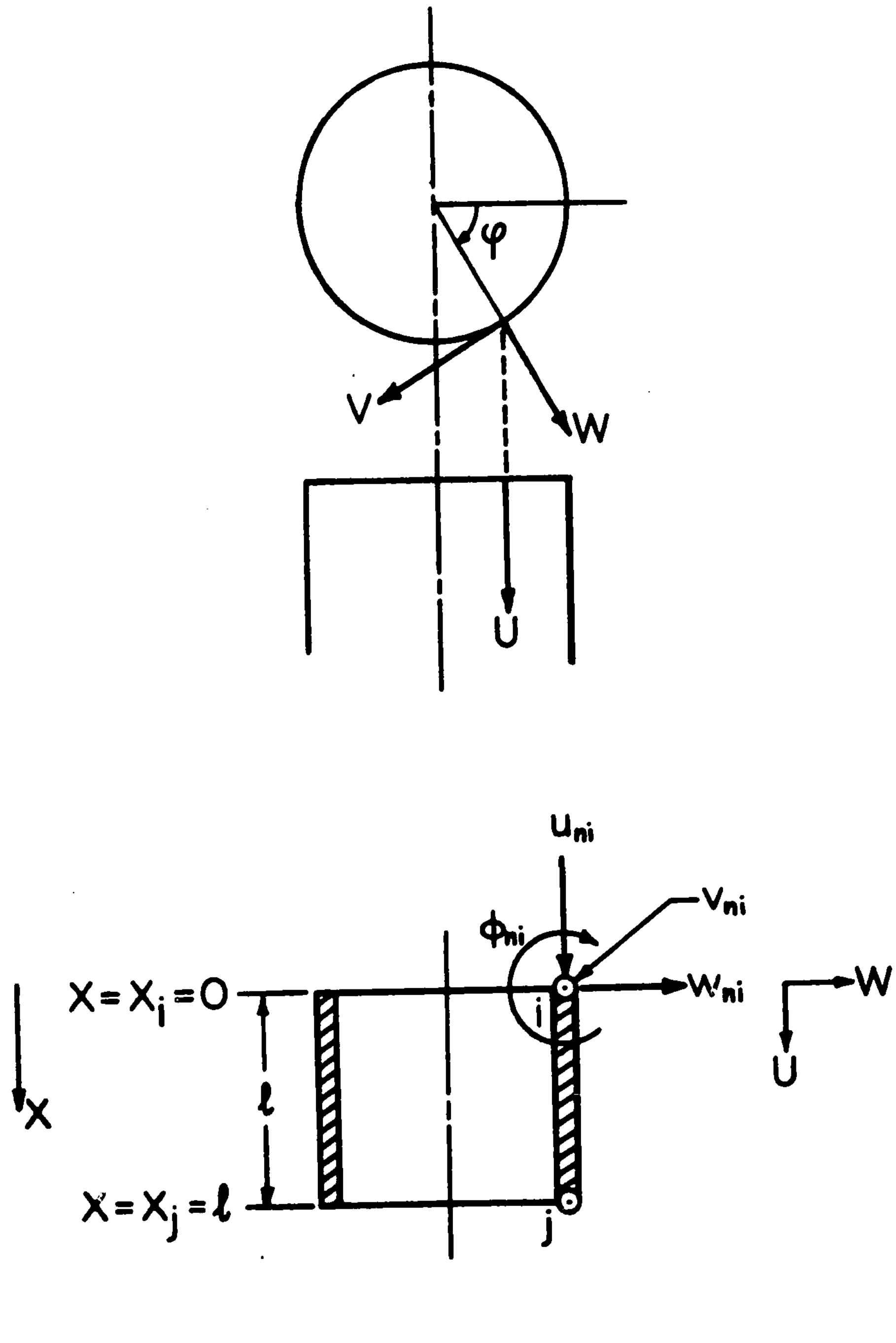


FIGURE 2. Nodal displacements at points i and j.

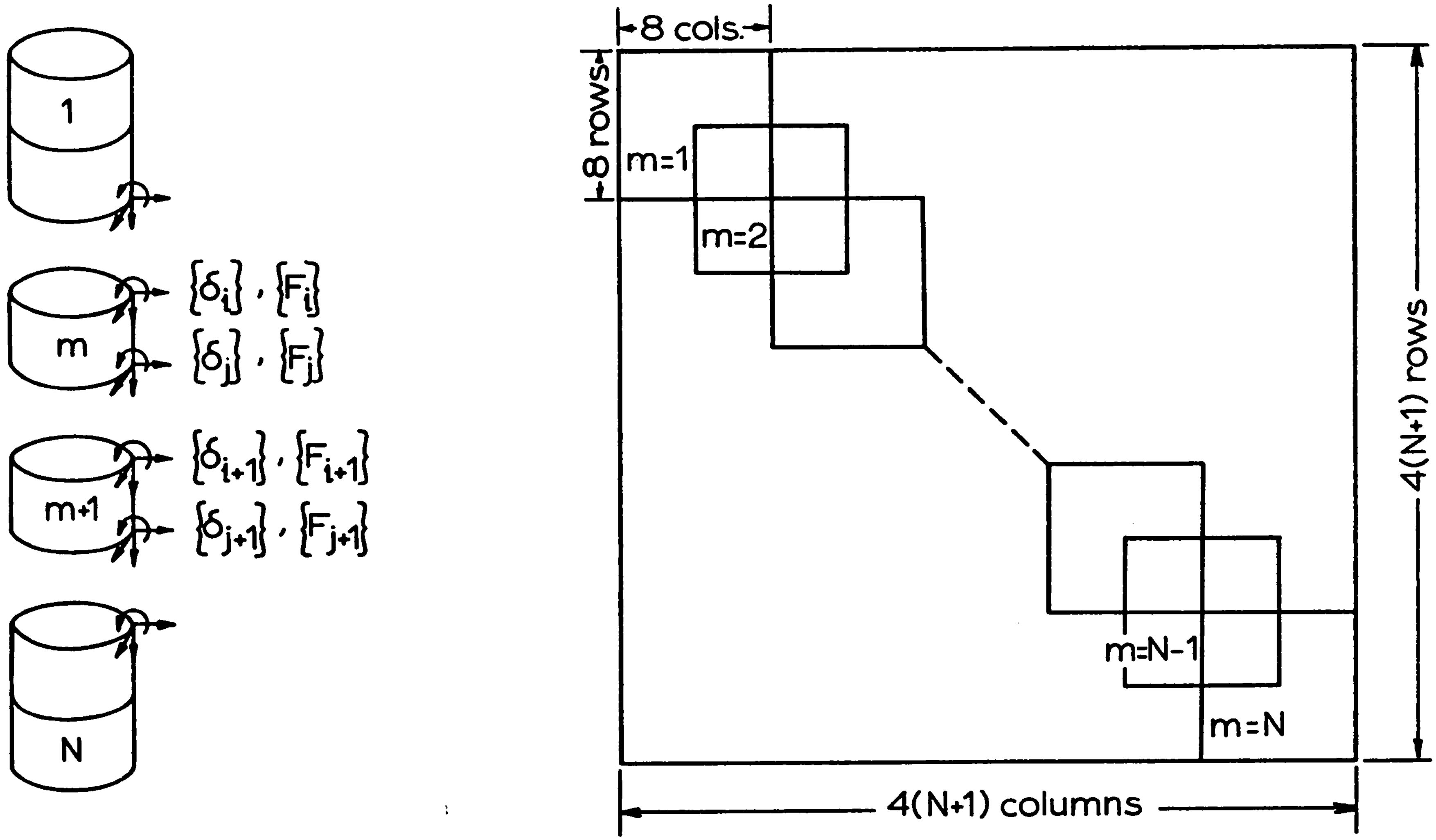


FIGURE 3. Illustration of the construction of stiffness and mass matrices for the whole shell. (N = number of elements).

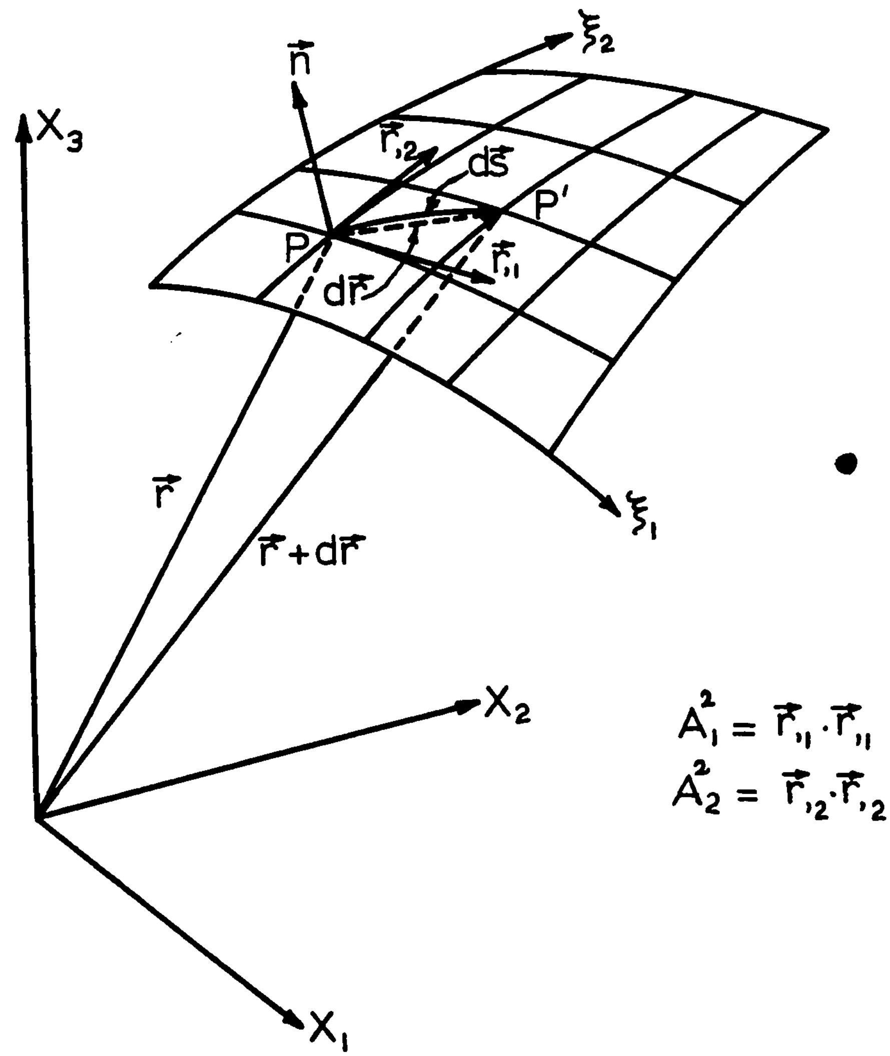


FIGURE 4. Parametric curves of the surface where

$$A_1^2 = \vec{r}_{,1} \cdot \vec{r}_{,1} \quad \text{and} \quad A_2^2 = \vec{r}_{,2} \cdot \vec{r}_{,2}$$

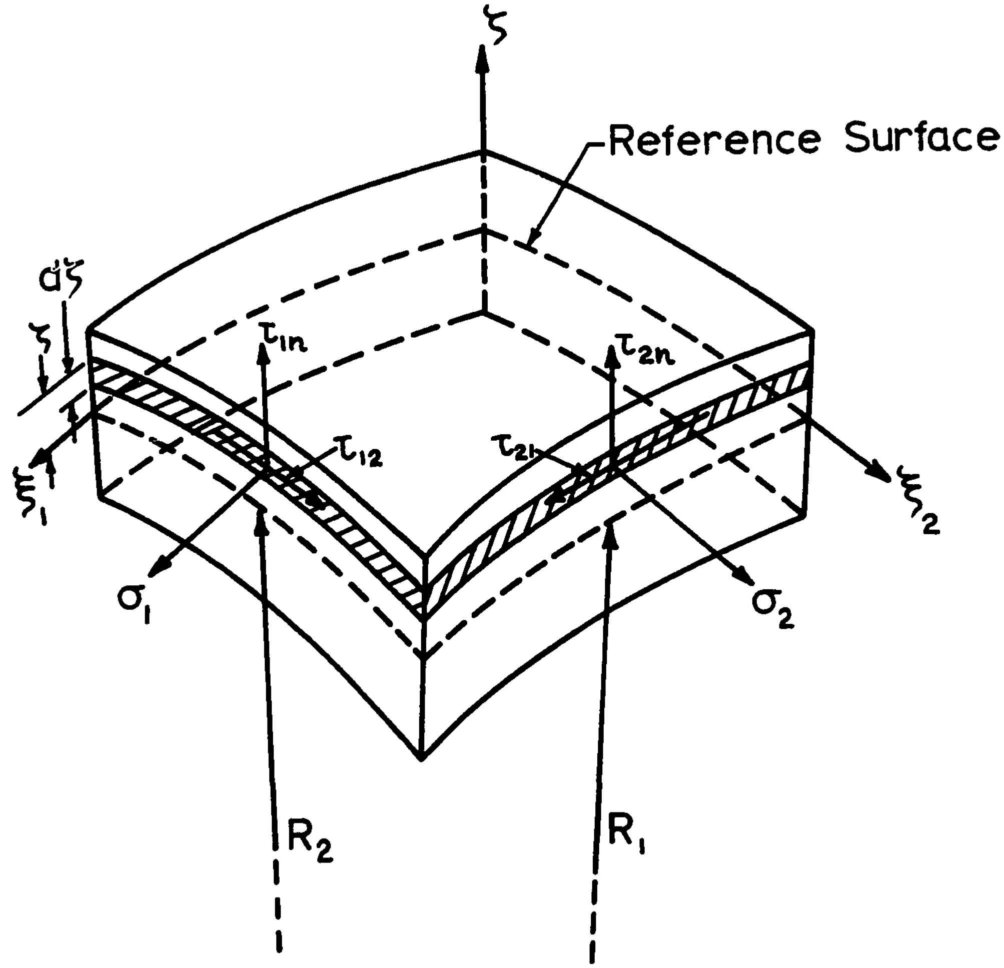


FIGURE 5. Differential element of a shell.

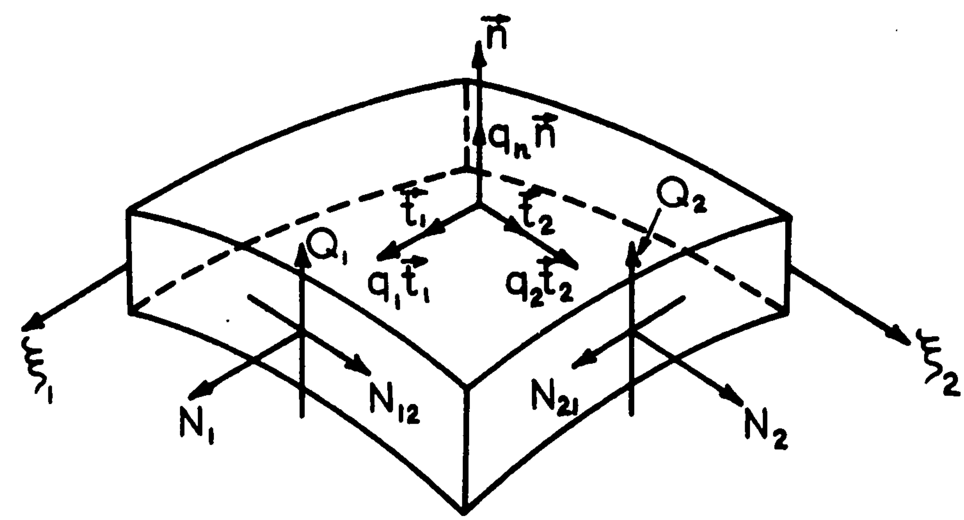


(a)

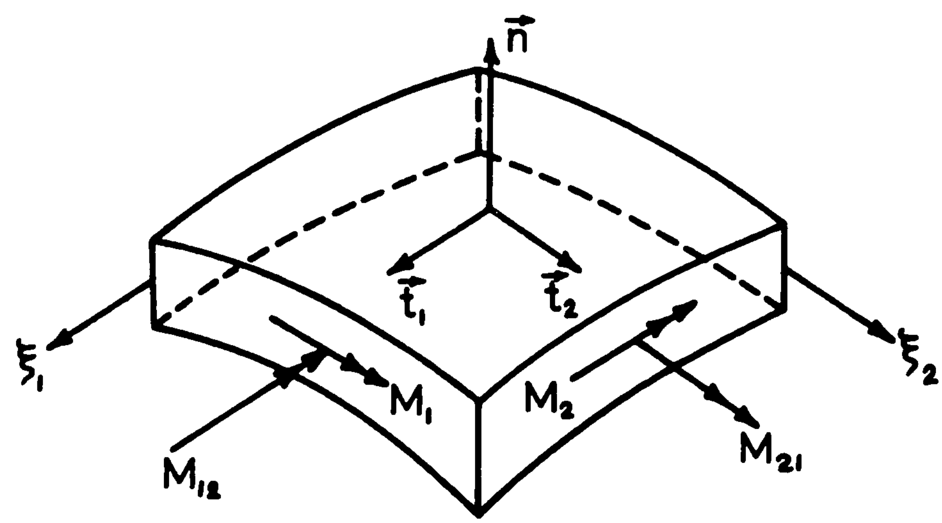


(b)

FIGURE 6. (a) Stress resultants and surface loads acting on a differential element, and (b) stress couples acting on a differential element.

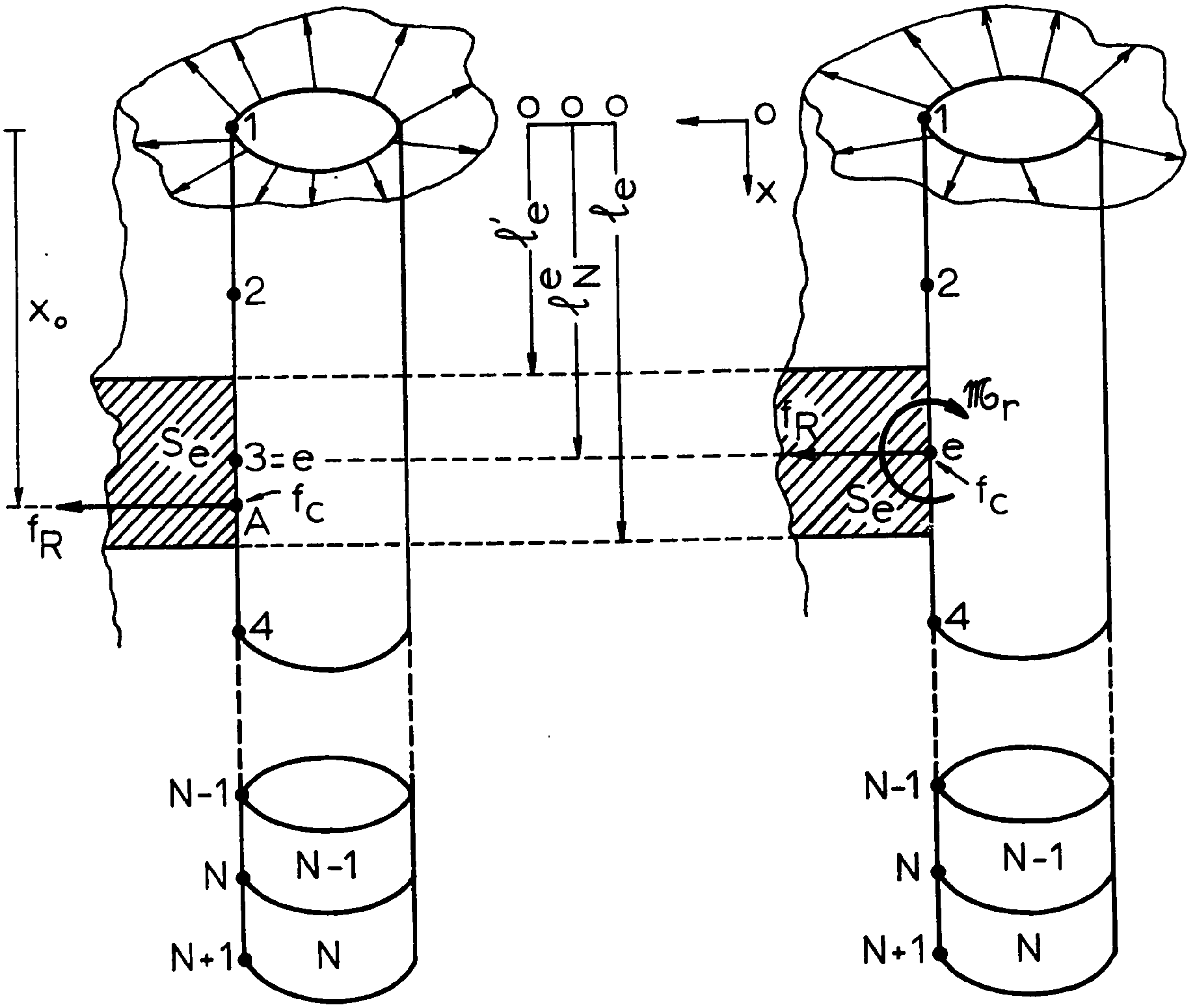


7a

7b

FIGURE 7. Illustration of the construction of the continuous random pressure field at the nodal points.

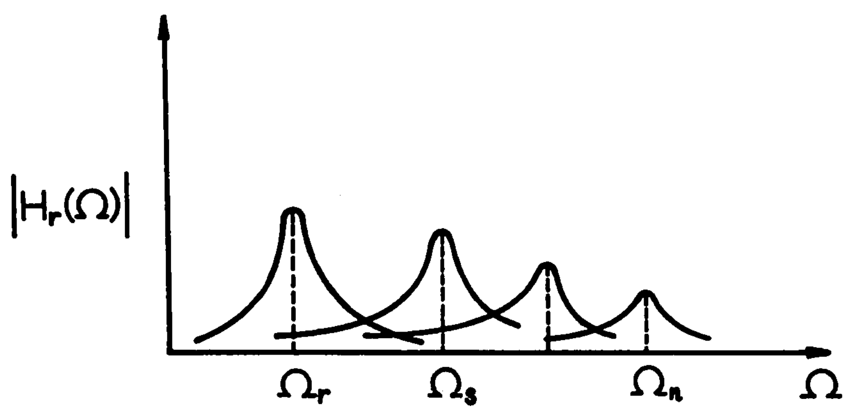


FIGURE 8. Magnification factors for a lightly damped multi-degree-of-freedom system.

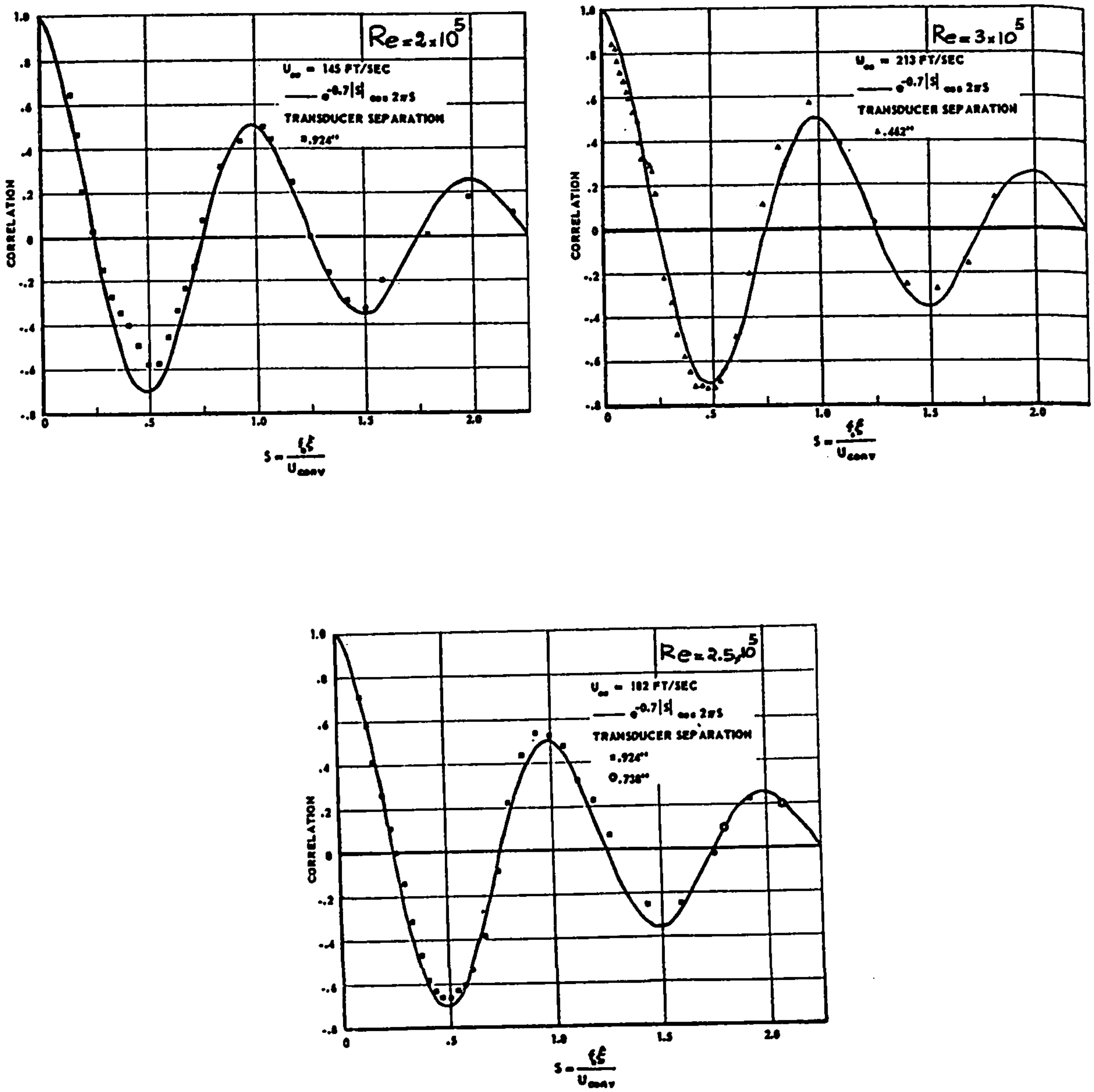


FIGURE 9. Longitudinal correlation versus Strouhal number based on convection velocity ($U_{CONV}$).

(Reproduction of Bakewell (44), figures 3,4 and 5)

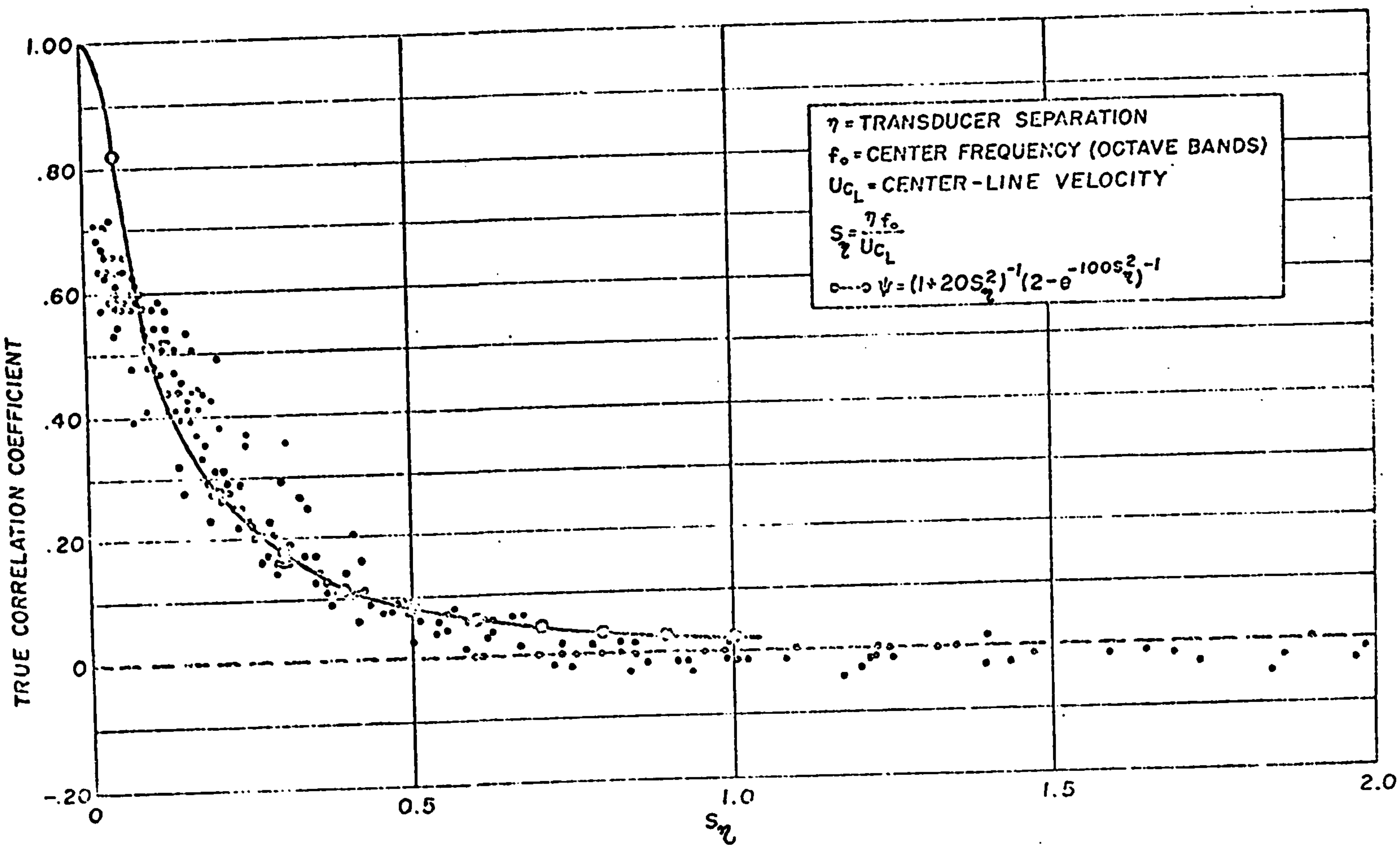


FIGURE 10. Lateral correlation versus Strouhal number based on centerline velocity.

(Reproduction of Bakewell (39), figure 30)

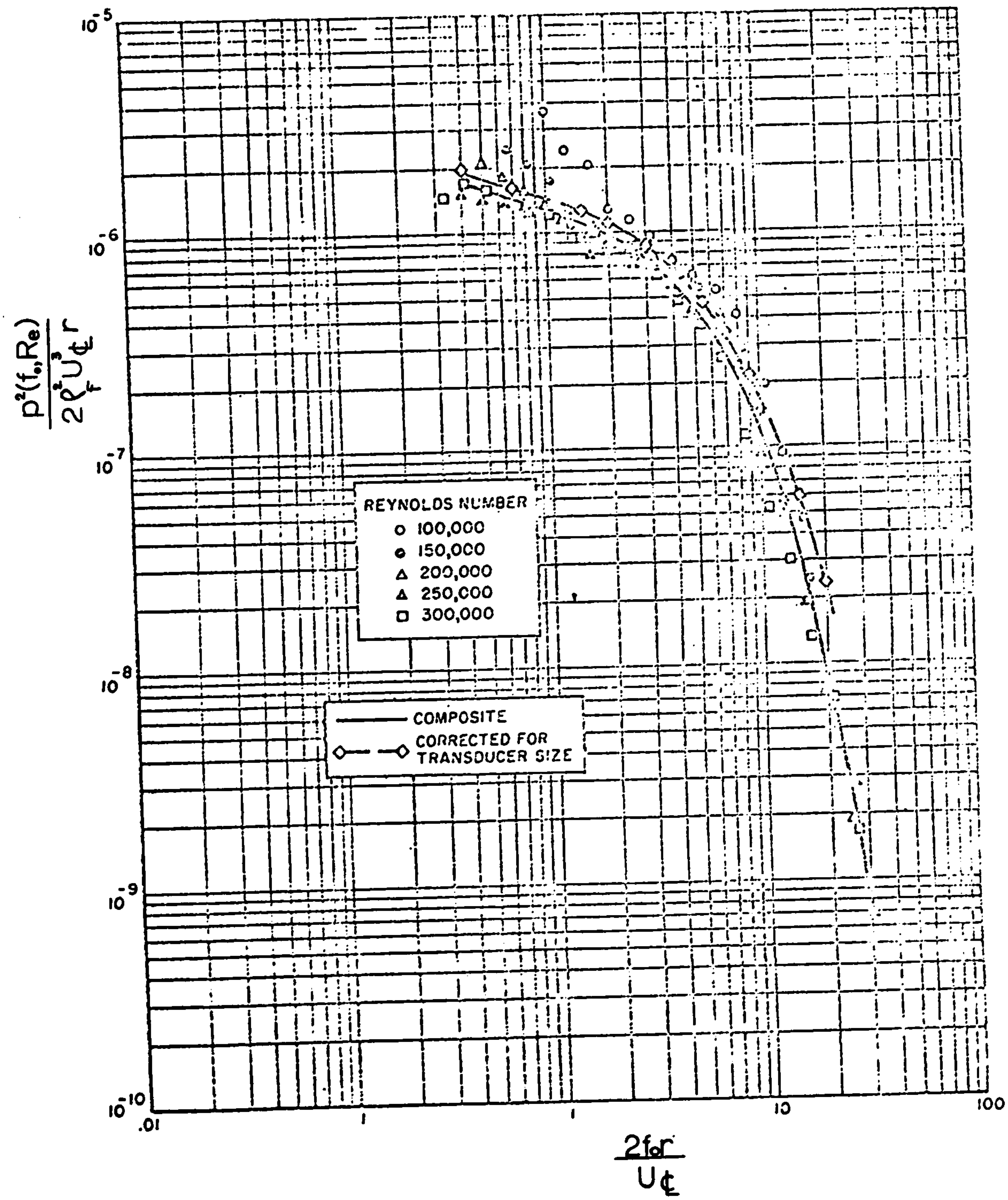


FIGURE 11. The non-dimensionalized frequency spectrum. (Reproduction of Bakewell (39), figure 5)

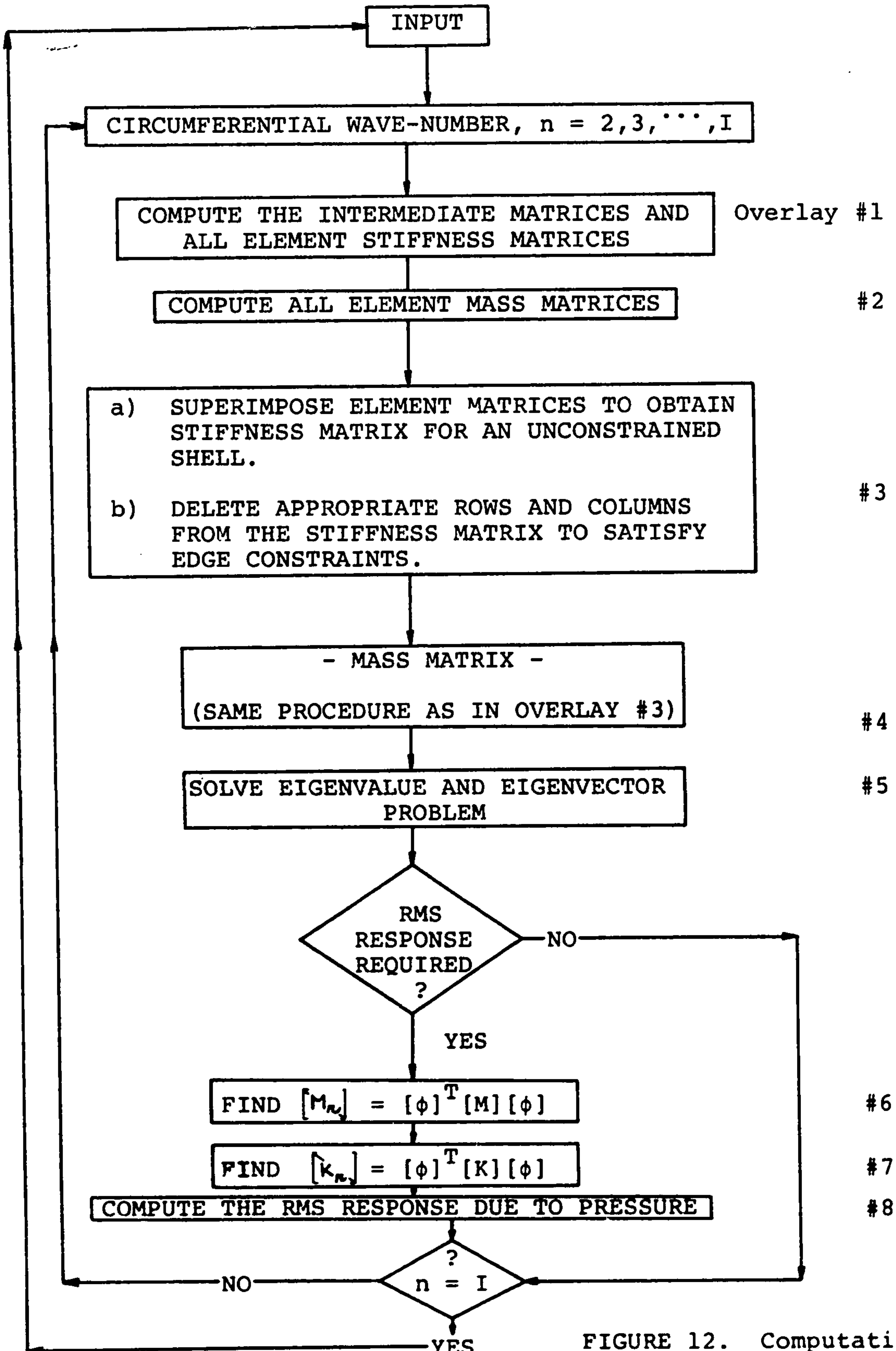


FIGURE 12. Computational flow diagram.

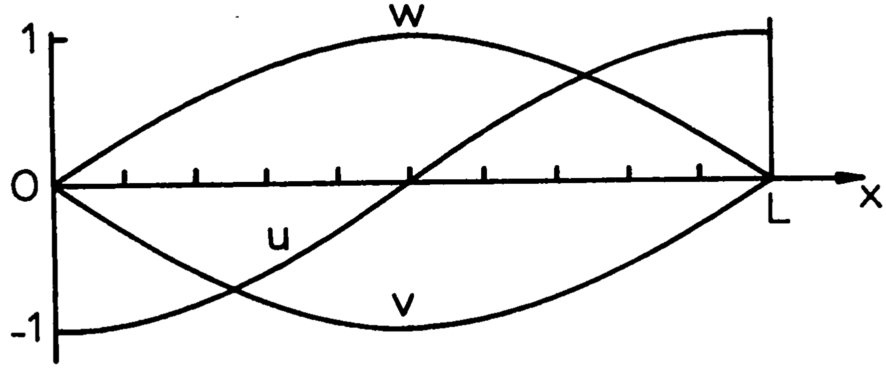


| n | $u_{max}/w_{max}$ | $v_{max}/w_{max}$ |
|---|---|---|
| 2 | 0.1342 | 0.5098 |
| 3 | 0.0683 | 0.3374 |
| 4 | 0.0404 | 0.2520 |
| 5 | 0.0265 | 0 2011 |

FIGURE 13 Normalized eigenvectors for n = 2,3,4,5 and m = 1 for a uniform, simply-supported shell.

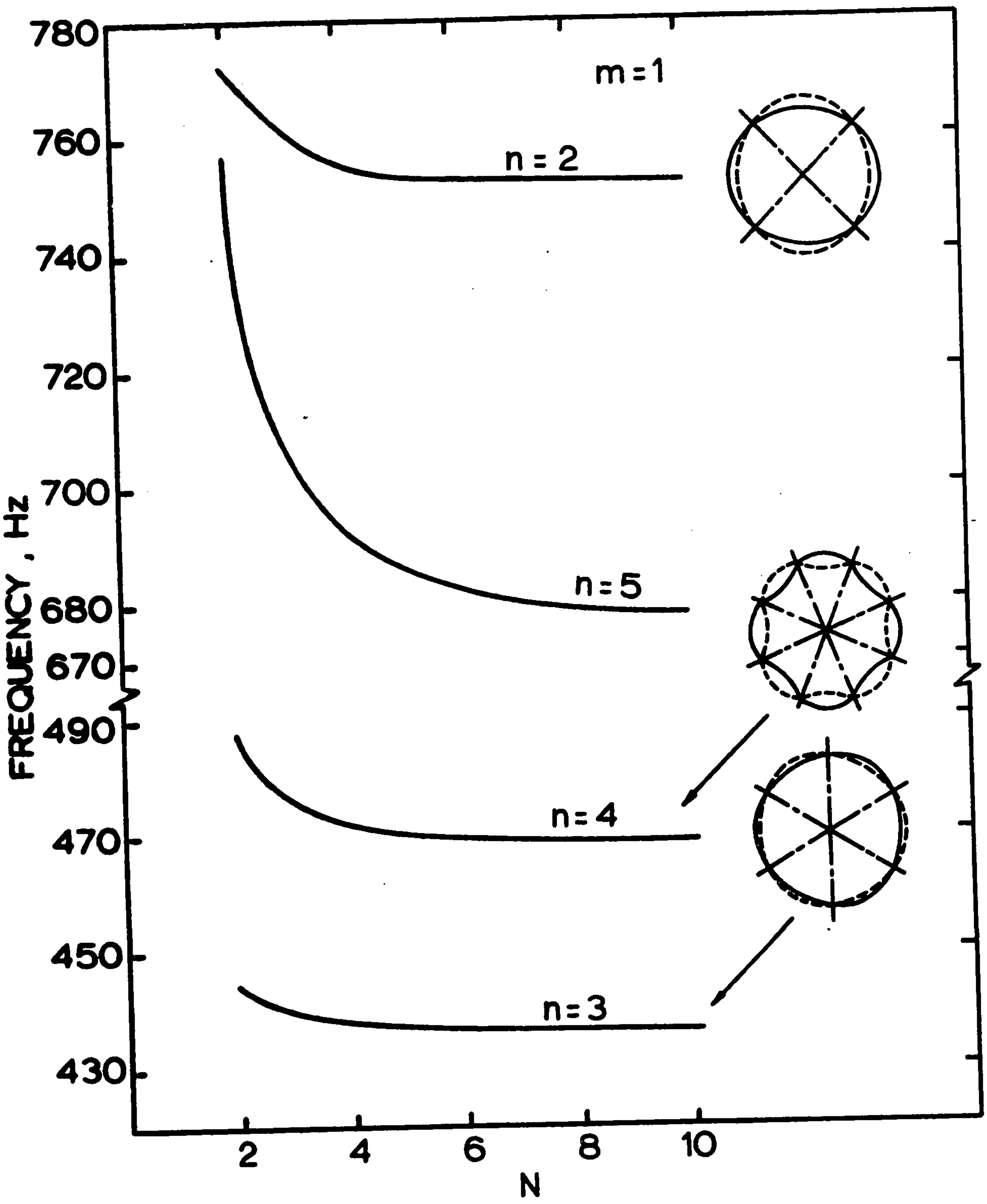


FIGURE 14a The natural frequencies of a uniform simply-supported shell as a function of the number of finite elements, N, for m = 1. (Continuous lines drawn through discrete points at integral N.)

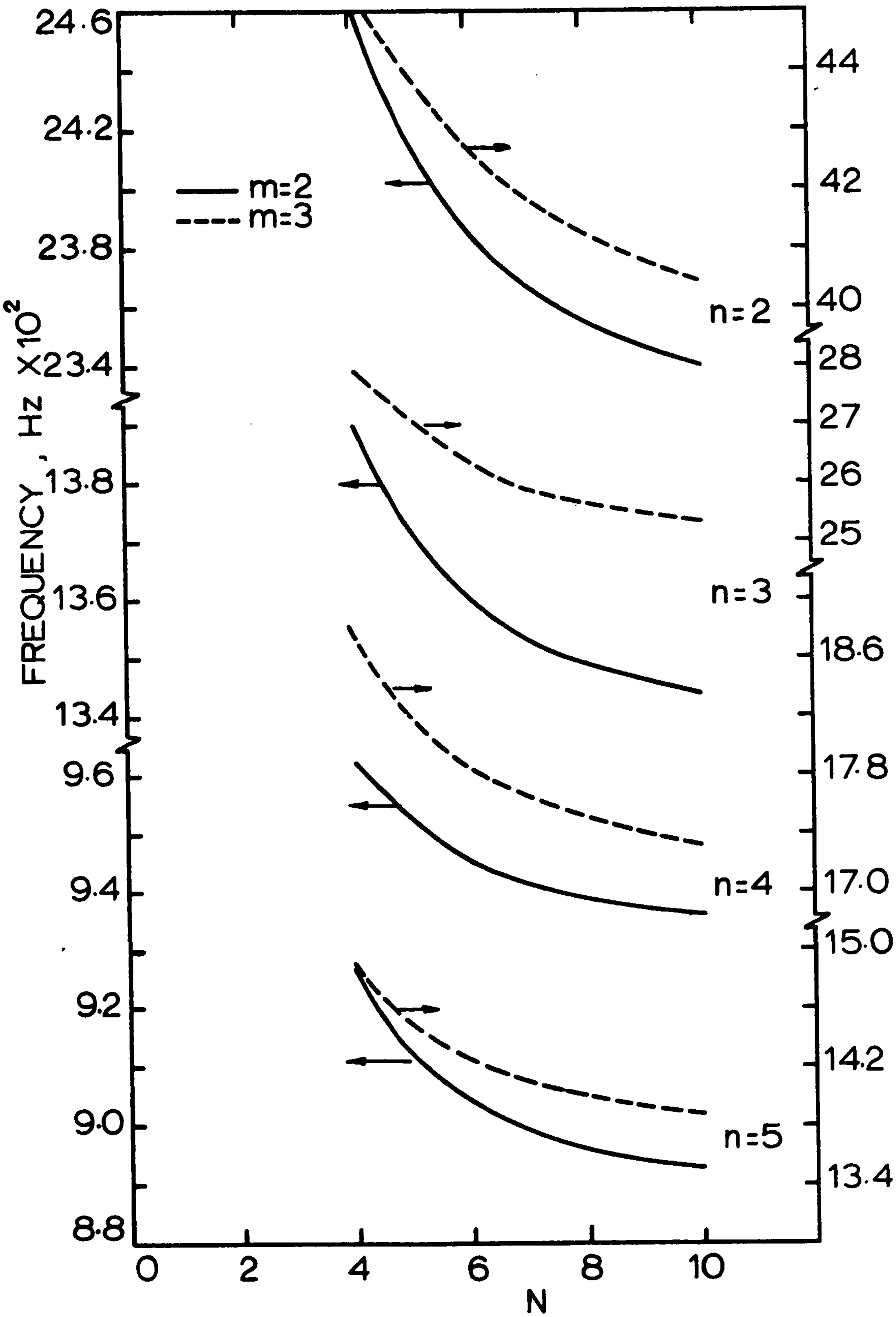


FIGURE 14b The natural frequencies of a uniform simply-supported shell as a function of N, for m = 2 and 3. (Continuous lines drawn through discrete points at integral N.)

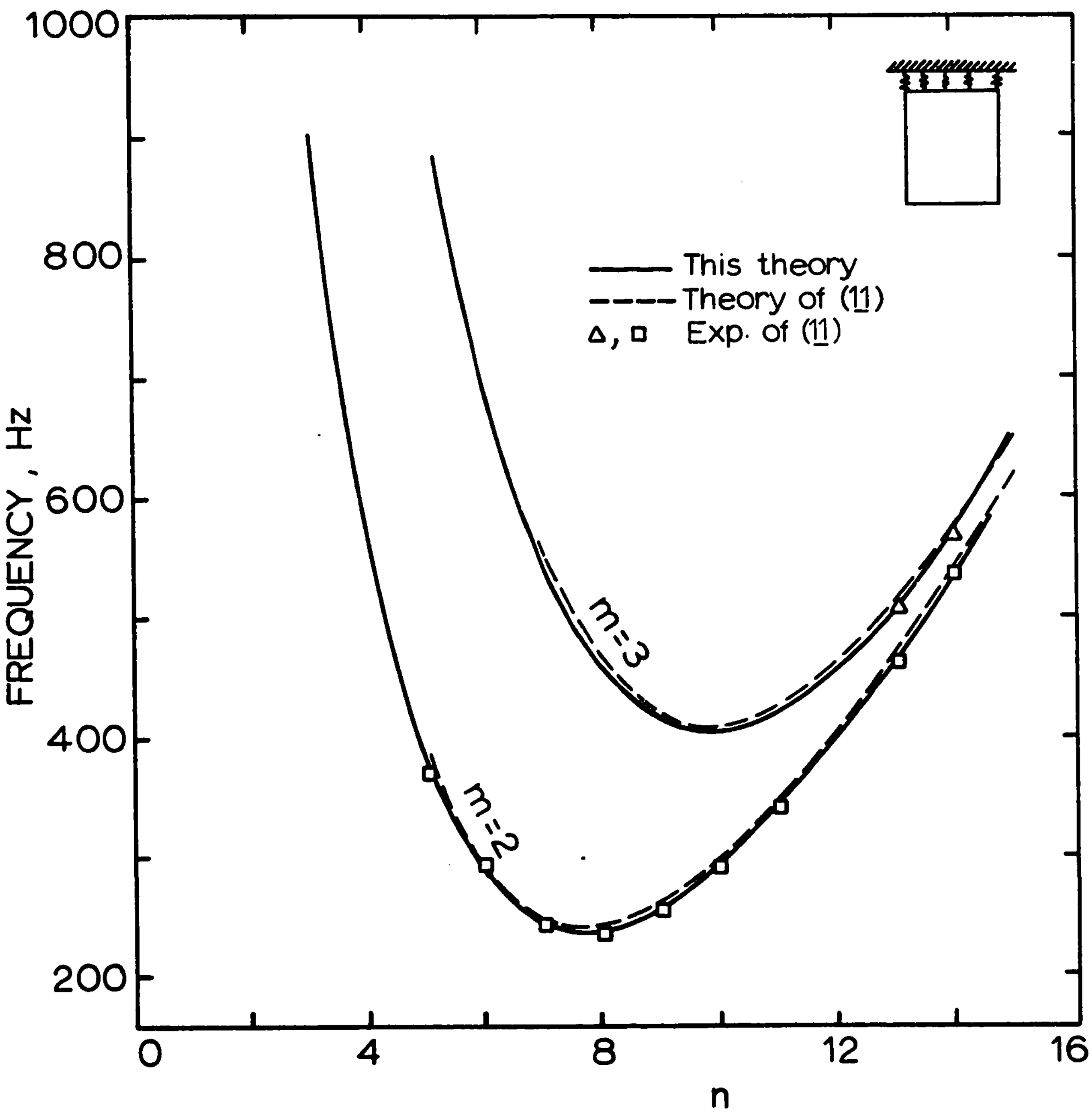


**FIGURE 15** Natural frequencies of a free-free uniform shell as a function of the number of circumferential waves, n.

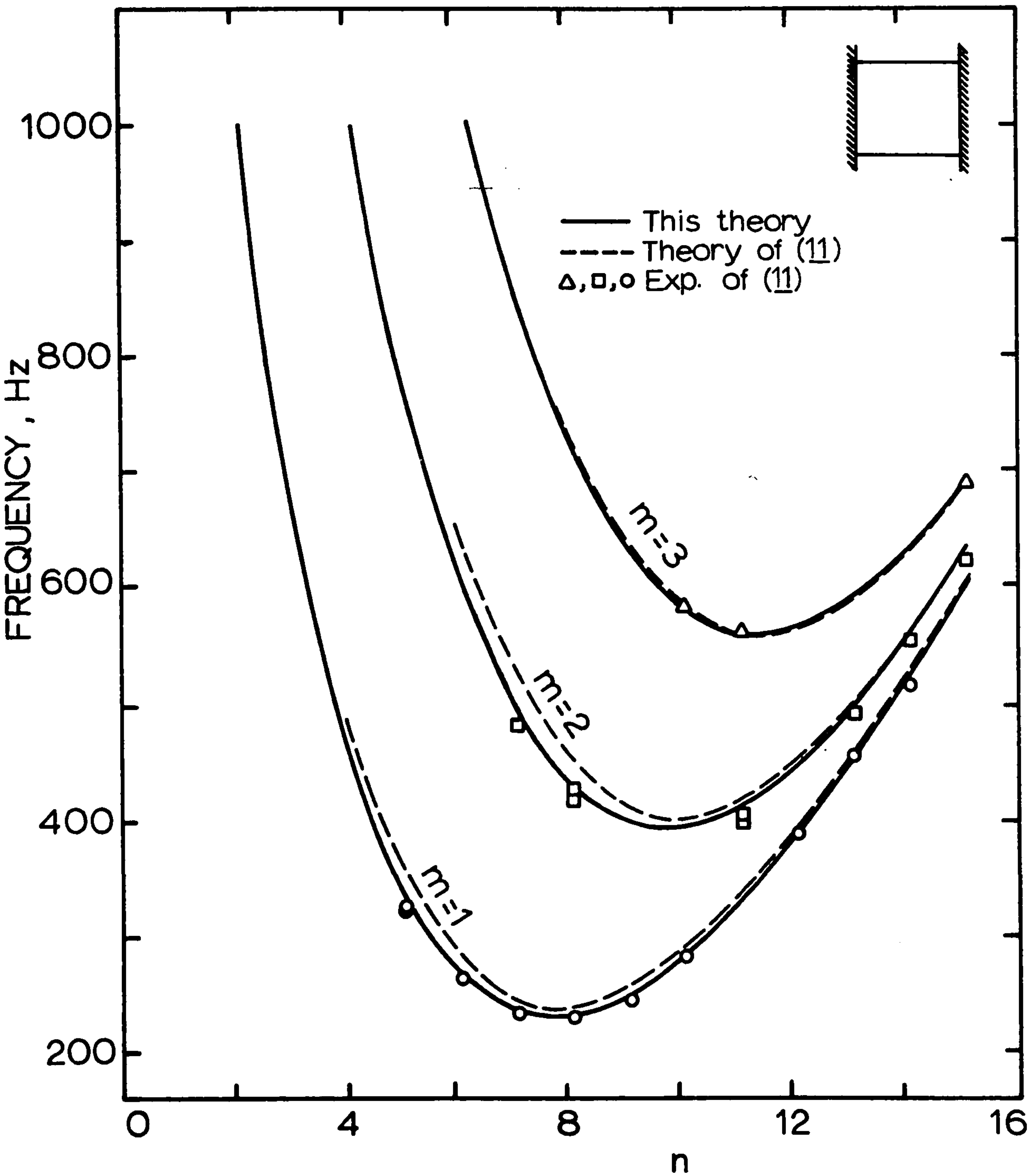


**FIGURE 16** **Natural frequencies of a clamped-clamped uniform shell.**

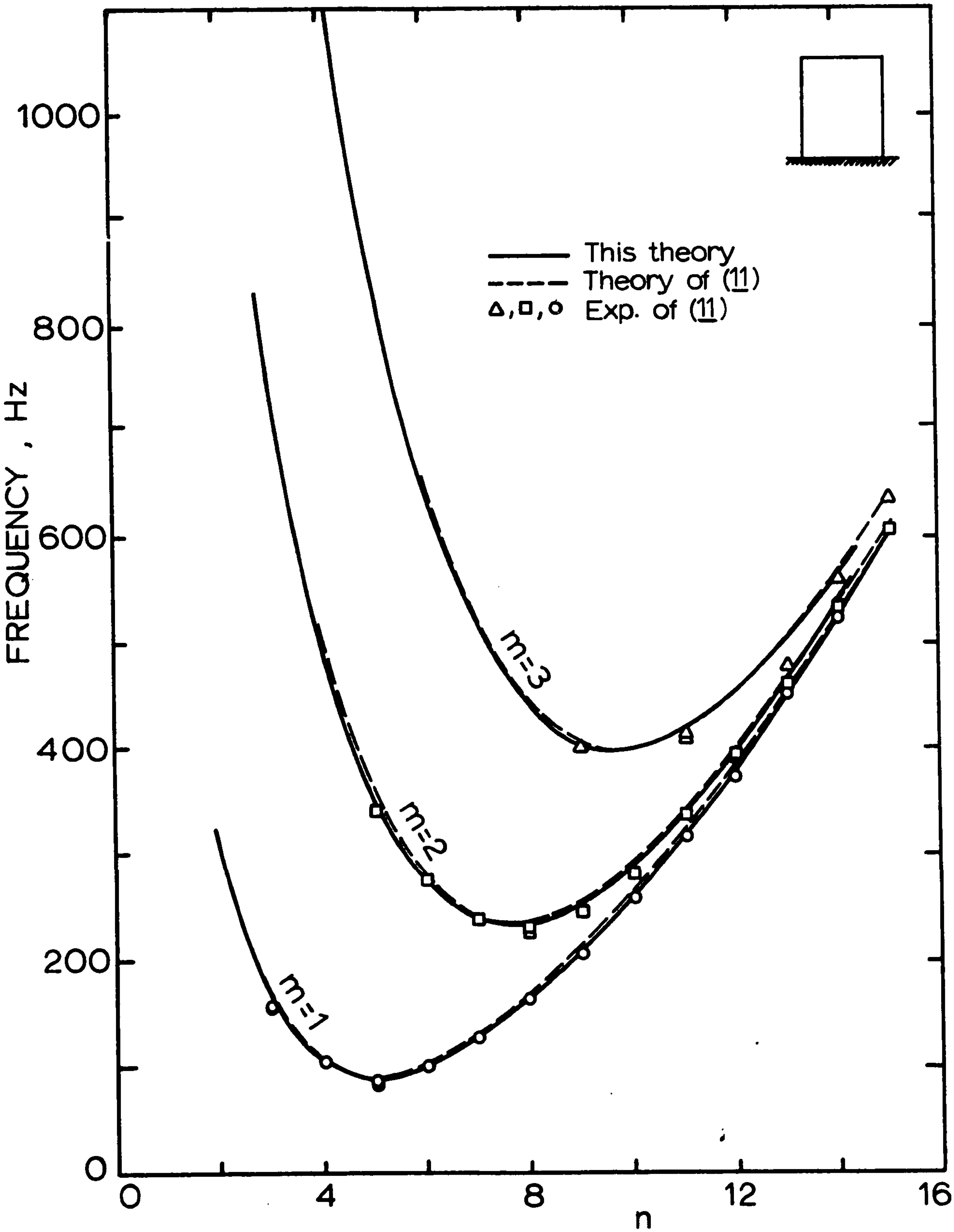


**FIGURE** 17 **Natural frequencies of a clamped-free uniform shell.**

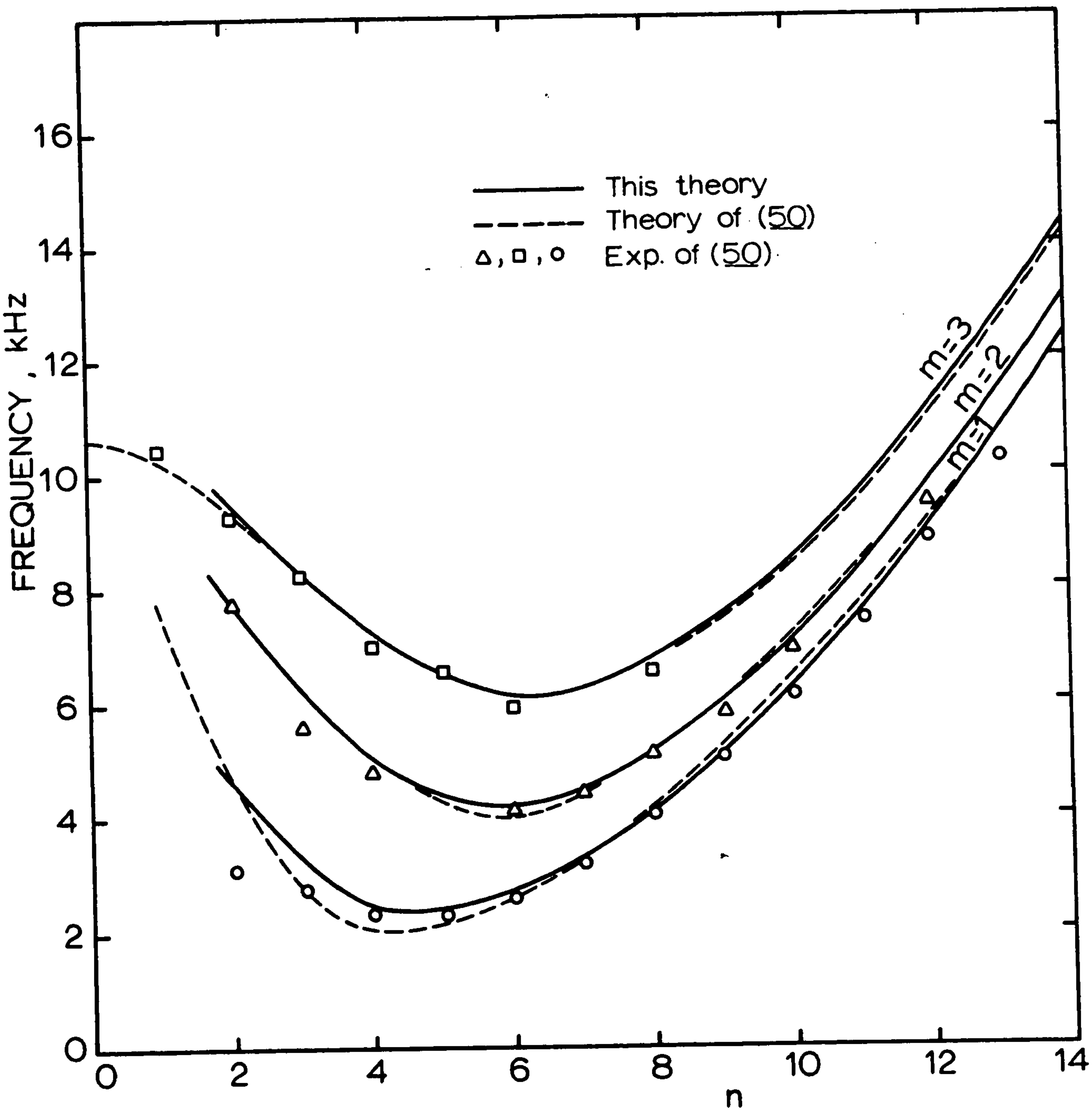


**FIGURE 18** Natural frequencies of the unstiffened (uniform) shell studied by Weingarten (50).

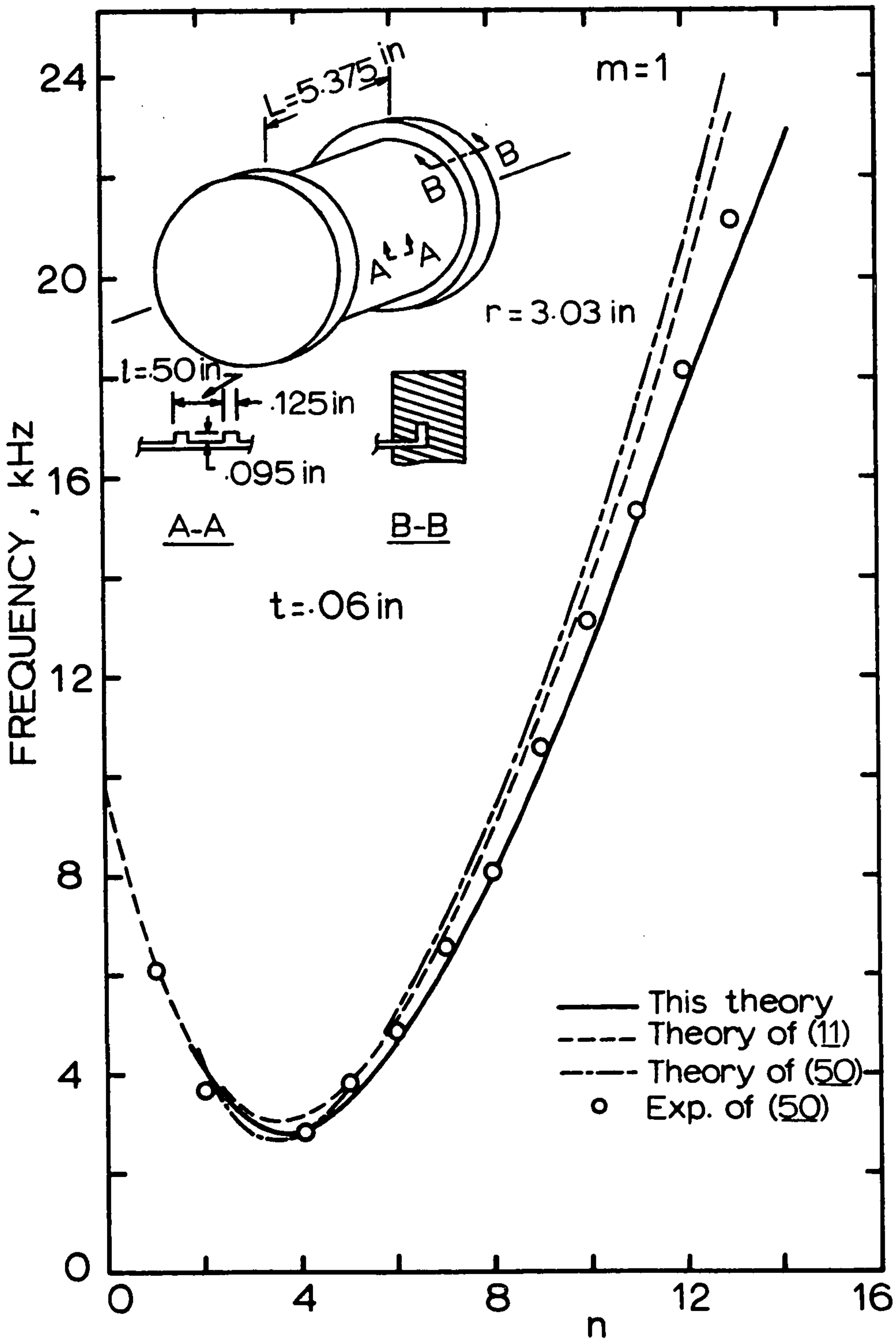


FIGURE 19 Natural frequencies of the ring-stiffened shell first studied by Weingarten (50); $m = 1$.

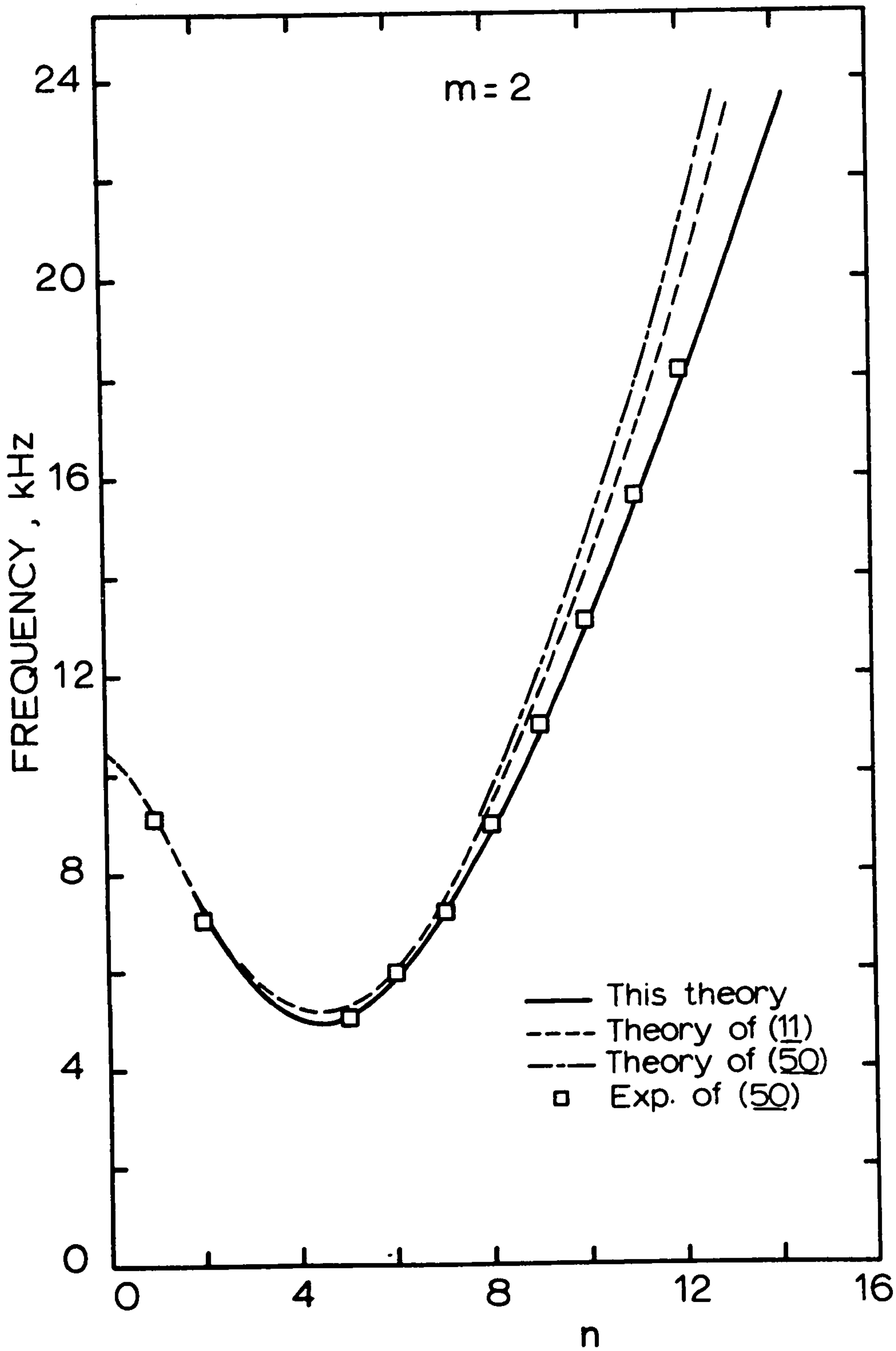


**FIGURE** 20 **Natural frequencies of the ring-stiffened shell first studied by Weingarten (50); m = 2.**

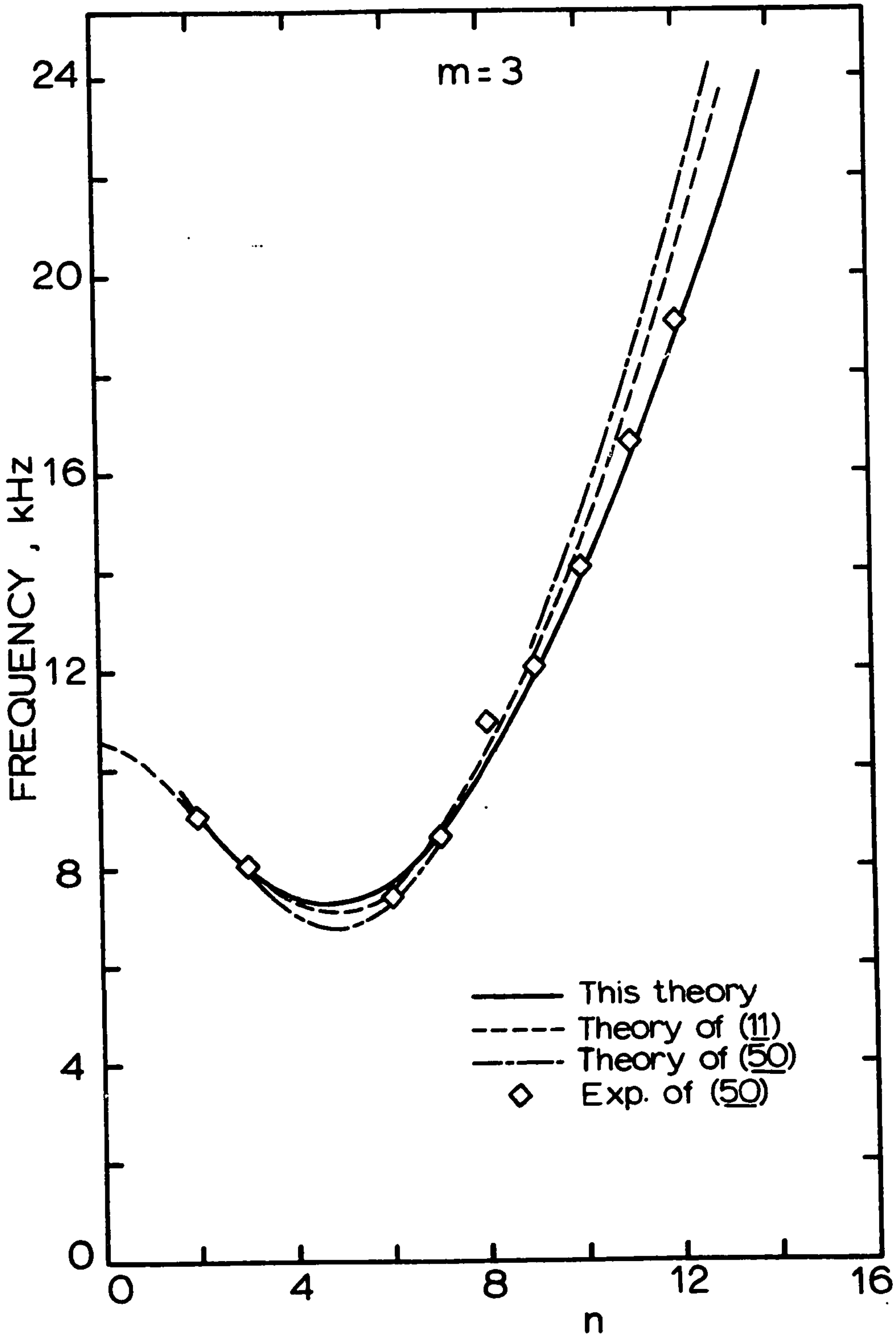


**FIGURE 21** **Natural frequencies of the ring-stiffened shell first studied by Weingarten (50); m = 3.**

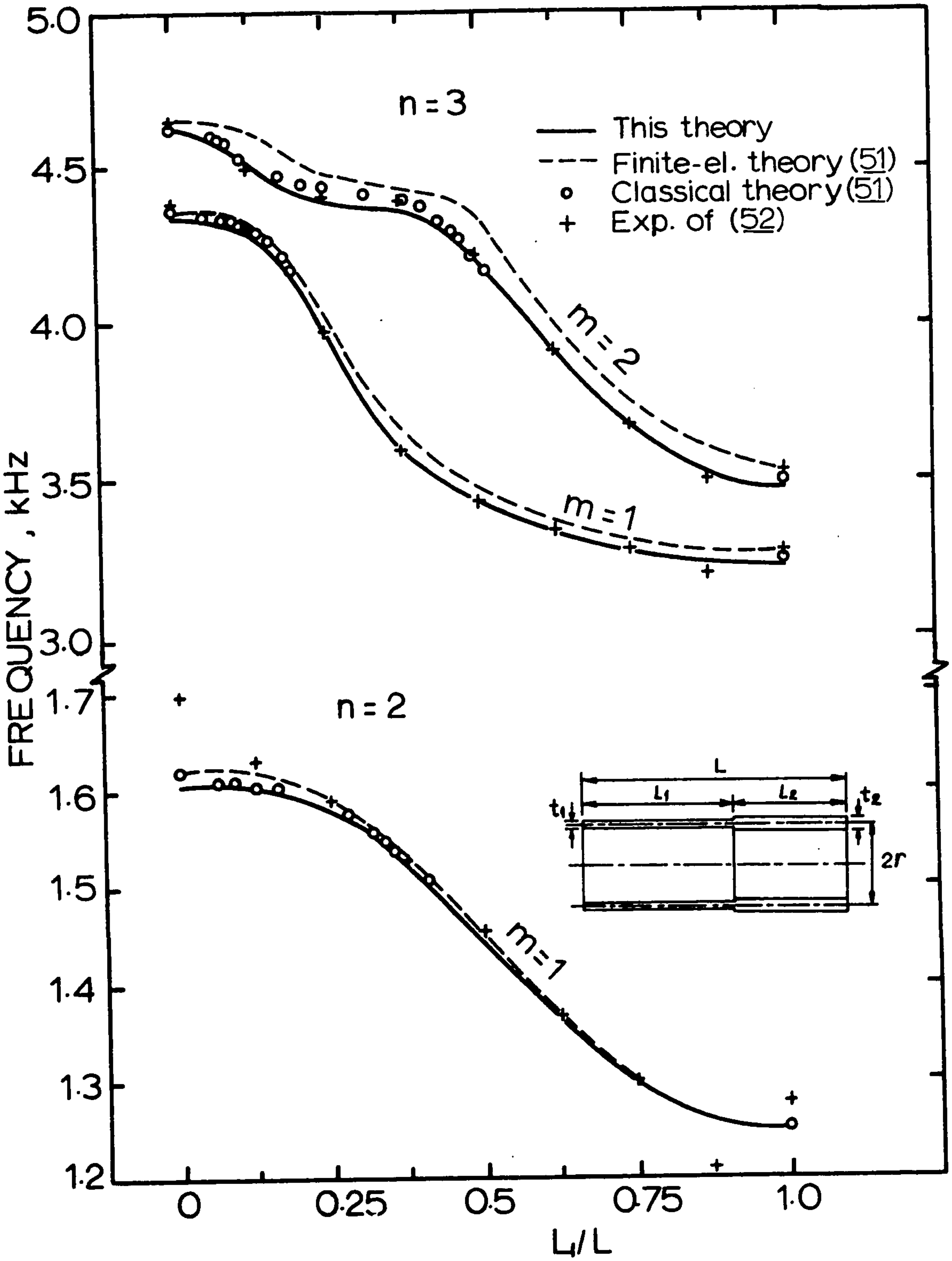


FIGURE 22 Some natural frequencies of a simply-supported shell with thickness discontinuity ($t_1$ = 0.1875 in., $t_2$ = 0.25 in.)

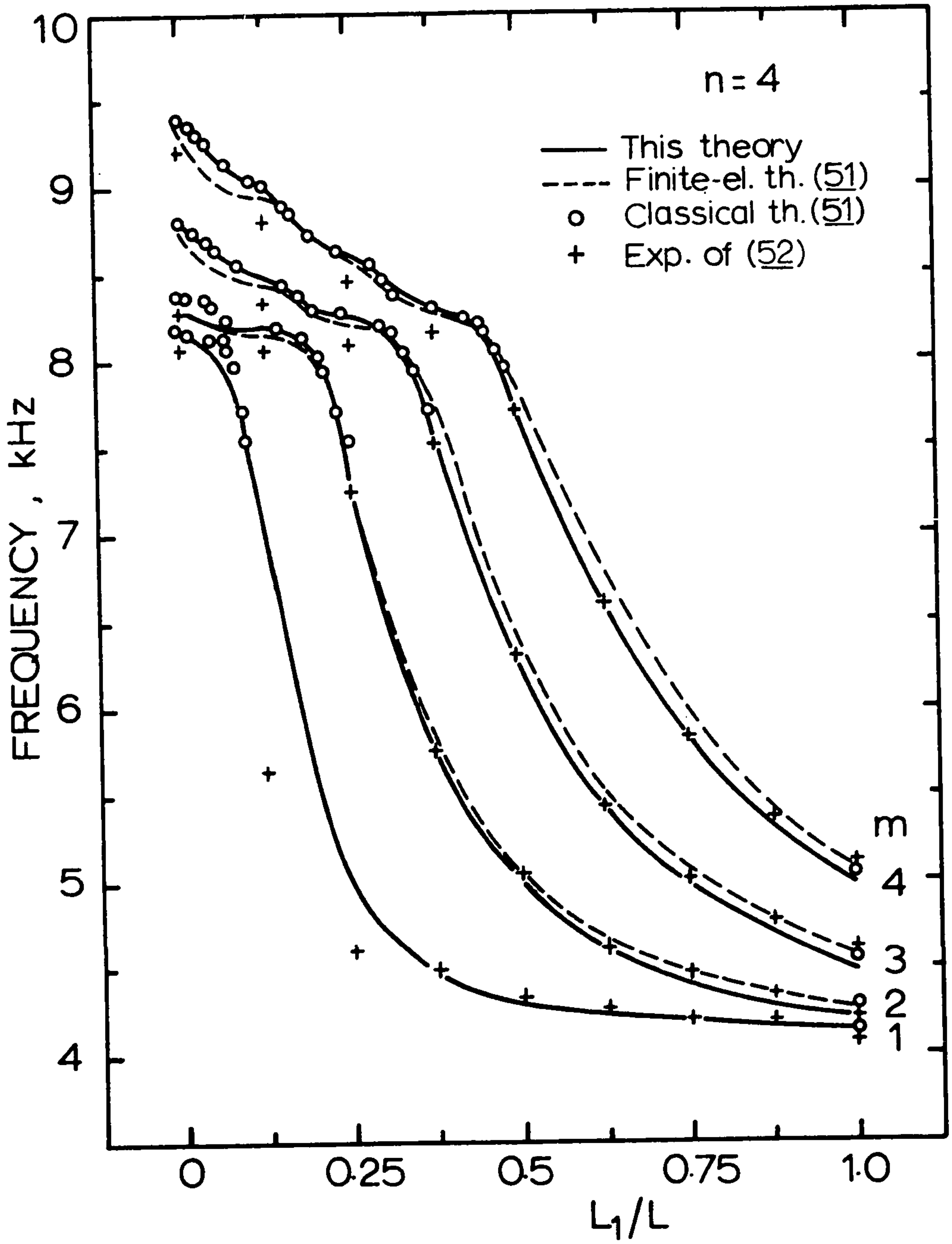


FIGURE 23 Natural frequencies of a simply-supported shell with thickness discontinuity ($t_1$ = 0.125 in., $t_2$ = 0.25 in.); n = 4.

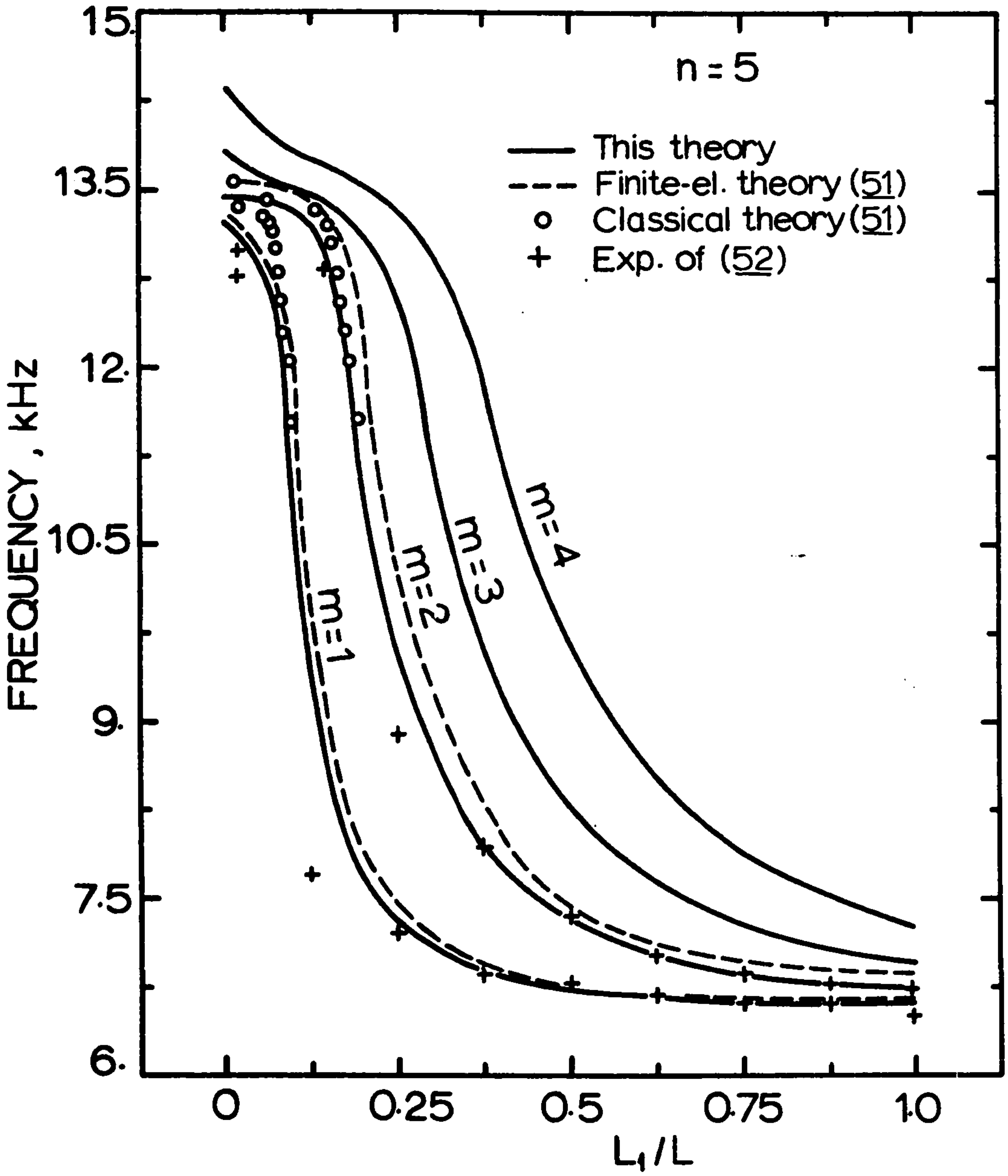


**FIGURE 24** **Natural frequencies of a simply-supported shell with thickness discontinuity ($t_1$ = 0.125 in., $t_2$ = 0.25 in.); n = 5.**

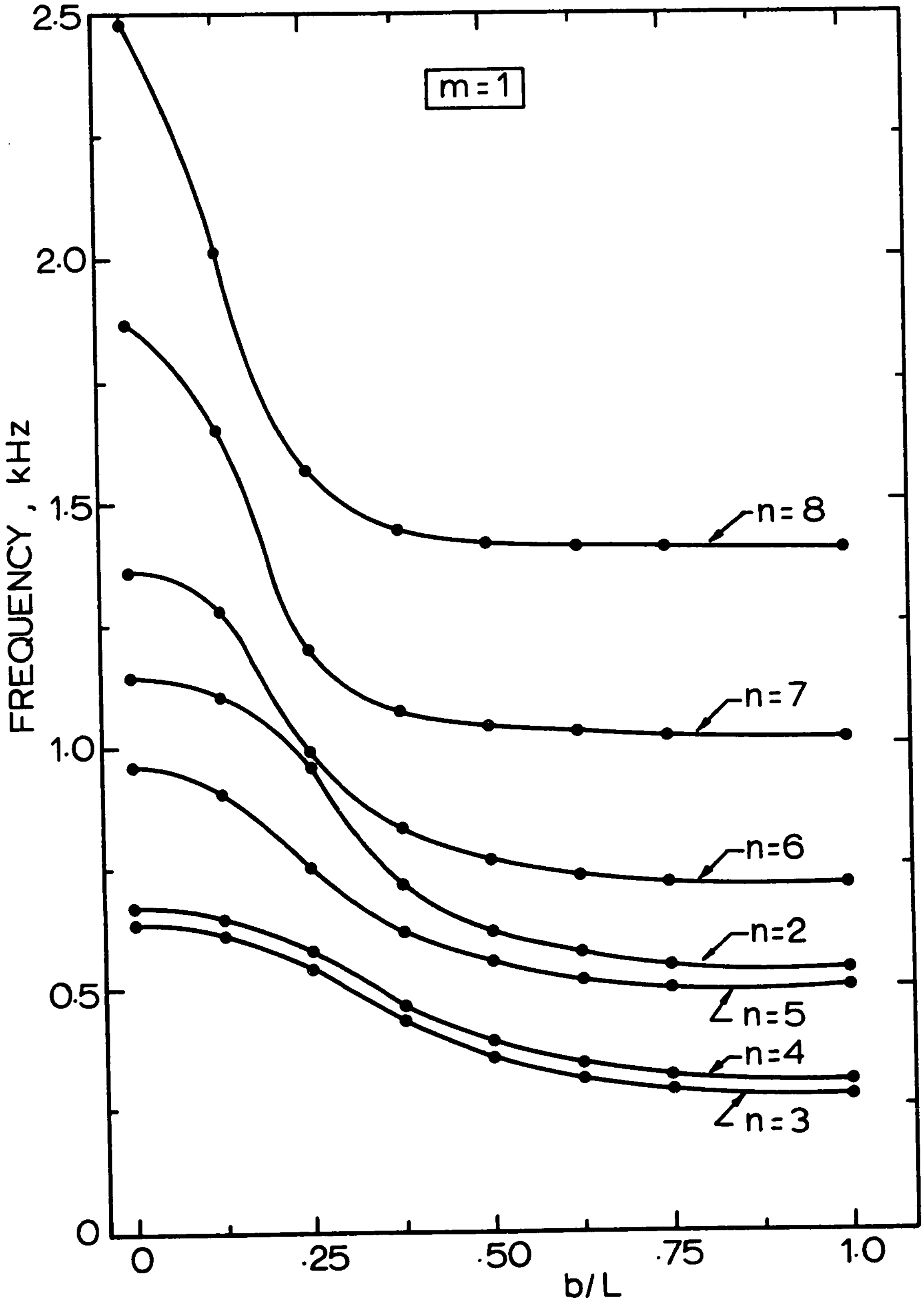


FIGURE 25. Variation of natural frequencies with liquid depth of a liquid filled shell, this theory: m = 1.

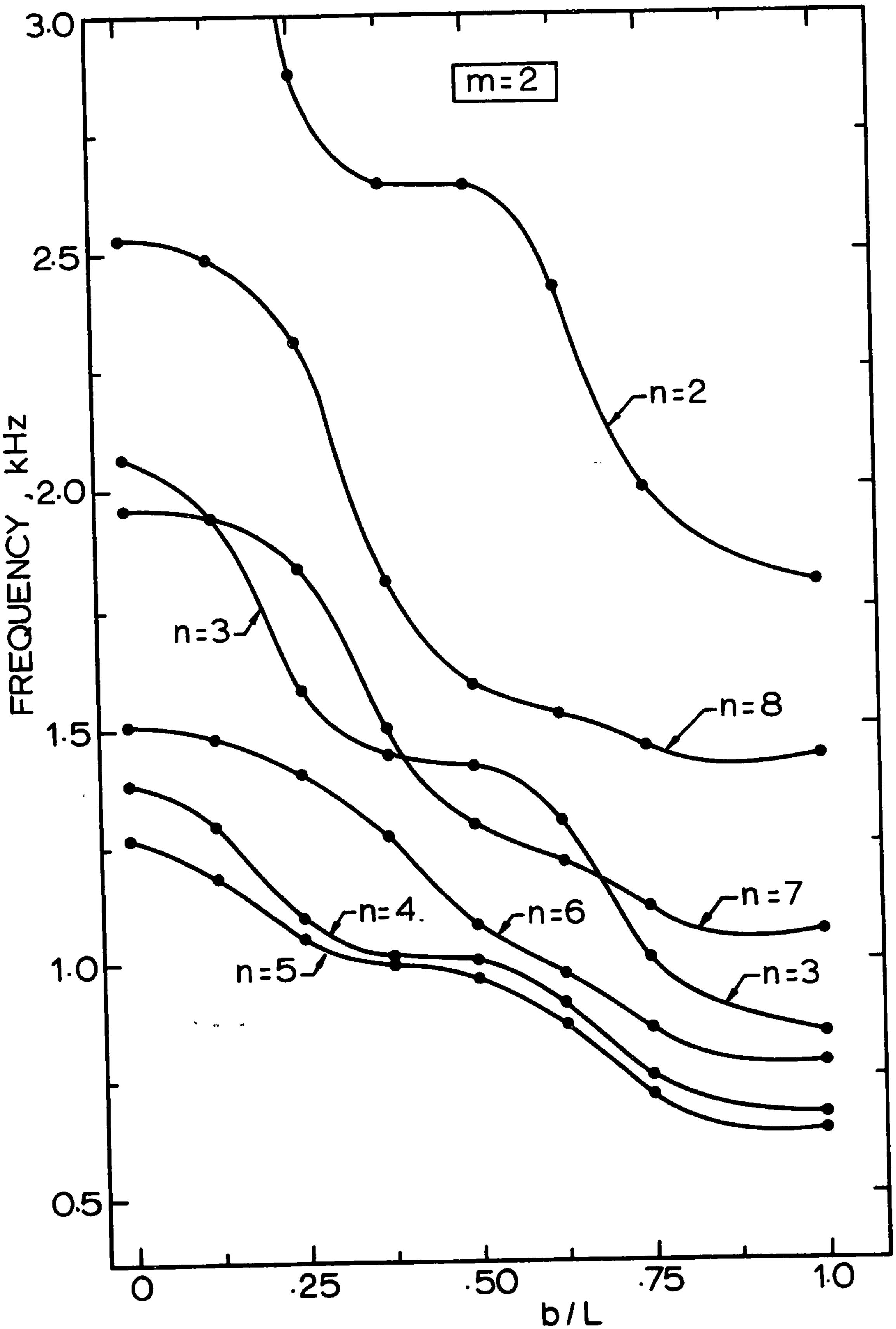


FIGURE 26. Variation of natural frequencies with liquid depth of a liquid-filled shell, this theory: m = 2.

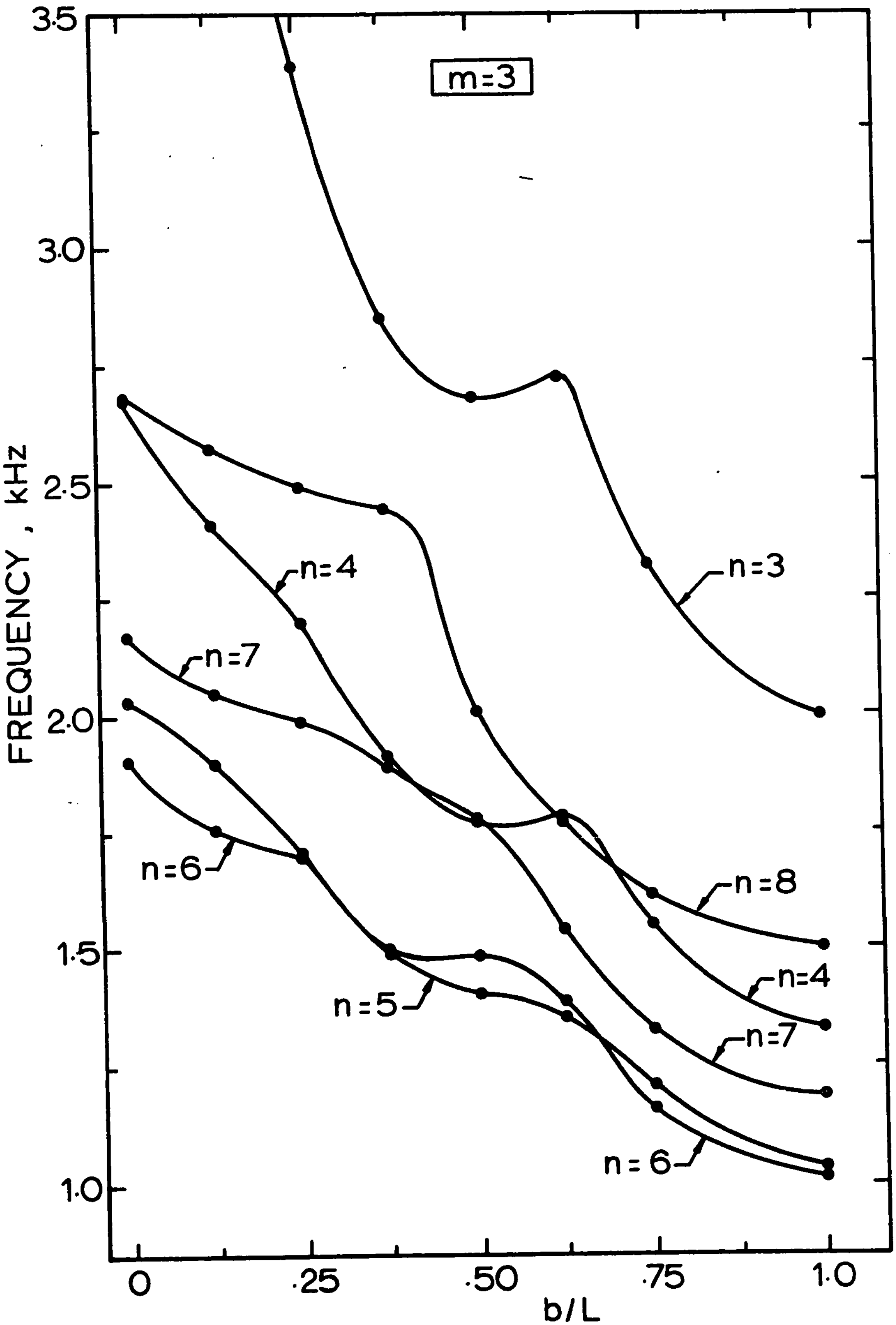


FIGURE 27. Variation of natural frequencies with liquid depth of a liquid-filled shell, this theory; m = 3.

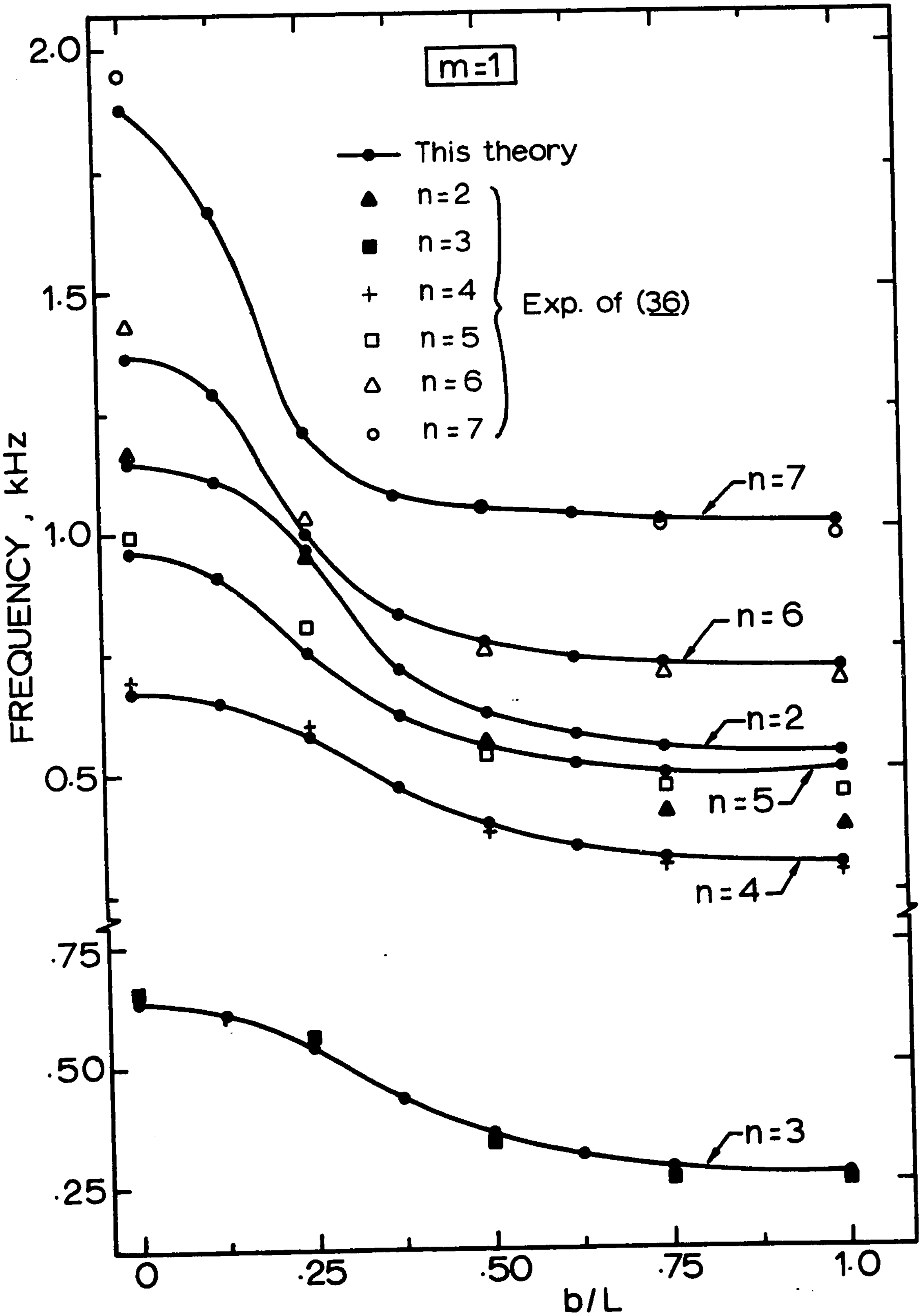


FIGURE 28. Comparison of this theory with experiments of (36) for liquid-filled shells; m = 1.

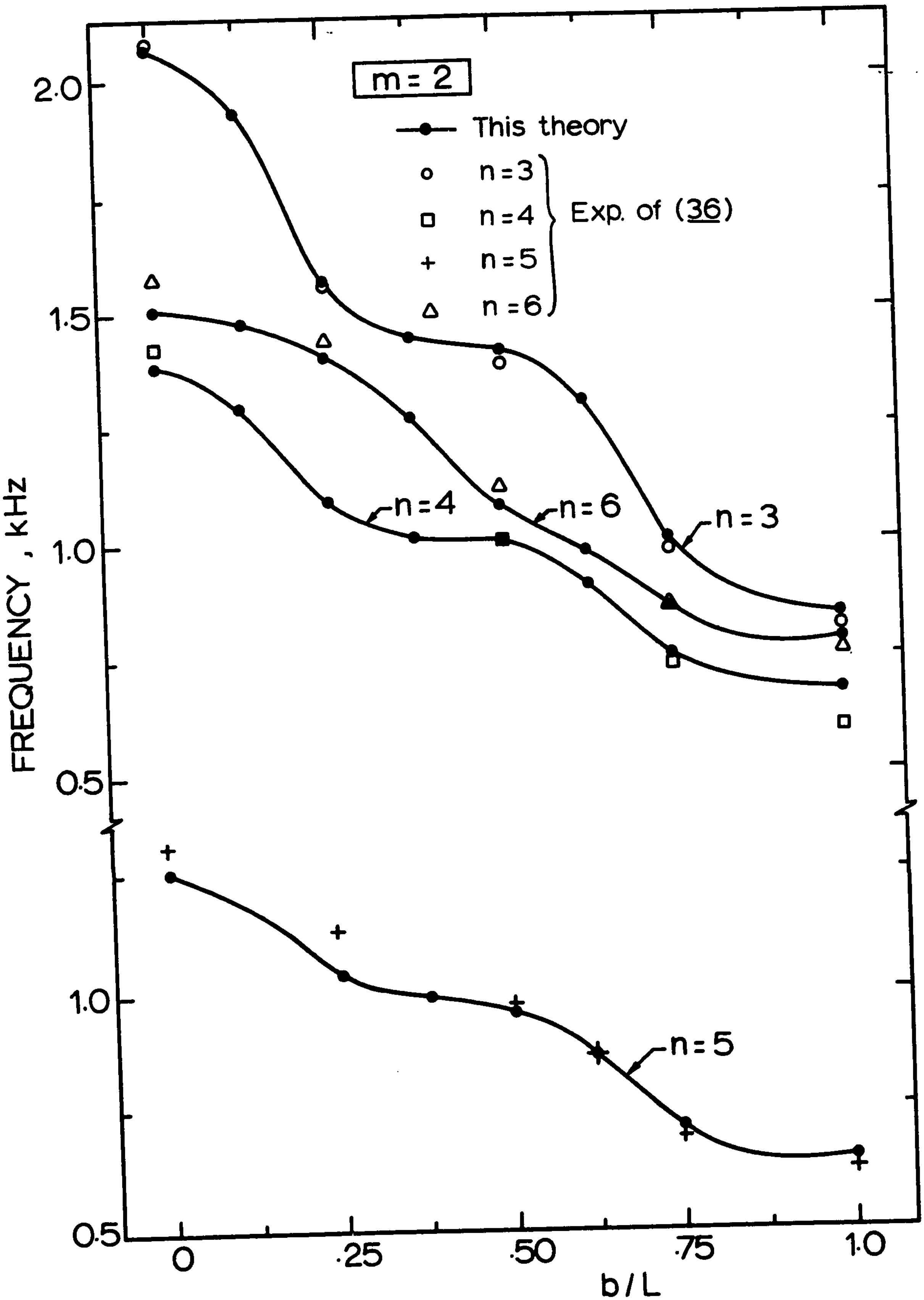


**FIGURE 29.** Comparison of this theory with experiments of (36) for liquid-filled shells; m = 2.

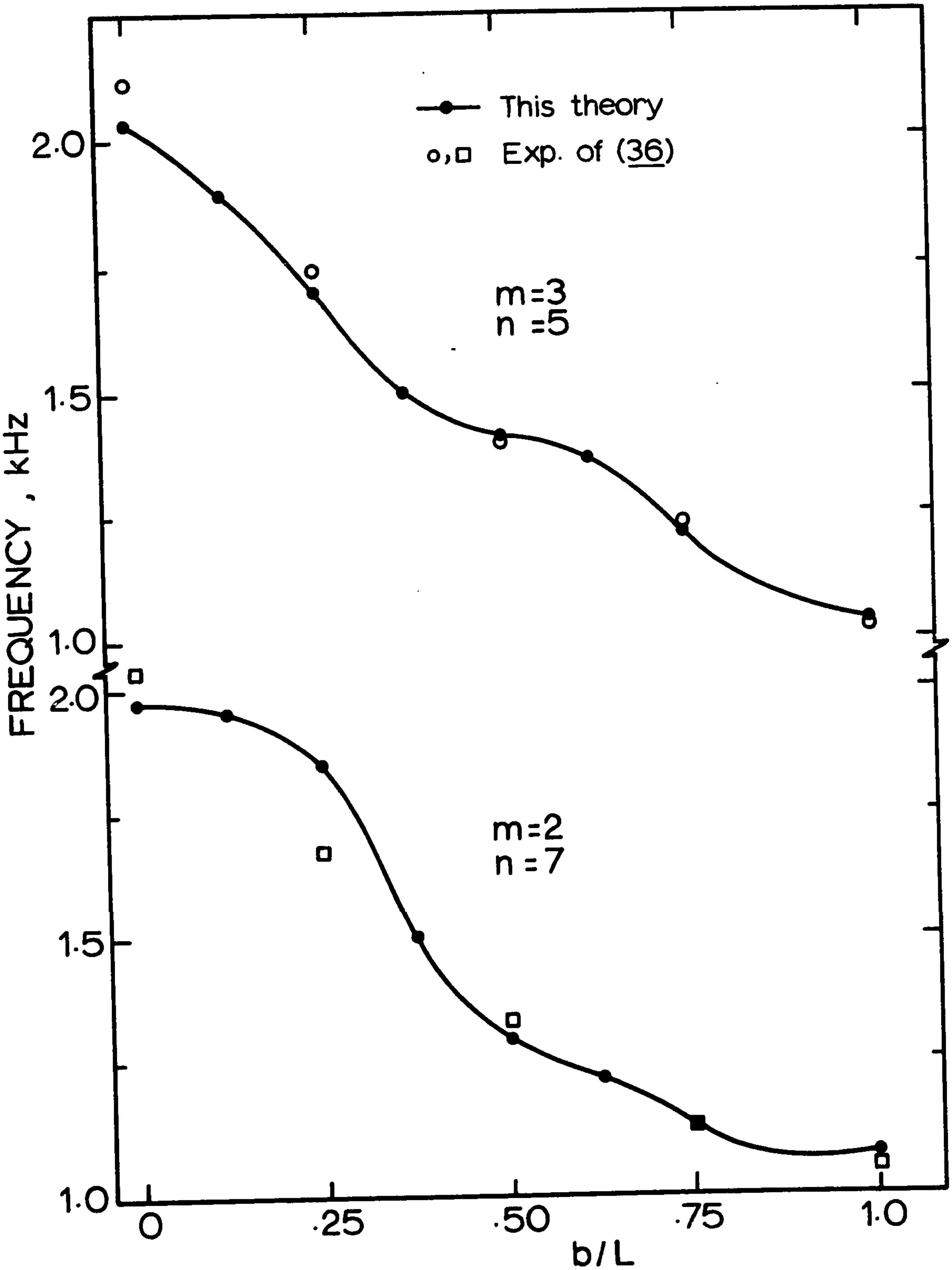


FIGURE 30. Comparison of this theory with experiments of (36) for liquid-filled shells; m = 2 and 3.

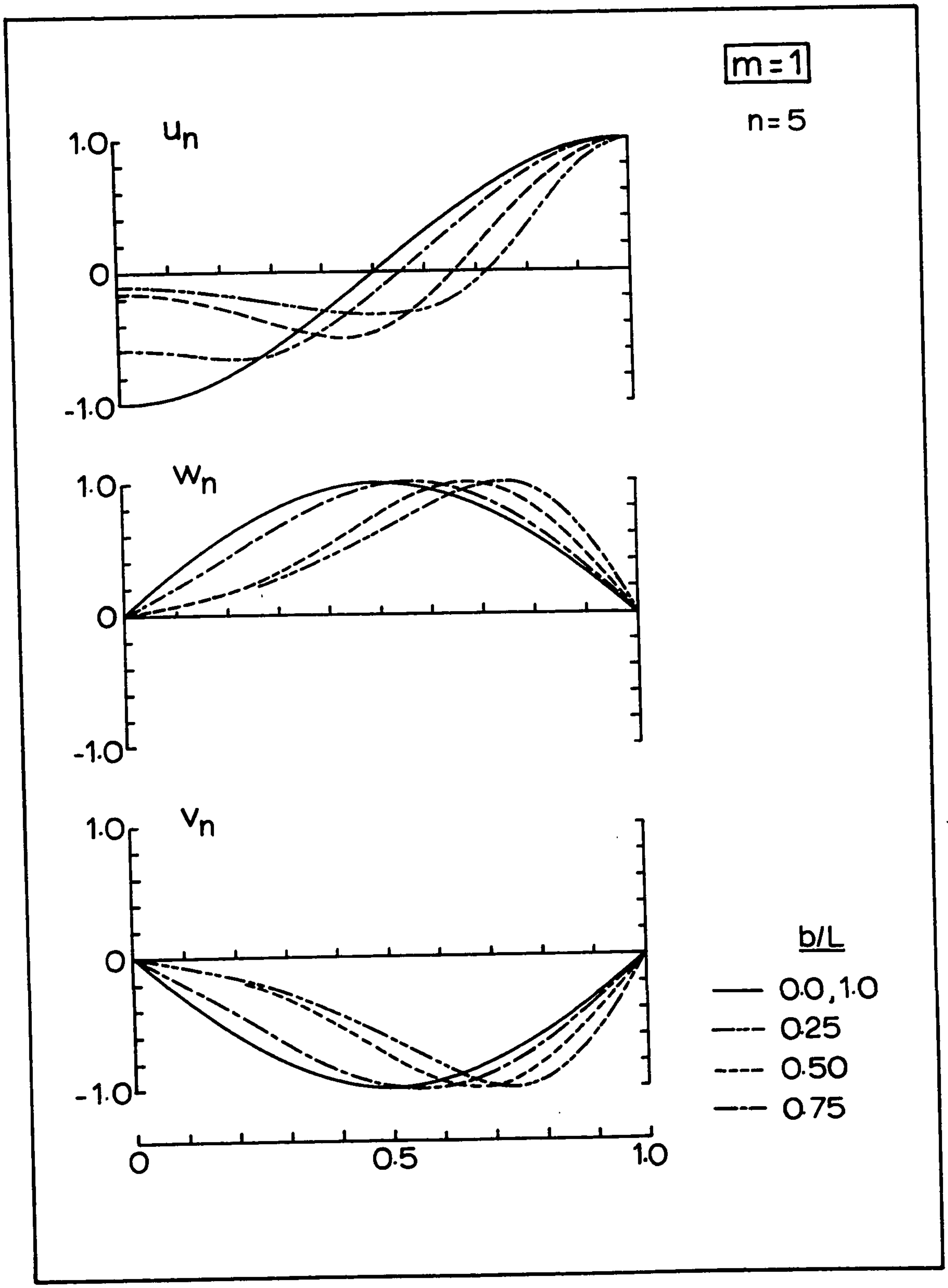


FIGURE 31. Eigenvectors of liquid-filled shells, as functions of liquid depth, b; for n = 5, m = 1.

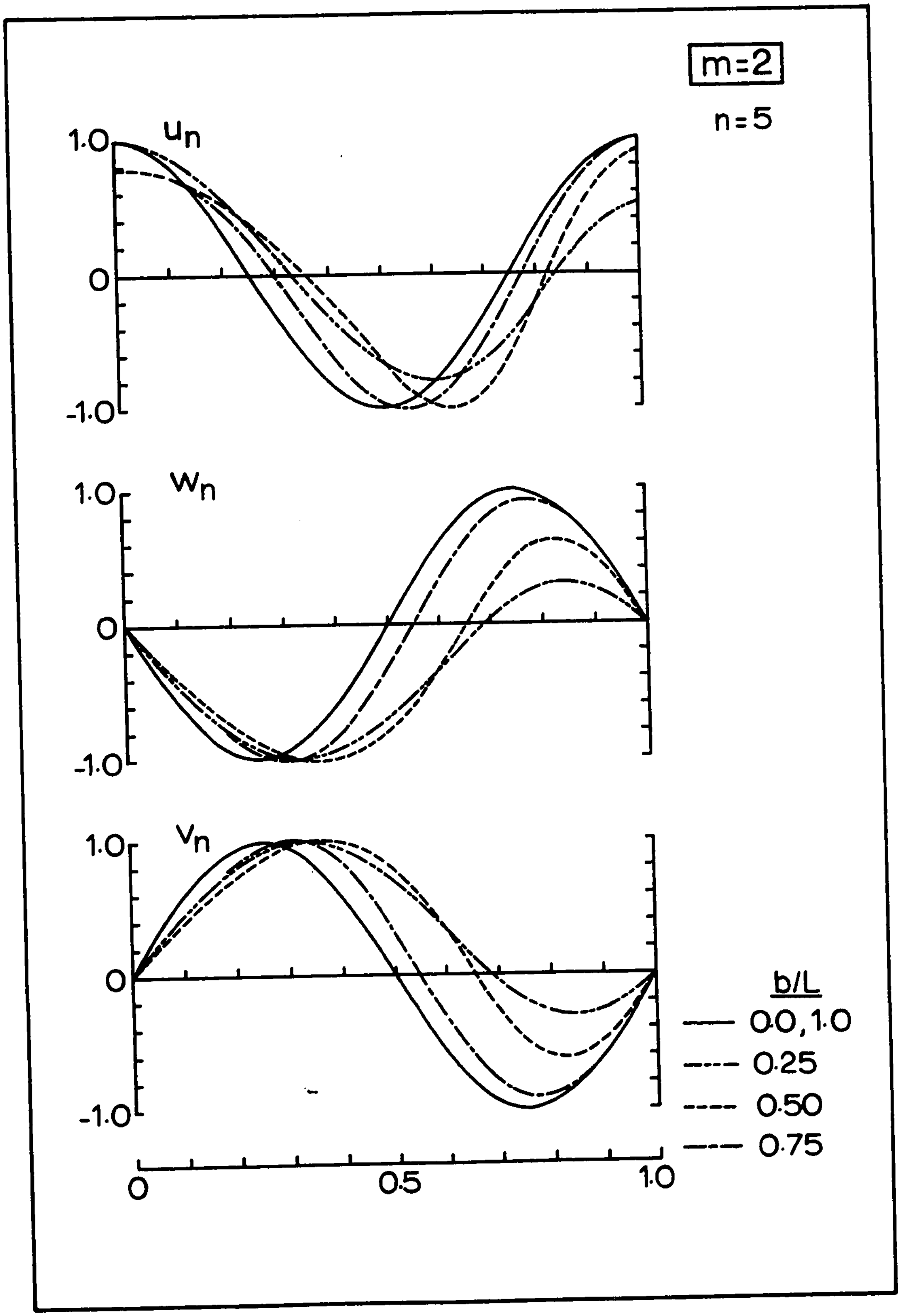


FIGURE 32. Eigenvectors of liquid-filled shells, as functions of liquid depth, b; for n = 5, m = 2.

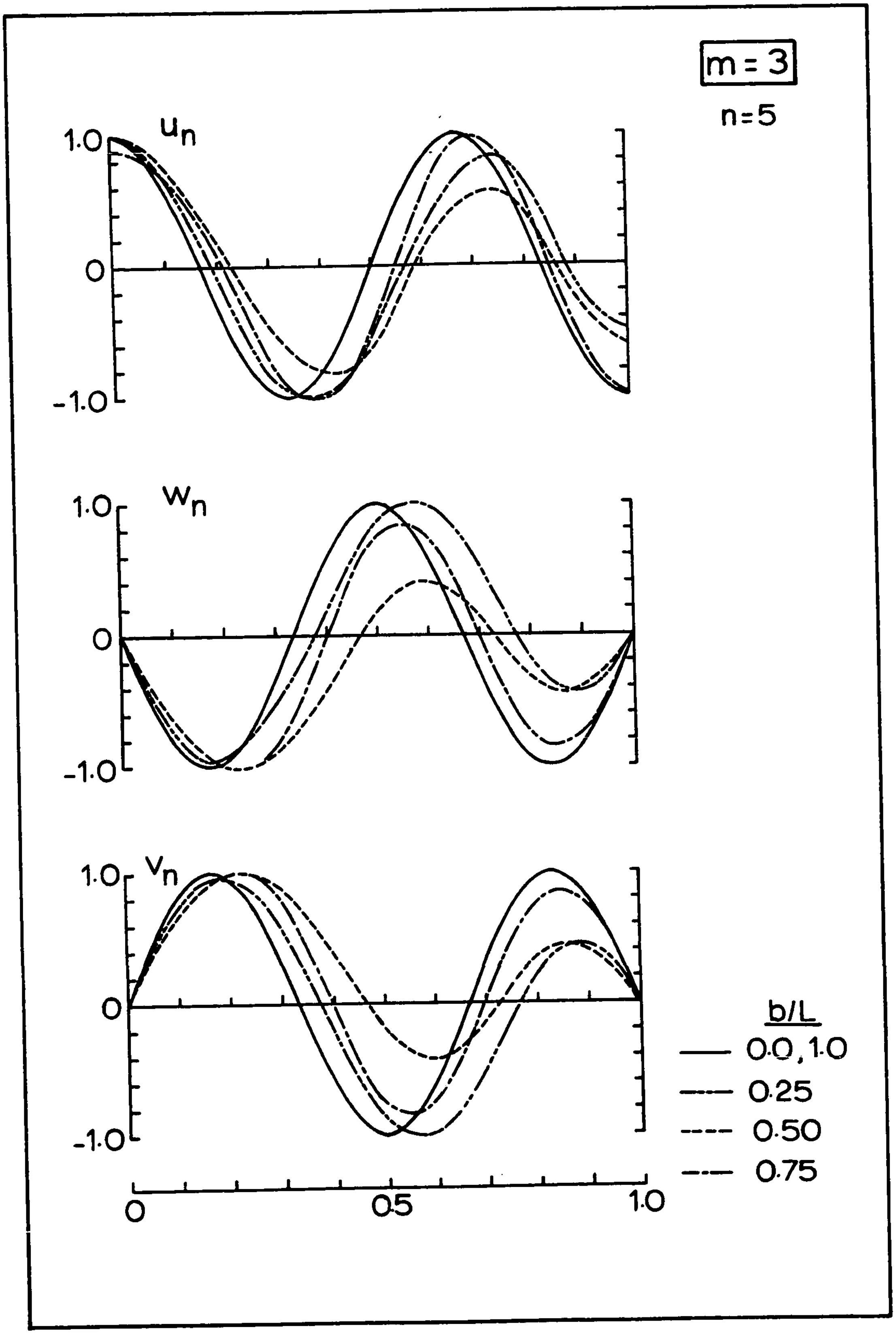


<u>FIGURE 33.</u> Eigenvectors of liquid-filled shells, as functions of liquid depth, b: for <u>n = 5</u>, m = 3.

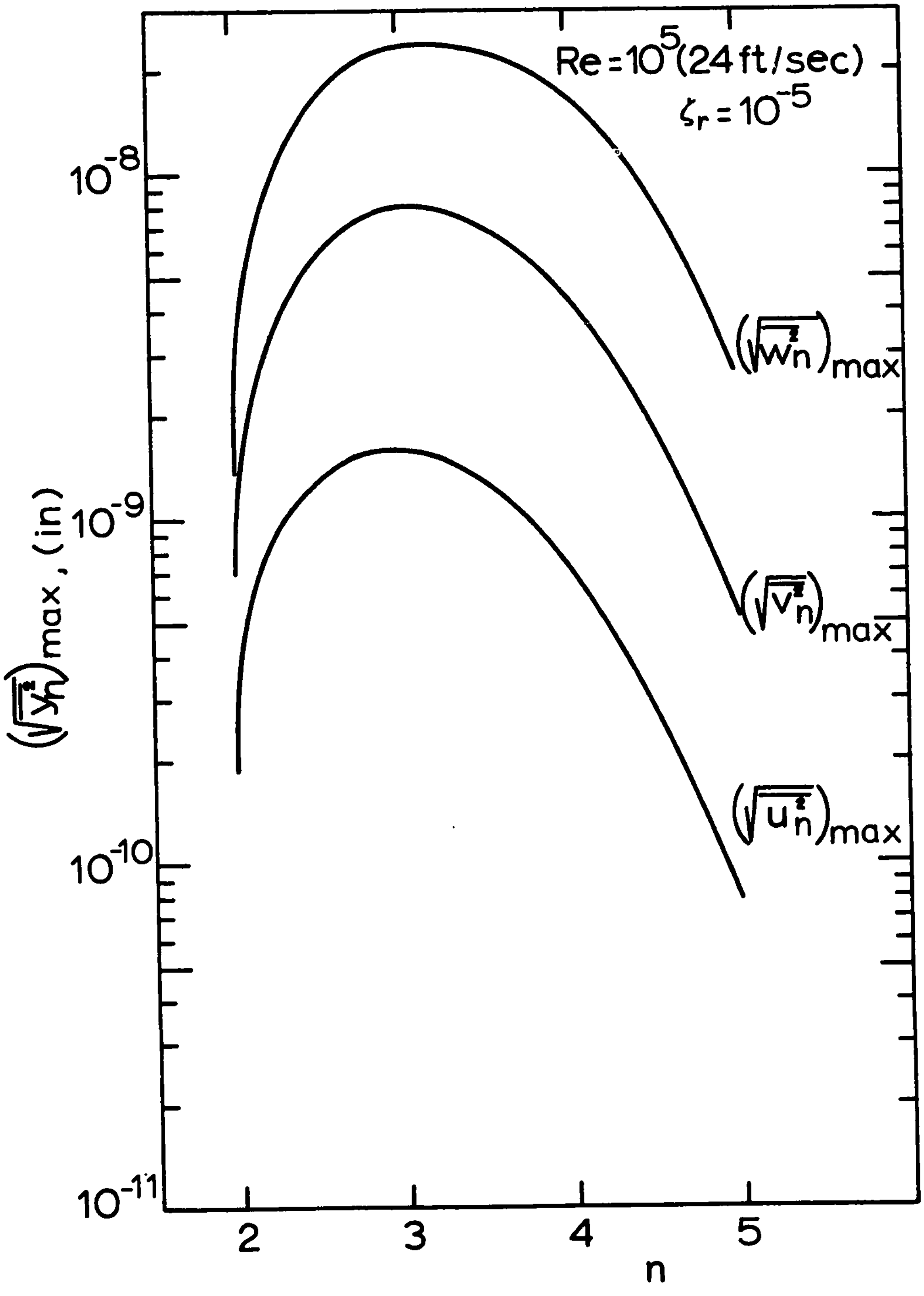


FIGURE 34. Maximum of r.m.s. displacements as functions of n; Re = $10^5$ and $\zeta_r = 10^{-5}$.

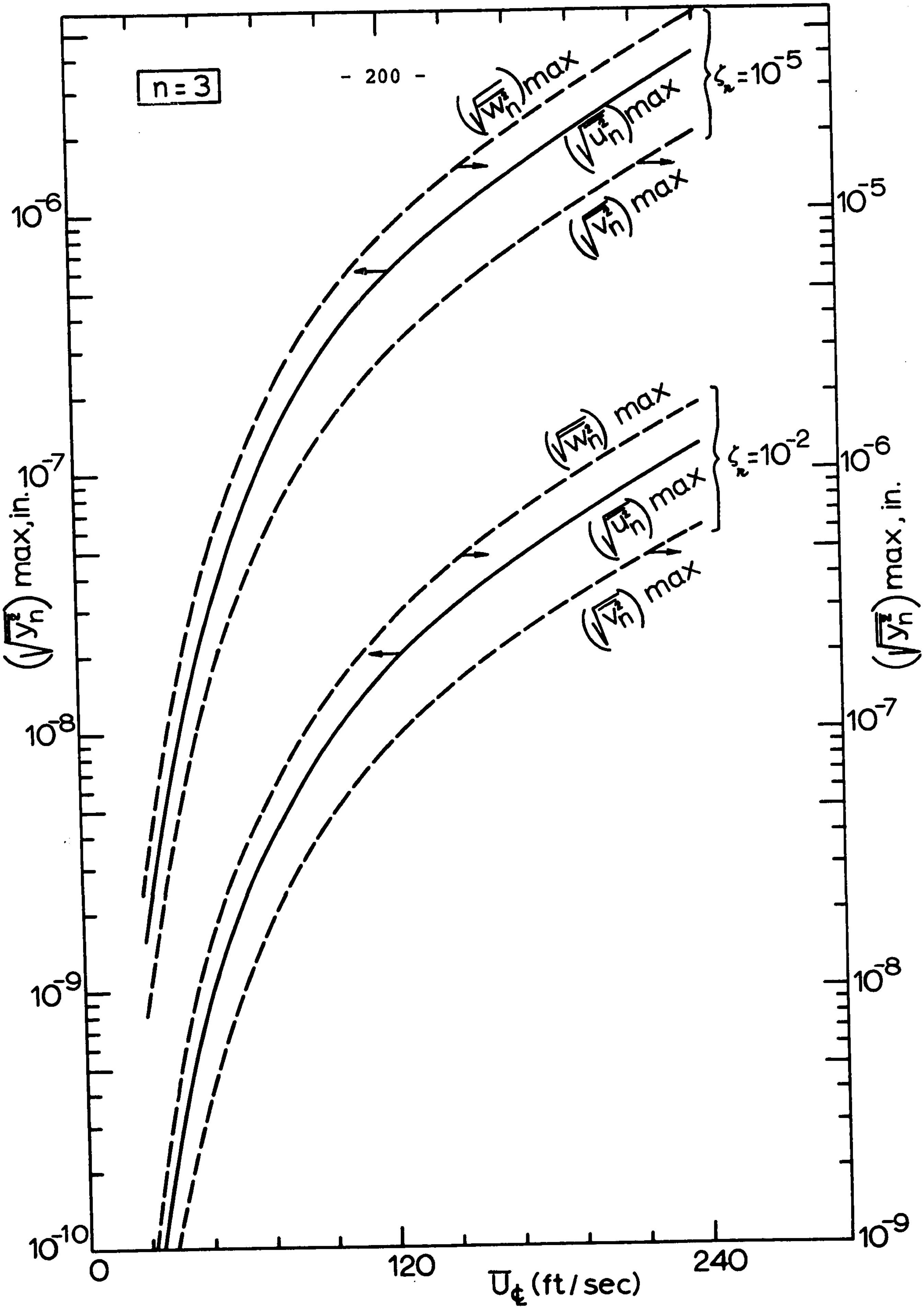


FIGURE 35. Maximum of r.m.s. displacements as functions of the mean centerline velocity, $\overline{U}_{\mathbb{C}}$ ; n = 3.